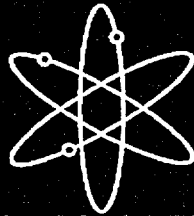
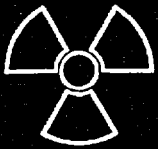




Knowledge Base for the Effect of Debris on Pressurized Water Reactor Emergency Core Cooling Sump Performance



Los Alamos National Laboratory



U.S. Nuclear Regulatory Commission
Office of Nuclear Regulatory Research
Washington, DC 20555-0001



**AVAILABILITY OF REFERENCE MATERIALS
IN NRC PUBLICATIONS**

NRC Reference Material

As of November 1999, you may electronically access NUREG-series publications and other NRC records at NRC's Public Electronic Reading Room at <http://www.nrc.gov/reading-rm.html>. Publicly released records include, to name a few, NUREG-series publications; *Federal Register* notices; applicant, licensee, and vendor documents and correspondence; NRC correspondence and internal memoranda; bulletins and information notices; inspection and investigative reports; licensee event reports; and Commission papers and their attachments.

NRC publications in the NUREG series, NRC regulations, and *Title 10, Energy*, in the Code of *Federal Regulations* may also be purchased from one of these two sources.

1. The Superintendent of Documents
U.S. Government Printing Office
Mail Stop SSOP
Washington, DC 20402-0001
Internet: bookstore.gpo.gov
Telephone: 202-512-1800
Fax: 202-512-2250
2. The National Technical Information Service
Springfield, VA 22161-0002
www.ntis.gov
1-800-553-6847 or, locally, 703-605-6000

A single copy of each NRC draft report for comment is available free, to the extent of supply, upon written request as follows:

Address: Office of the Chief Information Officer,
Reproduction and Distribution
Services Section
U.S. Nuclear Regulatory Commission
Washington, DC 20555-0001

E-mail: DISTRIBUTION@nrc.gov
Facsimile: 301-415-2289

Some publications in the NUREG series that are posted at NRC's Web site address <http://www.nrc.gov/reading-rm/doc-collections/nuregs> are updated periodically and may differ from the last printed version. Although references to material found on a Web site bear the date the material was accessed, the material available on the date cited may subsequently be removed from the site.

Non-NRC Reference Material

Documents available from public and special technical libraries include all open literature items, such as books, journal articles, and transactions, *Federal Register* notices, Federal and State legislation, and congressional reports. Such documents as theses, dissertations, foreign reports and translations, and non-NRC conference proceedings may be purchased from their sponsoring organization.

Copies of industry codes and standards used in a substantive manner in the NRC regulatory process are maintained at—

The NRC Technical Library
Two White Flint North
11545 Rockville Pike
Rockville, MD 20852-2738

These standards are available in the library for reference use by the public. Codes and standards are usually copyrighted and may be purchased from the originating organization or, if they are American National Standards, from—

American National Standards Institute
11 West 42nd Street
New York, NY 10036-8002
www.ansi.org
212-642-4900

Legally binding regulatory requirements are stated only in laws; NRC regulations; licenses, including technical specifications; or orders, not in NUREG-series publications. The views expressed in contractor-prepared publications in this series are not necessarily those of the NRC.

The NUREG series comprises (1) technical and administrative reports and books prepared by the staff (NUREG-XXXX) or agency contractors (NUREG/CR-XXXX), (2) proceedings of conferences (NUREG/CP-XXXX), (3) reports resulting from international agreements (NUREG/IA-XXXX), (4) brochures (NUREG/BR-XXXX), and (5) compilations of legal decisions and orders of the Commission and Atomic and Safety Licensing Boards and of Directors' decisions under Section 2.206 of NRC's regulations (NUREG-0750).

DISCLAIMER: This report was prepared as an account of work sponsored by an agency of the U.S. Government. Neither the U.S. Government nor any agency thereof, nor any employee, makes any warranty, expressed or implied, or assumes any legal liability or responsibility for any third party's use, or the results of such use, of any information, apparatus, product, or process disclosed in this publication, or represents that its use by such third party would not infringe privately owned rights.

Knowledge Base for the Effect of Debris on Pressurized Water Reactor Emergency Core Cooling Sump Performance

Manuscript Completed: February 2003
Date Published: February 2003

Prepared by
D.V. Rao, Principal Investigator

C.J. Shaffer,* D.V. Rao,
M.T. Leonard,** K.W. Ross***

Los Alamos National Laboratory
Los Alamos, NM 87545

Subcontractors:
*ARES Corporation
851 University Blvd. S.E., Suite 100
Albuquerque, NM 87106

**dycoda, LLC
70 Andres Sanchez Blvd.
Belen, NM 87002

***Innovative Technology Solutions Corporation
6000 Uptown Blvd. N.E., Suite 300
Albuquerque, NM 87110

B.P. Jain, NRC Project Manager

Prepared for
Division of Engineering Technology
Office of Nuclear Regulatory Research
U.S. Nuclear Regulatory Commission
Washington, DC 20555-0001
NRC Job Code Y6041



**NUREG/CR-6808, has been reproduced
from the best available copy.**

ABSTRACT

This report describes the substantial base of knowledge that has been amassed as a result of the research on boiling-water reactor (BWR) suction-strainer and pressurized-water reactor (PWR) sump-screen clogging issues. These issues deal with the potential insulation and other debris generated in the event of a postulated loss-of-coolant accident within the containment of a light-water reactor and subsequently transport to and accumulation on the recirculation sump screens. This debris accumulation could potentially challenge the plant's capability to provide adequate long-term cooling water to the emergency core cooling system (ECCS) and the containment spray system pumps.

This report describes analytical and experimental approaches that have been used to assess the different aspects of sump and strainer blockage and to identify the strengths, limitations, important parameters and plant features, and appropriateness of the different approaches. The report is organized in the same order that an evaluation of the potential of sump screen blockage would be performed. The report provides background information on the issues, including significant United States regulatory developments regarding the resolution of the issue. The report is designed to serve as a reference for plant-specific analyses with regard to whether a sump or strainer would perform its function without preventing the operation of the ECCS pumps.

CONTENTS

	<i>Page</i>
Abstract.....	iii
Executive Summary.....	xiii
Acknowledgements	xv
Abbreviations	xvii
Units Conversion Table	xix
1.0 Introduction	1-1
1.1 Historical Overview	1-1
1.2 Description of Safety Concern	1-8
1.3 Criteria for Evaluating Sump Failure	1-9
1.3.1 Fully Submerged Sump Screens	1-10
1.3.2 Partially Submerged Sump Screens	1-10
1.4 Description of Postulated Pressurized-Water Reactor Accidents.....	1-11
1.4.1 Overview	1-11
1.4.2 Large Loss-of-Coolant Accident.....	1-15
1.4.2.1 Reactor Coolant System Blowdown Phase	1-15
1.4.2.2 Emergency Core Cooling System Injection Phase.....	1-20
1.4.2.3 Recirculation Phase.....	1-21
1.4.3 Medium Loss-of-Coolant Accident.....	1-21
1.4.3.1 Reactor Coolant System Blowdown Phase	1-21
1.4.3.2 Emergency Core Cooling System Injection Phase.....	1-21
1.4.3.3 Recirculation Phase.....	1-21
1.4.4 Small Loss-of Coolant Accident.....	1-25
1.4.4.1 Reactor Coolant System Blowdown Phase	1-25
1.4.4.2 Emergency Core Cooling System Injection Phase.....	1-25
1.4.4.3 Recirculation Phase.....	1-25
1.4.5 Other Plant Design Features that Influence Accident Progression	1-25
1.5 Description of Relevant Plant Features that Influence Accident Progression	1-30
1.6 Regulatory Considerations.....	1-31
1.6.1 Code of Federal Regulations	1-32
1.6.2 Regulatory Guidance	1-34
1.7 Report Outline	1-35
1.8 References.....	1-35
2.0 Debris Sources	2-1
2.1 Actual Debris Found During Inspections	2-1
2.2 Loss-of-Coolant-Accident-Generated Debris.....	2-2
2.3 Loss-of-Coolant-Accident Exposure-Generated Debris.....	2-3
2.4 Operational Debris	2-4
2.5 Aging Effects on Mineral Fiber Thermal Insulation	2-5
2.6 Relative Timing and Debris Bed Composition	2-5
2.7 References.....	2-6
3.0 Debris Generation.....	3-1
3.1 Overview of the Mechanics of Debris Generation	3-1
3.1.1 Break-Jet Phenomena	3-4
3.1.1.1 Size/Configuration of Pipe Rupture	3-4
3.1.1.2 Break Effluent	3-4

3.1.1.3	Obstacles	3-5
3.1.2	Debris Classification	3-5
3.1.2.1	Size Classification of Fibrous Debris	3-6
3.1.2.2	Size Classification of RMI Debris	3-6
3.2	Debris-Generation Testing	3-6
3.2.1	Air-Jet Testing	3-9
3.2.1.1	NRC BWR Drywell Inertial Capture Tests	3-9
3.2.1.2	BWROG Air-Jet Impact Testing (AJIT)	3-10
3.2.2	Steam and Two-Phase Jet Testing	3-12
3.2.2.1	Marviken Full-Scale Containment Experiments	3-12
3.2.2.2	HDR Tests	3-12
3.2.2.3	Karlshamn Caposil and Newtherm Tests	3-13
3.2.2.4	Siemens Metallic Insulation Jet Tests (MIJITs)	3-14
3.2.2.5	Ontario Power Generation Test	3-15
3.2.2.6	Battelle/KAEFER Tests	3-19
3.3	Debris-Generation Models and Analytical Approaches	3-22
3.3.1	Cone Models	3-23
3.3.1.1	ANSI/ANS Standard	3-23
3.3.1.2	Three-Region Conical Jet	3-25
3.3.2	Spherical Models	3-26
3.3.2.1	Three-Region Spherical Model	3-26
3.3.2.2	Equivalent-Volume Sphere Model	3-27
3.3.3	Debris-Size Distribution as a Function of Local Jet Pressure	3-28
3.4	References	3-29
4.0	Airborne/Washdown Debris Transport in Containment	4-1
4.1	Overview on Mechanics	4-2
4.1.1	Accident Characterization Relevant to Debris Transport	4-2
4.1.2	Plant Features Affecting Debris Transport	4-3
4.1.3	Physical Processes and Phenomena Affecting Debris Transport	4-4
4.1.4	Debris Characteristics Affecting Transport	4-8
4.2	Airborne/Washdown Debris-Transport Testing	4-8
4.2.1	Airborne Phase Debris-Transport Testing	4-8
4.2.1.1	Separate-Effects Debris-Transport Tests	4-8
4.2.1.2	Integrated-Effects Debris-Transport Tests	4-13
4.2.1.3	Blowdown Experiments at Heissdampfreaktor (HDR) Facility	4-17
4.2.1.4	Karlshamn Steam Blast Tests	4-18
4.2.2	Airborne/Washdown Combined Phase Debris-Transport Testing	4-20
4.2.2.1	BWROG Testing of Debris Transport Through Downcomers/Vents	4-20
4.2.3	Washdown-Phase Debris-Transport Testing	4-23
4.2.3.1	Separate-Effects Insulation Debris Washdown Tests	4-23
4.2.3.2	Oskarshamn Nuclear Power Plant Containment Washdown Tests	4-25
4.3	Airborne/Washdown Debris-Transport Analyses	4-25
4.3.1	Evaluations of Operational Incidents	4-27
4.3.1.1	Evaluation of Incident at Gundremmingen-1	4-27
4.3.1.2	Evaluation of Incident at Barsebäck-2	4-27
4.3.2	Phenomena Identification and Ranking Tables	4-31
4.3.2.1	BWR PIRT	4-31
4.3.2.2	PWR PIRT	4-31
4.3.3	Airborne/Washdown Debris-Transport Evaluations	4-33
4.3.3.1	MELCOR Simulation of Karlshamn Tests	4-33
4.3.3.2	BWR Drywell Debris Transport Study (DDTS)	4-34
4.3.3.3	PWR Volunteer Plant Analysis	4-41
4.3.4	Generalized Debris-Transport Guidance	4-44
4.3.4.1	BWR URG Guidance for Drywell Debris Transport and the NRC Review	4-44

	4.3.4.2	Transport Fractions for Parametric Evaluation.....	4-48
4.4		Types of Analytical Approaches.....	4-49
4.5		Rules of Thumb.....	4-50
4.6		References.....	4-50
5.0		Sump Pool Debris Transport.....	5-1
5.1		Overview of Mechanics.....	5-1
	5.1.1	Accident Characterization.....	5-2
	5.1.2	Plant Features.....	5-3
	5.1.3	Physical Processes/Phenomena.....	5-4
	5.1.4	Debris Characteristics.....	5-7
5.2		Debris Transport in Pooled Water Testing.....	5-7
	5.2.1	Alden Research Laboratory Buoyancy and Transport Testing on Fibrous Insulation Debris.....	5-7
	5.2.2	Pennsylvania Power and Light Debris Transport Tests.....	5-10
	5.2.3	Alden Research Laboratory Suppression Pool Debris Sedimentation Testing.....	5-11
		5.2.3.1 Fibrous Debris Sedimentation Testing.....	5-12
		5.2.3.2 Reflective Metal Insulation Debris Sedimentation Testing.....	5-15
	5.2.4	Alden Research Laboratory Reflective Metallic Insulation Materials Transport Testing.....	5-15
	5.2.5	University of New Mexico Separate Effects Debris Transport Testing.....	5-17
	5.2.6	University of New Mexico Integrated Debris Transport Testing.....	5-24
	5.2.7	Bremen Polytechnic Testing of KAEFER Insulation Systems.....	5-29
	5.2.8	Alden Research Laboratory Testing of Owens-Corning Fiberglass (NUKON) Insulation.....	5-32
	5.2.9	STUK Metallic Insulation Transport and Clogging Tests.....	5-33
5.3		Debris Transport in Pooled Water Analysis.....	5-34
	5.3.1	Phenomena Identification and Ranking Tables.....	5-34
		5.3.1.1 Boiling-Water Reactor Phenomena Identification and Ranking Table.....	5-34
		5.3.1.2 Pressurized-Water Reactor Phenomena Ranking and Identification Table.....	5-34
	5.3.2	Boiling-Water Reactor Drywell Floor Pool Debris Transport Study.....	5-36
	5.3.3	Boiling-Water Reactor Suppression-Pool Debris-Transport Analysis.....	5-37
	5.3.4	Pressurized-Water Reactor Volunteer Plant Pool Debris Transport Analysis.....	5-38
	5.3.5	Nuclear Regulatory Commission Review of Licensee Experimental Approach to Sump Blockage Potential.....	5-38
	5.3.6	Computational Fluid Dynamic Simulations of UNM Integrated Debris-Transport Testing.....	5-41
5.4		Summary of Approaches to Modeling Containment Pool Transport.....	5-41
5.5		Guidance.....	5-43
5.6		References.....	5-44
6.0		Debris Accumulation.....	6-1
6.1		Locations of Concern.....	6-1
	6.1.1	Sump Screens.....	6-1
	6.1.2	Containment Flow Restrictions.....	6-3
6.2		Accumulation Patterns.....	6-3
6.3		Parameters Affecting Debris Accumulation.....	6-8
	6.3.1	Local Flow Field.....	6-8
	6.3.2	Local Geometry.....	6-9
	6.3.3	Submergence.....	6-9
	6.3.4	Debris Characteristics.....	6-10
6.4		Test Data.....	6-10
	6.4.1	BWR Strainer Tests.....	6-10
	6.4.2	Test Results for Vertical PWR Sump Screen Configurations.....	6-11
6.5		References.....	6-14

7.0	Debris Head Loss	7-1
7.1	Factors Affecting Debris-Bed Build-Up and Head Loss.....	7-1
7.1.1	Fibrous Debris Beds	7-1
7.1.2	Mixed Particulate and Fiber Beds.....	7-4
7.1.3	Reflective Metallic Insulation.....	7-6
7.1.4	Mixed Fiber and RMI Debris Beds.....	7-8
7.2	Review of Experimental Programs.....	7-9
7.2.1	Flat-Plate Strainers	7-11
7.2.2	Flat-Plate Strainers in Flumes.....	7-18
7.2.3	Prototype Module Strainer Testing	7-20
7.2.4	Semi-Scale Installed Strainer Testing.....	7-28
7.3	Analysis of Test Data	7-29
7.3.1	United States Nuclear Regulatory Commission Characterization of Head Loss Data	7-29
7.3.1.1	Fiberglass and Particulate Debris.....	7-29
7.3.1.2	Reflective Metallic Insulation	7-29
7.3.2	Analysis of Non-Flat-Plate Strainer Data	7-35
7.3.2.1	Phenomena of Debris Build-Up on Stacked-Disk Strainers	7-37
7.3.2.2	Application of the NUREG/CR-6224 Correlation to the PCI Strainer	7-37
7.4	Ongoing Research on Outstanding Issues	7-41
7.4.1	Long-Term Fibrous Debris Bed Stability.....	7-41
7.4.2	Calcium Silicate Debris Head Loss.....	7-42
7.4.3	Vertically Oriented Screens	7-42
7.5	References.....	7-42
8.0	Resolution Options	8-1
8.1	Overview of Resolution Options.....	8-1
8.2	Replacement Strainer Designs	8-2
8.2.1	Passive Strainer Designs Installed in U.S. Nuclear Power Plants.....	8-2
8.2.1.1	PCI Stacked-Disk Strainers	8-4
8.2.1.2	General Electric Stacked-Disk Strainers	8-6
8.2.1.3	ABB Combustion Engineering Strainers.....	8-6
8.2.1.4	Mark III Strainers	8-7
8.2.2	Active Strainer Designs.....	8-8
8.2.2.1	BWROG Research Into Active Strainer Concepts	8-8
8.3	Overview of U.S. BWR Plant Implementation.....	8-9
8.3.1	NRC Review of U.S. Plant Implementation	8-9
8.3.2	Onsite Plant Audits	8-10
8.4	Special Considerations for PWR Resolution Options	8-12
8.4.1	Flow Path Blocking	8-12
8.4.2	Strainer Penetration	8-12
8.4.2.1	Spray Nozzles.....	8-13
8.4.2.2	Fuel Bundles.....	8-13
8.4.3	LOCA Jet and Missile Considerations	8-15
8.4.4	Feasibility and Efficiency of Backflushing	8-15
8.4.5	Debris Induced Mechanical Structural Loadings	8-15
8.5	References.....	8-16
9.0	Significant Events	9-1
9.1	LOCA Debris Generation Events.....	9-1
9.2	Events Rendering a System Inoperable	9-2
9.3	Debris-Found-in-Containment Events	9-5
9.4	Inadequate Maintenance Leading to Potential Sources of Debris.....	9-8
9.5	Sump-Screen Inadequacies.....	9-10
9.6	References.....	9-12

10.0	Summary and Conclusions.....	10-1
10.1	Summary of Knowledge Base.....	10-1
10.2	Conclusions.....	10-13

Figures

1-1	Illustration of Sump Features and Parameters.....	1-9
1-2	Sump-Screen Schematics.....	1-10
1-3	Flow Chart of Analysis Process.....	1-12
1-4	PWR LLOCA Accident Progression in a Large Dry Containment.....	1-19
1-5	PWR MLOCA Accident Progression in a Large Dry Containment.....	1-24
1-6	PWR SLOCA Accident Progression in a Large Dry Containment.....	1-29
3-1	Example ZOI at a Postulated Break Location.....	3-2
3-2	Variation in the ZOI Shape with DEGB Separation and Offset.....	3-5
3-3	Fiberglass Insulation Debris of Two Example Size Classes.....	3-7
3-4	Inner Construction and Installation of a Typical RMI Cassette.....	3-8
3-5	RMI Foil Before/After "Crumpling" (Left) and Crumpled RMI Foil Debris (Right).....	3-8
3-6	Configuration of the CEESI Test Facility for the NRC/SEA BWR Drywell Debris-Transport Tests.....	3-10
3-7	Typical RMI Debris Generated by Large Pipe Break.....	3-15
3-8	RMI Debris Observed in Siemens Steam-Jet Impact Tests.....	3-15
3-9	Insulation Target Mounting Configuration in OPG Test (Longitudinal Seam at 45°, Circumferential Seam Offset).....	3-17
3-10	Typical Calcium-Silicate Debris Collected from an OPG Two-Phase Jet Test.....	3-18
3-11	Test Configuration of Aluminum-Clad Calcium-Silicate Insulation (Distance from Break of 9D and Longitudinal Seam at 45°).....	3-19
3-12	Post-Test Configuration of Aluminum-Clad Fiberglass Insulation (Distance from Break of 10D and Longitudinal Seam at 45°).....	3-20
3-13	Configuration of the Target Field in the Battelle/KAEFER Tests.....	3-20
3-14	Typical View of Target Destruction in Battelle/KAEFER Tests.....	3-22
3-15	ANSI/ANS Standard Free-Expanding Jet Model.....	3-24
3-16	Isobar of Damage Pressure P_x within a Fixed, Free-Expanding Jet.....	3-24
3-17	Illustration of the Three-Region, Two-Phase Conical-Jet ZOI Model.....	3-26
3-18	Illustration of the Three-Region, Two-Phase Spherical ZOI Model.....	3-27
3-19	Debris Size as a Function of Local Jet Pressure.....	3-30
4-1	Separate-Effects Insulation Debris-Transport/Capture Test Apparatus.....	4-12
4-2	Typical Fibrous Debris Capture by a Wetted Pipe.....	4-13
4-3	CEESI Air-Jet Test Facility.....	4-14
4-4	Samples of Debris Generated in the CEESI Tests.....	4-16
4-5	Typical Debris Deposition on a Grating in CEESI Tests.....	4-16
4-6	Capture of Small Debris by Grating.....	4-17
4-7	ABB-Atom Containment Experimental Arrangement.....	4-19
4-8	Schematic of 1/8-Scale Mark I Configuration Test Apparatus.....	4-21
4-9	Schematic of 1/8-Scale Mark II Configuration Test Apparatus.....	4-22
4-10	Schematic of Washdown Test Apparatus.....	4-24
4-11	Time-Dependency of 1-in. Insulation Blanket Material Under Break-Flow Conditions.....	4-26
4-12	Typical Condition of Debris After Exposure to Water.....	4-26
4-13	Schematic Illustrating the Complexity of Drywell Debris Transport.....	4-36
4-14	Sample Drywell Debris Transport Logic Chart.....	4-37
5-1	Suppression Pool Sedimentation Test Apparatus.....	5-13
5-2	Fibrous Debris Classifications.....	5-14
5-3	Fibrous Debris Terminal Settling Velocities.....	5-14
5-4	Typical Large (6-in.) RMI Debris in Suspension During Chugging.....	5-16
5-5	Photo of Large UNM Flume Test Apparatus.....	5-19
5-6	Diagram of Large UNM Flume Test Apparatus.....	5-19

5-7	Photo of Large UNM Flume Inlet Flow Conditioning Apparatus.....	5-20
5-8	Typical Test Sample of LDFG Insulation Debris	5-20
5-9	Typical Test Sample of Aluminum RMI Insulation Debris	5-21
5-10	Typical Test Sample of Paint-Chip Debris.....	5-21
5-11	Comparison of Terminal Settling Velocities.....	5-22
5-12	Comparison of Incipient and Bulk Tumbling Velocities	5-23
5-13	Comparison of Incipient Lift Velocities to Incipient Tumbling Velocities	5-23
5-14	Steel Tank Used in Integrated Testing	5-26
5-15	Integrated Test Tank Outlet Box	5-26
5-16	Test Configuration A.....	5-27
5-17	Test Configuration B.....	5-27
5-18	Test Configuration C.....	5-27
5-19	Test Configuration D.....	5-27
5-20	Samples of KAEFER Insulation Systems Tested.....	5-31
5-21	Bremen Buoyancy Test Illustration.....	5-32
5-22	Typical Fibrous Debris Transport in the Suppression Pool	5-39
5-23	Configuration of Millstone-2 Debris-Transport Experiment	5-39
5-24	Sample CFD Prediction of Flow Velocities for One Test Configuration	5-42
6-1	Examples of Various Recirculation Sump Configurations in PWRs.....	6-2
6-2	Example of Containment Floor Flow Restriction that Might Result in Diversion of Flow From the Recirculation Sump.....	6-3
6-3	Debris Accumulation Profiles Observed in Linear Flume Experiments.....	6-6
6-4	Photographs of Debris Accumulation on a 1-ft X 1-ft Vertical Screen in a Large Linear Flume ...	6-7
6-5	Typical Buildup of Fine Fibrous Debris that Easily Remains Suspended	6-8
6-6	Example Installation of a BWR Stacked-Disk ECCS Recirculation Suction Strainer.....	6-12
6-7	Fibrous Debris Accumulation on a Stacked-Disk Strainer	6-12
6-8	RMI Debris Accumulation on a Stacked-Disk Strainer.....	6-13
7-1(a)	High-Resolution Scanning Electron Microscope Image of Fibrous Debris	7-2
7-1(b)	Low-Resolution Scanning Electron Microscope Image of Fibrous Debris	7-2
7-2	Head Losses vs Fiber Volume for Fixed Quantities of Particulate	7-5
7-3	Aluminum RMI Accumulation on a Stacked Disk Strainer	7-8
7-4(a)	RMI/Fiber/Sludge Post Head Loss Test Debris Bed	7-10
7-4(b)	RMI and Fiber Accumulation on a Strainer	7-10
7-5	Equivalency Between a Truncated Cone Strainer Debris Accumulation and Flat-Plate Strainer Simulation	7-12
7-6	Vertical Flat-Plate Strainer Head Loss Facility at Alden Research Laboratory.....	7-13
7-7(a)	Flat-Plate-Strainer Head Loss Facility Used in KKL Test.....	7-16
7-7(b)	Gravity Head Loss Test Setup Used in the BWROG Tests	7-17
7-8(a)	Schematic of the Horizontal Flume Used in NRC-Sponsored ARL-Conducted PWR Sump Screen Tests).....	7-19
7-8(b)	Picture of Large RMI Foil Accumulation on the Vertical Screen	7-19
7-9(a)	Flume Test Setup Used in the CDI Experiments for Millstone 2.....	7-21
7-9(b)	Test Setup Used for Transport and Head Loss Measurement in the KKB Plant-Specific Tests.....	7-22
7-10	STUK RMI Head Loss Test Setup for Prototype Strainer	7-23
7-11	BWROG Prototype Strainer Module Test Setup	7-25
7-12	Measured Head Loss as Function of Strainer Debris Loading for Specialty Strainers	7-26
7-13	Semi-Scale Test Facility Used in Grand Gulf Quarter-Scale Testing	7-29
7-14	Prototype Strainer Module Test Setup Used in Grand Gulf Prototype Tests.....	7-30
7-15	Idealized View of Flow Through an RMI Bed	7-32
7-16	Comparison of NRC/ARL Test Data with LANL Correlation	7-34
7-17	Comparison of BWROG Test Data for Truncated Cone Strainer with LANL RMI Correlation....	7-34
7-18	Comparison of LANL RMI Correlation Predictions for Truncated Cone Strainer with the Experimental Data Obtained from LaSalle Tests	7-36
7-19	Comparison of LANL RMI Predictions with the STUK Head Loss Data	7-36
7-20	Schematic Representation of Debris Build-Up on a Stacked-Disk Strainer.....	7-38

7-21	Point-by-Point Comparison of Correlation Predictions with PCI Head Loss Data	7-39
7-22	Dimensionless Representation of Stacked-Disk Strainer Effective Area as a Function of Debris Volume	7-40
7-23	Example of Long Term Head Loss for a NUKON™ Debris Bed	7-41
8-1	BWROG Prototype Module Test Program	8-3
8-2	Measured Head Loss as a Function of Strainer Debris Loading for Typical Advanced Passive Strainers.....	8-3
8-3	PCI Stacked-Disk Strainer Being Installed at Pilgrim Nuclear Power Plant.....	8-5
8-4	The Core Tube Used in the PCI Stacked-Disk Strainers	8-5

Tables

1-1	Important Parameters Tracked and Their Relevance	1-13
1-2	Debris Generation and Transport Parameters: LLOCA-Large Dry Containment.....	1-16
1-3	Debris Generation and Transport Parameters: LLOCA-Ice Condenser Containment.....	1-17
1-4	PWR LLOCA Sequences	1-18
1-5	Debris Generation and Transport Parameters: MLOCA-Large Dry Containment	1-22
1-6	Debris Generation and Transport Parameters: MLOCA-Ice Condenser Containment.....	1-23
1-7	Debris Generation and Transport Parameters: SLOCA-Large Dry Containment	1-26
1-8	Debris Generation and Transport Parameters: SLOCA-Ice Condenser Containment	1-27
1-9	Debris Generation and Transport Parameters: SLOCA-Sub-Atmospheric Containment	1-28
3-1	Damage Pressures for Insulation Materials Found in U.S. PWRs	3-4
3-2	Size Classification Scheme for Fibrous Debris	3-7
3-3	Typical Size Characteristics of RMI Debris	3-9
3-4	Measured Particle-Size Distribution from Newtherm 1000 (Calcium-Silicate) Erosion Tests.....	3-14
3-5	Test Matrix for the OPG Calcium-Silicate Jet Impact Tests	3-17
3-6	Size Distribution of Calcium-Silicate Debris in Tests Where Insulation Was Liberated	3-18
3-7	Size Distribution of Fiberglass Debris in Tests Where Insulation Was Liberated	3-20
4-1	Physical Processes and Phenomena Affecting Airborne/Washdown Debris Transport	4-4
4-2	Thermal-Hydraulic Airborne Processes and Phenomena	4-5
4-3	Airborne Debris-Transport Mechanisms.....	4-6
4-4	Thermal-Hydraulic Processes and Phenomena.....	4-7
4-5	Washdown Debris-Transport Mechanisms	4-7
4-6	Airborne/Washdown Debris Transport Testing	4-9
4-7	Small Fibrous Debris Capture Fractions	4-18
4-8	Airborne/Washdown Debris-Transport Analyses	4-28
4-9	Highly Ranked Phenomenon from BWR Drywell Transport PIRT Table	4-32
4-10	Processes and Phenomena Ranked as High.....	4-33
4-11	Highly Ranked Processes and Phenomena for the Containment Above the Sump Pool.....	4-34
4-12	Study Transport Fractions for Main-Steam-Line Breaks	4-40
4-13	Study Transport Fractions for Recirculation Line Breaks	4-40
4-14	Study Transport Fractions for All Insulation Located in ZOI.....	4-41
4-15	Debris Size Categories and Their Capture and Retention Properties	4-43
4-16	Fractions of Blanket Material with Low Transport Efficiency.....	4-45
4-17	URG Drywell Transport Fractions	4-46
4-18	URG Combined Debris-Generation and Transport Fractions for Mark I, III.....	4-47
4-19	Debris-Transport Fractions Estimates Used in Parametric Evaluation	4-50
5-1	Summary Data for Diffused Flow Entry Inlet Conditions	5-22
5-2	Water Chemical Conditions in KAEFER Insulation Buoyancy Tests	5-31
5-3	Flow Velocity Needed to Initiated Motion of NUKON Insulation Fragments	5-33
5-4	Highly Ranked Phenomena from BWR Drywell Floor Pool Debris Transport PIRT Table	5-35
5-5	Highly Ranked Processes and Phenomena for the Debris Transport in a PWR Containment Sump Pool.....	5-35
6-1	Minimum Screen Approach Velocity for Debris to "Flip Up" or be Hydraulically "Lifted" Onto a Sump Screen	6-13
7-1	Head Loss Test Data for Mixtures of Calcium-Silicate and Fiberglass Insulation Debris	7-6

7-2	Characteristic Parameters for RMI Debris Beds	7-32
7-3	Geometric Details of the Portion of the Strainer Tested in the LaSalle Test Program.....	7-35
8-1	Total Strainer Area and Vendor for Each BWR Plant Responding to NRCB 96-03.....	8-10
8-2	Issue Resolution Summary for Audited Plants	8-11
8-3	Fibre Penetration, 4-mm Perforated Plate.....	8-14
8-4	Fibre Penetration, 4-mm Perforated Plate.....	8-14
9-1	Events With LOCA Generated Insulation Debris	9-2
9-2	Events Rendering a System Inoperable.....	9-3
9-3	Events With Debris Found Inside Containment.....	9-6
9-4	Events of Inadequate Maintenance Potentially Leading to Sources of Debris	9-9
9-5	Events Where Inadequacies Found in Sump Screens.....	9-11

EXECUTIVE SUMMARY

In the event of a loss-of-coolant accident (LOCA) within the containment of a light-water reactor, piping thermal insulation and other materials in the vicinity of the break will be dislodged by the pipe break and steam/water-jet impingement. A fraction of this fragmented and dislodged insulation and other materials, such as paint chips, paint particulates, and concrete dust, will be transported to the containment floor by the steam/water flows induced by the break and by the containment sprays. Some of this debris eventually will be transported to and accumulated on the recirculation-sump suction screens in pressurized-water reactor (PWR) containments or on the pump-suction strainer in boiling-water reactor (BWR) containments. Debris accumulation on the sump screen or strainers could challenge the plant's capability to provide adequate, long-term cooling water to the emergency core cooling system (ECCS) and the containment spray system pumps.

As a result of the research on the BWR suction-strainer and PWR sump-screen clogging issues, a substantial base of knowledge has been amassed that covers all aspects of the issues from the generation of debris to the head loss associated with a debris bed on a strainer or screen. This report describes the different analytical and experimental approaches that have been used to assess the various aspects of sump and strainer blockage and identify the strengths, limitations, important parameters and plant features, and appropriateness of the different approaches. The report also discusses significant United States (U.S.) Nuclear Regulatory Commission (NRC) regulatory actions regarding resolution of this issue. In essence, the report is designed to serve as a reference for plant-specific analyses in regard to whether the sump or strainer would perform its function without preventing the operation of the ECCS pumps.

This report is intended primarily for analyzing PWR sump-screen clogging issues, largely because the BWR issue had been resolved at the time the report was written. Nevertheless, the report also will be valuable in the review of any additional analyses for BWR plants as well. A majority of the strainer blockage research to date was conducted specifically for the resolution of the BWR issue; however, most of this research is also directly applicable to the

resolution of the PWR issue. Therefore, both BWR and PWR research and analytical approaches are discussed, and the applicability of that research, i.e., BWR vs PWR, is stated.

The report provides background information (Section 1) regarding the PWR containment sump and the BWR suction-strainer debris clogging issues. This background information includes a brief historical overview of the resolution of the BWR issue with a lead into the PWR issue, a description of the safety concern relative to PWR reactors, the criteria for evaluating sump failure, descriptions of postulated accidents, descriptions of relevant plant features that influence accident progression, and a discussion of the regulatory considerations.

The purpose of a sump screen is to prevent debris that may damage or clog components downstream of the sump from entering the ECCS and reactor coolant system. Debris accumulation across a sump screen would create a pressure drop across that screen that potentially could cause insufficient flow to reach the pump inlet. The knowledge-base report is organized in the same manner that an evaluation of the potential of sump screen blockage would be performed. These steps are the identification of sources of potential debris (Section 2); the potential generation of insulation debris by the effluences from a postulated LOCA (Section 3); the potential transport of the LOCA-generated debris to the containment sump (Section 4); the potential transport of debris within the sump pool to the recirculation sump screen (Section 5); the potential accumulation of the debris on the sump screen, specifically the uniformity and composition of the bed of debris (Section 6); and the potential head loss associated with the accumulated debris (Section 7). The report also summarizes the resolution options available to BWR plant licensees to resolve the BWR suction-strainer clogging issue and the advanced features of the new replacement strainers that were implemented in the BWR plants so that the strainers can accumulate the potential debris loading without the associated debris-bed head loss (Section 8). Domestic and foreign plant events relevant to the PWR sump-screen clogging issue are discussed (Section 9). Finally, an overall summary of the knowledge base is provided in Section 10.

ACKNOWLEDGMENTS

The U.S. Nuclear Regulatory Commission (NRC) Office of Nuclear Regulatory Research (RES) sponsored the work reported here. Dr. B. P. Jain is the Technical Monitor for this task. He provided technical direction and actively participated in reviewing the report and provided valuable comments. The authors would also like to acknowledge R. E. Architzel and J. Lehning of the NRC, Dr. J. Hyvarinen of Radiation and Nuclear Safety Authority (STUK), Finland, and Dr. M. Maqua of Gesellschaft fuer Anlagen- und Reaktorsicherheit (GRS) mbH, Germany, for their timely technical review of the report and

Gordon Hart of Performance Contracting Inc. for the information he supplied regarding the aging of insulation during normal plant operations.

The authors would like to acknowledge the contributions of Mrs. N. Butner. Nancy was primarily responsible for producing this document, from developing the project plan through incorporating the review comments. Ms. M. Timmers, J. Lujan, and J. Snyder, LANL, spent numerous hours editing and generally fixing the document.

ABBREVIATIONS

ABB	ABB Atom/Combustion Engineering
AJIT	Air-Jet Impact Testing
ANS	American Nuclear Society
ANSI	American National Standards Institute
ARL	Alden Research Laboratory
BWR	Boiling-Water Reactor
BWROG	Boiling Water Reactor Owners' Group
CCW	Component Cooling Water
CDF	Core-Damage Frequency
CDI	Continuum Dynamics Inc.
CE	Combustion Engineering
CEESI	Colorado Engineering Experiment Station, Inc.
CFD	Computational Fluid Dynamics
CFR	Code of Federal Regulations
CS	Containment Spray
CSNI	Committee on the Safety of Nuclear Installations
CSS	Containment Spray System
DBA	Design-Basis Accident
DB-LOCA	Design-Basis Loss-of-Coolant Accident
DDTS	Drywell Debris Transport Study
DEGB	Double-Ended Guillotine Break
DPSC	Diamond Power Specialty Company
ECCS	Emergency Core Cooling System
EOP	Emergency Operating Procedures
EPRI	Electric Power Research Institute
ESF	Engineered Safeguard Feature
FME	Foreign Material Exclusion
FSAR	Final Safety Analysis Report
GDC	General Design Criteria
GE	General Electric Nuclear Energy
GGNS	Grand Gulf Nuclear Station
GL	Generic Letter
GSI	Generic Safety Issue
HDFG	High-Density Fiberglass
HDR	Heisdampfreaktor
HELB	High Energy Line Break
HEPA	High-Efficiency Particulate Air
HPSI	High-Pressure Safety Injection
IN	Information Notice
ITS	Innovative Technology Solutions, Inc.
IVO	Imatran Voima Oy
KKL	Kernkraftwerk, Liebstadt
KWU	Siemens AG Power Generation Group
LDFG	Low-Density Fiberglass
LOCA	Loss-of-Coolant Accident
LLOC	Large Loss-of-Coolant Accident
LPCI	Low-Pressure Coolant Injection
LPCS	Low-Pressure Core Spray
LPSI	Low-Pressure Safety Injection
LTP	Licensing Topical Report
LWR	Light-Water Reactor
MIJIT	Metallic Insulation Jet Impact Testing Facility
MLOCA	Medium Loss-of-Coolant Accident

MSL	Main Steam Line
MSLB	Main-Steam-Line Break
NDE	Non Destructive Evaluation
NEA	Nuclear Energy Agency
NEI	Nuclear Energy Institute
NPSH	Net Positive Suction Head
NRC	Nuclear Regulatory Commission
NRCB	NRC Bulletin
OECD	Organization for Economic Cooperation and Development
OPG	Ontario Power Generating
PCI	Performance Contracting Inc.
PIRT	Phenomena Identification and Ranking Table
PORV	Power-Operated Relief Valve
PVC	Polyvinyl Chloride
PWR	Pressurized-Water Reactor
RCP	Reactor Coolant Pump
RCS	Reactor Coolant System
RG	Regulatory Guide
RHR	Residual Heat Removal
RL	Recirculation Line
RLB	Recirculation-Line Break
RMI	Reflective Metal Insulation
RWST	Refueling Water Storage Tank
SAT	Spray Additive Tank
SEA	Science and Engineering Associates, Inc.
SER	Safety Evaluation Report
SI	Safety Injection
SKI	Statens Kärnkraftenspektion
SLOCA	Small Loss-of-Coolant Accident
SRP	Standard Review Plan
SRV	Safety Relief Valve
SSC	System, Structure, and Component
STUK	Finnish Centre for Radiation and Nuclear Safety
TPI	Transco Products, Inc.
TVO	Teollisuuden Voima Oy
UNM	University of New Mexico
URG	Utility Resolution Guidance
US	United States
USI	Unreviewed Safety Issue
ZOI	Zone of Influence

UNITS CONVERSION TABLE

Convert From	Convert To	Multiply By
Length		
in.	m	0.02540
mil*	m	2.540E-5
ft	m	0.3048
Area		
in. ²	m ²	6.452E-4
ft ²	m ²	0.09290
Volume		
ft ³	m ³	0.02832
gal.	m ³	0.003785
gpm	m ³ /s	6.308E-5
Pressure		
psi	Pa	6895
Mass		
lbm**	kg	0.4536
Density		
lbm/ft ³	kg/m ³	16.02
Velocity		
ft/s	m/s	0.3048
Temperature		
°F***	°C	0.5556

* mil = one-thousandth of an inch

** lbm is often simply given as lb

*** Subtract 32 before multiplying

1.0 INTRODUCTION

In the event of a loss-of-coolant accident (LOCA)¹ within the containment of a light-water reactor (LWR), piping thermal insulation and other materials in the vicinity of the break will be dislodged by the pipe break and the ensuing steam/water-jet impingement. A fraction of this fragmented and dislodged insulation and other materials, such as chips of paint, paint particulates, and concrete dust, will be transported to the containment floor by the steam/water flows induced by the break and by the containment sprays. Some of this debris will eventually be transported to and accumulate on the recirculation-sump suction screens in pressurized water reactor (PWR) containments or a pump suction strainer in boiling water reactor (BWR) containments. Debris accumulation on the sump screen or strainers could challenge the plant's capability to provide adequate, long-term cooling water to the emergency core cooling system (ECCS) and to the containment spray system (CSS) pumps.

As a result of the research on the BWR suction-strainer and PWR sump-screen clogging issues, a substantial base of knowledge has been amassed that covers all aspects of the issues, from the generation of debris to the head loss associated with a debris bed on a strainer or screen. This report describes the different analytical and experimental approaches that have been used to assess the various aspects of sump and strainer blockage and identifies the strengths, limitations, important parameters, and plant features and the appropriateness of the different approaches. The report also discusses significant U.S. Nuclear Regulatory Commission (NRC) regulatory actions regarding resolution of the issue. In essence, the report is designed to serve as a reference for plant-specific analyses with regard to whether the sump or strainer would perform its function without preventing the operation of the ECCS pumps.

This report is intended for use in resolving the PWR issue because the BWR issue had been resolved. Nevertheless, the report will serve the review of any additional analyses for BWR

plants, as well. A majority of the strainer blockage research to date was conducted specifically for the resolution of the BWR issue; however, most of this research is also directly applicable to the resolution of the PWR issue. Therefore, both BWR and PWR research and analytical approaches are discussed, and the applicability of that research, i.e., BWR vs PWR, is stated.

The following background information is presented as preparation to understanding the discussions of the current state of knowledge in the succeeding sections.

- A brief historical overview of the resolution of the BWR issue with a lead into the PWR issue
- A description of the safety concerns relative to PWR reactors
- Criteria for evaluating sump failure
- Descriptions of postulated PWR accidents
- Relevant plant features that influence accident progression
- The regulatory considerations

1.1 Historical Overview

In January 1979, the NRC originally declared sump-screen blockage to be an Unresolved Safety Issue, USI A-43,¹⁻¹ titled "Containment Emergency Sump Performance" and published the concerns identified in the USI in NUREG-0510, "Identification of Unresolved Safety Issues Relating to Nuclear Power Plants."¹⁻² USI A-43 dealt with concerns regarding the availability of adequate long-term recirculation cooling water following a LOCA. This cooling water must be sufficiently free of debris so that pump performance is not impaired and long-term recirculation flow capability is not degraded.

Although USI A-43 was derived principally from concerns regarding PWR containment emergency sump performance, these concerns applied to BWR ECCS suction, as well. The BWR residual heat removal (RHR) system performs the low-pressure coolant injection (LPCI) function of the ECCS and the safety-related CSS. In addition, BWR designs incorporate a low-pressure core spray (LPCS) system as part of the ECCS. The suction

¹ The focus of this safety issue is on LOCAs, but the issue may also apply to other high-energy line breaks (HELBs) within the design basis that would require long-term recirculation cooling.

strainers located in the BWR suppression pool are analogous to the PWR sump debris screen.

Substantial experimental and analytical research was conducted to support the resolution of USI A-43. In 1985, the regulatory analysis results and the technical findings of research related to resolving USI A-43 were reported in NUREG-0869¹⁻³ and NUREG-0897,¹⁻⁴ respectively. The bases for these findings were documented in a series of NRC contractor reports, which are listed in the NUREG-0897 reference section.¹⁻⁴ In NUREG-0897,¹⁻⁴ the NRC concluded the following.

- The formation of an air-core vortex that would result in unacceptable levels of air ingestion that potentially could severely degrade pump performance was a concern. This concern was more applicable to PWRs but was still relevant to BWRs. Hydraulic tests showed that the potential for air ingestion was less severe than previously hypothesized. In addition, under normal flow conditions and in the absence of cavitation effects, pump performance is only slightly degraded when air ingestion is less than 2%.
- The effects of LOCA-generated insulation debris on RHR recirculation requirements depend on:
 1. the types and quantities of insulation,
 2. the potential of a high-pressure break to severely damage large quantities of insulation,
 3. the transport of debris to the sump screen or strainer,
 4. the blockage potential of the transported debris, and
 5. the impact on available net positive suction head (NPSH).
- The effects of debris blockage on the NPSH margin must be dealt with on a plant-specific basis. Insulation debris transport tests showed that severely damaged or fragmented insulation readily transported at relatively low velocities (0.2 to 0.5 ft/s). Therefore, the level of damage near the postulated break location became a dominant consideration. The level of damage to insulation was correlated with distance between the insulation and the break, in terms of L/Ds (distance divided by the pipe-break diameter). Data showed that jet load pressures would inflict severe damage to insulation within 3 L/Ds, and

substantial damage in the 3- to 5-L/D range with damage occurring out to about 7 L/D.

- The types and quantities of debris small enough to pass through screens or suction strainers and reach the pump impeller should not impair long-term hydraulic performance. In pumps with mechanical shaft seals, debris could cause clogging or excessive wear, leading to increased seal leakage. However, catastrophic failure of a shaft seal as a result of debris ingestion was considered unlikely. If the seal did fail, pump leakage would be restricted.
- Nineteen nuclear power plants were surveyed in 1982 to identify the insulation types used, the quantities and distribution of insulation, the methods of attachment, the components and piping insulated, the variability of plant layouts, and the sump designs and locations. The types of insulation found were categorized into two major groups: reflective metallic insulation (RMI) and fibrous insulations. The RMI was manufactured by at least four different manufacturers. The fibrous insulation included NUKON™ fiberglass blankets, fiberglass molded blocks, mineral wool fiber blocks, calcium-silicate molded blocks, and expanded perlite-molded blocks. Insulations sometimes were enclosed in an outer shell or jacket or cloth cover.

USI A-43 was declared resolved in 1985. The NRC resolution of USI A-43 was presented to the Commission in October 1985.¹⁻⁵ The resolution consisted of:

1. publishing NUREG-0897¹⁻⁴ as a summary of the key technical findings for use as an information source by applicants, licensees, and the staff;
2. revising the Standard Review Plan (SRP), Section 6.2.2,¹⁻⁶ and Regulatory Guide (RG) 1.82,¹⁻⁷ "Water Sources for Long-Term Recirculation Cooling Following a Loss-of-Coolant Accident," to reflect the staff's technical findings; and
3. issuing Generic Letter (GL) 85-22,¹⁻³³ "Potential for Loss of Post-LOCA Recirculation Capability Due to Insulation Debris Blockage," to all holders of an operating license or construction permit outlining safety concerns and recommending the use of Regulatory Guide (RG) 1.82, Revision 1¹⁻⁷ as guidance for

conducting 10 Code of Federal Regulations (CFR) 50.59 analyses.¹⁻⁸

In addition, a regulatory analysis was performed (see NUREG-0869¹⁻³) to serve as a basis for the final resolution of USI A-43.

The regulatory analysis did not support a generic backfit action because plant-specific design features and post-LOCA recirculation flow requirements govern debris blockage effects. As a result, the analysis conclusion was that the issue must be resolved on a plant-specific basis. The staff recommended that RG 1.82, Revision 1,¹⁻⁷ be used as guidance for the evaluation (10 CFR 50.59)¹⁻⁸ of plant modifications involving replacement and/or modification of thermal insulation installed on the primary coolant system piping and components. The 50% blockage criterion of Revision 0 of RG 1.82¹⁻⁷ was considered inadequate to address this issue.

After the closure of USI A-43,¹⁻¹ several ECCS strainer and foreign material discovery events prompted a review of the strainer blockage issue for BWRs. (These events are described in more detail in Section 9.) Perhaps the most notable of these events occurred on July 28, 1992, during the startup of Barsebäck, Unit 2, in Sweden. This is discussed in NRC Information Notice (IN) 92-71, "Partial Blockage of Suppression Pool Strainers at a Foreign BWR," September 30, 1992.¹⁻⁹ In this event, a spurious opening of a safety valve while the reactor was pressurized discharged steam into the drywell, dislodging mineral wool insulation that subsequently transported to the suppression pool, resulting in suction-strainer blockage and pump cavitation. The Barsebäck-2 event demonstrated that larger quantities of fibrous debris could reach the strainers than had been predicted by models and analysis methods developed for the resolution of USI A-43.¹⁻¹

ECCS suction-strainer clogging events also occurred at U.S. plants. These included the following.

- Two events (1992 and 1993) occurred at the Mark III Perry Nuclear Power Plant.¹⁻¹⁰ Debris was found on the suppression pool floor and on the RHR suction strainers during a refueling outage inspection. In addition, the buildup of debris on the strainer caused an excessive differential pressure,

which deformed the strainers. After the damaged strainers were replaced and the suppression pool was cleaned, the strainers were again found to be fouled by debris such that the pump suction pressure dropped to 0 during a test. The debris consisted of glass fibers, corrosion products, and other materials. Fibrous material acted as a filter for suspended particles—a phenomenon not previously recognized by either the NRC or industry.

- An event occurred at Limerick Generating Station Unit 1 in 1995¹⁻¹¹ in which a safety relief valve (SRV) opened while Unit 1 was at 100% power. Subsequently, a thin mat of fibrous material and sludge covering the RHR pump suction strainers in the suppression pool caused fluctuating motor current and flow, indicating pump cavitation was occurring. Limerick subsequently removed about 635 kg of debris from the pool.
- In 1988 and 1989, the Grand Gulf Nuclear Station experienced strainer blockage events during testing of the RHR pumps. Pump suction pressures fell below the in-service inspection acceptance criteria.¹⁻¹⁰
- In 1994, divers discovered numerous pieces of cloth-like material on the bottom of the torus and on the ECCS strainers at Browns Ferry Nuclear Plant Unit 2.¹⁻¹² This debris had partially blocked the strainers.

Substantial quantities of debris were discovered in suppression pools on other occasions. In other cases, plant inspections have found deteriorated insulation that would render these materials more likely to form debris following a LOCA. In other plant inspections, previously unidentified unqualified coatings that could form debris following a LOCA have been found.

All of these events occurred despite existing NRC regulations and regulatory guidance. Foreign materials, degraded coatings inside the containment that detach from their substrate, ECCS components not consistent with their design basis, and LOCA-generated debris are potential common-cause failure mechanisms for the ECCS and containment spray system (CSS). Debris may clog suction strainers, sump screens, filters, nozzles, and small-clearance flow paths in the ECCS and safety-related CSS and interfere with the long-term cooling function, source-term reduction and/or pressure-reduction capabilities of the plant. The NRC has

consistently emphasized the need to minimize the presence of foreign material in the containment [e.g., a strong foreign material exclusion (FME) program].

The string of operational events described above demonstrated that

- larger quantities of debris could reach the ECCS strainers than had been predicted by models and analysis methods developed during the resolution of USI A-43;¹⁻¹
- fibrous material acts as a filter for suspended particles, a phenomenon not previously recognized by the NRC or industry;
- head loss correlations developed during the resolution of USI A-43¹⁻¹ under-predicted strainer head losses for combined fiber/particulate debris beds; and
- Extensive quantities of foreign materials were being found in suppression pools despite ongoing FME programs.

The ECCS strainer and foreign material discovery events prompted a review of the strainer blockage issue; hence, the NRC sponsored research to estimate possible shortcomings of existing suction strainer designs in U.S. BWR plants and to evaluate the actions taken by the nuclear power industry to ensure the availability of long-term recirculation of cooling water in BWR plants.

Concerns generated by these strainer-blockage events prompted the NRC to issue Bulletin 93-02,¹⁻¹³ "Debris Plugging of Emergency Core Cooling Suction Strainers," on May 11, 1993, to both BWR and PWR licensees. Licensees were requested to:

- identify fibrous air filters and other temporary sources of fibrous material in the primary containment not designed to withstand a LOCA,
- take prompt action to remove the identified material, and
- take any other immediate compensatory measures necessary to ensure the functional capability of the ECCS.

The NRC sponsored research to evaluate the adequacy of existing suction strainer designs in U.S. BWR plants by initiating a detailed plant-specific study in September 1993 using a

reference BWR/4 reactor with a Mark I containment. The results were published in NUREG/CR-6224¹⁻¹⁴ in 1995. This plant-specific analysis developed analytical models applicable to the reference BWR that considered debris generation, drywell debris transport, suppression-pool debris transport, and strainer blockage. The NUREG/CR-6224 study identified a lack of critical data needed to complete the study.¹⁻¹⁴ As a result, the NRC sponsored a series of small-scale experiments designed to gain insights into the behavior of debris in the suppression pool and acquire mixed debris bed head loss data. A computer program called BLOCKAGE was developed to calculate debris generation, debris transport, fiber/particulate debris bed head losses and the effect of the debris on the available ECC NPSH.^{1-15,1-16} Probabilistic analyses were performed that focused on evaluating the likelihood of ECCS strainer blockage and blockage-related core damage from large loss of coolant accident (LLOCA) initiators. The final results of the reference plant study, which is documented in NUREG/CR-6224,¹⁻¹⁴ demonstrated that for the reference plant, there was a high probability that the available NPSH margin for the ECCS pumps would be inadequate if insulation and other debris caused by a LOCA transported to the suction strainers. In addition, the study calculated that the loss of NPSH could occur quickly (less than 10 min into the event). The study also concluded that determining the adequacy of the NPSH margin for a given ECCS system is highly plant-specific because of the large variations in such plant characteristics as containment type, ECCS flow rates, insulation types, plant layout, plant cleanliness, and available NPSH margin.

The NRC also exchanged information and experience with the international community. The Swedish nuclear power inspectorate, Statens Kärnkraftinspektion (SKI), hosted a workshop to study the strainer blockage issue in 1994. The workshop revealed a confusing picture of the available knowledge base, including examples of conflicting information and a variety of interpretations of the regulatory guidance in the NRC's RG 1.82, Rev. 1.¹⁻⁷ Following this workshop, SKI requested the formation of an international working group to establish an internationally agreed-upon knowledge base for assessing the reliability of emergency core cooling water recirculation systems. The NRC compiled a source book of

available knowledge for the CSNI of the Organization for Economic Cooperation and Development (OECD) Nuclear Energy Agency.¹⁻¹⁷

Based on the NRC's preliminary research and information learned at the OECD/Nuclear Energy Agency (NEA) workshop, the NRC issued Supplement 1 to Bulletin 93-02 on February 18, 1994, requesting BWR licensees to take further interim actions pending final resolution.¹⁻¹³ These actions involved implementing operating procedures and conducting training and briefings designed to enhance the capability to prevent or mitigate loss of ECCS following a LOCA as a result of strainer clogging. The purpose of these interim actions was to ensure the reliability of the ECCS so that the staff and industry would have sufficient time to develop a permanent resolution.

To provide time to conduct research to resolve the strainer clogging issue, the NRC first ensured that public health and safety were protected adequately. In responding to NRC Bulletin 93-02¹⁻¹³ and its supplement, BWR licensees implemented interim measures to ensure adequate protection of public health and safety. Specifically, licensees ensured that:

1. alternate water sources (both safety- and non-safety-related sources) to mitigate a strainer clogging event were available,
2. emergency operating procedures (EOPs) provided adequate guidance on mitigating a strainer-clogging event,
3. operators were trained adequately to mitigate a strainer-clogging event, and
4. loose and temporary fibrous materials stored in the containment were removed.

The responses to NRC Bulletin 93-02¹⁻¹³ showed that most suppression pools had already been cleaned recently and that those licensees who had not cleaned their suppression pools recently were scheduled to do so during their next refueling outage. In addition, a generic safety assessment conducted by the Boiling Water Reactor Owners' Group (BWROG) concluded that operators would have adequate time to make use of alternate water sources (25–35 min) if needed during a LOCA and that the probability of the initiating event is low. For these reasons, the NRC allowed continued operation by BWR licensees until the final

resolution to the strainer clogging issue was developed and implemented. The NRC initiated the final resolution to the strainer issue with the issuance of NRC Bulletin 96-03.¹⁻¹⁸ Satisfactory implementation of the requested actions in NRC Bulletin 96-03 ensured that the ECCS can perform its safety function and minimize the need for operator action to mitigate a LOCA.

The NRC issued RG 1.82, Revision 2, in May 1996.¹⁻⁷ This regulatory guide describes acceptable methods for implementing applicable design requirements for sumps and suppression pools functioning as water sources for emergency core cooling, containment heat removal, or containment atmosphere cleanup. In addition, guidelines for evaluating the adequacy of the sump and suppression pool for long-term recirculation cooling following a LOCA are provided. This regulatory guide was revised to update the BWR debris-blockage evaluation guidance because operational events, analyses, and research work that have occurred since the issuance of Revision 1 indicated that the previous guidance was not comprehensive enough to evaluate a BWR plant's susceptibility to the detrimental effects caused by suction-strainer debris blockage adequately.

An essential aspect of predicting the potential for strainer clogging is estimating the amount of debris that is likely to transport from the drywell into the wetwell. The transport processes are complex in that they involve transport during both the reactor blowdown phase (i.e., entrainment in steam/gas flows) and the post-blowdown phase (i.e., via water flowing out of the break and/or containment sprays). In Revision 2 of RG 1.82,¹⁻⁷ the NRC recommended assuming 100% debris transport unless analyses or experiments justified lower transport fractions. To facilitate a better understanding of debris transport, the NRC initiated a study in September 1996, referred to as the drywell debris transport study (DDTS), to investigate debris transport in BWR drywells using a bounding analysis approach. The focus of the DDTS was to provide a description of the important phenomena and plant features that control and/or dominate debris transport and the relative importance of each phenomenon as a function of the debris size. The results of the DDTS, which are documented in NUREG/CR-6369,¹⁻¹⁹ provide reasonable engineering insights that can be used to evaluate the

adequacy of the debris-transport factors used in plant-specific strainer-blockage analyses.

The NRC staff issued NRC Bulletin 96-03,¹⁻¹⁸ "Potential Plugging of Emergency Core Cooling Suction Strainers by Debris in Boiling-Water Reactors," on May 6, 1996. All BWR licensees were requested to implement appropriate measures to ensure the capability of the ECCS to perform its safety function following a LOCA. The staff had identified three potential resolution options but allowed licensees to propose others that provided an equivalent level of assurance. The three options identified by the staff were to install:

1. a large-capacity passive strainer designed with sufficient capacity to ensure that debris loadings equivalent to a scenario calculated in accordance with Section C.2.2 of RG 1.82, Revision 2¹⁻⁷ do not cause a loss of NPSH for the ECCS;
2. a self-cleaning strainer that automatically prevents strainer clogging by providing continuous cleaning of the strainer surface with a scraper blade or brush; and
3. a backflush system that relies on operator action to remove debris from the surface of the strainer to prevent it from clogging.

All licensees were requested to implement these actions by the end of the first refueling outage starting after January 1, 1997.

The staff closely followed the BWROG's efforts to resolve this issue. The BWROG evaluated several potential solutions, and completed testing on three new strainer designs: two passive designs and one self-cleaning design. The BWROG effort was consistent with the options proposed in NRCB 96-03¹⁻¹⁸ for resolution of the potential ECCS strainer clogging issue. The BWROG then developed topical report NEDO-32686,¹⁻²⁰ "Utility Resolution Guidance for ECCS Suction Strainer Blockage," November 1996 [the Utility Resolution Guidance (URG)], to provide utilities with:

1. guidance on evaluation of the potential ECCS strainer clogging issue for their plant;
2. a technically sound, standard industry approach to resolution of the issue; and
3. guidance that is consistent with the requested actions in NRCB 96-03¹⁻¹⁸ for

demonstrating compliance with 10 CFR 50.46.¹⁻⁸

The URG includes guidance on calculational methodologies for performing plant-specific evaluations. The BWROG and the industry conducted several small-scale tests to obtain the data needed to develop the URG and to qualify plant-specific strainer designs. The URG included substantial portions of these data.

The NRC reviewed the URG and issued its Safety Evaluation Report (SER) on August 20, 1998.¹⁻²¹ In the SER, the staff noted that the issue of potential strainer blockage is complex in that head loss across suction strainers is not only a function of the amount of debris but also of the types of debris (e.g., fibrous insulation, paint, reflective metallic insulation, dirt, corrosion products, etc.) and characteristics of the debris (size, shape, etc.). The analyst must evaluate the worst case for potential strainer debris loadings; consider the potential for foreign material to be introduced during normal plant evolutions such as refueling and maintenance outages; and evaluate maintenance practices, including the maintenance of qualified coatings in the drywell and wetwell.

The staff found the URG to be comprehensive, providing general guidance on resolution options and detailed guidance on performing plant specific analyses to estimate potential worst-case debris loadings on ECCS suction strainers during a LOCA. However, the URG lacked complete guidance and/or adequate supporting analysis in several areas. Because insufficient detail and supporting justification on the "resolution options," were included in the URG, further supporting justification from a licensee or the BWROG was required for the staff to reach a conclusion on their acceptability.

The NRC staff issued GL 97-04, "Assurance of Sufficient Net Positive Suction Head for Emergency Core Cooling and Containment Heat Removal Pumps," to all holders of operating licenses for nuclear power plants on October 7, 1997.¹⁻²² The staff wanted to ensure that the NPSH available for ECCS and containment heat-removal pumps would be adequate under all design-basis accident (DBA) scenarios. The staff was concerned that changes to plant configuration, operating procedures, environmental conditions, or other operating parameters over the life of the plant could result

in inadequate NPSH. Some licensees discovered that they needed to have their licensing basis include credit for containment overpressure to meet the NPSH requirements of the ECCS and containment heat-removal pumps. Some licensees were assuming containment overpressure credit inconsistent with the plant's licensing basis. GL 97-04 requested addressees to provide current information regarding their NPSH analyses.

The staff evaluated its position on the use of containment overpressure in calculating NPSH margin as part of its review of industry responses to GL 97-04.¹⁻²² The concerns that led to the issuance of GL 97-04 illustrated an existing uncertainty and variability in the application of the methods used to calculate the NPSH margin. These concerns were confirmed by the review of the industry submittals.¹⁻²³ Crediting containment overpressure in the NPSH margin requires supporting analyses. "Overpressure analyses" are detailed and comprehensive analyses performed to conservatively predict the minimum containment pressure available during a DBA. All means of removing heat from the containment are considered, including all installed pressure-reducing systems and processes. These systems and processes include heat transfer to structures, containment leakage, containment sprays, pool-surface heat and mass transfer, fan coolers, RHR heat exchangers, and power conversion systems. Because the NPSH is strongly dependent on the accident scenario, a comprehensive range of accident scenarios is evaluated to ensure that the minimum pressure is determined conservatively for the purpose of granting an overpressure credit. Because there is substantial uncertainty associated with the strainer clogging issue, the staff did not recommend licensing basis changes as a "resolution option."

The NRC issued GL 98-04,¹⁻²⁴ "Potential for Degradation of the Emergency Core Cooling System and the Containment Spray System After Loss-of-Coolant Accident Because of Construction and Protective Coating Deficiencies and Foreign Material in Containment," on July 14, 1998, to all holders of operating licenses for operating nuclear power reactors. GL 98-04¹⁻²⁴ alerted addressees of additional strainer-blockage concerns, including problems associated with:

1. the material condition of Service Level 1 protective coatings inside the containment,
2. foreign material found inside operating nuclear power plant containments, and
3. design and construction deficiencies with the material condition of ECCS systems, structures, and components inside the containment.

The NRC expected addressees to ensure that the ECCS and the safety-related CSS remain capable of performing their intended safety functions.

The industry addressed the requirements of NRC Bulletin 96-03¹⁻¹⁸ by installing large capacity passive strainers in each plant (NRCB 96-03 Option 1) with sufficient capacity to ensure that debris loadings equivalent to a scenario calculated in accordance with Section C.2.2 of RG 1.82, Revision 2,¹⁻⁷ do not cause a loss of NPSH for the ECCS. Four BWR plants were chosen for detailed audits by the NRC staff: Limerick (BWR/4 Mark II), Dresden (BWR/3 Mark I), Duane Arnold (BWR/4 Mark I), and Grand Gulf (BWR/6 Mark III).

The research and regulatory developments associated with the resolution of the strainer-blockage issue for the U.S. BWR plants were summarized in Los Alamos National Laboratory report LA-UR-01-1595.¹⁻²⁵ This report contains a more thorough history of events and developments than was just presented in this introduction. The report also includes brief summaries of the various experiments and analyses conducted to support the issue resolution.

As a result of research findings related to resolving the BWR ECCS strainer blockage safety issue, the NRC conducted further research into the PWR sump-screen blockage issue to determine if further action was needed beyond the original resolution of USI A-43.¹⁻¹ The Generic Safety Issue (GSI)-191, "PWR Sump Blockage," study was established to determine if the transport and accumulation of debris in a containment following a LOCA would impede the operation of the ECCS in operating PWRs.

A parametric evaluation¹⁻²⁶ was performed as part of the GSI-191 study to demonstrate the credibility of recirculation-sump clogging for operating PWRs. Each of the 69 domestic

PWRs was modeled in the evaluation using a mixture of generic and plant-specific data. The minimum amount of debris accumulation on the sump screen needed to exceed the required NPSH margin for the ECCS and CSS pumps was determined for each of the 69 representative models. Further, both completed and ongoing GSI-191 PWR research, as well as existing BWR research, were used to support the development of these models and the input to these models.¹⁻²⁶⁻¹⁻²⁹ The evaluation considered small, medium, and large LOCAs using both favorable and unfavorable assumptions, relative to the plant, to a number of parameters. The results of the parametric evaluation formed a credible technical basis for making the determination that sump blockage was a credible concern.

A risk study that supported the parametric evaluation¹⁻³⁰ was performed to estimate the amount by which the core damage frequency (CDF) would increase if failure of PWR ECCS recirculation cooling resulting from debris accumulation on the sump screen were accounted for in a manner that reflects the results of recent experimental and analytical work. Further, the estimate was made in a manner that reflected the total population of U.S. PWR plants. Results suggest that the conditional probability of recirculation sump failure, given a demand for recirculation cooling, is sufficiently high at many U.S. plants to cause an increase in the total CDF of an order of magnitude or more.

However, the parametric evaluation had a number of limitations; the most notable were attributed to the extremely limited plant-specific data available to the study. The need for more accurate plant-specific assessments of the adequacy of the recirculation function of the ECCS and CSS to be performed for each operating PWR was indicated clearly. The Nuclear Energy Institute (NEI) also recognized this need and has since initiated a program to develop evaluation guidance for the industry, a program being closely monitored by the NRC.

1.2 Description of Safety Concern

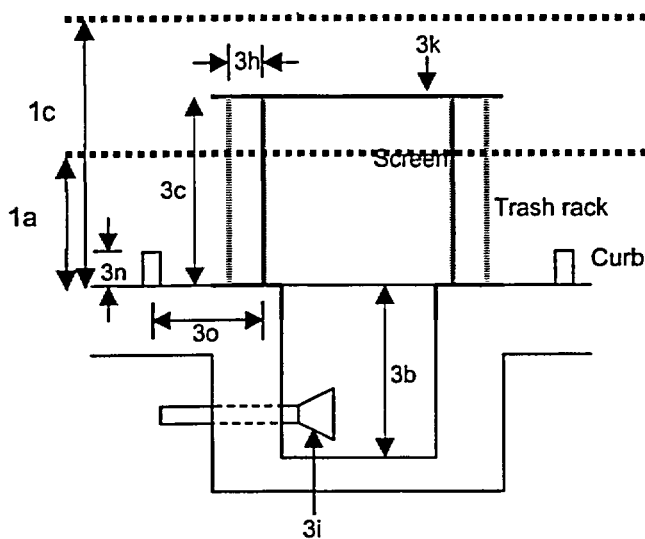
In the event of a LOCA within the containment of a PWR, piping thermal insulation and other materials in the vicinity of the break will be dislodged by break-jet impingement. A fraction of this fragmented and dislodged insulation and

other materials such as paint chips, paint particulates, and concrete dust will be transported to the containment floor by the steam/water flows induced by the break and the containment sprays. Some of this debris eventually will be transported to and accumulated on the recirculation sump suction screens. Debris accumulation on the sump screen may challenge the sump's capability to provide adequate, long-term cooling water to the ECCS and the containment spray (CS) pumps.

Generally speaking, the sump is the space enclosed by the trash rack; the space enclosed by the sump screen is referred to as the sump pit or sump region. Figure 1-1 illustrates the general features of a PWR sump layout generically; the parameters indicated were those queried of the industry during a survey conducted as part of the GSI-191 study.¹⁻²⁶ Actual sump designs vary significantly from this figure, but all share similar geometric features. The purpose of the trash rack and sump screen is to prevent debris that may damage or clog components downstream of the sump from entering the ECCS and reactor coolant system (RCS). The area outside of the sump is referred to as the containment floor or pool.

An examination of plant drawings, preliminary analyses, and ongoing tests suggests that a prominent mechanism for recirculation sump failure involves pressure drop across the sump screen induced by debris accumulation. However, sump-screen failure through other mechanisms is also possible for some configurations. Three failure mechanisms were considered as part of the GSI-191 study.

1. Loss of NPSH margin caused by excess pressure drop across the screen resulting from debris buildup. This concern applies to all plant units having sump screens that are completely submerged in the containment pool in combination with other plant features that permit generation and accumulation of debris on the sump screen.
2. Loss of the static head necessary to drive recirculation flow through a screen because of excess pressure drop across the screen resulting from debris buildup. This concern applies to all plant units having sump screens that are not completely submerged in combination with other plant features that permit generation and accumulation of debris on the sump screen.



Symbol	Description
3b	Sump depth
3c	Height above floor
3h	Distance between trash rack and screen
3i	Vortex suppressor
3k	Solid plate
3n	Debris curb height
3o	Distance between debris curb and screen
1a	Height of water pool on containment floor at time of switchover
1c	Max. Height of water pool on containment floor

Figure 1-1 Illustration of Sump Features and Parameters

- Blockage of water-flow paths could (a) cause buildup (and retention) of water in some regions of the containment and result in lower water levels near the sump and thus a lower NPSH margin than estimated by the licensees, or (b) altogether prevent adequate water flow through these openings.

Realistically, an analysis of the likelihood of any of the above three recirculation-flow failure mechanisms required plant-specific data that only the licensee has in sufficient quantity to perform a definitive analysis. The parametric evaluation discussed in the preceding section²⁶ attempted to evaluate the likelihood, but those results were not definitive. Rather, the objective of that study, which was conducted using a mixture of generic and plant-specific data, was simply to demonstrate the credibility of recirculation-sump clogging for operating PWRs. For each of the 69 representative models, the minimum amount of debris accumulation on the sump screen needed to exceed the required NPSH margin for the ECCS and CSS pumps was determined and then compared with the potential for generating debris within the containment. The sump-clogging credibility was demonstrated effectively.

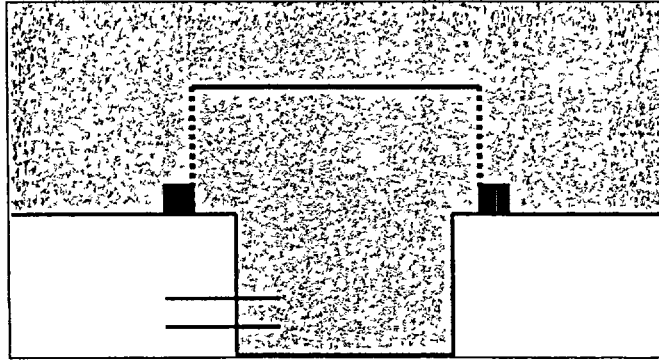
Other concerns related to debris generated during postulated accidents include:

- the potential for debris to pass through the sump screen, enter the RCS, and damage or block ECCS or RCS components and
- structural failure of the sump screens as a result of loads from debris or direct jet impingement.

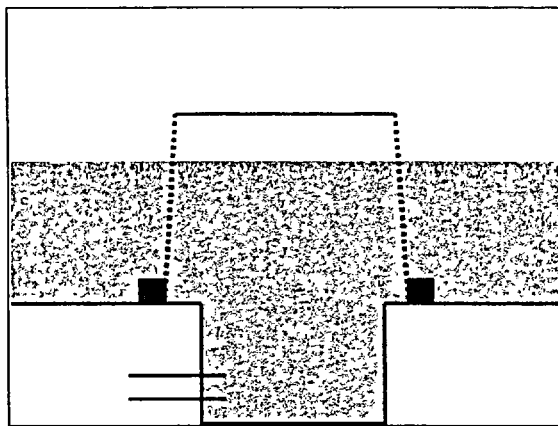
These concerns were considered beyond the scope of the GSI-191 study and the parametric evaluation.

1.3 Criteria for Evaluating Sump Failure

The sump-failure criterion applicable to each plant is determined primarily by sump submergence. Figure 1-2 illustrates the two basic sump configurations of fully and partially submerged screens. Although only vertical sump configurations are shown here, the same designations are applicable for inclined-screen designs. The key distinction between the fully and partially submerged configurations is that partially submerged screens allow equal pressure above both the pit and the pool, which are potentially separated by a debris bed. Fully submerged screens have a complete seal of water between the pump inlet and the containment atmosphere along all water paths passing through the sump screen. The effect of this difference in evaluation of the sump-failure criterion is described below.



(a) Fully submerged screen configuration showing solid water from pump inlet to containment atmosphere



(b) Partially submerged screen configuration showing containment atmosphere over both the external pool and the internal sump pit with water on lower portion of screen

Figure 1-2 Sump-Screen Schematics

1.3.1 Fully Submerged Sump Screens

Figure 1-2(a) is a schematic of a sump screen that is fully submerged at the time of switchover to ECCS from the injection phase to the recirculation phase. The most likely mode of failure for sumps in this configuration would be cavitation within the pump housing if the head loss caused by debris accumulation exceeds the NPSH margin. The NPSH margin is the excess in the available NPSH over that required by the pump per the manufacturer's specifications. The excess or margin is determined with the sump screens clean, i.e., no debris. The available NPSH is a function of the water level in the containment sump, the temperature of the sump water, the containment pressure, and the piping friction losses between sump and pump inlet. Because the NPSH margin is higher at the

maximum sump pool level than at the switchover pool level, the evaluation of sump blockage must consider the margin at the time of switchover. The accumulation of debris on the screen also would be transient; however, accurately determining the timing of debris accumulation on the screens would be a very difficult analysis. Conservatively, the head loss associated with the maximum accumulation of debris usually is compared with the minimum NPSH margin, which usually would occur at the time of switchover rather than the time of maximum debris loading.

1.3.2 Partially Submerged Sump Screens

Figure 1-2(b) is a schematic of a sump that is partially submerged at the time of switchover. Failure can occur for sumps in this configuration

in one of two ways: by pump cavitation as explained above or when head loss caused by debris buildup prevents sufficient water from entering the sump. As debris accumulates on the screen and causes a drop in pressure across it, the water level behind the screen would drop somewhat lower than the water level in front of the screen. In other words, this additional hydrostatic head resulting from the differing water levels compensates for the added head loss of the debris to maintain the volumetric demands of the pump, which remains relatively constant. Because the pit and the pool are at equal atmospheric overpressure, the only force available to move water through a debris bed is the static pressure head in the pool. After the pool level behind the screen drops to the bottom of the screen, the maximum hydrostatic pressure head will have been reached and the subsequent volumetric flow will decrease below the required pump flow, causing pump cavitation.

The effective maximum hydrostatic head loss actually would be less than the difference between the sump-pool level and the bottom of the sump screen. The pressure differential across the debris bed on the screen increases from 0 at the top of the debris bed to the maximum head at the bottom of the screen. Numeric simulations have confirmed that the effective maximum hydrostatic head loss across a debris bed is approximately equal to one-half of the height of the sump pool. To summarize, after the head loss across the sump screen resulting from debris accumulation exceeds the hydrostatic head corresponding to one-half the height of the sump pool, the volumetric flow to the pump decreases below the required flow to the pump and the pump will fail.

In some plants, the sump could be partially submerged at pump switchover but be totally submerged later as the sump reached its full level. This can occur for a number of reasons, including accumulation of CS water, continued melting of ice-condenser reservoirs, and continued addition of refueling water storage tank (RWST) inventory to the containment pool. As the pool depth changes during recirculation, the wetted or submerged area of the sump screens also would change. The depth of the pool also determines the average velocity of water approaching the screen, which, in turn, affects both debris transport to the screen and the pressure drop across the debris bed.

1.4 Description of Postulated Pressurized-Water Reactor Accidents

1.4.1 Overview

This section presents the results of thermal-hydraulic simulations performed to achieve three objectives.²

1. Identify important RCS and containment thermal-hydraulic parameters that influence the generation and/or transport of debris in PWR containments.
2. Determine time-dependent values for these parameters as a function of the assumed system's response (where applicable) by performing plant simulations using NRC-approved computer codes.
3. Use the calculated plant-response information to construct accident progression sequences that form the basis for strainer-blockage evaluations and probabilistic risk evaluations.

Evaluations were made for seven accident scenarios:

1. an LLOCA (cold- and hot-leg breaks),
2. a medium loss-of-coolant accident (MLOCA) (6-in. cold-leg break),
3. a small loss-of-coolant accident (SLOCA) (2-in. cold-leg break),
4. a small-small LOCA (1/4-in. cold-leg break),
5. a pressurizer surge line break,
6. a loss of offsite power with simultaneous failure of feedwater, and
7. inadvertent opening and stuck-open power-operated relief valve (PORV).

Figure 1-3 shows the major steps involved in the calculational effort. These include the following.

- RELAP5/MOD3.2¹⁻³¹ was used for simulating the RCS response to each of the postulated accident sequences. The RELAP5 simulations incorporated realistic initial and boundary conditions and a full representation of a Westinghouse four-loop RCS design. Selected simulations were also performed for Combustion Engineering (CE) plants.

² These results are documented in more detail in Ref. 1-27.

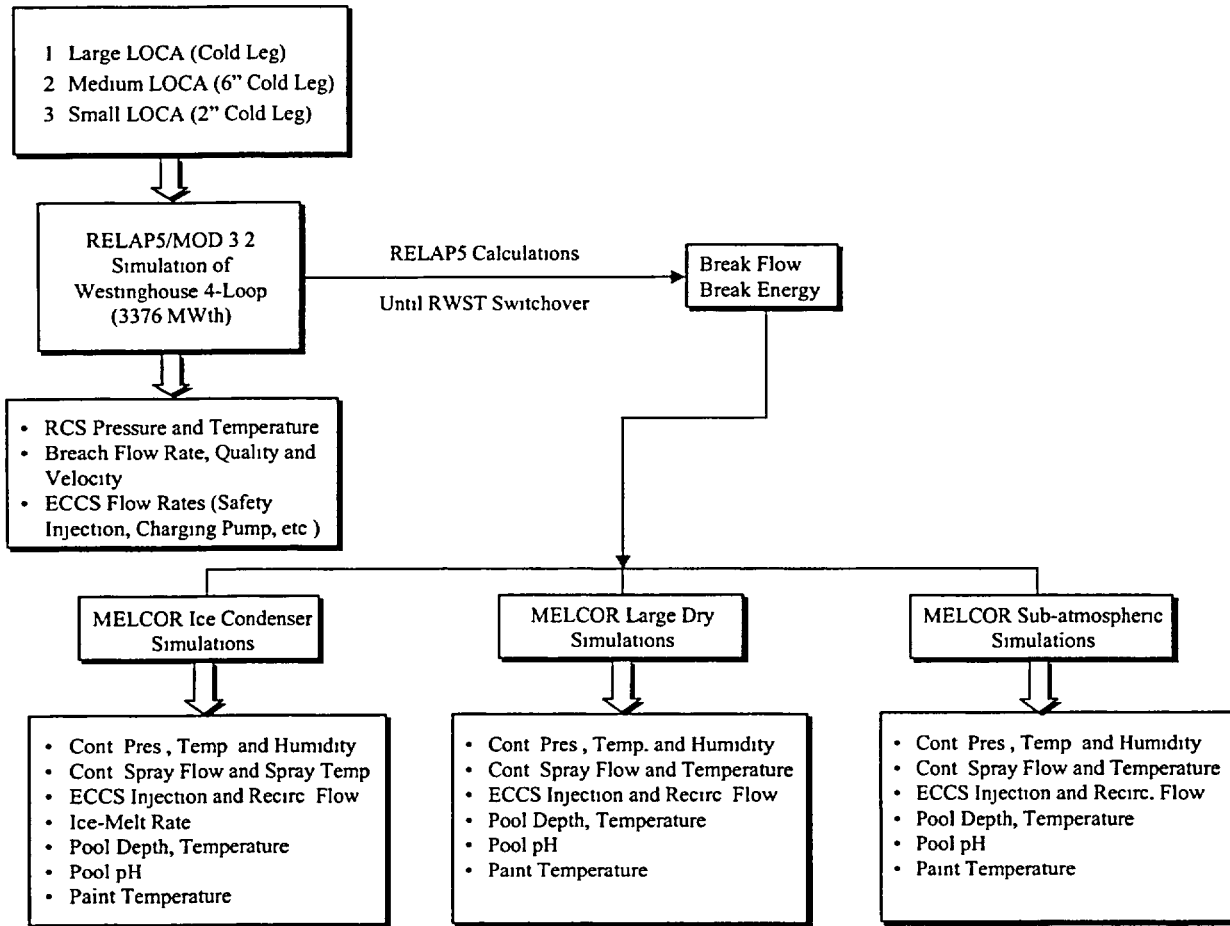


Figure 1-3 Flow Chart of Analysis Process

- MELCOR Version 1.8.2¹⁻³² was used for simulating the response of the ice condenser, large dry, and sub-atmospheric containments to a release of steam/water into the containment as a result of each accident sequence (as predicted by RELAP5).

The parameters tracked for each code simulation are shown in Figure 1-3. These parameters were limited to those that could influence debris generation and transport following a LOCA. A brief description of each of the important parameters and their potential effects is provided in Table 1-1.

Brief discussions of the simulation results are provided in Sections 1.4.2 through 1.4.4 for an LLOCA, an MLOCA, and an SLOCA, respectively. An examination of the data summarized in these sections reveals that

accident progression differs markedly with event type and containment type. The important differences are as follows

1. *Time at which blowdown commences and the duration over which blowdown occurs varies considerably with accident type.* In one extreme, the RCS blowdown following an LLOCA commences immediately and terminates within 30 s. The stagnation pressure at the break plane over that time period varies between 2000 and 300 psia. On the other extreme, blowdown following the SLOCA occurs over the first hour of the transient; even after 1 h, it is possible that the pressure vessel remains at pressures as high as 500 psi. Debris-generation estimates must account for these differences, especially for those insulations for which generation is driven by erosion. It is possible that a small-break zone of

Table 1-1 Important Parameters Tracked and Their Relevance

RCS PRESSURE AND TEMPERATURE: The flow through an RCS breach would be choked as long as the RCS temperature (and hence pressure) remains elevated. The critical (choked) flow rate through the breach would depend strongly on upstream pressure and temperature, which define the thermodynamic state of the fluid. The state of the fluid largely determines the expansion characteristics of a two-phase flashing jet.

BREACH FLOW CONDITIONS (FLOW RATE, VELOCITY, AND QUALITY): The destructive potential of a break jet depends strongly on break flow conditions. The velocities of both phases (liquid and vapor) are important here. The values calculated are the velocities at the choke plane. The moisture content of the fluid exiting the breach influences the damage potential of the jet. The quantity calculated here is the ratio of vapor mass flow rate to total mass flow rate at the choke plane.

ECCS SAFETY INJECTION FLOW: The rates of ECCS safety injection determine when the inventory of the RWST would be depleted, requiring switchover to ECCS recirculation through the emergency sump. The timing of switchover is important with regard to debris settling opportunities. Flow patterns in the water pool formed on the floor of the containment would be influenced by injection rates. Injection rates determine accident progression as related to the rate at which the RCS is cooled down.

ECCS RECIRCULATION FLOW: The rate at which flow is recirculated through the emergency sump will determine the flow patterns, velocities, and turbulence levels in the containment pool. The potential for debris transport is governed by these traits.

CONTAINMENT SPRAY FLOW: Containment sprays have the potential to wash settled debris from containment structures and suspended debris from the containment atmosphere down to the containment pool. Whether the sprays are operating or not largely determines the time at which the RWST inventory is expended and the magnitude of the recirculation flow through the emergency sump. The flow patterns and turbulence levels in the containment pool may be affected by where and how the sprays drain.

The potential for containment sprays to influence debris transport is thought to be considerable. As such, it is important to note the large variability in spray activation logic that exists from plant to plant, e.g., containment high-high pressure set points. Additionally, actions taken by the operators to shut containment sprays down would influence debris transport.

CONTAINMENT SPRAY TEMPERATURE: In some plants, recirculated spray water passes through heat exchangers. The heat removal would influence containment pressure and temperature trends. This phenomenon is of particular interest in ice-condenser containments. Therefore, special emphasis was put on modeling RHR heat exchangers and determining spray temperatures as close to reality as possible.

POOL DEPTH AND TEMPERATURE: The available NPSH at the recirculation pumps depends on the depth of the containment pool and its temperature. The velocities, flow patterns, and turbulence levels (and hence debris transport potential) in the pool depend on pool depth.

POOL PH: Basic or acidic tendencies in recirculating water may change the corrosion, dissolution, or precipitation characteristics of metal or degraded metal-based paints in containment. A specific concern is the possible precipitation of ZnOH formed from chemical interaction between zinc (in the zinc-based paints) and water at high temperature. The dissolution/precipitation of ZnOH in water is influenced by the degree of boration.

CONTAINMENT ATMOSPHERIC VELOCITY: The atmospheric velocities generated in the containment in response to an RCS breach determine to what degree generated debris initially disperses within the containment. These are the velocities developed as containment is subjected to the shock and pressurizing effects of the flashing break jet.

PAINT TEMPERATURE: Sustained elevated temperatures may degrade containment paints. An elaborate paint representation model was included in the MELCOR input model.

influence (ZOI) may be characterized by a larger L/D compared with large or medium breaks.³

2. *The magnitude of the ECCS recirculation flow through the emergency sump varies between events.* In the case of an SLOCA, the maximum ECCS flow through the sump during recirculation corresponds to the make-up flow for the high-pressure safety injection (HPSI) and charging pump discharge into the RCS (at about 500 psi) and subsequently leaking into the containment through the breach. On the other hand, following a LLOCA or a MLOCA, the maximum ECCS flow approaches the design flow (which is approximately 11,000 gpm for the cases simulated). The implication is that the potential for debris transport would be higher following an LLOCA than for the SLOCA analyzed. The plant-specific estimates for ECCS recirculation flow for each case can be obtained as follows.

- A generic value⁴ of 10,000 gpm (large break) could be used for most plants, or alternately, the plant response to NRC GL 97-04¹⁻²² may be used.
- A generic value of 2500 gpm (small break) could be used for most plants. A survey of plant data suggests that actual ECCS flow following a SLOCA could vary between 1800 gpm and 4800 gpm, with a median value of 2500 gpm (Ref. 1-26, Volume 2).

3. *A CS actuation is accident-specific and plant-specific.* In an accident where containment fan coolers sufficiently managed containment pressure and temperature to below the engineered safeguard feature (ESF) actuation set point, sprays would not actuate. If the sprays were not used or were used only sparingly, the

³ The ZOI is defined as the zone within which the break jet would have sufficient energy to generate debris of transportable size and form. L/D is a unitless measure of the size of the ZOI, where L is the maximum linear distance from the location of the break to the outer boundary of the ZOI and D is the diameter of the broken pipe.

⁴ The generic values presented here originally were developed for use in the parametric evaluation where plant-specific data were lacking. In plant-specific analyses, plant-specific values should be used where possible

length of time that ECCS injection could draw from the RWST would be increased largely. This also would minimize the potential for debris washdown by the cascading spray water. Note that for SLOCA events, sprays were not required for large dry containments whose actuation set points are higher than 10 psi, thereby limiting the maximum flow expected through the sump. Sprays were required for the ice condenser containment, resulting in sump flow rates nearly 4 times that required for the large dry plants. Sprays also are required for many large dry plants (including, but not limited to, sub-atmospheric containments) whose actuation set points are equal to or lower than 10 psi.⁵ This is because of the following:

- In several plants, the chilled water supply to the fan coolers is isolated following the LOCA, which reduces the efficiency of the fan coolers for removing containment heat. [The ultimate heat sink is via the component cooling water (CCW), which may not be sufficiently sized to handle such heat loads.]
- Degradations in fan coolers also may be possible if LOCA debris reaches or deposits on the fan cooler heat exchangers.
- Fan coolers are not safety-class equipment in most PWRs.⁶ For those plants, it is not clear that such fan coolers can be relied on for pressure control for a variety of reasons ranging from the fact that their functionality is not tested for these conditions to the fact that the heat removal source for fan coolers may be isolated as a result of a hi-hi or hi containment pressure set point (differs from containment to containment). However, for plants with safety-class fan coolers, those coolers can be relied upon to cool the containment, e.g., the fan coolers at

⁵ A SLOCA simulation was performed assuming fan coolers were not operational. The maximum containment pressure for this calculation was estimated to be approximately 18 psi, as opposed to 6 psi (see Table 1-7) for the case where fan coolers are assumed to operate.¹⁻²⁷

⁶ In the thermal-hydraulic simulations discussed in this section, all plant systems including the fan coolers were assumed to operate as designed.

Combustion Engineering (CE) plants with safety related CCW and safety related power to low speed fans.

The plant estimates for CS recirculation flow for each plant can be obtained as follows.

- A generic value of 6000 gpm can be used for most PWRs or preferably one can use appropriate flow rates applicable to each plant. Individual plant flow is generally not significantly different and thus will not influence the accident outcome.

1.4.2 Large Loss-of-Coolant Accident

The LLOCA simulated was a cold-leg, pump-discharge, double-ended guillotine break (DEGB). The RCS pressure and average temperature before the break were 2250 psia and 570°F. The cold-leg inside diameter was 27.5 in., corresponding to a cross-section area of 4.12 ft². The break was assumed to be instantaneous with a discharge coefficient of unity. A cold-leg break was chosen as the LLOCA event because design-basis accidents typically are cold-leg breaks. With respect to debris generation and transport, any differences between a cold-leg and hot-leg break likely would be small. This is not the case for core response, but with respect to emergency sump blockage, differences between large hot-leg and large cold-leg breaks are probably negligible. This assumption is supported by the results (not presented here) of a supplementary RELAP5 large-hot-leg-break calculation that compares closely with the results of the large-cold-leg-break calculation with respect to break-flow characteristics.

The calculated results for the LLOCA events in large dry and ice condenser containments are provided in Tables 1-2 and 1-3, respectively.⁷ These simulations were used to develop a generic description of LLOCA accident progression in a PWR, both in terms of the system's response and its implications on debris generation and transport. Table 1-4 provides a

⁷Large dry containment LLOCA results are representative of those expected for sub-atmospheric containments as well, with the exception that inside recirculation pump flow for the sub-atmospheric containment would have to be added.

general chronology of events for a PWR LLOCA sequence. Figure 1-4 summarizes key findings to supplement the tabulated results, with further explanation as follows.

1.4.2.1 Reactor Coolant System Blowdown Phase

In this report, the RCS blowdown refers to the event (or process) by which elevated energy in the RCS inventory is vented to the containment as the RCS vents through the breach. Blowdown and the subsequent flashing⁸ in the containment cause rapid decay in the RCS pressure and rapid buildup of containment pressure. Either of these initiates reactor scram.⁹ With delay built-in, it is expected that reactor scram would occur within the first 2 s. It is during RCS blowdown that flow from the break occurs and the highest (and most destructive) energy is released. Therefore, debris generation by jet impingement would be greatest during this time. Also, debris could be displaced from the vicinity of the break as the flashing two-phase break jet expands into the containment. Large atmospheric velocities may develop in the containment, approaching 200 ft/s in the ice condenser containment and 300 ft/s in the large dry containment, as breach effluent quickly expands to all regions of the containment. In the vicinity of the breach, containment structures would be drenched by water flowing from it. Increase in containment pressure also causes immediate automatic actuation of containment sprays, for all plant types, condensing steam and washing structures throughout containment. Spray water drains over and down containment walls and equipment, carrying both insulation and particulate (e.g., dirt and dust) debris to a growing water pool on the containment floor. In most containments, NaOH liquid stored in the spray additive tank (SAT) will be added to the borated water to facilitate absorption of iodine that may be released to the containment. Therefore, a secondary CS effect is a potential

⁸Flashing refers to the phenomenon by which the mainly liquid inventory of the RCS turns into a steam and liquid mixture as it is expelled into the containment atmosphere, which is at a significantly lower pressure.

⁹The accident progression in sequences in which scram does not occur is significantly different and will not be discussed in this document.

Table 1-2 Debris Generation and Transport Parameters: LLOCA—Large Dry Containment

Parameter	Blowdown Phase			Injection Phase			Recirculation Phase		
	0+	20 s	45 s	45 s	15 min	27 min	27 min	2 h	24 h
RCS pressure at break (psia)	2250	393	55						
RCS temperature at break (°F)	531	291	250	250	173	144	144		
Break flow (lb/s)	7.97e4	1.28e4	4.89e3						
Break flow velocity (ft/s)	296	930	100						
Break flow quality	0	0.25	0.3	0.3	0				
Safety injection (gpm)				11500	11500	11500			
Recirculation flow (gpm)							17500	11800	11800
Spray flow (gpm)				0	5700	5700	5700	0	
Spray temperature (°F)					105	190	190		
Containment pressure (psig)	0	36	33	33	11.5	7	7	1.5	0
Containment temperature (°F)	110	305	250	250	190	163	163	115	95
Pool depth (ft)					2	3.5	3.5	3.5	3.5
Pool temperature (°F)					212	187	187	125	100
Pool pH									
Containment atmosphere velocity (ft/s)	282		7						
Containment relative humidity (%)	50	100	100	100	100	90	90	100	100
Paint temperature (°F)	100			215	240	220	220	145	112
Peak break flow: 7.97e4 lb/s at 0+ s			Peak break flow velocity: 930 ft/s at 21 s						
Quality at peak break flow: 0			Quality at peak break flow velocity: 0.25						
Peak containment pressure: 36 psig at 20 s			Peak containment atmosphere velocity: 282 ft/s at 0+ s						

Table 1-3 Debris Generation and Transport Parameters: LLOCA—Ice Condenser Containment

Parameter	Blowdown Phase			Injection Phase			Recirculation Phase		
	0+	20 s	45 s	45 s	10 min	17 min	17 min	2 h	24 h
RCS pressure at break (psia)	2250	393	55						
RCS temperature at break (°F)	531	291	250	250	200	160	160		
Break flow (lb/s)	7.97e4	1.28e4	4.89e3						
Break flow velocity (ft/s)	296	930	100						
Break flow quality	0	0.25	0.3	0.3	0				
Safety injection (gpm)				11500	11500	11500			
Recirculation flow (gpm)							18000	18000	18000
Spray flow (gpm)				6400	6400	6400	6400	6400	6400
Spray temperature (°F)				105	105	97	97	95	89
Containment pressure (psig)	0+	14	10.1	10.1	4.5	4.5	4.5	3	2
Containment temperature (°F)	100	168	160	160	103	105	105	98	100
Pool depth (ft)				4	8.5	10.75	10.75	10.8	10.1
Pool temperature (°F)				180	157	159	159	148	126
Pool pH									
Containment atmosphere velocity (ft/s)	184	18	1						
Containment relative humidity (%)	0	50	100	100	80	96	96	97	98
Paint temperature (°F)	100	106	112	112	113	112	112	90	90
Peak break flow: 7.97e4 lb/s at 0+ s			Peak break flow velocity: 930 ft/s at 21 s						
Quality at peak break flow: 0			Quality at peak break flow velocity: 0.25						
Peak containment pressure: 14.4 psig at 15 s			Peak containment atmosphere velocity: 184 ft/s at 0+ s						

Table 1-4 PWR LLOCA Sequences

Time after LOCA (s)	Accum. (SI Tanks)	HPSI	LPSI	CS	Comments
0-1	Reactor scram Initially high containment pressure. Followed by low pressure in the pressurizer Debris generation commences caused by the initial pressure wave, followed by jet impingement The blowdown flow rate is large. But mostly saturated water. Quality ≤ 0.05 . Saturated jet-models are appropriate SNL/ANSI Models suggest wider jets, but pressures decay rapidly with distance				
2		Initiation signal	Initiation signal	Initiation signal	Initiation signal from low pressurizer pressure or high containment pressure/temp
5	Accumulator injection begins	Pumps start to inject into vessel (bypass flow out)	Pumps start (RCS P > pump dead head)	Pump start and sprays on	In cold-leg break, ECCS bypass is caused by counter-current injection in the downcomer. Hot-leg does not have this problem.
10	The blowdown flow rate decreases steadily from $\approx 20,000$ lb/s to 5000 lb/s Cold-leg pressure falls considerably to about 1000 psia At the same time, effluent quality increases from 0.1 to 0.5 (especially that from steam generator side of the break) Flow is vapor continuum with water droplets suspended in it. Saturated water or steam jet-models are appropriate. At these conditions, SNL/ANSI models show that jet expansion induces high pressures far from the break location.				
25		End of bypass; HPSI injection			
25-30	Break velocity reaches a maximum > 1000 ft/s. Quality in excess of 0.6. Steam flow at less than 500 lb/s. Highly energetic blowdown is probably complete. However, blowdown continues as residual steam continues to be vented				
35	Accumulators empty		Vessel LPSI ramps to design flow.		
40	Blowdown is terminated, and therefore, debris generation is complete. Blowdown pressure at the nozzle less than 150 psi. Debris would be distributed throughout the containment. Pool is somewhat turbulent. Height < 1 ft.				
55-200	Reflood and quenching of the fuel rods ($T_{max} = 1036$ °F). In cold-leg break, quenching occurs between 125 and 150 s. In the case of hot-leg break, quenching occurs between 45 and 60 s ($T_{max} = 950$ °F).				
200-1200	Debris added to lower containment pool by spray washdown drainage and break washdown. The containment floor keeps filling. No directionality to the flow. Heavy debris may settle down.				
1200	RWST low level indication received by the operator. Operator prepares to turn on ECCS in sump recirculation mode. Actual switchover when the RWST low-low level signal is received				
1500		Switch suction to sump	Switch suction to sump	Terminate or to sump	Many plants have containment fan coolers for long-term cooling
1500-18000	Debris may be brought to the sump screen. Buildup of debris on the sump screen may cause excessive head loss. Containment sprays may be terminated in large dry containments at the 2-h mark.				
>36000		Switch to hot-leg recirculation	Switch to hot-leg recirculation		

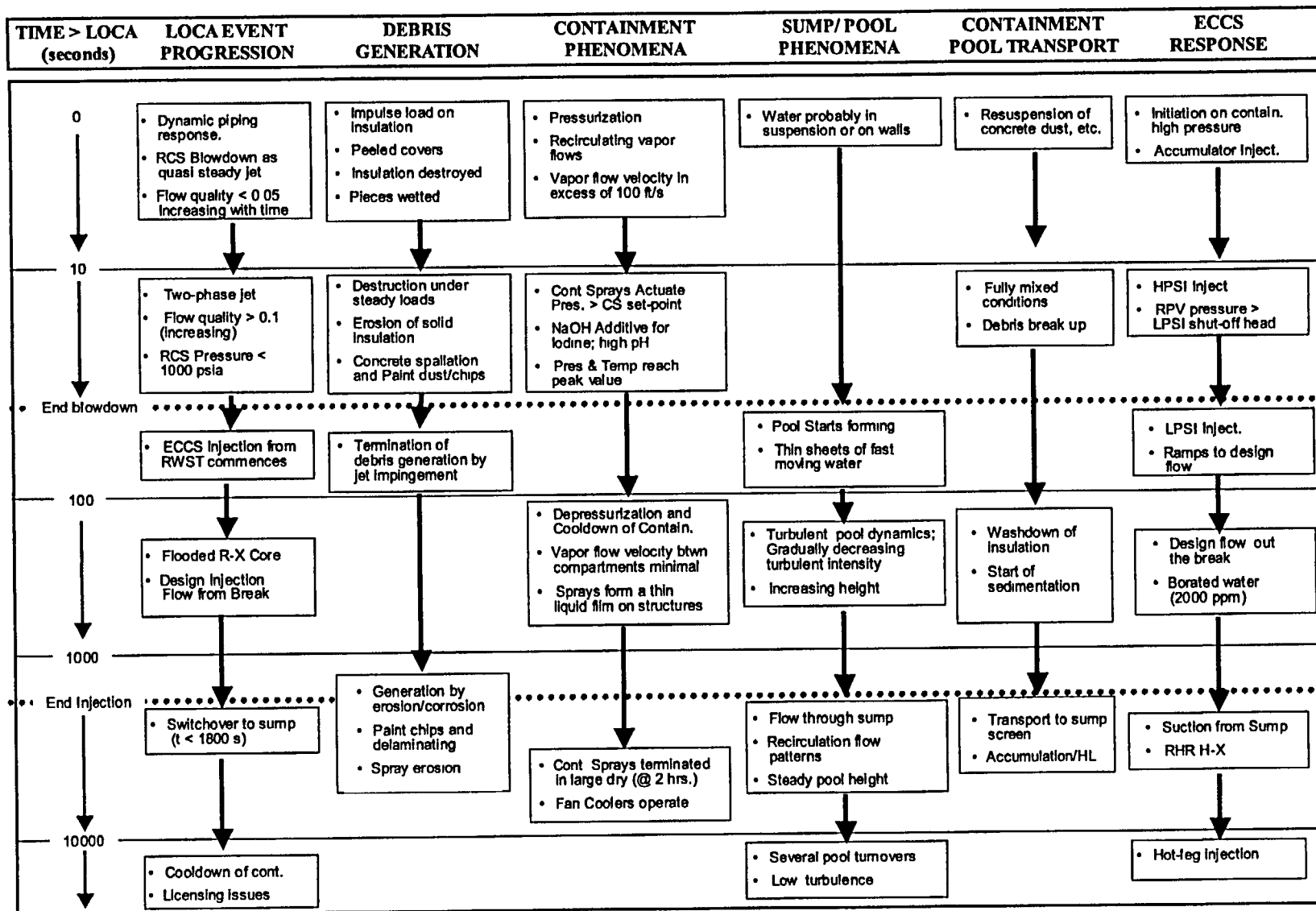


Figure 1-4 PWR LLOCA Accident Progression in a Large Dry Containment

increase in pool pH, which in turn, could play a role in particulate debris precipitation caused by the interaction of hot, borated, high-pH water with zinc and aluminum surfaces. The rates of these reactions are used in many Final Safety Analysis Reports (FSARs) to estimate the hydrogen source term and evaluate the potential for hydrogen accumulation in the containment.

Accurate characterizations of conditions that exist during the blowdown phase are important for estimating debris generation and, to some degree, debris transport. For LLOCA events, RCS blowdown occurs over a period of approximately 30 s, during which vessel pressure goes from 2250 psia to near containment pressure. During this time, the reactor pressure vessel thermodynamic conditions undergo a rapid change. Initially, the break flow is subcooled at the break plane and flashes as it expands into the containment. Within 2 s, the vessel pressure drops below 2000 psi and the flow in the pipes and the vessel becomes saturated. Thereafter, the break flow quality is equal to or higher than 10%. On the other hand, the void fraction increases to approximately 1.0, clearly indicating that the water content would be dispersed in the vapor continuum in the form of small droplets. The corresponding flow velocity at the break plane reaches a maximum of about 930 ft/s. This clearly indicates that jets would reach supersonic conditions during their expansion upon exiting the break. Based on these simulations, the energetic blowdown terminates within 25–30 s as the vessel pressure decreases to near 150 psig. Although steam at high velocities continues to exit, the stagnation pressure is not sufficient to induce very high pressures at distances far from the break. Thus, it is reasonable to assume that debris generation following an LLOCA occurs within the first minute. (Note: Debris generation by non-jet-related phenomena may occur over a prolonged period of time as a result of high temperature, humidity, and sprays.) The RCS blowdown continues until the vessel pressure falls below the shut-off head for the accumulator tank,¹⁰ the HPSI, and the low-pressure safety injection (LPSI). This causes increasingly large quantities of cooler, borated RWST water to quench the core and terminate blowdown.

¹⁰The accumulators are also known as safety injection tanks in some designs.

1.4.2.2 Emergency Core Cooling System Injection Phase

The injection phase refers to the period during which the RCS relies on safety injection, drawing on the RWST for decay heat removal. In the case of an LLOCA, the injection phase immediately succeeds the initial RCS blowdown. During this phase, core reflood is accomplished and quasi-steady conditions are arrived at in the reactor, where decay heat is removed continually by injection flow. In ice condenser containments, the ice condenser compartment doors open and the recirculation fans move the containment atmosphere through the ice condensers. Opportunities would exist for debris to settle in the pool during this relatively quiescent time before ECCS recirculation. Containment pressure would decrease from its maximum value (reached in the blowdown phase). The injection phase is considered to be over when the RWST inventory is expended and switchover to sump recirculation is initiated.

Accurate characterization of conditions that exist during injection phase may be important for estimating the quantity of debris transported from the upper containment to the pool and for estimating the quantity of debris that may remain in suspension. Following the initial break, safety injection (SI) begins immediately with the combined operation of the accumulators, the charging pumps, the HPSI pumps, and the LPSI (RHR) pumps. The SI flow approaches the design value (which is 11,500 gpm in the plant simulated) in about a minute and continues at that rate until switchover. Current simulations did not take credit for potential reduction in the injection flow (e.g., system-failure scenarios). Containment sprays continue to operate; spray water and water exiting the break will cause washdown of debris from the upper portions of the containment to the pool on the containment floor.

It has been determined that large quantities of water would be introduced into the containment within a few minutes following an LLOCA. As a result, the water-pool depth on the containment floor increases steadily. In the case of a large dry containment, the peak pool height is reached at the end of the injection phase; in an ice-condenser containment, the peak value is reached several hours into the accident after all the ice has melted.

1.4.2.3 Recirculation Phase

After the RWST inventory is expended, the ECCS pumps would be realigned to take suction from the emergency sump in the containment floor. This would begin the ECCS recirculation phase, in which water would be pulled from the containment pool, passed through heat exchangers, and delivered to the RCS, where it would pick up decay heat from the reactor core, flow out the breach, and return to the containment pool. Pool depth would reach a steady state during the recirculation phase, and containment pressure and temperature would be decreasing gradually. It would be during this accident phase that the potential would exist for debris resulting from an RCS breach (or residing in containment beforehand) to continue to be transported to the containment emergency sump. Because of the suction from the sump, this pool debris may accumulate on the sump screens, restrict flow, and either reduce available NPSH or starve the ECCS recirculation pumps.

The primary observation regarding the RCS and containment conditions during the recirculation phase is that the sump flow rate reaches the design capacity of all the pumps, which in the plants analyzed is 17,500 gpm for the large dry and sub-atmospheric containments and 18,000 gpm for the ice condenser containment.

1.4.3 Medium Loss-of-Coolant Accident

The MLOCA simulated was 6-in. in diameter circular hole, corresponding to a cross-section area of 0.1963-ft², in a cold leg downstream of the reactor coolant pump (RCP). The hole became full-sized instantaneously. It was situated on the side of the cold leg and centered halfway up. A discharge coefficient of unity was used, which made these simulations very conservative. The cold-leg location of the hole was chosen arbitrarily and is not expected to be a determining factor in the simulation results.

The calculated results for the MLOCA events in large dry and ice condenser containments are provided in Tables 1-5 and 1-6, respectively. Figure 1-5 presents the time scales associated with the occurrence of some of the events. The following sections highlight the differences between the MLOCA event and the LLOCA event described above.

1.4.3.1 Reactor Coolant System Blowdown Phase

In the case of an MLOCA, RCS blowdown occurs over a prolonged period (3 min) compared with that in an LLOCA. Blowdown starts at 0 s when the vessel is at 2250 psia and terminates as the RCS pressure and liquid subcooling decrease. Peak break flow for the MLOCA is at least a factor of 15 less than that observed for the LLOCA. In addition, the resulting vapor velocity in the containment peaks around 30 ft/s, as opposed to 200–300 ft/s for the LLOCA. These observations suggest less severe debris generation and transport caused by the LOCA jet itself. Another significant observation is that after MLOCAs, the exit flow at the break plane remains subcooled throughout the blowdown, at least until the vessel pressure falls to a point where blowdown would have little effect on debris generation. This may affect the ZOI over which debris would be generated.

1.4.3.2 Emergency Core Cooling System Injection Phase

There are three fundamental differences between an MLOCA and an LLOCA.

- ECCS injection begins before termination of the RCS blowdown. Initiation of injection occurs after 20–60 s, whereas the blowdown phase is not terminated until approximately 180 s.
- The LPSI does not inject significant quantities of water into the core in the short term. The LPSI (or RHR) pumps start injecting into the core at about 15 min.
- In the plants analyzed, spray actuation occurs shortly after ECCS injection begins (approximately 3 min, right around the termination of the RCS blowdown).

1.4.3.3 Recirculation Phase

The recirculation-phase accident characteristics for the MLOCA are similar to those described in Sec. 1.4.2.3 for the LLOCA. The sump recirculation flow rate for each plant analyzed was approximately half of that for the LLOCA simulation. The containment pressure and temperature increased following the ECCS switchover to the recirculation mode at 57 min. due to an increase in the spray water temperature, from approximately 105° to 150°F.

Table 1-5 Debris Generation and Transport Parameters: MLOCA—Large Dry Containment

Parameter	Blowdown Phase			Injection Phase			Recirculation Phase		
	0+	30 s	180 s	20 s	15 min	57 min	57 min	2 h	24 h
RCS pressure at break (psia)	2250	900	508						
RCS temperature at break (°F)	537	521	392		330	274	274		
Break flow (lb/s)	4940	1670	1000						
Break flow velocity (ft/s)	510	190	108						
Break flow quality	0	0	0		0.03	0.03	0.03	0	
Safety injection (gpm)				885	2500	2500			
Recirculation flow (gpm)							8250	2550	2550
Spray flow (gpm)		0	5700		5700	5700	5700	0	
Spray temperature (°F)			105		105	150	150	150	
Containment pressure (psig)	0	6	9.5		5	3	3	4.2	1.5
Containment temperature (°F)	110	170	182		160	140	140	148	120
Pool depth (ft)					0.9	3.3	3.3	3.3	3.3
Pool temperature (°F)					170	145	145	147	125
Pool pH									
Containment atmosphere velocity (ft/s)	35	10	5						
Containment relative humidity (%)	50	100	100		98	98	98	98	100
Paint temperature (°F)	110		160		175	160	160	155	121
Peak break flow:	4940 lb/s at 0+ s			Peak break flow velocity:			510 ft/s at 0+ s		
Quality at peak break flow:	0			Quality at peak break flow velocity:			0		
Peak containment pressure:	10.2 psig at 2 min			Peak containment atmosphere velocity:			35 ft/s at 0+ s		

Table 1-6 Debris Generation and Transport Parameters: MLOCA—Ice Condenser Containment									
Parameter	Blowdown Phase			Injection Phase			Recirculation Phase		
	0+	30 s	180 s	20 s	15 min	34 min	34 min	2 h	24 h
RCS pressure at break (psia)	2250	900	508						
RCS temperature at break (°F)	537	521	392		330	300	300		
Break flow (lb/s)	4940	1670	1000						
Break flow velocity (ft/s)	510	190	108						
Break flow quality	0	0	0		0.03	0.03	0.03	0	
Safety injection (gpm)				885	2500	2500			
Recirculation flow (gpm)							9000	9000	9000
Spray flow (gpm)		0	6400		6400	6400	6400	6400	6400
Spray temperature (°F)			105		105	105	92.5	86.5	84
Containment pressure (psig)	0+	9.8	7.8		4	4	4	1.8	1.4
Containment temperature (°F)	100	145	151		110	110	110	87	90
Pool depth (ft)					4	7.9	7.9	8	9.6
Pool temperature (°F)					150	146	146	117	104
Pool pH									
Containment atmosphere velocity (ft/s)	30	2.5	1.25						
Containment relative humidity (%)	0	10	40		80	97	97	97	98
Paint temperature (°F)	100	101	125		130	125	125	95	90
Peak break flow: 4940 lb/s at 0+ s			Peak break flow velocity: 510 ft/s at 0+ s						
Quality at peak break flow: 0			Quality at peak break flow velocity: 0						
Peak containment pressure: 11 psig at 55 s			Peak containment atmosphere velocity: 30 ft/s at 0+ s						

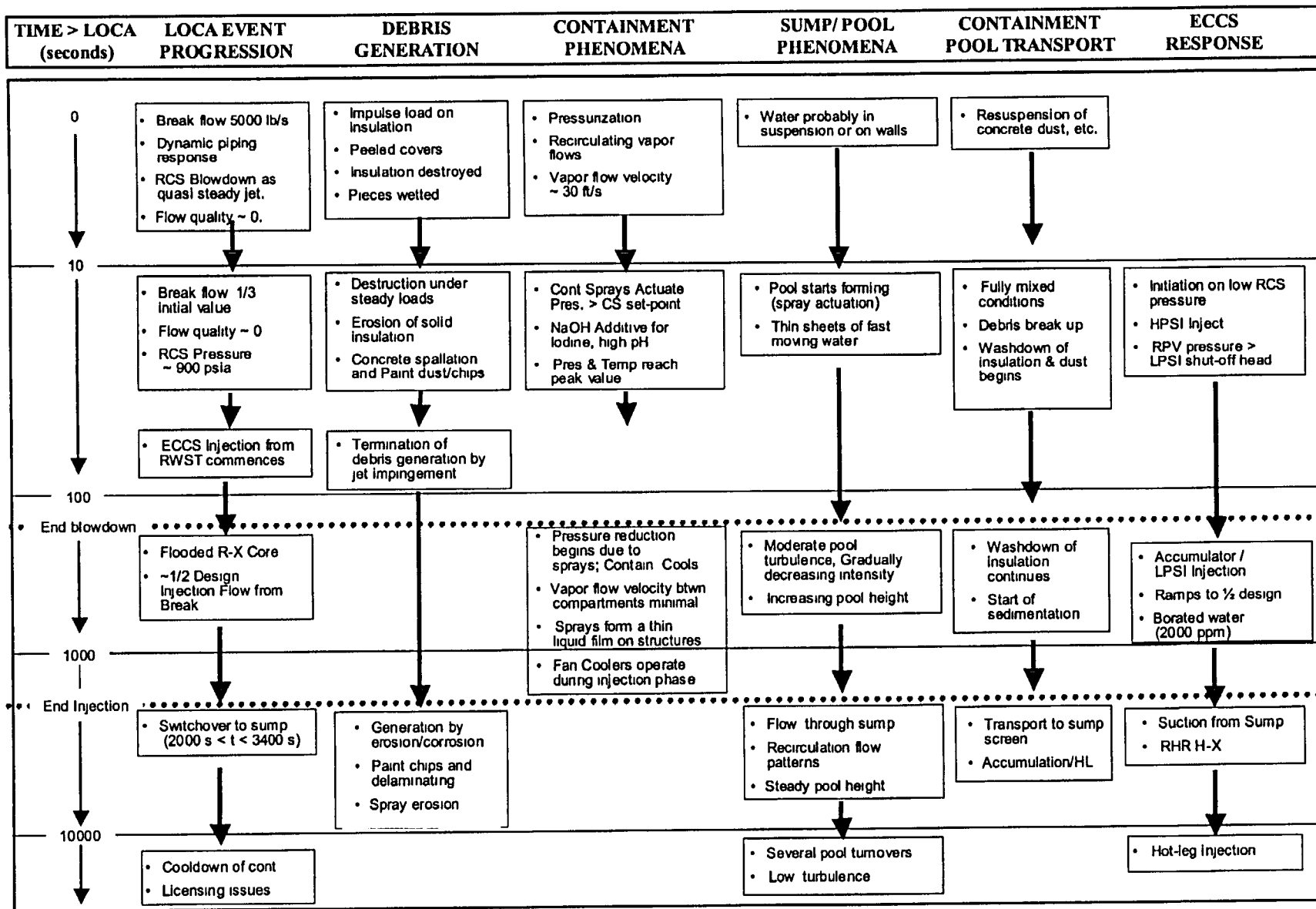


Figure 1-5 PWR MLOCA Progression in a Large Dry Containment

1.4.4 Small Loss-of-Coolant Accident

The SLOCA studied was a 2-in. diameter, circular hole in a cold leg, corresponding to a cross-section area of 0.0218-ft², downstream of the RCP.¹¹ The hole became full-sized instantaneously. It was situated on the side of the cold leg and centered halfway up. A conservative discharge coefficient of unity was defined. The cold-leg location of the hole was chosen arbitrarily and is not expected to be a determining factor in the simulation results. The 2-in. specification of this hole was made with the expectation that the RCS pressure would stabilize above the accumulator pressure such that the accumulators would not inject.

The calculated results for the SLOCA events in large dry, ice condenser, and sub-atmospheric containments are provided in Tables 1-7 through 1-9, respectively. Figure 1-6 presents the time scales associated with the occurrence of some of the events.

1.4.4.1 Reactor Coolant System Blowdown Phase

RCS blowdown in the case of an SLOCA occurs over a prolonged period (60 min). Blowdown starts at 0 s when the vessel is at 2000 psia and terminates mainly as the RCS pressure and liquid subcooling decrease. Peak break-flow velocities for the SLOCAs are a factor of 30 less than those for the LLOCA and a factor of 2 less than those for the MLOCA. Containment atmosphere velocities are a factor of 30–60 less than those for the LLOCA and a factor of 2 less than those for the MLOCA. Another significant observation is that following SLOCAs, the exit flow at the break plane remains subcooled throughout the blowdown (at least until the vessel pressure falls to a point where blowdown would have little effect on debris generation). This may affect the ZOI over which debris would be generated.

1.4.4.2 Emergency Core Cooling System Injection Phase

There are fundamental differences between an SLOCA and an LLOCA.

¹¹The study also simulated a 1.75-in. break. The results were found to be very similar to the 2-in. break.

- The LPSI does not inject into the core at all; the HPSI and charging pumps are sufficient to make up for lost inventory.
- Actuation of containment sprays is highly plant-specific and may not be needed at all. In the large dry containment plant analyzed (which has a CS actuation set point of 9.5 psig), spray operation is not required.¹² Spray actuation is seen after 30 min in the ice condenser simulation and after 15 min in the sub-atmospheric plant. Even then, the operator may terminate sprays during the SLOCA event to prolong RWST availability and rely on fan coolers (or the ice condenser) for decay heat removal from the containment. Note that washdown of debris from the upper containment to the floor pool may be limited to more localized areas (near the break) for plants in which containment sprays are not required. As noted in Section 1.4.1, some plants, such as CE plants, have containment heat removal capability that can be relied upon to cool the containment indirectly without spray cooling.
- Paint is exposed to significantly higher peak temperatures following a LLOCA than it would be following a SLOCA.

1.4.4.3 Recirculation Phase

The recirculation-phase accident characteristics for the SLOCA are similar to those described in Sec. 1.4.2.3 for the LLOCA. The primary difference is that the required flow rates for the SLOCA are significantly less than those for the LLOCA (as low as 2500 gpm for plants in which containment sprays do not actuate). The paint temperatures for paint on thin steel remains a few degrees hotter in the long-term for a SLOCA compared with a LLOCA, but the paint temperatures would be about the same for paint on concrete surfaces.

1.4.5 Other Plant Design Features That Influence Accident Progression

Other plant design features (beyond those previously discussed) may influence the debris-

¹²Again, the results presented here are for an accident scenario in which fan coolers operate. Other calculations suggest a peak containment pressure during an SLOCA in a large-dry containment could reach values nearing 18 psig if fan coolers fail to operate.¹⁻²⁷

Table 1-7 Debris Generation and Transport Parameters: SLOCA—Large Dry Containment

Parameter	Blowdown Phase			Injection Phase			Recirculation Phase		
	0+	30 min	1 h	60 s	2 h	3 h	3 h	12 h	24 h
RCS pressure at break (psia)	2250	605	512						
RCS temperature at break (°F)	538	354	371		270	236	236		
Break flow (lb/s)	550	343	300						
Break flow velocity (ft/s)	320	320	320						
Break flow quality	0	0	0						
Safety injection (gpm)				1500	2500	2500			
Recirculation flow (gpm)							2500	2500	2500
Spray flow (gpm)	Sprays not required								
Spray temperature (°F)									
Containment pressure (psig)	0	5	5		4	3	3	1	0.75
Containment temperature (°F)	110	160	160		150	140	140	115	110
Pool depth (ft)			0.8		1.5	2.25	2.25	3	3
Pool temperature (°F)			157		157	150	150	125	118
Pool pH									
Containment atmosphere velocity (ft/s)	9	4	4						
Containment relative humidity (%)	50	100	100		100	100	100	100	100
Paint temperature (°F)	100	160	160		157	153	153	127	117
Peak break flow: 550 lb/s at 0+ s			Peak break flow velocity: 320 ft/s at 0+						
Quality at peak break flow: 0			Quality at peak break flow velocity: 0						
Peak containment pressure: 6 psig at 38 min			Peak containment atmosphere velocity: 9 ft/s at 20 s						

Table 1-8 Debris Generation and Transport Parameters: SLOCA—Ice Condenser Containment

Parameter	Blowdown Phase			Injection Phase			Recirculation Phase		
	0+	30 min	1 h	60 s	15 min	35 min	35 min	5 h	24 h
RCS pressure at break (psia)	2250	605	512						
RCS temperature at break (°F)	538	354	371		391	362	362		
Break flow (lb/s)	550	343	300						
Break flow velocity (ft/s)	320	320	320						
Break flow quality	0	0	0						
Safety injection (gpm)				1500	2500	2500			
Recirculation flow (gpm)							9000	9000	9000
Spray flow (gpm)		6400	6400	0	6400	6400	6400	6400	6400
Spray temperature (°F)		105	91		105	105	91	87.5	86
Containment pressure (psig)	0+	4.1	3.6	3.4	4.4	4.2	4.2	2.25	1.8
Containment temperature (°F)	100	111	96.5	94	112	110	110	92	95
Pool depth (ft)		5.5	6.75		2.5	6.5	6.5	9	8.9
Pool temperature (°F)		137	132		137	137	137	120	114
Pool pH									
Containment atmosphere velocity (ft/s)	2.9	0.7	0.7						
Containment relative humidity (%)	0	97	97	6	100	97	97	97	97
Paint temperature (°F)	100	110	104	100	106	110	110	92	96
Peak break flow: 550 lb/s at 0+ s			Peak break flow velocity: 320 ft/s at 0+						
Quality at peak break flow: 0			Quality at peak break flow velocity: 0						
Peak containment pressure: 4.4 psig at 15 min			Peak containment atmosphere velocity: 2.9 ft/s at 23 s						

Table 1-9 Debris Generation and Transport Parameters: SLOCA—Sub-Atmospheric Containment

Parameter	Blowdown Phase			Injection Phase			Recirculation Phase		
	0+	30 min	1 h	60 s	1 h	3 h	3 h	12 h	24 h
RCS pressure at break (psia)	2250	605	512						
RCS temperature at break (°F)	538	354	371		270	236	236		
Break flow (lb/s)	550	343	300						
Break flow velocity (ft/s)	320	320	320						
Break flow quality	0	0	0						
Safety injection (gpm)				1500	2500	2500			
Recirculation flow (gpm)							2500	2500	2500
Spray flow (gpm)					9000	9000	9000	9000	9000
Spray temperature (°F)					105	150	150	125	120
Containment pressure (psig)	0	5	5		4	3	3	1	0.75
Containment temperature (°F)	110	160	160		150	140	140	115	110
Pool depth (ft)			0.8		1.5	2.25	2.25	3	3
Pool temperature (°F)			157		157	150	150	125	118
Pool pH									
Containment atmosphere velocity (ft/s)	9	4	4						
Containment relative humidity (%)	50	100	100		100	100	100	100	100
Paint temperature (°F)	100	160	160		157	153	153	127	117
Peak break flow: 550 lb/s at 0+ s			Peak break flow velocity: 320 ft/s at 0+						
Quality at peak break flow: 0			Quality at peak break flow velocity: 0						
Peak containment pressure: 6 psig at 38 min			Peak containment atmosphere velocity: 9 ft/s at 20 s						

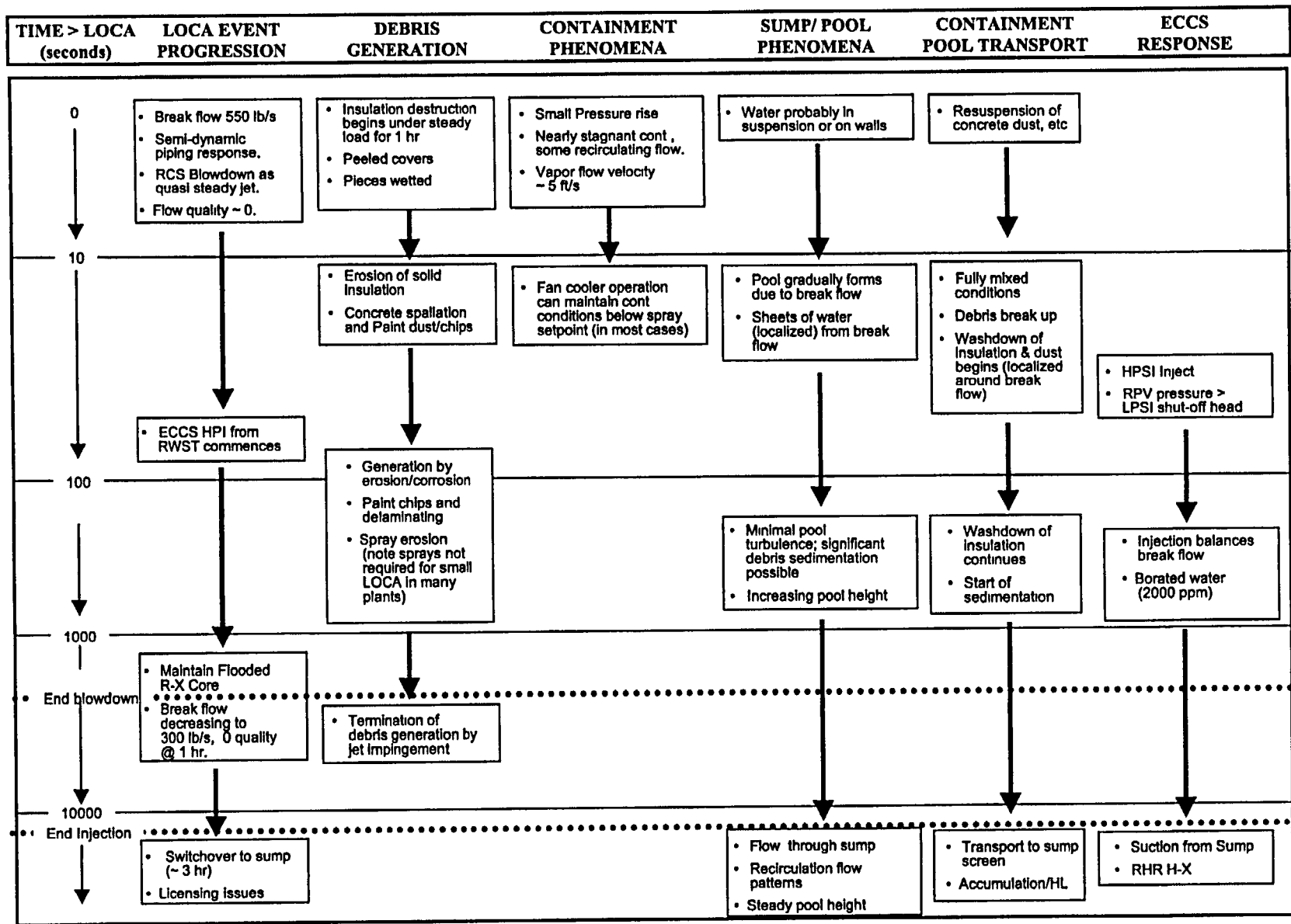


Figure 1-6. PWR SLOCA Accident Progression in a Large Dry Containment

related accident progression. For example, in many plants, heat exchangers are installed directly in the core-cooling recirculation flow paths to ensure that the water is cooled before it is returned to the core. However, in some plants, the core cooling recirculation systems do not have dedicated heat exchangers and instead make indirect use of heat exchangers from other systems (i.e., CS) to ensure that heat is removed from the reactor coolant. Examples of plants where core cooling makes indirect use of heat exchangers from CS includes the plants with sub-atmospheric containments and CE plants. For these types of plants, successful core cooling during recirculation may require (1) direct sump flow from the core cooling system and (2) sump recirculation cooling from the CS system.

For plants with sub-atmospheric containments, switchover for the set of "inside" recirculation spray pumps is performed quickly (approximately 2 min), whereas the switchover for ECCS pumps and CS pumps is considerably longer (on the order of 30 min or more depending on LOCA type). The relatively quick switchover of the inside recirculation spray pumps is accomplished to minimize containment pressure and temperature. The inside recirculation spray system is equipped with a heat exchanger, and it appears that its actuation is credited in estimating the NPSH margin for the ECCS and CS system during the recirculation phase.

Recovery from a stuck-open PORV may be possible at many plants through operator actions to close the associated block valve. The need for sump recirculation could be avoided by this action.

The containment structures are sufficiently robust that failure of CS is not expected to cause containment failure from overpressure.

1.5 Description of Relevant Plant Features that Influence Accident Progression

Some general conclusions regarding important plant features that influence accident outcome

are listed below. The primary source for this information is the PWR plant survey published in 2002.¹⁻²⁶

Sump Design and Configurations

- The ECCS and/or CSS pumps in nearly one-third of the PWR plants surveyed have an NPSH margin less than 2 ft-water, and another one-third have an NPSH margin between 2-ft water and 4-ft water. In general, PWR sumps have low NPSH margins compared with the head loss effects of debris accumulation on the sump screen.
- PWR sump designs vary significantly, ranging from horizontal screens located below the floor elevation to vertical screens located on pedestals. The sump-screen surface areas vary significantly from unit to unit, ranging from 11 ft² to 700 ft² (the median value is approximately 125 ft²). Some plants employ curb-like features to prevent heavier debris from accumulating on the sump screen, and some do not have any noticeable curbs.
- In 19 PWR units, the sump screen would not be completely submerged at the time that ECCS recirculation starts. The mode of failure is strongly influenced by sump submergence.
- Sump-screen clearance size varies considerably. A majority of the plants used a sump-screen opening size of 0.125 in., reportedly to ensure that the maximum size of the debris that can pass through the sump screen is less than the smallest clearance in the RCS and the CSS. However, 26 PWR units indicated that sump-screen clearance is higher than 0.125 in., reaching up to 1 in. Two units reported not having fine screens, other than the standard industrial grating used to filter out very large debris.

Sources and Locations of Debris

- U.S. PWRs employ a variety of types of insulation and modes of encapsulation, ranging from non-encapsulated fiberglass to fully encapsulated stainless steel RMI. A significant majority of PWRs have fiberglass and calcium-silicate insulations in the containment, either on primary piping or on

supporting systems.¹³ The types of fibrous insulation varied significantly, but much of it is in the form of generic low-density fiberglass (LDFG) and mineral wool. It appears that many of the newer plants (or plants replacing steam generators) have been replacing RMI insulation on the primary systems with "high-performance" fiberglass. In general, the smaller pipes and steam generators are more likely to be insulated with fiberglass and calcium-silicate than the reactor pressure vessel or the hot leg or cold leg. Other sources of fibrous materials in the containment for some plants include up to approximately 13,000 ft³ of filter media on the air-handling units and up to 1500 ft³ of fibrous insulation (e.g., Kaowool) used as fire barrier materials. Given that (a) very small quantities of fibrous insulation would be necessary to induce large pressure drops across the sump screens (less than 10 ft³) and (b) most plants have comparatively very large inventories of fibrous insulation, it is clear that plant-specific analyses are necessary before the recirculation sumps of any particular plant can be declared safe with respect to screen blockage.

- Other sources of debris in the PWR containments include cement dust and dirt (either present in the containment *a priori* or generated by a LOCA), particulate insulations used on the fire barriers (e.g., Marinite), failed containment coatings (a medium-sized PWR has approximately 650,000 ft² of coated surfaces in the containment), and precipitants (zinc and aluminum precipitation by-products).¹⁴ Estimates for this type of debris range from 100 lb to several 1000 lb; either of these bounds would result in very large head losses when combined with fibrous material.

¹³About 40 PWR units have in excess of 10% of the plant insulation in the form of fiberglass and another 5–10% in the form of calcium-silicate. A typical plant has approximately 7500 ft³ of insulation on the primary pipes and supporting systems pipes that are in close proximity to the primary pipes.

¹⁴PWR DBAs evaluate the potential for precipitation of aluminum and zinc when they are subjected to high-pH, hot, borated water because these chemical reactions generate H₂.

Containment Features Affecting Debris Transport

- CS set points typically are defined based on LLOCA and equipment qualification considerations. Consequently, sprays may not (automatically) actuate during SLOCAs¹⁵ because of the lower peak containment pressures associated with SLOCAs. CS actuation following an SLOCA event plays an important role in the transport of debris to the sump, and at the same time, it affects the timing of sump failure.¹⁶ Set points for CS actuation vary considerably and span a wide range: 2.8 psig to 30 psig. Consistently lower values are observed in sub-atmospheric and ice condenser containment designs, as would be expected. Nevertheless, values at or below 10 psig¹⁷ are observed for large dry containments, as well.

1.6 Regulatory Considerations

Federal regulations were established to govern the design and operational aspects of nuclear power reactors that affect the safety of those plants. These regulations are codified in the CFR. Title 10¹⁻⁸ of the CFR deals with energy and Part 50 of Title 10¹⁻⁸ consists of regulations promulgated by the NRC to provide for the licensing of production and use of facilities. The NRC published RG documents to guide the nuclear power industry to compliance with the regulations. Regulations and regulatory guidance applicable to the strainer blockage

¹⁵Fan cooler response to LOCAs also plays a vital role in determining spray actuation following SLOCA. These concerns are not applicable to LLOCAs or MLOCAs, where automatic actuation of sprays is expected in every plant.

¹⁶The drainage of the spray water from the upper reaches of the containment down to the containment sump could transport substantial quantities of debris to the sump that otherwise would likely remain where deposited following the RCS depressurization (i.e., the containment sprays would substantially increase the fraction of debris transported to the sump screens over the fraction that would be transported without spray operation).

¹⁷The 10-psig set point is important because MELCOR simulations showed that if both fan coolers in a large dry containment are not operating at full capacity, containment pressure could exceed 10 psig for breaks ≥ 2 in.¹⁻²⁷

issue are summarized in Sections 1.6.1 and 1.6.2, respectively.

1.6.1 Code of Federal Regulations

This section provides a description of the regulations that apply to the strainer blockage issue. Title 10 of the CFR¹⁻⁸ provides the authority to the NRC to regulate nuclear power plants. Section 50.46, "Acceptance Criteria for Emergency Core Cooling Systems for Light-Water Nuclear Power Reactors," of 10 CFR¹⁻⁸ requires that licensees of a BWR or PWR design their ECCS systems to meet five criteria. Specifically, the rule provides acceptance criteria for peak cladding temperature, maximum cladding oxidation, maximum hydrogen generation, coolable core geometry, and long-term cooling. The long-term cooling criterion states, "After any calculated successful initial operation of the ECCS, the calculated core temperature shall be maintained at an acceptably low value and decay heat shall be removed for the extended period of time required by the long-lived radioactivity remaining in the core." Licensees are required to demonstrate this capability while assuming the most conservative (worst) single failure. Some licensees may credit CSSs in the licensing basis for radioactive source-term and pressure reduction. The capability of the ECCS and safety-related CSS pumps to fulfill the criteria of limiting the peak cladding temperature and to provide long-term cooling over the duration of the postulated accident could be seriously compromised by the loss of adequate NPSH and the resulting cavitation. Operational experience and detailed analysis demonstrated that excessive buildup of debris from thermal insulation, corrosion products, and other particulates on ECCS pump strainers is highly likely to cause a common-cause failure of the ECCS thereby preventing the ECCS from providing long-term cooling following a LOCA. Therefore, Section 50.46 clearly applies to the strainer blockage issue, and licensees must resolve this issue for their respective plants in order to ensure compliance with the regulations.

General Design Criteria (GDC) 35, 36, 37, 38, 39, and 40 in Appendix A to 10 CFR Part 50¹⁻⁸ require appropriate design, inspectability, and testability of the ECCS and the containment heat

removal systems.¹⁸ These GDC establish minimum requirements for the principal design criteria for water-cooled nuclear power plants similar in design and location to plants for which the NRC has issued construction permits. The GDC also are considered to be generally applicable to other types of nuclear power units and are intended to provide guidance in establishing the principal design criteria for such other units. Specifically, these criteria state the following.

Criterion 35 – Emergency core cooling. A system to provide abundant emergency core cooling shall be provided. The system safety function shall be to transfer heat from the reactor core following any loss of reactor coolant at a rate such that (1) fuel and clad damage that could interfere with continued effective core cooling is prevented and (2) clad metal-water reaction is limited to negligible amounts. Suitable redundancy in components and features, and suitable interconnections, leak detection, isolation, and containment capabilities shall be provided to assure that for onsite electric power system operation (assuming offsite power is not available) and for offsite electric power system operation (assuming onsite power is not available) the system safety function can be accomplished, assuming a single failure.

Criterion 36 – Inspection of emergency core cooling system. The emergency core cooling system shall be designed to permit appropriate periodic inspection of important components, such as spray rings in the reactor pressure vessel, water injection nozzles, and piping, to assure the integrity and capability of the system.

¹⁸ GDC 41, 42, and 43, which define criteria for containment atmosphere cleanup, apply in regards to the availability of containment spray systems to remove fission products from the containment atmosphere. In addition, Section 50.67 of 10 CFR Part 50, which addresses accident source terms, would be affected should ECCS be lost due to sump blockage. Further, 10 CFR Part 100 details reactor site criteria including factors considered when evaluating reactor sites such as the expectation those reactors will reflect through their design, construction, and operation an extremely low probability for accidents that could result in release of significant quantities of radioactive fission products

Criterion 37 – Testing of emergency core cooling system. The emergency core cooling system shall be designed to permit appropriate periodic pressure and functional testing to assure (1) the structural and leaktight integrity of its components, (2) the operability and performance of the active components of the system, and (3) the operability of the system as a whole and, under conditions as close to design as practical, the performance of the full operational sequence that brings the system into operation, including operation of applicable portions of the protection system, the transfer between normal and emergency power sources, and the operation of the associated cooling water system.

Criterion 38 – Containment heat removal. A system to remove heat from the reactor containment shall be provided. The system safety function shall be to reduce rapidly, consistent with the functioning of other associated systems, the containment pressure and temperature following any loss-of-coolant accident and maintain them at acceptably low levels. Suitable redundancy in components and features, and suitable interconnections, leak detection, isolation, and containment capabilities shall be provided to assure that for onsite electric power system operation (assuming offsite power is not available) and for offsite electric power system operation (assuming onsite power is not available) the system safety function can be accomplished, assuming a single failure.

Criterion 39 – Inspection of containment heat removal system. The containment heat removal system shall be designed to permit appropriate periodic inspection of important components, such as the torus, sumps, spray nozzles, and piping to assure the integrity and capability of the system.

Criterion 40 – Testing of containment heat removal system. The containment heat removal system shall be designed to permit appropriate periodic pressure and functional testing to assure (1) the structural and leaktight integrity of its components, (2) the operability and performance of the active components of the system, and (3) the operability of the system as a whole, and under conditions as close to the design as practical the performance of the full operational sequence that brings the system into operation, including operation of applicable portions of the protection system, the transfer

between normal and emergency power sources, and the operation of the associated cooling water system.

Section 50.65 of 10 CFR Part 50, "Requirements for monitoring the effectiveness of maintenance at nuclear power plants"¹⁻⁸ (referred to hereafter as the Maintenance Rule) provides the requirements for monitoring and maintenance of plant structures, systems, and components (SSCs). The maintenance rule requires the licensee of a nuclear power plant to monitor the performance or condition of SSCs in a manner sufficient to provide reasonable assurance that the SSCs are capable of fulfilling their intended functions. When the performance or condition of an SSC does not meet its established goals, appropriate action shall be taken. Based on the criteria in the rule, the maintenance rule includes in its scope BWR suction strainers, all safety-related CSSs, and those non-safety-related CSSs that fall into the following categories.

1. Those that are relied on to mitigate accidents or transients or are used in plant emergency operating procedures
2. Those whose failure could prevent safety-related CSSs from fulfilling their safety-related function
3. Those whose failure could cause a reactor scram or an actuation of a safety-related system.

Protective coatings also are covered by the Maintenance Rule to the extent that coating activities can affect safety-related equipment, e.g., suction strainers. On the basis of the guidelines in the rule, the maintenance rule requires that licensees monitor the effectiveness of maintenance for these protective coatings. The staff also considers the requirements of 10 CFR Part 50, Appendix B, "Quality Assurance Criteria for Nuclear Power Plants and Fuel Reprocessing Plants,"¹⁻⁸ to be applicable to safety-related containment coatings. Criterion IX of Appendix B, "Control of Special Processes," is especially relevant requiring that "Measures shall be established to assure that special processes are controlled and accomplished by qualified personnel using qualified procedures in accordance with applicable codes, standards, specifications, criteria, and other special requirements."

Appendix K of 10 CFR Part 50,¹⁻⁸ "ECCS Evaluation Models," establishes requirements

for analytical determinations that impact aspects of the strainer blockage issue. These analytical requirements include:

1. fission product decay heat generation rate (affects the calculated suppression pool temperature),
2. break flow characteristics and discharge model (affects the estimated amounts of debris),
3. post-blowdown phenomena and heat removal by the ECCS, and
4. required ECCS model documentation.

Appendix K also specifies that single failures be considered and the containment pressure to be used for evaluating cooling effectiveness.

1.6.2 Regulatory Guidance

This section provides a description of regulatory guidance that applies to the strainer/sump blockage issue. The NRC provided guidance on ensuring adequate long-term recirculation cooling following a LOCA in RG 1.82, "Water Sources for Long-Term Recirculation Cooling Following a Loss-of-Coolant Accident."¹⁻⁷ The guide describes acceptable methods for implementing applicable GDC requirements with respect to the sumps and suppression pools functioning as water sources for emergency core cooling, containment heat removal, or containment atmosphere cleanup. Guidelines for evaluating availability of the sump and suppression pool for long-term recirculation cooling following a LOCA are included in the RG 1.82.¹⁻⁷

Revisions 1 and 2 of RG 1.82 were issued in November 1985 and May 1996, respectively; Revision 3 is scheduled for September 2003. The first revision, Revision 1, reflected the staff's technical findings related to USI A-43¹⁻¹ that were reported in NUREG-0897.¹⁻⁴ A key aspect of the revision was the staff's recognition that the 50% strainer blockage criterion of Revision 0 did not address the issue adequately and was inconsistent with the technical findings developed for the resolution of USI A-43.¹⁻¹ It was assumed in Revision 0 that the minimum NPSH margin could be computed by assuming that 50% of the screen area was blocked by debris. GL 85-22¹⁻³³ recommended use of RG 1.82 Revision 1¹⁻⁷ for changeout and/or modifications of thermal insulation installed on primary coolant system piping and components. Revision 2 altered the strainer blockage

guidance for BWRs because operational events, analyses, and research following Revision 1 indicated that the previous guidance was not comprehensive enough to adequately evaluate a BWR plant's susceptibility to the detrimental effects caused by debris blockage of the suction strainers.

RG 1.82 Revision 2¹⁻⁷ guidance addressed operational debris, as well as debris generated by a postulated LOCA. Specifically, the Regulatory Guide stated that all potential debris sources should be evaluated, including, but not limited to, insulation materials (e.g., fibrous, ceramic, and metallic), filters, corrosion material, foreign materials, and paints/coatings. Operational debris included corrosion products (such as BWR suppression pool sludge), and foreign materials (FME procedures were not specifically introduced into Rev. 2). Revision 2 also noted that debris could be generated and transported by the washdown process, as well as, the blowdown process. Other important aspects of Revision 2 included: the use of debris interceptors (i.e., suction strainers) in BWR designs to protect pump inlets and NPSH margins; the design of passive and/or active strainers; instrumentation, in-service inspections; suppression pool cleanliness; the evaluation of alternate water sources, analytical methods for debris generation, transport, and strainer blockage head loss, and the need for appropriate supporting test data. Revision 2 references provide further detailed technical guidance for the evaluation of potential strainer clogging. Guidance for the evaluation of potential sump clogging for PWR plants will be provided in Revision 3 of RG 1.82.

RG 1.82 Revision 2¹⁻⁷ cited RG 1.1,¹⁻³⁴ "Net Positive Suction Head for Emergency Core Cooling and Containment Heat Removal System Pumps," for specific conditions to be used in determining the available NPSH for ECCS pumps in a BWR plant's licensing basis. RG 1.1¹⁻³⁴ considered the potential for degraded pump performance for ECCS and containment heat removal, which could be caused by a number of factors, including inadequate NPSH. If the available NPSH to a pump is not sufficient, cavitation of the pumped fluid can occur, thereby significantly reducing the capability of the system to accomplish its safety functions. It is important that the proper performance of the ECCS and containment heat removal systems be independent of calculated increases in

containment pressure caused by postulated LOCAs to ensure reliable operation under a variety of postulated accident conditions. The NRC's regulatory position is that the ECCS and containment heat removal systems should be designed with adequate NPSH margin assuming the maximum expected temperatures of the pumped fluids and no increase in containment pressure above atmospheric.

The NRC issued Revision 1 of RG 1.54, "Quality Assurance Requirements for Protective Coatings Applied to Water-Cooled Nuclear Power Plants," in July 2000¹⁻³⁵ to provide guidance regarding compliance with quality assurance requirements related to protective coating systems applied to ferritic steel, aluminum, stainless steel, zinc-coated (galvanized) steel, and masonry surfaces. The revision encourages industry to develop codes, standards, and guide that can be endorsed by the NRC and carried out by industry. With noted exceptions, the ASTM standards cited in the Regulatory Position of Revision 1 for the selection, qualification, application, and maintenance of protective coatings in nuclear power plants have been reviewed by the NRC staff and found acceptable.

Additional guidance is found in the applicable sections of the NRC SRP.¹⁻⁶ These sections include:

1. Section 6.2.2, "Containment Heat Removal Systems,"
2. Section 6.1.2, "Protective Coating Systems (Paints) – Organic Materials," and
3. Section 6.2.1.5, "Minimum Containment Pressure Analysis for Emergency Core Cooling System Performance Capability Studies."

1.7 Report Outline

This report is organized in the order that screen blockage analyses are usually performed. The analysis is usually decomposed into several steps as listed below.

- Section 2 discusses the identification of the potential sources of debris at the plant under evaluation.
- Section 3 discusses the testing and analytical models associated with estimating the volumes of debris that could potentially be generated.
- Section 4 discusses the testing and analytical models associated with the transport of the debris within the upper containment, i.e., blowdown debris transport and subsequent washdown debris transport by the containment sprays.
- Section 5 discusses the testing and analytical models associated with the transport of the debris within the sump pool.
- Section 6 discusses the accumulation of debris on a sump screen or a pump suction strainer.
- Section 7 discusses the estimation of the head loss associated with a particular debris bed on a sump screen or a pump suction strainer.
- Section 8 discusses the redesigns of sump screens or pump suction strainers that have occurred during the resolutions of strainer blockage issue.
- Section 9 discusses the related significant events that have occurred both in the U.S. and internationally.
- Section 10 discusses the summary and conclusions of the report.

1.8 References

- 1-1. NUREG-0933, R. Emrit, R. Riggs, W. Milstead, J. Pittman, "A Prioritization of Generic Safety Issues," U.S. Nuclear Regulatory Commission, Revision 16, November 1993.
- 1-2. NUREG-0510, "Identification of Unresolved Safety Issues Relating to Nuclear Power Plants," U.S. Nuclear Regulatory Commission, January 1979.
- 1-3. NUREG-0869, Revision 1, A. W. Serkiz, "USI A-43 Regulatory Analysis," U.S. Nuclear Regulatory Commission, October 1985.
- 1-4. NUREG-0897, Revision 1, A. W. Serkiz, "Containment Emergency Sump Performance," U.S. Nuclear Regulatory Commission, October 1985.
- 1-5. SECY-85-349, "Resolution of Unresolved Safety Issue A-43, 'Containment Emergency Sump Performance,'" October 31, 1985.
- 1.6. NUREG-0800, Revision 4, "Standard Review Plan for the Review of Safety

- Analysis Reports for Nuclear Power Plants," LWR Edition, Section 6.2.2: Containment Heat Removal Systems, U.S. Nuclear Regulatory Commission, June 1987.
- 1.7 RG-1 82, Regulatory Guide 1.82, Revision 1, "Water Sources for Long-Term Recirculation Cooling Following a Loss-of-Coolant Accident," U.S. Nuclear Regulatory Commission, Revision 1, November 1985 and Revision 2, May 1996.
 - 1-8. 10 CFR Part 50, Title 10, Code of Federal Regulations, published by the Office of the Federal Register, National Archives and Records Administration, U.S. Government Printing Office, January 1, 1997.
 - 1-9. NRC Information Notice, IN-92-71, "Partial Blockage of Suppression Pool Strainers at a Foreign BWR," NRC Information Notice, September 30, 1992
 - 1-10 NRC Information Notice, IN-93-34, "Potential for Loss of Emergency Cooling Function Due to a Combination of Operational and Post-LOCA Debris in Containment," NRC Information Notice, April 26, 1993.
Supplement 1, "Potential for Loss of Emergency Cooling Function Due to a Combination of Operational and Post-LOCA Debris in Containment," NRC Information Notice, May 6, 1993.
 - 1-11. NRC Information Notice, IN-95-47, Revision 1, "Unexpected Opening of a Safety/Relief Valve and Complications Involving Suppression Pool Cooling Strainer Blockage," NRC Information Notice, November 30, 1995.
 - 1-12. NRC Information Notice, IN-95-06, "Potential Blockage of Safety-Related Strainers by Material Brought inside Containment," NRC Information Notice, January 25, 1995.
 - 1-13. NRC Bulletin 93-02, "Debris Plugging of Emergency Core Cooling Suction Strainers," NRC Bulletin to Licensees, May 11, 1993, and Supplement 1, February 18, 1994.
 - 1-14. NUREG/CR-6224, G. Zigler, J. Brideau, D. V. Rao, C. Shaffer, F. Souto, W. Thomas, "Parametric Study of the Potential for BWR ECCS Strainer Blockage Due to LOCA Generated Debris," Final Report, U.S. Nuclear Regulatory Commission, October 1995.
 - 1-15. NUREG/CR-6370, D. V. Rao, W. Bernahl, J. Brideau, C. Shaffer and F. Souto, "BLOCKAGE 2.5 User's Manual," SEA96-3104-A:3, December 1996.
 - 1-16. NUREG/CR-6371, C. Shaffer, W. Bernahl, J. Brideau, and D. V. Rao, "BLOCKAGE 2 5 Reference Manual," SEA96-3104-A:4, December 1996.
 - 1-17. NEA/CSNI/R (95) 11, "Knowledge Base for Emergency Core Cooling System Recirculation Reliability," Prepared by U.S. Nuclear Regulatory Commission for the Principal Working Group 1 (PWG-1), International Task Group, Committee on the Safety of Nuclear Installations, Organization for Economic Cooperation and development (OECD) Nuclear Energy Agency (NEA), February 1996.
 - 1-18. NRC Bulletin 96-03, "Potential Plugging of Emergency Core Cooling Suction Strainers by Debris in Boiling-Water Reactors," NRC Bulletin to BWR Licensees, May 6, 1996.
 - 1-19 NUREG/CR-6369, Volume 1, D. V. Rao, C. Shaffer, and E. Haskin, "Drywell Debris Transport Study," U.S. Nuclear Regulatory Commission, SEA97-3501-A:14, September 1999.
NUREG/CR-6369, Volume 2, D. V. Rao, C. Shaffer, B. Carpenter, D. Cremer, J. Brideau, G. Hecker, M. Padmanabhan, and P. Stacey, "Drywell Debris Transport Study: Experimental Work," SEA97-3501-A:15, September 1999.
NUREG/CR-6369, Volume 3, C. Shaffer, D. V. Rao, and J. Brideau, "Drywell Debris Transport Study: Computational Work," SEA97-3501-A:17, September 1999.
 - 1-20. NEDO-32686, Rev. 0, "Utility Resolution Guidance for ECCS Suction Strainer Blockage," BWROG, November 1996.
 - 1-21. NRC-SER-URG, "Safety Evaluation by the Office of Nuclear Reactor Regulation Related to NRC Bulletin 96-03 Boiling Water Reactor Owners Group Topical Report NEDO-32686, 'Utility Resolution Guidance for ECCS Suction Strainer Blockage,'" Docket No. PROJ0691, August 20, 1998.

- 1-22. GL-97-04, "Assurance of Sufficient Net Positive Suction Head for Emergency Core Cooling and Containment Heat Removal Pumps," NRC Generic Letter to All Holders of Operating Licenses for Nuclear Power Plants, October 7, 1997.
- 1-23. SEA97-3705, Clint Shaffer and Willard Thomas, "Reliance on Containment Overpressure for Ensuring Appropriate NPSH," Technical Evaluation Report to U.S. NRC, SEA97-3705-A:5, April 29, 1998.
- 1-24. GL-98-04, "Potential for Degradation of the Emergency Core Cooling System and the Containment Spray System After Loss-of-Coolant Accident Because of Construction and Protective Coating Deficiencies and Foreign Material in Containment," NRC Generic Letter to All Holders of Operating Licenses for Nuclear Power Plants, July 14, 1998.
- 1-25. LA-UR-01-1595, D. V. Rao, Clinton J. Shaffer, and Robert Elliott, "BWR ECCS Strainer Blockage Issue: Summary of Research and Resolution Actions," Prepared for U.S. Nuclear Regulatory Commission, Los Alamos National Laboratory, LA-UR-01-1595, March 21, 2001.
- 1-26. NUREG/CR-6762, "GSI-191 Technical Assessment," U.S. Nuclear Regulatory Commission (2002).
 Volume 1: D. V. Rao, B. Letellier, C. Shaffer, S. Ashbaugh, and L. Bartlein, "GSI-191 Technical Assessment: Parametric Evaluation for Pressurized Water Reactor Recirculation Sump Performance," LA-UR-01-4083, 2002.
 Volume 2: D. V. Rao, B. Letellier, K. W. Ross, L. Bartlein, and M. T. Leonard, "GSI-191 Technical Assessment: Summary and Analysis of U.S. Pressurized Water Reactor Industry Survey Responses and Responses to GL 97-04," LA-UR-01-1800, 2002.
 Volume 3: C. J. Shaffer, D. V. Rao, and S. G. Ashbaugh, "GSI-191 Technical Assessment: Development of Debris-Generation Quantities in Support of the Parametric Evaluation," LA-UR-01-6640, 2002.
 Volume 4: S. G. Ashbaugh, and D. V. Rao, "GSI-191 Technical Assessment: Development of Debris Transport Fractions in Support of the Parametric Evaluation," LA-UR-01-5965, 2002.
- 1-27. NUREG/CR-6770, K. W. Ross, D. V. Rao, and S. G. Ashbaugh, "GSI-191: Thermal-Hydraulic Response of PWR Reactor Coolant System and Containments to Selected Accident Sequences," NUREG/CR-6770, LA-UR-01-5561, 2002.
- 1-28. NUREG/CR-6772, D. V. Rao, B. C. Letellier, A. K. Maji, and B. Marshall, "GSI-191: Separate-Effects Characterization of Debris Transport in Water," NUREG/CR-6772, LA-UR-01-6882, 2002.
- 1-29. NUREG/CR-6773, D. V. Rao, C. J. Shaffer, B. C. Letellier, A. K. Maji, and L. Bartlein, "GSI-191: Integrated Debris-Transport Tests in Water Using Simulated Containment Floor Geometries," NUREG/CR-6773, LA-UR-02-6786, 2002.
- 1-30. NUREG/CR-6771, J. L. Darby, W. Thomas, D. V. Rao, B. C. Letellier, S. G. Ashbaugh, and M. T. Leonard, "GSI-191: The Impact of Debris-Induced Loss of ECCS Recirculation on PWR Core Damage Frequency," NUREG/CR-6771, LA-UR-02-0279, 2002.
- 1-31. NUREG/CR-5535, Lockheed Idaho Technologies Co., "RELAP5/MOD3 Code Manual," Volumes I through VII, NUREG/CR-5535, Rev. 1, Idaho National Engineering Laboratory, June 1995.
- 1-32. NUREG/CR-6119, Summers, R. M., et al., "MELCOR Computer Code Manuals," Volumes 1 and 2, NUREG/CR-6119, SAND93-1285, Sandia National Laboratories, September 1994.
- 1-33. GL-85-22, "Potential for Loss of Post-LOCA Recirculation Capability Due to Insulation Debris Blockage," NRC Generic Letter to All Licensees of Operating Reactors, Applicants for Operating Licenses, and Holders of Construction Permits, December 3, 1985.
- 1-34. RG-1.1, Regulatory Guide 1.1, "Net Positive Suction Head for Emergency Core Cooling and Containment Heat Removal System Pumps," U.S. Nuclear Regulatory Commission, November 2, 1970.

1-35. RG-1.54, Regulatory Guide 1.54, "Quality Assurance Requirements for Protective Coatings Applied to Water-Cooled Nuclear Power Plants," Rev. 1, July 2000.

2.0 DEBRIS SOURCES

Sources of debris that could contribute to the potential clogging of a strainer or sump screen include LOCA-generated debris, exposure-generated debris, and operational debris.

- LOCA-generated debris would be any materials damaged or destroyed by the effluents of a primary-system depressurization such that these materials subsequently could transport from their original location (e.g., piping insulation).
- Exposure-generated debris would be any materials damaged by prolonged exposure to the LOCA environment that subsequently could transport (e.g., failed unqualified coatings).
- Operational debris would be any resident material that normally is not considered permanently part of the plant (e.g., dust/dirt, rags, and plastic bags).

Each of these types of debris has been found following operational events and/or plant inspections.

The NEI conducted a survey on PWR sump design and operations for PWR reactors operating within the US in 1999 and forwarded the survey results to the US NRC. The NRC reviewed the survey results and published their findings in Volume 2 of NUREG/CR-6762.²⁻¹ In addition, an earlier survey was conducted in 1982.²⁻² These two surveys provide an overview of the types of insulation used by nuclear power plants in the US.

This section describes

- the debris actually found inside plant containments,
- the types of debris formed by LOCA depressurization effluents,
- the types of debris formed by prolonged exposure to a LOCA environment, and
- the types of debris formed by operational processes.

2.1 Actual Debris Found During Inspections

A wide variety of debris has been found inside the containments of operating nuclear power

plants. In some cases, the debris has rendered systems inoperable. The associated event reports are described in Section 9. Operational debris has included materials left over from the actual construction of the containment and materials left inside the containment during maintenance, repairs, and modifications. The operational and/or potential debris also includes such materials as equipment covers intended for removal before operation, tools, rope, and dust/dirt. Many event reports simply stated that miscellaneous operational debris was found without specifying the content of that debris. Failed coatings have been found where the coating pieces had or could have formed debris. The types of debris found are now listed by very general screen-blockage characteristics.

Fibrous Debris

Fibrous debris from sources such as temporary cooling filters used during an outage has been found inside the containment. In the most notable events, the fibers were found in suppression pools after excessive strainer head loss rendered a system inoperable.

Particulate Debris

Operational particulate debris has included corrosion products, construction/maintenance residues, and operational accumulations.

- Sludge buildup in suppression pools resulted from the continuous corrosion of structural steel.
- Dirt, dust, and pebble accumulations found in sumps were the result of insufficient housekeeping.
- Weld slag found in sumps was the result of insufficient cleanup following construction or modifications.

Transportable Sheet-Like Materials

Numerous miscellaneous, relatively transportable materials were found that would essentially behave like a solid sheet of material when they were on a strainer/screen, i.e., totally blocking a small section of the screen. These included the following.

- Sheets of thin plastic, e.g., bags or wraps
- Cloth-like materials

- Oil cloth
- Coveralls
- Nylon bags
- Duct tape
- Downcomer cleanliness covers
- Rubber mats
- Step-off pads
- Gasket materials
- Foam rubber plug

Relatively Non-Transportable Materials

Numerous miscellaneous materials were found that were relatively nontransportable and therefore less likely to contribute to significant strainer/sump-screen blockage, including the following.

- Tools
 - Hammer
 - Slugging wrench
 - Socket
 - Grinder wheel
 - Flashlight
- Miscellaneous hardware
 - Nuts and bolts
 - Scaffold knuckle
 - Antenna
 - Metal sheeting
 - Welding rod
 - Hoses and hose clamps
 - Tygon tubing
 - Tie wraps
 - Rope
 - Hardhats
 - Pens/Pencils

Although these materials are less likely to transport or cause strainer/sump-screen blockage, these types of debris can render a system inoperable under certain circumstances and have done so. Certainly, if the debris were left inside a sump screen, a pump could ingest it. For example, in 1980, a welding rod was found jammed between the impeller and the casing ring of an RHR system at the Trojan plant.

Failed Coatings

Several incidences of failed coatings and of the identification of unqualified coatings where only qualified coating should have been used were found during inspections. For example, in 1993 at North Anna Unit 1, most of the unqualified silicon-aluminum paint covering the steam

generators and pressurizer had detached from those surfaces and was held in place only by the surrounding insulation jackets.

Adherence to the FME and other housekeeping programs by the licensees will limit the extent of operational debris within the containment.

These include periodic inspections and cleanings to minimize the amount of foreign material and suppression-pool sludge. However, despite the ongoing FME programs, extensive quantities of foreign materials still were being found in suppression pools.

2.2 Loss-of-Coolant-Accident-Generated Debris

The break effluent following a LOCA would generate substantial quantities of debris within the containment, mostly within the vicinity of the break. The majority of the destruction to materials near the break would occur within the region generally designated as the ZOI. The size of the ZOI (refer to Section 3), which usually is considered to be spherical, depends on the type of material, i.e., the region of destruction could extend further for some materials than for others. However, some debris could be generated well beyond the ZOI. As the containment pressurizes, equipment covers, loose coatings, etc., could be blown free to become debris. A rapid pressurization could burst light bulbs anywhere within the containment. All of these sources of debris should be considered.

The debris generated within the ZOI would almost certainly be the largest source of transportable debris. Sources of debris within the ZOI generally include

- insulation materials and their respective jacketing,
- fire barrier materials,
- surface coatings, and
- concrete erosion.

The largest source of debris within the ZOI usually would be destroyed or damaged insulation. There are several types of insulation materials (as well as manufacturers of insulation), and each has unique destruction and transport characteristics. The types of insulation include those listed below.

- Fibrous insulation
 - LDFG
 - High-density fiberglass (HDFG)
 - Mineral wool
 - Miscellaneous other types
- RMI
 - Aluminum RMI
 - Stainless-steel RMI
- Particulate insulation
 - Calcium silicate
 - Asbestos
 - Unibestos
 - Microtherm
 - Min-K
 - Gypsum board
- Foam insulation
 - Foamglass
 - Foamed plastic
 - Armaflex
 - Vinyl cell
 - Neoprene

A number of different types of fire-barrier materials is used inside containments, but the volume of debris generated from fire-barrier materials tends to be substantially less than that of insulation, primarily because there usually would be much less fire-barrier material inside the ZOI. The pieces of failed coatings, ranging from powder to large chips of paint, would contribute to the buildup of particulate on the strainer/screen, as would the by-product of concrete erosion.

Beyond the ZOI, the LOCA-generated debris could include such materials as cloth used in equipment covers, permanent tags and stickers, and glass from broken light bulbs. The various filters located within containment potentially could contribute to the generation of debris, even though these filters are usually considered sufficiently protected that the LOCA flows (beyond the ZOI) would not damage the filter sufficiently to form debris. These filter materials could include filter paper, fiberglass, high-efficiency particulate air (HEPA) filters, and charcoal.

2.3 Loss-of-Coolant-Accident Exposure-Generated Debris

After the primary system depressurization is complete, the materials inside the containment would be subject to the high temperatures and

humidity resulting from the depressurization. In addition, the containment sprays, if activated, would impact and wet surfaces throughout the containment continuously. Prolonged exposure to the LOCA environment (both during depressurization and afterward) could cause some materials to fail, thereby generating additional debris.

One concern is that protective coatings within containments would have the potential to detach from their substrate as a result of prolonged exposure to a LOCA environment. Qualified protective coatings are expected to adhere to their substrates during a design-basis LOCA (DB-LOCA), except those coatings directly impacted by the break jet. A research program conducted at the Savannah River Technology Center to investigate the performance and potential for debris formation of coating systems used in nuclear power plant containments²⁻³ concluded that qualified, properly applied coatings that have not been subjected to irradiation of 10^9 rads can be expected to remain fully adhered to and intact on a steel substrate following exposure to all simulated DB-LOCA conditions. However, coatings that have been subjected to irradiation of 10^9 rads exhibited profound blistering, even when properly applied, leading to disbondment of a near-surface coating layer (1–2 mils of the 10-mil thickness) when exposed to elevated temperatures and moisture conditions within the range of DBA conditions. This phenomenon likely would produce a coating-debris source term.

All coatings inside the containment are not qualified,²⁻⁴ and therefore, the amount of unqualified coatings must be controlled because the unqualified coatings are assumed to detach from their substrates during a DB-LOCA and may be transported to the emergency sump screens or suction strainers. Several instances have been reported to the NRC in which protective coatings either have not been applied/maintained properly or have not been qualified adequately for their intended use.²⁻⁵

The characteristics of failed coating debris have been examined by the BWROG for selected types of coatings and test conditions.²⁻⁶ Test samples were prepared by first exposing the coating to a minimum radiation dose of 10^9 rads at an average dose rate of 1.65 Mrads/h at the University of Massachusetts Lowell Radiation Laboratory. The specimens next were subjected

to a series of three LOCA tests at the Testing Department of the Carboline Company to investigate the post-LOCA failure mechanisms and the failure timing of the coating systems. A scanning electron microscope was used to perform a detailed examination of pieces of debris. Microhardness measurements also were taken and compared for selected coating types. The coating debris examined ranged from powder residues to large, slightly curved pieces.

The LOCA environment, especially with the containment sprays operating, also could fail the adhesive intended to attach tags or labels permanently to walls and equipment. This type of debris material could well transport to the sump screens or suction strainers.

The exposure of the LOCA environment would likely cause oxidation of metallic surfaces that could generate transportable particulate debris.¹ There are unpainted metallic surfaces (steel, zinc, and aluminum) in all PWR containments that would be exposed in an accident environment to hot and highly borated water. The borated water would react with those surfaces, generating particulates.²⁻¹ Estimating the potential quantity of these particulates is difficult because the oxidation rates depend on a variety of parameters, such as the type of chemistry, the water temperature, the pH of the water, and the aeration of the water. The investigation of this phenomenon is only cursory at this time, and the current estimates vary greatly, depending on the values of the assumed parameters.

In addition to generating certain types of debris, exposure to the LOCA environment can degrade previously generated debris further. For example, individual fibers from pieces of relatively nontransportable or trapped fibrous debris likely would break free, at least to some extent, forming transportable debris. In the case of calcium-silicate debris, small particles likely would break free from the larger pieces. This issue needs to be addressed in debris-transport calculations.

¹Ongoing research is studying the importance of this potential source of debris, but it likely is negligible in the short term.

2.4 Operational Debris

Operational debris is debris formed from the operational erosion of containment materials or from materials that normally would not be left inside the containment during operation. A tool would be an example of a material left inside the containment following a period of maintenance. The location of debris such as a tool would be important to whether that tool could have an adverse affect. An example of operational erosion would be the iron oxide sludge that forms continuously in a BWR wetwell. Some of this sludge likely would always be found in the wetwell, but it should be kept to a minimum by cleaning of the wetwell during outages. Good general housekeeping is needed to limit debris such as dirt/dust that can accumulate throughout the containment. Even if an area of the containment looks clean, small quantities of dirt/duct could be located out of sight in and around equipment where the containment sprays would transport that debris to the sump. Operational debris has included (but is not limited to) the following.

- Wetwell sludge
- Dirt and dust
- Rust on unpainted surfaces
- Products of wear and tear (e.g., paint chips)
- Temporary air treatment filters
- Tools
- Rags
- Sheeting of various materials
- Plastic products (e.g., plastic bags)
- Paper products
- Rope
- Tape
- Wire ties
- Fire hoses

The quantities of operational debris present inside containment are plant-specific. The FME and other housekeeping programs might well be able to reasonably ensure that certain operational debris is not present, at least in places where the debris can transport to the sump screens or suction strainers. Much of the history of foreign materials inside containment predates the FME program. However, foreign material continues to be found inside containment.²⁻⁴

2.5 Aging Effects on Mineral Fiber Thermal Insulation

The effects of aging on mineral fiber thermal insulation would affect, at least to some extent, the generation of insulation debris, its subsequent transport to a PWR sump screen or a BWR suction strainer, and the resultant head loss across a bed of debris on that screen/strainer. The aging effects could include exposure to high temperatures, exposure to radiation, and operational damage. Of these types of aging or damage, the exposure to high temperature is the most significant effect. Insulation damaged significantly during normal operational of the plant normally would be replaced because of its reduced ability to perform its function. Although gamma and neutron radiation at sufficient intensity would decompose organic binders, operational observations do not indicate a significant aging resulting from exposure to radiation.

Mineral fiber insulation consists of either of two different types of material: fiberglass insulation and mineral or rock wool insulation. Fiberglass insulation is made from melted glass that is spun into fibers about 2 in.-long and, for mechanical products, with a 5- to 7-micron fiber diameter and a product bulk density of 2 to 3 lbs/ft³. These fibers are very flexible and resilient and essentially are free of "shot" or inorganic particles and short fibers. In contrast, mineral wool insulation is made from melted rock and/or slag and spun into fibers about ½ in. long and 3 to 10 microns in diameter. Typical bulk densities for mechanical mineral wool products are 6 to 10 lb/ft³. Mineral wool insulation products typically have a significant "shot," or particle and short fiber content, of 15 to 30% by weight.

The important aging effect appears to be the degradation of fiber insulation as a result of exposure to the high temperatures of the piping being insulated. Mineral fiber insulations all use a binder to essentially adhere the fibers to one another, thereby forming a fiber matrix that creates the pack of fibers. Binders are usually made from a phenolic resin and typically constitute about 3% by weight²⁻⁷ for LDFG insulation. These binders are hydrophobic in nature but decompose chemically (into gases) at temperatures greater than about 450°F.²⁻⁸ Typical RCS coolant temperatures range from

about 560°F at the vessel inlet to about 620°F at the vessel outlet, well above the fibrous insulation decomposition temperature. Because of the temperature gradient through the fiber pack, only part of the binder decomposes; i.e., only the portion where the insulation temperature exceeds 450°F. On a 600°F surface, this decomposed portion is typically about 1/3 of the total binder content.

A reduction in the binder that cements the fibers together could increase the generation of the very fine debris during a LOCA, which in turn would enhance debris transport to the sump screen or suction strainer. Less binder in the fibrous debris bed could allow the fiber to compact tighter with a corresponding reduction in bed porosity and increase in head loss across the bed. The aging effect would vary with the type insulation (e.g., LDFG insulation compared with mineral wool insulation). Head-loss testing has included tests using fibrous insulation artificially aged by heat-treating the test specimens. A typical heat treatment has been to place the specimen on a 650°F hot plate for a few days (4 days per ASTM C411), thereby heating only one side of the specimen as would occur to insulation installed around a pipe.²⁻⁹ Definitive data regarding the effects of aging on debris generation, transport, and head loss are scarce. Realistically, at this time, it can be said only that the effect could be significant and perhaps substantial for specific types of fibrous insulation.

2.6 Relative Timing and Debris Bed Composition

The relative arrival time of debris onto the sump screens or suction strainers can affect the composition of the accumulated debris and the associated head loss. The head loss also would depend on the timing of the recirculation pump operation and the pool height at activation. The initial formation of a bed of debris on the screens after the activation of recirculation pumping likely would consist of debris located in the sump at the time of the accident and debris transported to the sump in the short term. Debris initially located in the sump could consist of operational debris left in the sump area and LOCA generated debris deposited in the sump during blowdown debris transport. During the period of short-term transport (the first few hours following the break), a majority of the transportable debris

likely would be transported to the sump by the containment sprays (assuming the containment spray systems were activated). In the longer term, debris transport would consist primarily of exposure-generated debris and the erosion of larger non-transportable debris.

2.7 References

- 2-1. NUREG/CR-6762, D. V. Rao, B. C. Letellier, C. Shaffer, S. Ashbaugh, and L. Bartlein, "GSI-191: Parametric Evaluations for Pressurized Water Reactor Recirculation Sump Performance," NUREG/CR-6762, Volume 1, 2002.
D. V. Rao, B. C. Letellier, K. W. Ross, L. S. Bartlein, and M. T. Leonard, "GSI-191 Technical Assessment: Summary and Analysis of U.S. Pressurized Water Reactor Industry Survey Responses and Responses to GL-97-04," NUREG/CR-6762, Volume 2, 2002.
- 2-2. NUREG/CR-2403, Reyer, R., E. Gahan, and J. W. Riddington, "Survey of Insulation Used in Nuclear Power Plants and the Potential for Debris Generation," NUREG/CR-2403, Burns and Roe, Inc. and Sandia National Laboratories, October 1981, and Supplement No 1, July 1982.
- 2-3. WSRC-TR-2001-00067, M. E. Dupont, et al., "Degradation and Failure Characteristics of NPP Containment Protective Coating Systems (U) Interim Report No. 3," Westinghouse Savannah River Company, WSRC-TR-2001-00067, February 2001.
- 2-4. GL-98-04, "Potential for Degradation of the Emergency Core Cooling System and the Containment Spray System After Loss-of-Coolant Accident Because of Construction and Protective Coating Deficiencies and Foreign Material in Containment," NRC Generic Letter to All Holders of Operating Licenses for Nuclear Power Plants, July 14, 1998.
- 2-5. IN-97-13, "Deficient Conditions Associated with Protective Coatings at Nuclear Power Plants," NRC Information Notice, March 24, 1997.
- 2-6. ITS-DDES, J. Bostelman, G. Zigler, and G. Ashley, "Failed Coating Debris Characterization," Prepared for: BWROG Containment Coating Committee, ITS Corporation and Duke Engineering Services, July 21, 1998.
- 2-7. Gordon Hart, "Tests for Long Term Head Loss Across Fiberglass Insulation Debris Using Warm, Alkaline Water," Paper presented to the OECD/NEA Workshop on Sump Screen Clogging, Stockholm, May 10-11, 1999.
- 2-8. "Knowledge Base for Emergency Core Cooling System Recirculation Reliability," Prepared by U.S. Nuclear Regulatory Commission for the Principal Working Group 1 (PWG-1), International Task Group, Committee on the Safety of Nuclear Installations, Organization for Economic Cooperation and development (OECD) Nuclear Energy Agency (NEA), Restricted, NEA/CSNI/R (95) 11, February 1996.
- 2-9. James B. Nystrom, "Extended Head Loss Testing in Alkaline Water of Thermal Insulation used in Nuclear Containments," Alden Research Laboratory, Inc., 72-92/M670F, May 1992.

3.0. DEBRIS GENERATION

This section describes the mechanisms by which the hydrodynamic forces created during a LOCA destroy insulation on neighboring piping and other components, creating debris available for transport to the containment sump.

Experimental measurements of the quantities of debris generated when insulation is subjected to these forces also are summarized. Finally, analytical models for estimating the quantity of debris generated during postulated LOCAs of various sizes and locations within the containment are described.

Critical locations within a PWR containment where the accumulation of debris would adversely affect recirculation performance also are described. What is currently known about the effect of parameters such as insulation type and debris size on the spatial distribution of debris fragments on the surface of the screen is discussed as well. This information was gathered primarily from experimental observations of debris accumulation on simulated PWR sump screens.

Various mechanisms have been postulated for generating debris as a consequence of a postulated LOCA in a PWR. Analysis performed to resolve USI A-43 indicated that dynamic (shock) forces and mechanical erosion caused by impingement of the steam/water jet from the broken pipe on neighboring pipe insulation, equipment coatings, and other structures would be the dominant mechanism for LOCA-generated debris.¹ This finding was retained in the subsequent re-evaluation of LOCA-generated debris in US BWR plants.²

¹ Other mechanisms include acceleration forces associated with pipe whip and mechanical damage caused by the impact of the broken pipe on neighboring structures. The potential for debris generation by these mechanisms was examined in support of the resolution to USI A-43.³⁻¹ This assessment concluded that "jet impingement is by far the most significant of the insulation debris generation mechanisms." Consequently, debris generation from pipe whip and pipe impact is not discussed further in this document

² This includes the NRC contractor analyses summarized in NUREG/CR-6224³⁻² and Utility Resolution Guidance (URG) prepared by the BWR Owners' Group (BWROG).³⁻³ The NRC issued a Safety Evaluation Report (SER) regarding the BWROG URG.³⁻⁴

The physical processes that govern debris generation by this mechanism, particularly as it relates to the damage or destruction of piping and component insulation, are described in Section 3.1. Published data on this subject are summarized in Section 3.2. As is often the case, much of the data collected in US and international research programs were collected in well-instrumented, but idealized, laboratory conditions. Therefore, an analytical method is required to apply the data to the more complex conditions associated with reactor/containment designs with varying configurations and potential debris sources. Useful models and methods for estimating the quantities of debris generated by a postulated LOCA are described in Section 3.3.

3.1 Overview of the Mechanics of Debris Generation

Component insulation is destroyed initially by the blast effects of a shock wave that expands away from the break in the RCS piping when it first opens.³ The strength of the shock wave decays rapidly as it expands away from the break plane because of the increased volume (decreased density) of the expanding steam/water mixture. This initial shock wave may cause substantial damage to even the most heavily reinforced insulating constructions (e.g., steel-jacketed RMI or fiber) if they are located sufficiently close to the break. After the shock wave passes, shear forces and consequential erosion of piping insulation, paint, coatings, and other materials in the wake of the break jet result in additional debris generation.⁴

In an ideal (unobstructed) environment, the shock wave expands away from the break in a spherical pattern. The steam/water jet expands

³ Analysis performed by General Electric for BWR coolant system pressures (1000 psia or 70 bar) suggests a shock wave might not be generated if the break opening time were sufficiently long, as might occur if the "leak-before-break" assumption were adopted [BWROG, 1996].

⁴ The current understanding of debris-generation phenomena is that the initial blast (shock) accompanying rupture of a high-pressure steam- or water-filled pipe does not have a significant effect on such debris sources as equipment or containment surface coatings. However, it would cause substantial resuspension of dirt, dust and other loose particulate material in the area.

away from the break plane in the shape of a cone. Experimental measurements and analytical studies have allowed the pressure distribution within a conical jet to be characterized with reasonable accuracy (see Section 3.1.1.). Unfortunately, the current state of knowledge regarding the specific mechanisms for the damage or destruction of component insulation is not sufficiently complete to discern how near-field shock dynamics and far-field jet erosion combine to dislodge insulation from its initial location and break it apart into debris fragments of various sizes. This is in part because experiments simulating the damage or destruction of piping insulation by impingement of a high-pressure steam/water jet are able to "measure" only the end-state of the insulation material, i.e., the amount of material dislodged from a target location, and the size distribution of fragmented debris (see Section 3.2.) It is not reasonably possible to determine accurately specifically how the fragments were generated.

Another factor that complicates an evaluation of debris generation is the high degree of congestion in close proximity to many candidate break locations in a typical PWR containment. The close proximity of insulated components, containment structures, and other obstacles limits the usefulness of break-jet pressure distributions measured in an idealized,

unobstructed environment. Rarefaction and reflected expansion waves are generated as the shock front encounters obstacles in its path. The steam/water jet also may impact neighboring obstacles, redirecting flow from portions of the jet and possibly dissipating some of its energy.

These complications, combined with the possibility that the break plane can move in space because of the motion of the ruptured pipe, cause the set of potential insulation "targets" to be rather large. Various analytical methods for characterizing the ZOI within which insulation might be damaged have been proposed as described in Section 3.3. These methods each attempt to correlate the energy contained in the steam/water jet to a region in space within which the jet pressure would be large enough to cause damage to various types of insulation material. In all cases, the extent of damage becomes less severe with distance from the break location. As shown in Figure 3-1, these factors lead to a damage pattern resembling concentric rings emanating from the postulated break location. The boundaries of these rings can be either conical or spherical, depending on the specific modeling assumptions used to define the ZOI. Alternative models for estimating the shapes and dimensions of these rings are described in Section 3.3

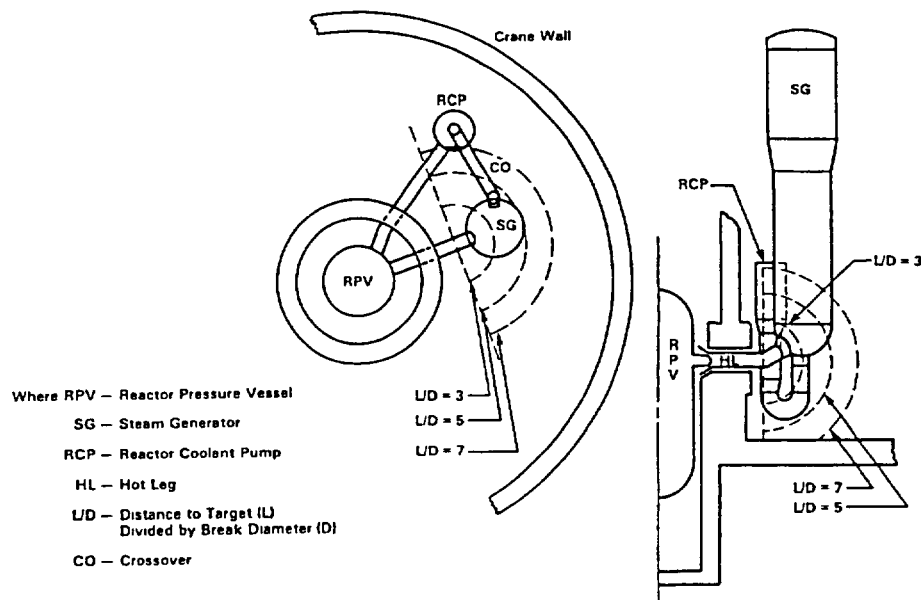


Figure 3-1 Example ZOI at a Postulated Break Location³⁻⁵

The extent of damage to insulation positioned at a given distance from the break depends on the following.

- The physical properties of the insulation component and its installation hardware
 - The material used to form the core of the insulation component (e.g., fiberglass with a blanket, layered metal sheeting within a cassette)
 - The composition and thickness of the insulation enclosure [e.g., steel jacket(s), woven fiber matting]
 - The construction and mechanical properties of the component installation hardware (e.g., banding, closure clasps, wire retainers)
- The orientation of the insulation relative to the jet⁵
- The exposure history of the insulation (thermal and radiation environment)⁶

These factors combine to affect the “damage pressure” for a particular insulating construction. “Damage pressure” is a characteristic of a particular insulating material and method of installation. It represents the maximum distance from the break plane at which an insulation blanket (if fiber) or cassette (if RMI) has been observed in controlled experiments to be dislodged from piping and break into smaller fragments (i.e., the distance where the jet pressure drops below the minimum pressure that can cause damage to the insulation).

In some analyses, this characteristic is measured simply in terms of the maximum number of pipe diameters away from the break plane where damage has been observed

⁵ Orientation has often been ignored in characterizing debris generation; however, as described in Section 3.2, the orientation of the seams of steel jacketing on fiber or calcium-silicate insulation can affect the extent of damage significantly.

⁶ Exposure of some forms of insulation to sustained high temperatures and/or radiation fields can cause the base insulation materials to become brittle. For example, the binding compounds used in some types of insulation can break down under sustained heating. The resulting changes in the mechanical properties of the insulation can lead to a decrease in its characteristic damage pressure and increase the proportion of small debris fragments.

experimentally.⁷ Another method for expressing the threshold for damage is to correlate the distance from the break to the stagnation pressure of the jet at that location (thus, the term damage “pressure”). Analytical models for associating the distance at which insulation damage is measured to stagnation pressure are described in Section 3.3. Damage pressures for various types of insulation are summarized in Table 3-1.

The term “destruction” pressure has been used interchangeably in the past (specifically during the BWR resolution studies) with “damage” pressure but herein the term “damage” pressure has been preferred to acknowledge that this pressure is a threshold pressure and that the destruction of insulation is incomplete at this pressure. The extent of damage increases as local pressures increase. The extent of damage within a ZOI is very dependent upon the type of insulation. Some more fragile types of insulations (e.g., calcium silicate) would likely be more extensively damaged than a less fragile type (e.g., RMI) in term of the fraction of the ZOI insulation turned into very fine or small debris. This subject is discussed further in Section 3.3.3.

The damage pressure also depends on (1) whether the insulation is jacketed, (2) the material and number of layers of jacketing, and (3) the orientation of the jacket seams relative to the axis of the break. The insulation jacket may provide some protection to the insulation (but not in all cases), which would be reflected in an increase in the damage pressure. The orientation of the jacket seam relative to the jet has been found to affect the damage pressure profoundly. At a seam orientation of 45°, the jacket can be opened up at the seam much more easily than if the seam was on opposite side from the jet (180°). In reality, the damage to insulation within the ZOI could be rather chaotic because the jet would impact insulation at a variety of seam and pipe orientations. Insulation closer to the jet but with its jacket seam opposite the jet might survive, whereas insulation further out was destroyed because its seam was oriented toward the jet.

⁷ Distance is expressed in terms of L/D, where L/D is the number of pipe diameters (D) away from the (guillotine) break plane where the insulating construction is positioned.

Insulating Construction (Fibrous)	Damage Pressure (psi)	Insulating Construction (RMI)	Damage Pressure (psi)
Min-K	4	Mirror [®] /std bands	4
Koolphen-K	6	Mirror [®] /Sure-hold [®] band	150
Unjacketed Nukon [®]	10	Transco RMI	190
Jacketed Nukon [®] /std bands	10	Darchem DARMET	190
Knaupf	10		
Temp-Mat/SS wire retainer	17	Insulating Construction (Other)	Damage Pressure (psi)
K-wool	40	Calcium-silicate/aluminum jacketing	20
Jacketed Nukon [®] /Sure-hold [®] bands	150		

*The listing of insulating materials, with the exception of the calcium-silicate pressure, was derived from responses to an NEI survey³⁻⁶ and industry responses to GL 97-04,³⁻⁷ information obtained from these sources is summarized in Ref. 3-10. The listed values for damage pressure are the minimum of those reported by the BWROG in its URG documents³⁻³ and the results of confirmatory analysis performed by NRC and documented in Appendix B of Ref. 3-4. These data were based on air-jet testing. The aluminum-jacketed calcium-silicate pressure of 20 psi was determined from the OPG two-phase (steam with droplets) jet test data (Section 3.2.2.5), which is considerably lower than the BWROG air-jet test result of 160 psi. The OPG test data indicate lower damage pressures when the jet is a two-phase jet rather than an air jet. Further, the damage pressure for the jacketed calcium-silicate depended on the seam angle, and the 20-psi value was based on the optimum seam angle for damage.

Finally, the hardware used to mount an insulation blanket or cassette to piping can affect its resistance to jet forces significantly. For example, tests performed by the BWROG indicated that Sure-hold[®] bands had significantly better mechanical properties than standard bands with common closure clasps. As indicated in Table 3-1, application of the Sure-hold[®] bands resulted in an approximately 30-fold increase in the damage pressure for Nukon[®] fiberglass blankets and DPSC Mirror[®] RMI.

A common way to measure the extent of damage inflicted on component insulation during jet impact tests is to sort the resulting debris into various sizes. Increasing local pressure causes the base insulation material to fragment into smaller pieces. The resulting size distribution of debris fragments is important for evaluating the efficiency of debris transport to the recirculation sump (see Sections 4 and 5), debris accumulation profiles on the sump screen (see Section 6), and finally, screen head loss (see Section 7). Standard schemes for classifying debris sizes and shapes are described in Section 3.1.2. The available data on debris-size distributions for various insulating material are summarized in Section 3.2

3.1.1 Break-Jet Phenomena

The shape of the break jet and its orientation in space depend on several factors. The most important factors are

- the size and configuration of the pipe rupture,
- the break effluent (steam, water or a two-phase mixture), and
- the size and orientation of neighboring obstacles.

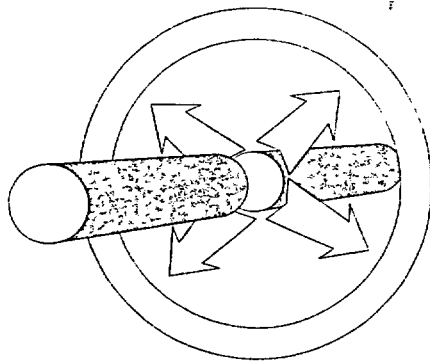
The effects of these factors on a free-expanding jet can be summarized as follows.

3.1.1.1 Size/Configuration of Pipe Rupture

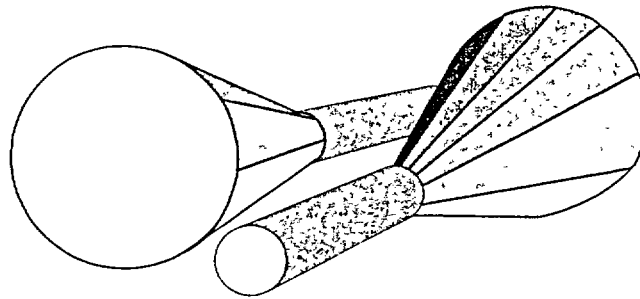
The total volume and shape of the jet emerging from a ruptured pipe depends on the size of the ruptured pipe, the shape and area of the opening in the pipe, and (for DEGBs) the relative positions of the opposing pipe ends. Two examples are shown in Figure 3-2.

3.1.1.2 Break Effluent

The thermodynamic state of the break effluent has been found to have an important effect on the rate at which jet pressure decays with distance from the break plane and the extent to which the jet expands in the radial direction. At any location along the jet centerline (beyond one pipe diameter), the local pressure for a two-phase jet (i.e., a steam/water mixture) is less than that for a steam-only jet with the same initial stagnation pressure.³⁻⁸ Further, the cross-sectional area of the jet is larger for a steam-only jet than for a two-phase jet with the same initial stagnation pressure.³⁻⁹



100% pipe separation, 0% offset



100% pipe separation, and 100% offset

Figure 3-2 Variation in the ZOI Shape with DEGB Separation and Offset

3.1.1.3 Obstacles

Postulated breaks in the coolant system piping are not likely to occur at locations in the containment where there is an unobstructed, clean, line-of-sight view of insulation on neighboring components. Walls, floors, catwalks, and other structures may interfere with the trajectory of fluid emerging from a ruptured pipe. Structures close to the break can cause the standing shock wave at the break exit to be reflected, increasing local pressures. Large structures further away from the break can divert subsonic jet flow significantly, changing the overall volume and shape of the area impacted by the break effluent. A large obstacle such as a floor, wall, or large vessel (e.g., steam generator) can cast a large "shadow," preventing jet forces from affecting insulation on components on its opposite side. These factors, combined with the high degree of congestion in many locations of the containment, cause the overall region of space affected by a ruptured pipe to be much different in terms of the impacted volume shape and size than the volume swept out by an imaginary cone protruding from the break plane. These factors are taken into account in developing models to characterize the shape and dimension of the ZOI surrounding a postulated break (see Section 3.3.)

3.1.2 Debris Classification

To handle the differences in generation and transport effectively, LOCA-generated debris is classified into distinct debris groups: fibrous insulation debris, RMI insulation debris,

particulate insulation debris,⁸ foam or rubber insulation debris, failed coatings debris, miscellaneous particulate, and miscellaneous operational material debris (examples are given in Section 2). Each of these groups generates debris of various sizes because of the variability in the break jet, the installed configuration of material, and other factors described above.⁹ The size distributions of these debris species, as well as other characteristics, play an important role in transport efficiency and sump-screen accumulation patterns (see Sections 4, 5, and 6, respectively) and therefore directly affect sump performance. This effect can be illustrated by contrasting the two very different sizes of fibrous debris: fine fibers (or fines) and large fibrous mat fragments.

Fines are transported easily to the containment floor and tend to remain suspended in the pool of water for prolonged periods of time. These characteristics greatly increase the potential for fines to be transported to, and collect on, the sump screen. Large fibrous fragments can

⁸ Calcium-silicate insulation is a common type of a particulate insulation; other types include asbestos, Unibestos, Min-K, Microtherm, and gypsum board.³⁻¹⁰

⁹ The size distribution of particulate matter may not be a concern in the assessment of sump-screen blockage, and this type of debris has often been treated as simply "particulate." However, the size of individual particles can vary considerably—from common dirt/dust with characteristic diameters on the order of micro-meters to granules of ablated concrete with diameters on the order of millimeters. The size distribution could be important in a transport analysis performed to reduce the assumed complete transport of the particulate to the sump screen.

become attached to structures or captured by floor grating at upper elevations of the containment and therefore may not be transported easily to the containment floor. If these fragments reach the floor, they tend to either float or (if saturated with water) sink to the floor of the pool of water. Relatively high local pool velocities are required to move large fragments to the screen, where they tend to collect near the base of a vertical screen, leaving the upper portions of the screen free of debris (of similar size). Additionally, fines tend to form more compact and uniform beds on the screen, resulting in larger pressure drops than beds of similar thickness formed by larger fragments.

3.1.2.1 Size Classification of Fibrous Debris

The results of debris-generation experiments involving fibrous insulating materials demonstrate that impingement of a high-pressure jet onto fibrous insulation (jacketed or not) generates debris that spans a wide range of sizes—from individual fibers to intact or nearly intact pillows. A scheme for classifying the size of fibrous debris was developed in the NRC's evaluation of debris generation for BWRs.¹⁰ Because the transport and head loss properties of fibrous debris depend on the debris shape and size, these physical characteristics are used to describe the various "classes" of debris generated when fibrous insulation is subjected to jet blasts of variable intensity. The size classification scheme is summarized in Table 3-2. Photographs of fibrous debris in Classes 3 and 5 are shown in Figure 3-3.

3.1.2.2 Size Classification of RMI Debris

The internal construction of a typical RMI cassette is shown in Figure 3-4. Transportable debris generated from this type of construction typically consists of small crumpled sheets of

¹⁰ Actually, a number of classification schemes have been devised through the years to meet the particular needs of a test program or analysis; they range from two general groupings (fines and everything else) to the NRC seven-group scheme. Some translating between the size classification schemes may have to be done while comparing studies on the base of knowledge. For example, fine debris has been used to describe everything in the NRC classification from Classes 1 through 6, but in other analyses, the fines only cover debris that would always remain suspended. For PWR analyses, it is important to distinguish between suspended and nonsuspended debris

the internal foil, which resembles shrapnel. Figure 3-5 is a photograph of cut pieces of RMI foil (roughly 2 in. square) and crumpled "debris."






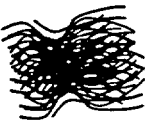

The spectrum of debris sizes typically observed in blast tests involving this type of insulation is more limited than that observed with fibrous insulation. A structured RMI debris-size classification was not developed in the NRC study of BWR strainer performance. However, four broad classes can be suggested based on observations of RMI debris generation tests (see Section 3.2) and are described in Table 3-3.

As described in the next section, the size distribution of RMI debris depends on the material used (aluminum vs stainless steel) and the cassette construction (banding, type of closure clasps, etc.).

3.2 Debris-Generation Testing

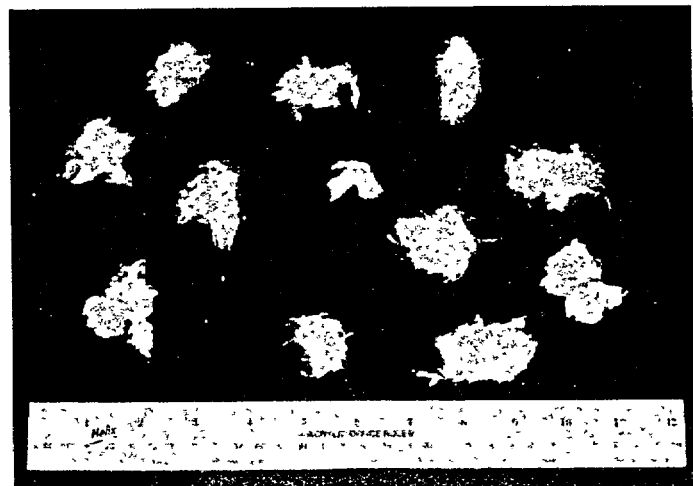
Investigators in several countries have performed experimental simulations of jet-blast impingement onto RCS insulation of various shapes, materials, and construction. One distinguishing feature of these tests is the jet effluent (air or steam/water). For reasons of economy, many early experimental studies of the destructive forces on RCS insulation materials were performed using high-pressure air jets rather than two-phase (steam/water) jets. However, analysis performed in support of a parametric evaluation of PWR recirculation sump performance³⁻²⁴ indicates that the ZOI associated with prototypic two-phase (steam/water) jets is larger than the ZOI indicated by air-jet simulant tests¹¹ and that the debris generated would be somewhat finer³⁻¹¹. The specific cause of these differences is not well understood. Further work in this area is needed to fully explain the observed effects. Nevertheless, it is generally agreed that some adjustment should be made to the results of the air-jet tests to interpret the results properly for use in reactor containment conditions. The following summaries of debris-generation testing separate the results obtained from air jets and those obtained with more prototypic steam/water jets.

¹¹ The radius of the ZOI in the parametric study was increased to 12D from the BWROG radius of 10 4D, corresponding to a lowering of the damage pressure from 6 to 4 psi. This increase in the ZOI radius increased the volume of the spherical ZOI by 50%

Table 3-2 Size Classification Scheme for Fibrous Debris ³⁻²		
No.	Description	
1		Very small pieces of fiberglass material; "microscopic" fines that appear to be cylinders of varying L/D
2		Single, flexible strands of fiberglass; essentially acts as a suspending strand.
3		Multiple attached or interwoven strands that exhibit considerable flexibility and that, because of random orientations induced by turbulent drag, can exhibit low settling velocities.
4		Fiber clusters that have more rigidity than Class 3 debris and that react to drag forces as a semi-rigid body.
5		Clumps of fibrous debris that have been noted to sink when saturated with water. Generated by different methods by various researchers but easily created by manual shredding of fiber matting.
6		Larger clumps of fibers lying between Classes 5 and 7.
7		Fragments of fiber that retain some aspects of the original rectangular construction of the fiber matting. Typically pre-cut pieces of a large blanket to simulate moderate-size segments of original blanket



Fiberglass shreds in size Class 3



Fiberglass shreds in size Class 5

Figure 3-3. Fiberglass Insulation Debris of Two Example Size Classes

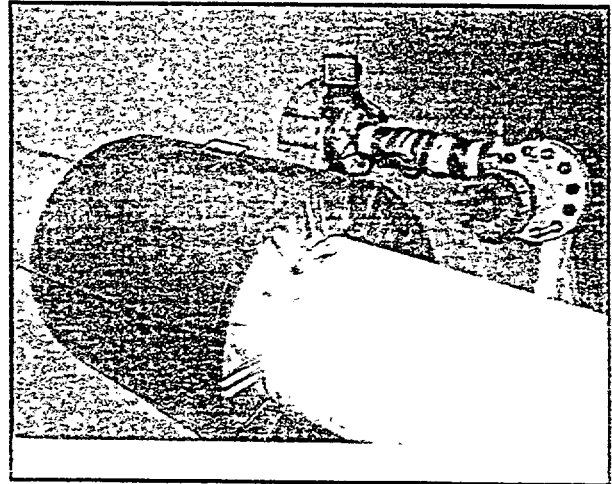
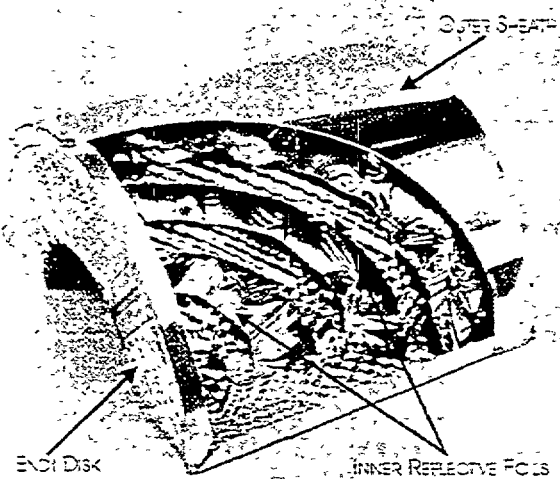




Figure 3-4 Inner Construction and Installation of a Typical RMI Cassette³⁻³



Figure 3-5 RMI Foil Before/After "Crumpling" (Left) and Crumpled RMI Foil Debris (Right)

No.	Description	
1		Small crumpled pieces of RMI foil typically 0.5 to 1.0 in across. The crumpled foils transport more readily than flat foils and tend to "roll" along the floor of moving pool of water.
2		Small flat pieces of RMI foil typically 2 in across
3	Photo not available for this type of debris	Large wrapped or crumpled pieces of RMI foil or crushed sections of the outer casing of the original cassette.
4	Photo not available for this type of debris	Large flat sheets of RMI foil.

3.2.1 Air-Jet Testing

3.2.1.1 NRC BWR Drywell Inertial Capture Tests³⁻¹²

The NRC commissioned Science and Engineering Associates, Inc. (SEA) to perform a series of tests designed to measure the extent to which LOCA-generated debris would be captured on structures internal to the drywell of a BWR during the blowdown period of a LOCA. One portion of these tests involved measurements of debris generation, transport, and inertial capture of typical BWR piping insulation materials. The tests were performed at the Colorado Engineering Experiment Station, Inc. (CEESI), which has an 11,000-ft³ air-storage tank and air-blast test chamber that can be used to simulate jet impingement (and debris-transport) conditions. Exhaust air exiting the far end of the test chamber passed through a fine mesh screen (1/8-in. mesh) to capture debris that was not collected on the simulated typical drywell structures placed downstream of the target pipe. Debris-generation and transport tests were conducted at nozzle stagnation pressures of approximately 1000 psig. The test facility is shown in Figure 3-6.

Although the primary objective of these tests was to study inertial capture of debris on drywell structures, data also were collected that provide insights into the amount and size distribution of

fibrous debris.¹² The target material in the NRC/SEA tests conducted at CEESI was Transco fiberglass insulation encased in a tough canvas bag and designed to wrap around a pipe. Each blanket was 3 ft long and approximately 3 in. thick. The blankets were held in place by canvas straps and supported by three stainless-steel bands and two end supports to prevent axial movement along the target assembly. The Transco blankets each had two seams (i.e., each blanket was formed from two half-sections) that were arranged so that the seams were aligned with the top and bottom of the pipe 90° from the jet centerline.

Debris fragments found dispersed through the test apparatus were collected and sorted according to their size and material composition. Seven debris classes were collected.

- A. Canvassed insulation consisting of large sections of canvas covers encapsulating insulation (protecting insulation)
- B. Insulation attached to Class A debris but extruding from the canvas (unprotected insulation)
- C. Large (greater than hand-size) pieces of exposed insulation
- D. Medium (less than hand-size but smaller than grating mesh) pieces of exposed insulation

¹² These tests did not examine jet impingement on RMI cassettes

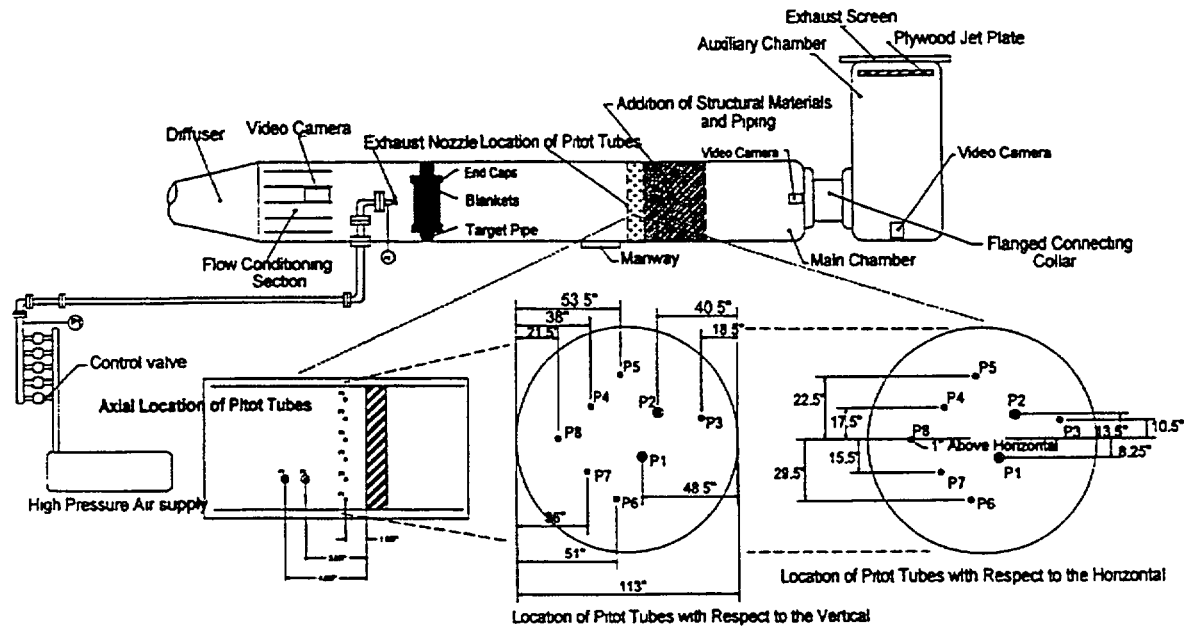


Figure 3-6 Configuration of the CEESI Test Facility for the NRC/SEA BWR Drywell Debris-Transport Tests

- E. Small (smaller than grating mesh) pieces of exposed insulation
- F. Pieces of shredded canvas without insulation
- G. Agglomerated debris consisting of a tangled mix of canvas and insulation

The findings related to fibrous-debris generation are summarized in the following paragraphs.

The target blankets were destroyed completely or nearly completely by the air blast, and the degree of destruction was generally similar among the various tests.¹³ From 15 to 25% of the original blanket insulation mass was

classified as nonrecoverable mass; i.e., the fibrous debris either exited the test chamber through a fine mesh screen or was too fine to collect by hand. This nonrecoverable mass translates into a generation of debris fine enough to remain suspended in a pool of water indefinitely that averages about 20% of the insulation in a totally destroyed blanket. Usually one relatively large section of canvas was found on the floor near the target or hanging on the continuous grating downstream of the target mounting). This section of canvas sometimes had a substantial quantity of fiberglass attached to it (45% of the total in one test) However, in some tests, this canvas was empty of fiberglass.

¹³ Because the main test objective was the study of debris transport, the blankets were positioned and oriented to maximize destruction, thereby creating more debris for transport. Positioning an insulation target blanket closer to the jet nozzle increased the pressure that the air jet applied to the target, hence increasing the damage to the insulation. However, if the blanket were placed too close, the ends of the target would extend beyond the flow of air from the jet so that some of the target would escape serious damage, e.g., placing the target directly in front of the jet and very close to the jet would destroy the center of the blanket but not the entire blanket. A distance was found that allowed each blanket to be essentially totally destroyed

3.2.1.2 BWROG Air-Jet Impact Testing (AJIT)³⁻³

General Electric Nuclear Energy (GE) conducted tests at CEESI to examine the failure characteristics of fibrous insulation and RMI when they are subjected to jet impingement forces. The tests also provided data on the size distribution of the resulting debris. CEESI has compressed air facilities with 11,000 ft³ of storage at 2500 psia. Insulation samples were mounted inside a wind tunnel with a perforated plate (containing 1/8-in. holes) covering an 86-in. man-way at its exit, thus allowing air to be

discharged from the facility but keeping most of the insulation debris within the test chamber. Debris-generation tests were conducted under conditions that resulted in a choked-flow stagnation pressure at the 3-in. exhaust nozzle of 1110 psig (+25/-100), simulating coolant circuit conditions in a BWR.

A total of 77 tests were performed involving four broad classes of insulation: aluminum RMI, stainless-steel RMI, fibrous insulation, and lead shielding. Four of the tests were designed to measure target pipe stagnation pressure at various distances from the jet nozzle. The insulating materials used, as well as their construction and installation, conformed to vendor standards. The following vendors and product names were examined.

RMI

Transco Products, Inc. (TPI)
 Diamond Power Specialty Company (DPSC)
 Mirror®
 Darchem Engineering, Ltd. DARMET

Fiber

NUKON® blankets (jacketed and unjacketed)
 Min-K (unjacketed)
 Temp-Mat™ (unjacketed)
 K-Wool (unjacketed)
 Knaufl® (jacketed and unjacketed)

Other

Calcium-silicate
 Koolphen-K® closed-cell phenolic with anti-sweat jacketing

The distances from the break nozzle ranged from an L/D of 2.5 to an L/D of 116.3. The general test conclusions were summarized as follows.³⁻³

Throughout the AJIT Program testing, the inner and outer sheaths of reflective metallic insulation and stainless steel jacketing used on fibrous insulation did not fail in a manner, which would contribute to transportable debris. Tests of RMI conducted at distances of 2.4 L/D (7.25 in.) resulted in deformation of the cassette outer sheath but did not cause the stainless steel to be penetrated. In tests that did generate transportable reflective foil debris, the debris occurred due to the separation of the outer sheath

of the RMI cassette from the cassette side and/or (end) disk panels. The tests that generated the largest amounts of transportable debris resulted when the outer sheath or jacketing material was completely separated from the internal or jacketed insulation.

Debris generation resulting from an RMI assembly or jacketed fibrous insulation material was typically due to failure of the fastening mechanism of the assembly. Latch and strike mechanism failures occurred in 76% of the tests conducted which used latch and strike attachment mechanisms (32 of 42 tests). The latch and strike failures included straightening of the "J" hook on the strike, failure of the latch assembly (i.e., the locking clip and articulated latch hook breaking into component parts), and compression of the outer sheath or jacket to dimensions where the latch and strike were capable of release without damage to the latch and strike.

With the exception of the testing performed on Darchem DARMET® RMI (with Cam-Lock® latches and strikes) and aluminum jacketed calcium-silicate insulation, failure of the latch and strikes occurred out to distances of 100 L/D (300 in.). This corresponds to a target pipe stagnation pressure of approximately 4 psig. In the case of fibrous insulation materials, the use of jacketing as a means of reducing debris generation does not appear to be effective without the use of an additional banding material, which better secures the jacketing to the insulation assembly and the pipe.

The following values for damage pressure were recommended for fibrous and other (non-RMI) insulation materials.

Calcium-Silicate	160 psig
K-Wool	40 psig
Temp-Mat™	17 psig
Knaufl® Fiberglass	10 psig
NUKON® Fiberglass (jacketed and unjacketed)	10 psig
Koolphen-K®	6 psig
Min-K	4 psig

3.2.2 Steam and Two-Phase Jet Testing

A large body of experimental work related to debris generation has been performed in facilities using steam or two-phase (steam/water) jets. These facilities are located in the U.S., Germany, Sweden, and Canada. The published test data are summarized in the following sections.

3.2.2.1 Marviken Full-Scale Containment Experiments³⁻¹³

The Marviken Power Plant originally was designed and built as a boiling, heavy-water, direct-cycle reactor with natural circulation and provisions for nuclear superheating of steam. It was constructed and tested up to light-water commissioning tests but was never charged with nuclear fuel. The facility subsequently was used for a wide range of containment safety experiments, among which were several high-pressure blowdown experiments in which damage to equipment paint, containment (concrete) coatings, and component insulation was examined.

A series of blowdown experiments was performed between 1972 and 1973 to examine the (BWR) pressure suppression containment response and iodine transport within the containment during a simulated pipe break. These experiments also provided useful information on the extent to which containment paint and thermal insulation materials were damaged from the resulting break flow.

Components inside the containment were insulated with jacketed and unjacketed rockwool and calcium-silicate. The locations and orientations of the insulation relative to the break were not measured quantitatively; rather, the initial conditions were described in qualitative terms and with schematic (isometric) layout diagrams. The simulated pipe break also was not configured in a manner that created a coherent jet. Rather, the break plane was oriented vertically, and the break effluent impacted a horizontal deflector plate to disperse flow throughout the containment atmosphere. As noted above, the primary purpose of these tests was to examine containment thermodynamic response and bulk transport of iodine; the evaluation of insulation damage was a secondary consideration.

Qualitative observations and photographs of the extent of damage to insulation were recorded. The major findings include the following.

- Significant damage was observed to all forms of insulation in close proximity to the break location (within a few meters). In some locations, material was completely removed from its original mounted positions, and large amounts of insulation debris were found large distances from the break.
- Sheets of aluminum jacketing were stripped from some locations and were found crumpled at large distances from their initial locations.
- Test pieces shielded from the break by large concrete structures were not destroyed.

3.2.2.2 HDR Tests³⁻⁵

The Heissdampfreaktor (HDR) facility is a decommissioned BWR nuclear facility in Karlsruhe, Germany, that was refit in the late 1970s for light-water-reactor research. The reactor internals were removed, and the facility was decontaminated. New equipment was installed specifically for reactor blowdown simulations in a small, but authentic, reactor containment facility. The initial thermodynamic state developed in the test vessel for blowdown simulations is 110 bar (~1600 psia) and 310°C (323°F).

Among the tests performed in the HDR (and documented in NUREG-0897³⁻⁵) were blowdown simulations specifically designed to evaluate the extent of damage to RMI and fiberglass blanket insulation during blowdown. One test (described in Appendix C of NUREG-0897) involved four specimens of stainless-steel Mirror[®] cassettes with fasteners installed according to manufacturer specifications. In a second series of two tests, NUKON[®] blankets were installed.¹⁴

The test specimens were installed on target piping or rectangular steel struts located at various positions in the HDR containment. The distance from the break nozzle and insulation samples spanned a wide range but was generally less than 7D.

¹⁴ Jacketed and unjacketed samples were used in the NUKON[®] tests

It is important to note that a deflection plate was positioned approximately 4 ft away from the break nozzle (450 mm inner diameter nozzle with break initiated using rupture disks) in the HDR tests to protect the containment wall. Therefore, the deflection plate distributed the break flow to the surrounding area, rather than the flow bearing down upon target material as a coherent jet.

The major observations made from these tests can be summarized as follows.

- The stainless-steel Mirror[®] insulation remained essentially intact when it was installed at distances greater than 7D from the break. The single sample installed closer to the break (approximately 2D) was torn apart. The outer casing was heavily damaged and compressed against neighboring structures. The inner stainless-steel foils were ripped from the casing and crumpled into relatively small pieces.
- Unjacketed NUKON[®] blankets positioned within 7D of the break were destroyed, with weight losses of the internal wool of 85 to 100%. Blankets jacketed with 22-gage stainless steel and installed at similar positions experienced less damage, with weight losses ranging from 7% to 75%.
- Flat NUKON[®] blankets covered with a metal mesh jacketing and placed above the impingement plate at a distance of 7.4D were totally destroyed.

3.2.2.3 Karlsruhn Caposil and Newtherm Tests^{3-14,3-15,3-16}

A series of steam-jet impact tests was conducted by Studsvik in 1993 to determine the extent to which blocks of calcium-silicate insulation material would be eroded at various distances from a postulated steam-line break. The specific material examined in these tests was Caposil HT1 and Newtherm 1000. The Caposil HT1 material was supplied by the Ringhals and Oskarshamn nuclear power plants; the Newtherm 1000 material was provided by Ringhals and ABB-Atom. The materials were tested in both aged and unaged (new installation) conditions. The aged insulation had been in service at one of the power plants at temperatures of 290°C (553°F) for approximately 15 yr.

Samples of material were cut and mounted into a firm steel casing and then mounted downstream of a steam jet. Tests were conducted in which the jet impacted the samples at 90° (i.e., perpendicular) to the sample and 45° from the sample surface. Erosion patterns on the samples were noted, and debris stripped from the sample blocks was collected for analysis. Tests were conducted with the jet positioned between 2 and 10 break-diameters from the sample. All tests involved steam jets delivered from a high-pressure storage tank at 80 bar (1160 psia) and 280°C (535°F).

Observations made from these tests included the following.

- The radius of the eroded zone was found to be roughly equal to the distance of the break plane from the material surface. This observation is consistent with the conceptual picture of an expanding 90° conical free jet.
- The stagnation pressure at the "erosion limit" (i.e., the maximum distance from the break where significant erosion was observed) was found to be 1.67 bar (24 psia).
- The extent of material erosion increased with decreasing distance from the break plane. The sample blocks were destroyed or broken into several pieces at distances of less than 5 nozzle diameters.
- The wear loss of Caposil HT1 was found to be less than that of unaged Newtherm 1000 for the same exposure time.

A series of four tests was conducted in a closed container with a filtered exhaust so that debris fragments could be collected and analyzed. After these tests, collected debris was sorted into three size bins for subsequent processing.

- Pieces picked up by hand
- Slurry separated using a 2-mm net
- "Fines" suspended in water.

ABB analyzed the particles for four cases as summarized in Table 3-4.

The "flow density" (steam mass flux) was higher in Tests 1 and 2 compared with Tests 3 and 4. This difference is cited as the reason for the lower fraction of large particle sizes in Tests 3 and 4. A deficit of approximately 10% of the

Table 3-4 Measured Particle-Size Distribution from Newtherm 1000 (Calcium-Silicate) Erosion Tests ³⁻¹⁶						
Test No.	Mass of Material (g)					
	Particle Size (µm)			Total	Quantity Before Test	Per Cent Lost
	> 850	20-850	< 20			
1	1135.3	43.8	71.1	1250.2	1475.4	15.3
2	1002.4	77.6	73.6	1153.6	1404.5	17.9
3	775	148.5	165.0	1088.5	1407.8	22.7
4	841.4	94.0	198.7	1134.1	1402.8	19.2

original insulating material mass was found in the total mass of debris collected in these experiments. This “mass” was ejected from the experimental facility (in spite of the exhaust filter) and is assumed to be “fine” particles.

3.2.2.4 Siemens Metallic Insulation Jet Impact Tests (MIJITs)^{3-17,3-18}

Between October 1994 and February 1995, the Swedish Nuclear Utilities conducted metallic insulation jet impact tests (MIJITs) at the Siemens AG Power Generation Group (KWU) test facility in Karlstein am Main, Germany. Although the Swedish tests were reasonably extensive, only a general summary of the test results was released. Specific test data from the RMI debris generation tests were not made publicly available. In addition, the data are not directly applicable to US power plants because the European RMI design was substantially different from the RMI currently installed in US power plants.

In 1995, the NRC conducted a single debris-generation test to generate representative RMI debris to obtain insights and data on the effects of RMI relative to US plants. These tests were contracted to Siemens AG/KWU in Karlstein, Germany.

Each of the Swedish tests examined the performance of RMI used in European nuclear stations, which was manufactured by Grünzweig and Hartmann or Darchem Engineering. The NRC test was performed using RMI cassettes frequently found in US nuclear plants. The NRC samples were provided by DPSC, the manufacturer of Mirror® RMI cassettes. The tests were performed with high-pressure, saturated water and (separately) saturated steam. The facility consisted of a tall vessel and a blowdown line with a double rupture disk and orifice (break plane) mounted at its end. Target insulation materials were installed on a 10-in.

pipe that was positioned downstream of the simulated break at distances up to 25 break-pipe diameters. The orientation and position of the target pipe relative to the jet centerline could be changed to examine the effects of an asymmetric jet impingement.

A total of seven saturated water tests and nine saturated steam tests were performed in the Swedish test program. The following observations were recorded in publicly distributed reports.

- All insulation panels directly impacted by the steam jet (up to L/D = 25) were destroyed.
- Insulation outside the core of the steam jet was not fragmented.
- The degree of destruction caused by saturated water jets was much less than that caused by saturated steam jets. Damage tended to take the form of crumpling the RMI panels rather than fragmenting them into small pieces. Panel disintegration was observed (with a water jet) only when the target became stuck in the mounting trestle and remained in the core of the jet during the 30-s blowdown. In this case, a small percentage of the panel was fragmented.

The NRC test was conducted on May 31, 1995. Most of the RMI debris was recovered and categorized by the location where it was found. Approximately 91% of the debris was recovered as loose foil pieces; the remainder was found wedged in place among the structures. The debris was analyzed with respect to size distribution. The overall size distribution for the total recovered debris mass is shown in Figure 3-7. A photograph of the RMI debris generated by this test where the RMI panel was positioned directly over the break is shown in Figure 3-8.

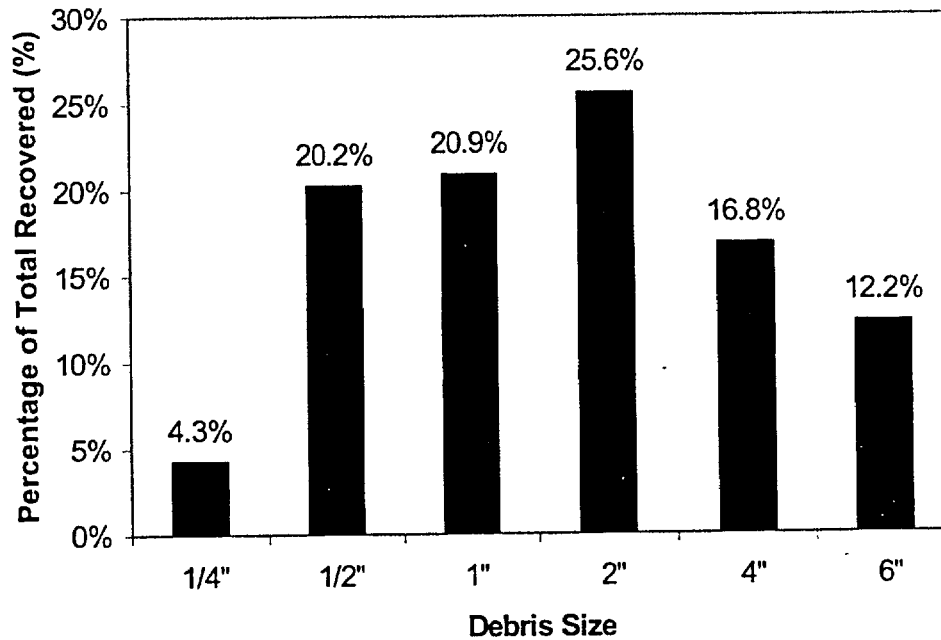


Figure 3-7 Typical RMI Debris Generated by Large Pipe Break

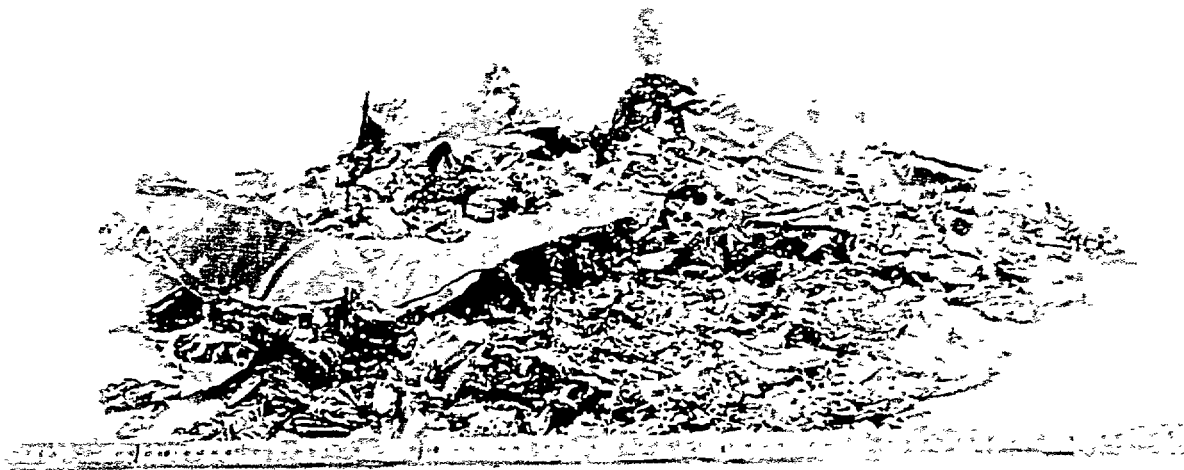


Figure 3-8 RMI Debris Observed in Siemens Steam-Jet Impact Tests

3.2.2.5 Ontario Power Generation Tests³⁻¹⁹

The OPG testing program was designed to address debris generation by two-phase jets created during a PWR blowdown through postulated breaks. The principal insulation of concern was aluminum-clad calcium-silicate; however, data from a single test performed with jacketed fiberglass also was made available to the NRC. In addition to broad objectives to collect data related to debris generation, an

additional (NRC) objective¹⁵ was to compare the insulation damage behaviors between the two-phase OPG tests and the BWROG AJIT tests.

The OPG jet-impact test rig consisted of a tank with a capacity of approximately 2.2 m³ filled with heated, pressurized water. A 3-in. schedule-160 nozzle was connected to the tank by a rupture-disk triggering mechanism,

¹⁵ The NRC contributed funding to the OPG tests

associated piping, and instrumentation. A robust sample-holding frame held the insulation in front of the nozzle at a predetermined position and orientation. A debris catch cage approximately 12 ft³ in volume surrounded the nozzle and target to capture insulation debris for analysis.

With the 3-in. nozzle, the duration of the blowdown was approximately 10 s when the tank was filled initially with saturated water at a pressure of 10 MPa (1450 psia). Typical initial conditions for the tests were 324°F and 1417 psig.

Calcium-Silicate Tests

The target insulation was mounted on two 2-in. schedule-160 pipes. Figure 3-9 is a photograph of a typical mounting configuration. The insulation targets were 48 in. long and 1 in. thick; thus, the target outer diameter was 4.375 in. A 0.016-in.-thick aluminum cladding surrounded the insulation. The cladding and banding specifications were based on large-scale piping used in OPG's (CANDU) nuclear plants. Two or three sections of cladding (depending on the test) were required because the standard cladding length was 24 in. Thus, each target had one or two circumferential seams in addition to a longitudinal seam running its length. For calcium-silicate targets, the bands were stainless steel with a thickness of 0.020 in. and standard crimp connectors. For the single fiberglass test, the bands were 0.5 in. wide and 0.05 in. thick. The average spacing between bands¹⁶ was 6.5 in.

The longitudinal seam was oriented at an angle relative to the jet centerline. The targets were always mounted with their centerlines perpendicular to the jet centerline. The convention used was 0° at the front, 90° on the top, 180° at the rear, and 270° at the bottom. Most tests were conducted at an angle of 45°.

Because clad failure was found to be sensitive to the angle of the longitudinal seam, a few tests were performed in which a second layer of cladding was added to the target with the longitudinal seam of the outer clad positioned 45° from the jet and the seam of the inner clad positioned 180° from the outer clad.

¹⁶ For tests in which the jet was centered between the bands (circumferential seam offset from the jet center), the spacing was 8 in.

In addition to orientation of the longitudinal seam of cladding, test variables included the distance of the target from the jet and the position of the circumferential seam relative to the jet centerline. One test also was performed in which the target was positioned with a radial offset relative to the jet centerline. A summary of the specific test conditions examined (for calcium-silicate insulation) is shown in Table 3-5. Note that some test conditions were repeated to examine the reproducibility of the results (e.g., tests 1, 2, and 4).

For test conditions in which insulation was liberated, debris was collected by hand and sorted into three size classes: over 3 in., between 3 in. and 1 in., and under 1 in. Substantial quantities of debris were too small to be collected, and this debris was termed "dust;" its mass was calculated by subtracting the collected mass from the initial target insulation mass. The results are shown in Table 3-6. Photographs of debris in each of the collectable size classes are shown in Figure 3-10.

In addition to the measured debris size distributions, the following observations were made.

- When failure occurred, the mode of failure was tearing of the cladding caused by pressure acting on the edge of the (longitudinal) seam, thus exposing insulating material to the jet. The failure mode was such that a large fraction of calcium-silicate remained on the piping, protected from the jet by cladding on the front of the pipe. However, rapid disintegration and/or erosion of the calcium-silicate on the back side of the pipe caused a substantial fraction of the initial insulation mass to be converted to dust.
- The fraction of calcium-silicate converted to dust was found to be as high as 46% at target distances between 5D and 11D from the break. The level of material disintegration remained significant but reduced to 14% at 20D.
- The position of the longitudinal seam of the aluminum cladding was an important factor in determining whether insulation damage occurred.
 - When the longitudinal seam of over-clad calcium-silicate insulation was directly in line with the jet (at 0°), damage was observed at distances up to 7D.

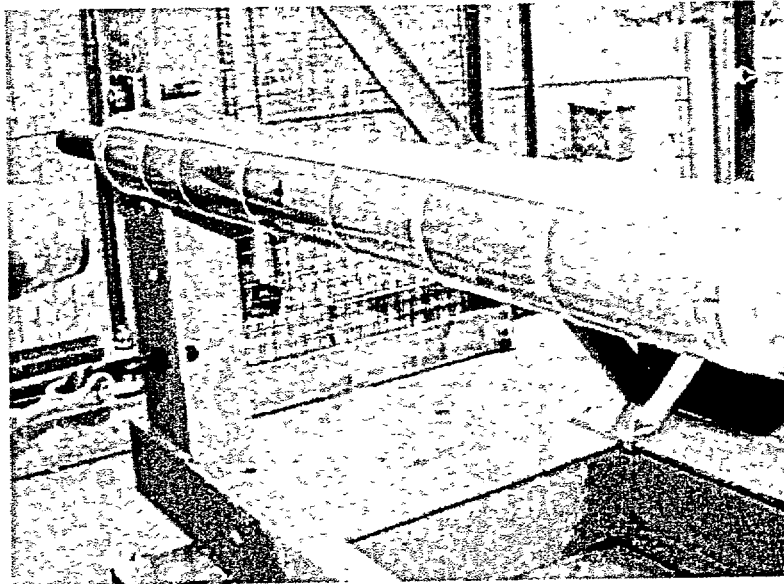


Figure 3-9 Insulation Target Mounting Configuration in OPG Test (Longitudinal Seam at 45°, Circumferential Seam Offset)

Table 3-5 Test Matrix for the OPG Calcium-Silicate Jet Impact Tests					
TEST	Target Distance from Break	Over-cladding?	Orientation of Longitudinal Seam	Position of Circumferential Seam	RESULTS Insulation Liberated?
1	7D	No	0°	Jet center	Yes (small amount)
2	7D	No	0°	Jet center	No
3	5D	No	0°	Jet center	Yes
4	7D	No	0°	Jet center	No
5	5D	No	0°	Jet center	Yes
6	5D	No	180°	Jet center	No
7	5D, 2D radial offset	No	0°	Jet center	No
8	7D	No	45°	Offset	Yes
9	4D	Yes	45°	Offset	No
10	3D	Yes	45°	Offset	No
11	4D	Yes	45°	Offset	No
12	9D	No	45°	Offset	Yes
13	11D	No	45°	Offset	Yes
14	13D	No	45°	Offset	Yes
15	20D	No	45°	Offset	Yes

TEST	Target Distance	Initial Weight (g)	Remaining on Target (g)	Debris Size Classes			
				Over 3 in (g)	1 to 3 in (g)	Under 1 in. (g)	Dust (g)
5	5D	2109	1112	238	247	31	481
7	5D, offset 2D	2074	1325	75	160	49	465
8	7D	2116	1578	52	118	34	334
12	9D	2089	1263	48	136	55	587
13	11D	2090	1252	114	120	37	567
14	13D	2143	1700	53	61	23	306
15	20D	2130	1654	98	60	17	301



Figure 3-10 Typical Calcium-Silicate Debris Collected from an OPG Two-Phase Jet Test

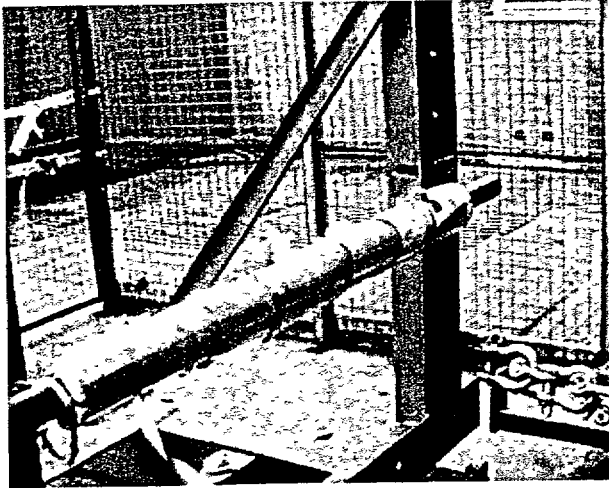
- When the seam was oriented 45° away from the jet, damage occurred out to 20D, the furthest distance tested¹⁷
- When the longitudinal seam was rotated away from the jet (180°), no damage was found at 5D.

- Application of a second layer of cladding (over-clad) successfully prevented damage with the insulation positioned as close as 3D from the break.

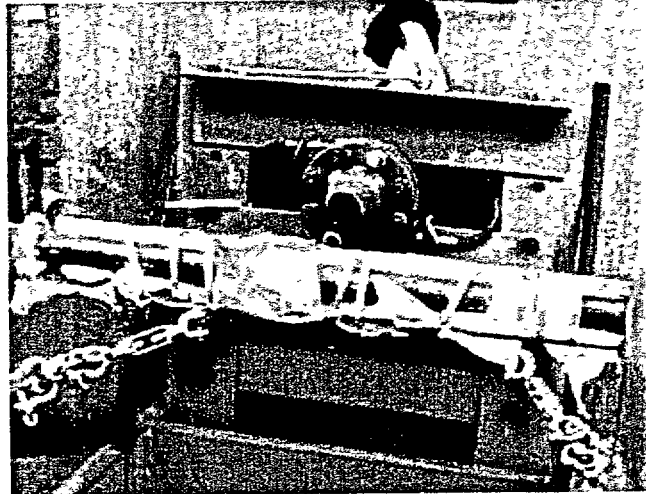
Photographs of the end state of the calcium-silicate target insulation for one of the OPG tests that resulted in insulation damage are shown in Figure 3-11

¹⁷ The jet centerline pressure at 20D estimated using the American National Standards Institute/American Nuclear Society (ANSI/ANS) 58.2 model (Section 3.3.1.1) was about 24 psi (Ref. 3-11, Volume 3). Because tests were not conducted at distances beyond 20D and damage could occur at distance somewhat greater than 20D, the minimum or onset pressure for damage would be somewhat less than 24 psi. When the jacket seam was oriented at 45°, the estimated minimum pressure for the onset of damage to the insulation was judged to be about 20 psi. Note that at distances of 20D, the analytical model used

to estimate the pressure could have significant uncertainty associated with the estimate



Front view



Back view

Figure 3-11 Post-Test Configuration of Aluminum-Clad Calcium-Silicate Insulation (Distance from Break of 9D and Longitudinal Seam at 45°)

Low-Density Fiberglass Test

The results of a single OPG test involving LDFG were available to the NRC. The general construction of the target insulation was similar to that described above for calcium-silicate: 0.016-in aluminum cladding and the 0.5-in.-wide, 0.05-in.-thick stainless-steel bands. The target was positioned 10D away from the break nozzle, and the longitudinal seam of the cladding was oriented at 45°.

Extensive damage was observed along the full length of the insulation target. Fiberglass on the back side of the target pipe was removed completely; fiberglass on the front side was compressed and remained trapped by dented (but not perforated) cladding.

Shreds of the dislodged fiberglass were collected and sorted into three size classes: over 3 in., between 3 in. and 1 in., and under 1 in. As with the calcium-silicate, substantial quantities of debris were too small to be collected; however, the debris mass was calculated by subtracting the collected mass from the initial target insulation mass. The results are shown in Table 3-7.

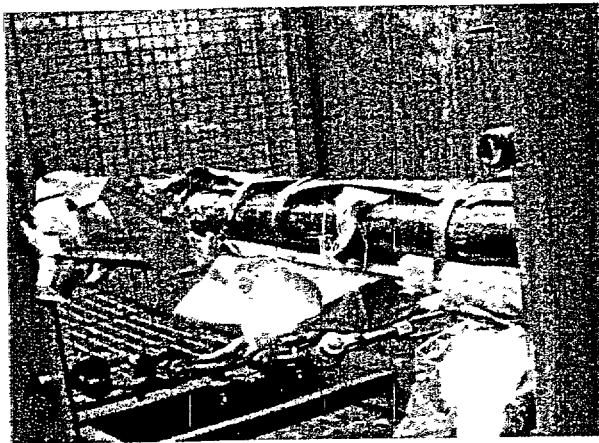
Photographs of the fiberglass target insulation at the conclusion of an OPG test are shown in Figure 3-12.

3.2.2.6 Battelle/KAEFER Tests³⁻²⁰

Battelle Ingenieurtechnik conducted a series of debris generation experiments in 1995 for a German manufacturer of insulating systems—KAEFER Isoliertechnik GmbH. The experiments were performed in a facility constructed at an earlier time for simulations of high-pressure, two-phase vessel blowdown. The facility consisted of an electrically heated pressure vessel and appended piping that were isolated from the environment by a fast-opening burst-disk assembly designed to not discharge any fragments that might interfere with downstream insulation targets. The burst-disk assembly was set to open at an internal pressure of approximately 140 bar (2030 psia). Therefore, debris-generation measurements could be performed at pressures close to those of typical PWR systems.

A unique feature of these experiments is the arrangement of target insulating systems downstream of the break orifice. In contrast to debris-generation experiments performed by other investigators, which positioned a single target in the wake of the jet, the Battelle/KAEFER tests were conducted using an array of targets as shown in Figure 3-13. The array included four insulated 80-mm (3 2-in.)-diameter pipes positioned at different distances and orientations from the break plane. Two of

Table 3-7 Size Distribution of Fiberglass Debris in Tests Where Insulation Was Liberated							
TEST	Target Distance	Initial Dry Weight (g)	Dry Weight Remaining on Target (g)	Debris Size Classes			Dry Weight of Unaccounted "fines" (g)
				Dry Weight Over 3 in. (g)	Dry Weight 1 to 3 in. (g)	Dry Weight Under 1 in. (g)	
22	10D	530	250	6	21	4	249



Back side of target pipe



Collected debris

Figure 3-12 Post-Test Configuration of Aluminum-Clad Fiberglass Insulation (Distance from Break of 10D and Longitudinal Seam at 45°)

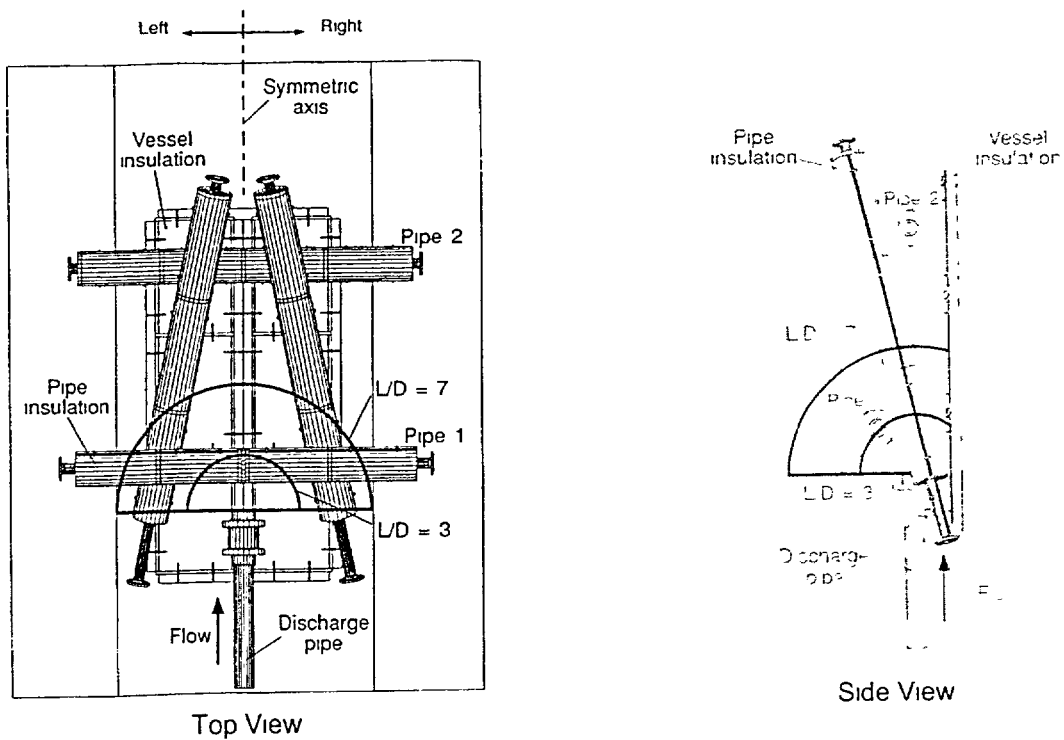


Figure 3-13 Configuration of the Target Field in the Battelle/KAEFER Tests³⁻²⁰

the pipes were oriented perpendicular to the jet (one close to the break plane, the other farther away). The other two pipes were mounted at a slight angle to, and laterally offset from the jet centerline. The four target pipes were positioned so that insulation response could be observed at distances covering three ranges: $L/D = 0$ to 3 , $L/D = 3$ to 7 , and $L/D > 7$. The test field also included an array of flat insulation that was located beneath the piping targets and installed flush onto the base of the test field. These flat insulation components were designed to represent vessel insulation assemblies. They were installed in two sections: one on the left-hand side of the test field and the other on the right hand side.

A total of four tests was performed with this arrangement. Each test involved a different combination of six types of insulating constructions on the piping and flat panel targets. The types of insulation studied were

- a stainless-steel RMI cassette,
- calcium-silicate in a steel cassette,
- a steel-jacketed Min-Wool blanket,
- steel-jacketed fiberglass,
- Min-Wool in a steel cassette, and
- fiberglass in a steel cassette.

In each test, a single type of insulating construction was installed on target locations on the left-hand side of the test field; a different type was installed on targets on the right-hand side. KAEFER Isoliertechnik GmbH manufactured all of the insulation.

The primary objective of the Battelle/KAEFER tests was to evaluate KAEFER insulation performance against the criteria described in US NRC Regulatory Guide 1.82,³⁻²¹ not to study the amount or characteristics of resultant debris. As a result, the Battelle/KAEFER test report describes the experimental findings in terms of the extent of damage to installed insulation rather than describing the shape, size or other characteristics of the debris generated (i.e., the complement of "debris generation" data.) Figure 3-14 shows the damage to the test specimens typical of these experiments. Specifically, the post-test condition of the insulation target field is described in terms of two quantities.

- Per cent remaining in "as-fabricated" or as-installed condition
- Per cent destroyed or fragmented

These quantities are estimated for each piece of insulation installed in the various target locations and are expressed simply in terms of per cent of the original installed target component. The data sheets for each test also recorded qualitative observations of target insulation conditions. For example, the surface conditions of partially damaged components were noted (e.g., dented or punctured), the size of fissures (if any) in weld seams on the outer cassette structure were estimated, and the fraction of the component's core insulating material lost was estimated.

The following general observations were made from the data collected in these tests.

- The insulating construction with the poorest overall performance was the jacketed fiberglass blanket, with 68% of the target material in the field destroyed or severely damaged. The jacketed Min-Wool construction performed slightly better with ~44% damaged. All types of insulation encased in steel cassettes had lower levels of destruction than these two types.
- The extent of damage to targets in the test field was generally higher at locations close to the break plane (i.e., $3 < L/D < 5$) than at locations distant from the break plane ($L/D > 5$). However, significant exceptions were noted. Tests with targets manufactured as steel cassettes often showed damage patterns in which the damage to near-field targets was lower than damage to targets at the mid- or far-field. One possible explanation for this unusual observation is collateral damage. That is, material stripped from targets near- or mid-field became projectiles that struck other targets downstream.
- The orientation of weld seams in steel cassettes relative to the axis of the steam jet was found to influence the amount of damage inflicted on this type of insulation. The cases in which damage levels to cassettes were high often correlated to conditions in which the jet impacted a weld seam and ripped open the cassette.
- The overall levels of damage observed for the flat-panel insulation installed at the base of the test field were not significantly different from those observed for pipe insulation (i.e., the same trends noted above

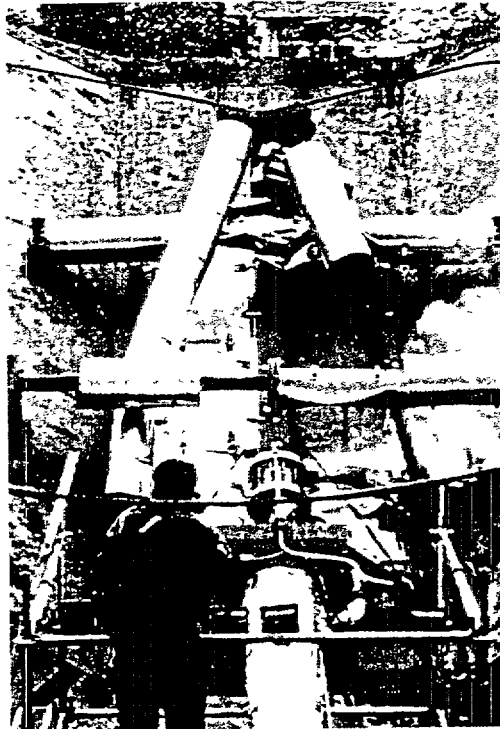


Figure 3-14 Typical View of Target Destruction in Battelle/KAEFER Tests³⁻²⁰

apply equally well to piping and flat-panel installations) However, after a flat-panel target located near the jet was damaged (i.e., ripped from its initial location), the damage appeared to propagate upward, removing subsequent pieces of insulation from the base of the target field. As a result, the flat targets either tended to remain intact or be removed completely.

3.3 Debris-Generation Models and Analytical Approaches

In Section 3.2, the test data described the minimum pressure at which various forms of insulation material would be dislodged from their installed locations and, to a lesser extent, the physical forms (shape and size) that the resulting debris would take. To use this information to characterize debris generation in a reactor containment, one must be able to first determine the forces (i.e., pressure field) surrounding a postulated break location.

Jet impingement forces resulting from stationary breaks in high-pressure piping have been measured experimentally³⁻²² and calculated using models for isentropic expansion and flow

across shock discontinuities.^{3-8,3-9} This information subsequently was used as a basis for designing piping systems and other structures within reactor containments to survive mechanical loads created by the two-phase effluent from postulated RCS piping breaks.³⁻²³ Another important application of this information was the development of a conceptual picture of the ZOI within which piping insulation might be affected by jet forces emerging from a postulated pipe break. The ZOI was described by a right-angle cone projected along the axis of the ruptured pipe, which was assumed to expand freely into unobstructed space. This model for characterizing the region of space where pressures would be higher than ambient and sufficient to inflict damage on component insulation is reviewed in Section 3.3.1.

Unfortunately, the idealized pipe-break configurations examined in experimental studies do not address the effects of pipe movement or jet deflection in a congested area. As a result, an alternative approach to defining the ZOI for estimating debris generation was developed in the evaluations of BWR suppression-pool strainer performance³⁻². This model, which is referred to as the "spherical debris-generation

model" accounts for the effects of jet reflection and pipe motion by transforming the total energy within an idealized conical jet into an equivalent sphere that surrounds the break location. This model also has the advantage of not requiring information about the angular orientation of the rupture pipe in space to map out the volume within which insulation of a particular material/construction would be damaged. This model is described in Section 3.3.2.

3.3.1 Cone Models

3.3.1.1 ANSI/ANS Standard

ANSI/ANS-58.2-1988³⁻²³ describes an analytical method for evaluating the geometry of a free-expanding jet. In addition to its basic purpose, which is to describe fluid forces on structures at various distances from a postulated pipe break, the basic mathematical model is the foundation of the conical ZOI used in Ref. 3-5.¹⁸

The model represents the free-expanding jet as a series of three regions, as shown in Figure 3-15. Region 1, which is described as the "jet core," represents the region of space immediately downstream of the break within which fluid striking an intervening object (target) would experience full recovery of the fluid stagnation pressure. This region is significant only for jets involving subcooled stagnation conditions. Region 2 extends from the end of the jet core to a distance downstream of the break, where the jet has expanded (in free, unimpeded space) to its asymptotic limit, i.e., isentropic expansion to near-ambient conditions. In practice, this means that the jet centerline pressure has decreased to less than twice the ambient pressure. In Region 3, the jet expands at a reduced rate and at an assumed angle of 10° to become fully equilibrated with ambient conditions.

The distance to the asymptotic plane from the break (L_a) and the cross-sectional area of the jet at the asymptotic plane (A_a) are calculated relative to the equivalent dimensions at the break plane; i.e., the break diameter D_b and

¹⁸ A number of experimentally based empirical correlations for jet expansion exist in the literature. Although these correlations may predict the data on which the correlations are based adequately, extreme care must be taken in extrapolating those correlations to other pipe-break configurations, sizes, pressures, etc.

break area A_b with the formulas listed in the right-hand side of Figure 3-15.

The diameters of the jet in Regions 2 and 3 (relative to the break diameter D_b) are calculated as follows.

Region 2:

$$\frac{D_j}{D_b} = \sqrt{C_T \left[1 + \frac{L}{L_a} \left(\frac{A}{C_T A_b} - 1 \right) \right]}$$

and

Region 3:

$$\frac{D_j}{D_b} = \sqrt{\frac{A_j}{A_b}} = \sqrt{\frac{A_j A_a}{A_b A_a}} = \left[1 + \frac{2(L - L_a)}{D_b} \tan 10^\circ \right] \sqrt{\frac{A_a}{A_b}}$$

where L = distance away from the break place at which the jet diameter is D_j .

In addition to determining the overall dimensions of the jet, applying the ANSI/ANS model to estimate debris generation requires information regarding the geometry of the isobar within the jet that encloses the region of space where pressures exceed a particular damage pressure. This region of space is shown in Figure 3-16 and is described by the following expressions.

The pressure at any distance downstream of the break plane (L) and distance away from the jet centerline (D_x) is calculated as follows.

Region 2:

$$\frac{P_x}{P_{jc}} = \left(1 - \frac{D_x}{D_j} \right) \left\{ 1 - 2 \frac{D_x}{D_j} \left[1 - 3C_T \left(\frac{D_b}{D_j} \right)^2 \left(\frac{P_o}{P_{jc}} \right) \right] \right\}$$

and

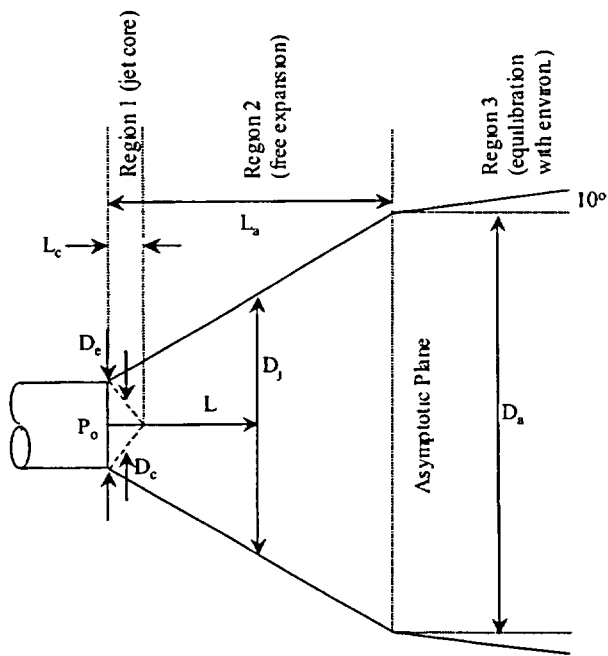
Region 3:

$$\frac{P_x}{P_{jc}} = 1 - \frac{D_x}{D_j}$$

where the pressure along the jet centerline (P_{jc}) is

Region 2:

$$\frac{P_{jc}}{P_o} = F_c - \left[F_c - 3C_{T_a} \left(\frac{D_b}{D_a} \right)^2 \right] \frac{\left(1 - \frac{L_c L_a}{L_a L_l} \right)}{\left(1 - \frac{L_c}{L_a} \right)}$$



$$\frac{L_a}{D_c} = \frac{1}{2} \left(\sqrt{\frac{A_a}{A_c}} - 1 \right)$$

$$\frac{A_a}{A_c} = \left(\frac{G_{crit}^2}{g_c \rho_{ma} C_T P_o} \right)$$

$$\rho_{ma} = \frac{1}{\frac{\chi_v}{\rho_g} + \frac{(1-\chi_v)}{\rho_l}}$$

where, ρ_g, ρ_l, χ are evaluated at P_a

$$\frac{P_g}{P_{amb}} = 1 - 0.5 \left(1 - \frac{2P_{amb}}{P_o} \right) f(h_o)$$

$$f(h_o) = \begin{cases} \sqrt{0.1 + \left(\frac{h_o - h_f}{h_{fg}} \right)^2} & \text{for } \left(\frac{h_o - h_f}{h_{fg}} \right) > -0.1 \\ 0 & \text{for } \left(\frac{h_o - h_f}{h_{fg}} \right) < -0.1 \end{cases}$$

where: G_{crit} = break flow rate (mass flux)
 ρ_{ma} = mixture density at asymptotic plane
 ρ_g, ρ_l = saturated vapor, liquid density
 C_T = thrust coefficient
 P_o = stagnation pressure
 χ = mixture vapor mass fraction (quality)
 h_o, h_f = stagnation, saturation liquid enthalpy

Figure 3-15 ANSI/ANS Standard Free-Expanding Jet Model

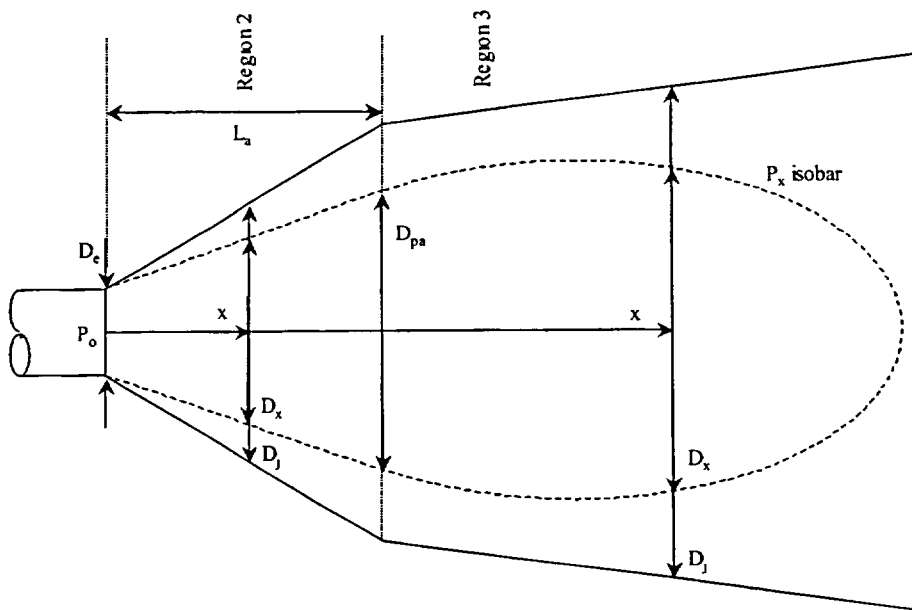


Figure 3-16 Isobar of Damage Pressure P_x within a Fixed, Free-Expanding Jet

where

$$F_c = \begin{cases} 1.0 & \text{for } \left(\frac{D_j}{D_e}\right)^2 \leq 6C_T \text{ at } L = L_c \\ 6C_T \left(\frac{D_e}{D_j}\right)^2 & \text{for } \left(\frac{D_j}{D_e}\right)^2 > 6C_T \text{ at } L = L_c \end{cases}$$

Region 3:

$$P_{jc} = 3P_o \frac{A_j}{A_e}$$

At any distance away from the break plane, the diameter of the volume defined by an isobar of a fixed pressure (P_x) can be calculated by solving the above equations for D_x . The result is

Region 2:

$$\frac{D_x}{D_j} = \frac{1}{4A} \left[(2A+1) - \sqrt{(2A+1)^2 - 8A \left(1 - \frac{P_x}{P_{jc}}\right)} \right]$$

where

$$A = \left[1 - 3C_{Te} \left(\frac{D_e}{D_j}\right)^2 \left(\frac{P_{oe}}{P_{jc}}\right) \right]$$

Region 3:

$$\frac{D_x}{D_j} = 1 - \frac{P_x}{P_{jc}}$$

3.3.1.2 Three-Region Conical Jet³⁻⁵

A variant of the three-region conical-jet expansion model was proposed in NUREG-0897 to describe the varying degrees of damage inflicted on insulation material, with distance away from the break, by the initial shock wave and subsequent mechanical erosion. The model did not calculate the pressure distribution within the free-expanding jet explicitly but described the distance downstream of the break plane at which the level of material damage decreased from "total destruction" (Region 1) to "high levels of destruction" (Region 2) to "dislodged, as-fabricated pieces" (Region 3). The distance away from the break plane at the interface between these regions was described in terms of the number of break diameters (L/D) as shown in Figure 3-17.

The boundaries of the three regions represented in this model were based on calculations of two-dimensional pressure distributions (similar to those described for the ANSI/ANS standard). The following significant findings were derived from the calculations and reported.³⁻⁵

1. "Target pressure loadings increase asymptotically at L/D's less than 3.0 to break exit pressures. At L/D's less than 3, survivability of insulation materials is highly unlikely.
2. At L/D's from 5 to 7, the centerline stagnation pressure becomes essentially constant at approximately 2 ± 1 bars.
3. The multidimensional pressure field loads the target over a large region; this region may be approximated by a 90° jet cone expansion model. A hemispherical expansion model could be another approximation for this expanding pressure field. These two-dimensional calculations do not support the use of the Moody jet model (a narrow cone) for targets close to the break locations."

Experiments performed in the HDR facility (see Section 3.2.2.2) formed the primary basis for connecting the two-phase pressure distributions calculated with the conical jet expansion model to observation of insulation damage. Sufficient experimental data were not available at the time that NUREG-0897³⁻⁵ was published to quantitatively distinguish "high levels of destruction" in Region 2 from either of its two neighbors. However, the following qualitative description of damage was offered.

... it appears that [in Region 2] the RMI debris could consist of damaged inner foils and damage assemblies or components that were the result of further LOCA damage. Experimental data available for fibrous insulations indicate that shredding and damage can extend into Region 2, with such damage decreasing with distance from the jet. However, if the 'inner core' of fibrous insulation is exposed to the break jet (as would occur if the cover blanket were breached), blowdown transport of this material would be expected to extend for distances much greater than 7 L/D's.

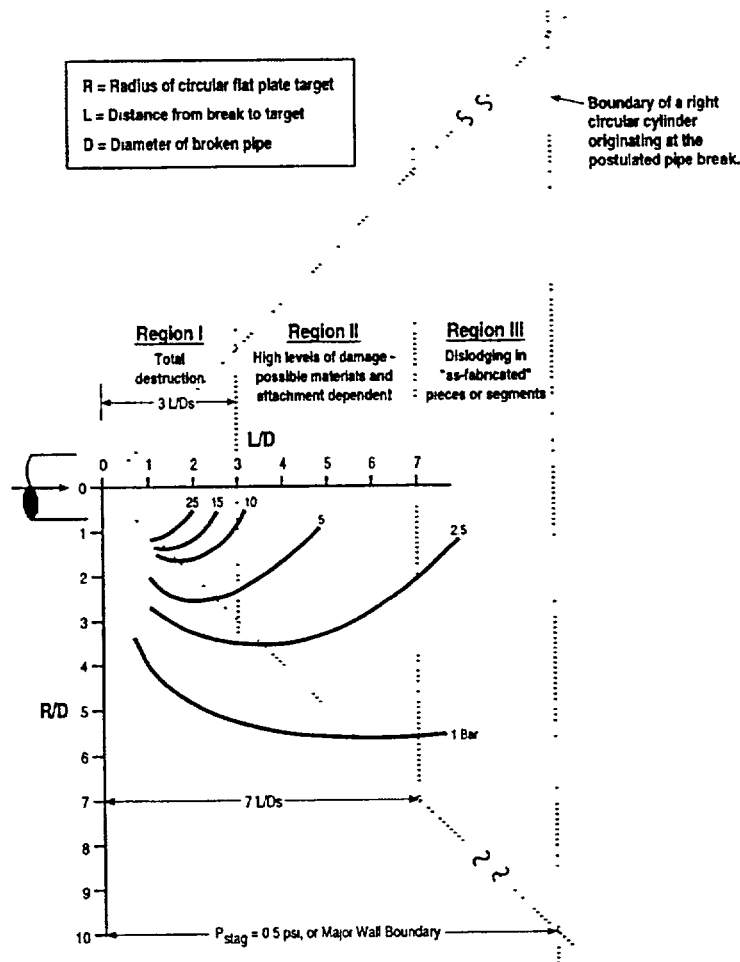


Figure 3-17 Illustration of the Three-Region, Two-Phase Conical-Jet ZOI Model³⁻⁹

3.3.2 Spherical Models

3.3.2.1 Three-Region Spherical Model³⁻²

A major limitation of the conical model is the inherent assumption that pipe separation and offset at the location of the break are fixed in space. That is, movement of the break plane(s) is not taken into account explicitly. The ANSI/ANS standard³⁻²³ acknowledges this limitation by stating that adjustments to the model are necessary to properly account for movement of the break plane(s) and/or reflection of the jet by intervening structures. In particular, the ANSI/ANS Standard states:

“Regardless of the fluid jet model used to determine affected structures and components, engineering judgment shall be applied in determining whether the jet will impinge upon a given target. The geometry

of the jet cannot be perfectly defined for all of the various fluid conditions under today’s state of the art .. Neither can the movement of the ruptured pipe, thus the jet centerline, be defined with complete accuracy.”

Also,

“The movement of the jet centerline due to pipe whip shall be taken into account in the characterization of jet impingement loads on a target.”

The so-called “three-region, spherical model” for characterizing the ZOI at a particular break location was developed to address uncertainties in break-plane movement and jet reflection.³⁻² The three-region, spherical model is illustrated in Figure 3-18.

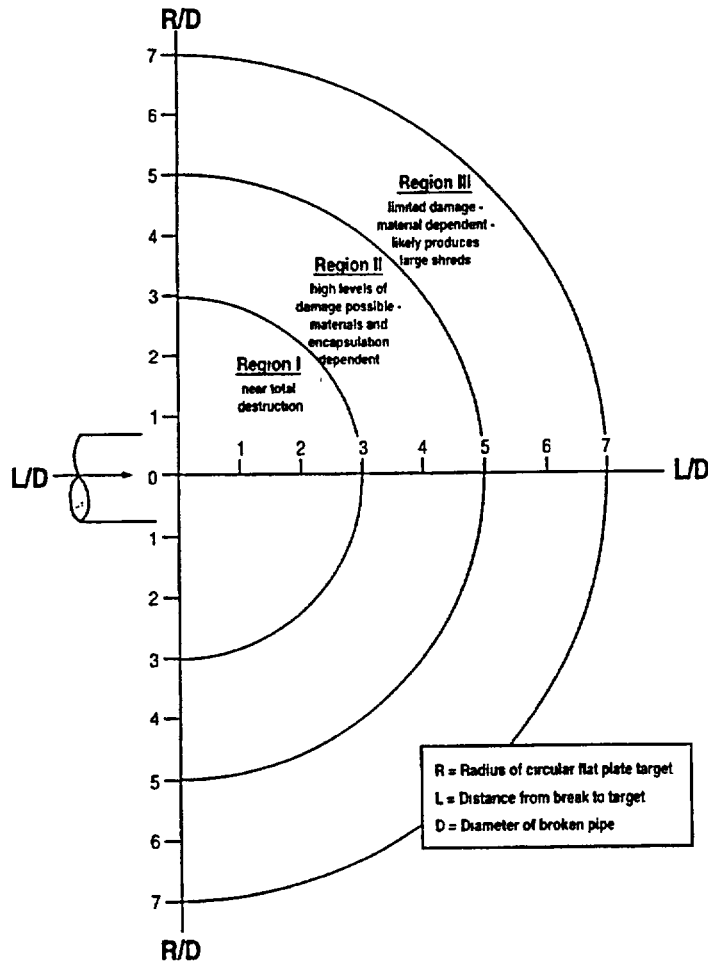


Figure 3-18 Illustration of the Three-Region, Two-Phase Spherical ZOI Model³⁻²

As in the three-region cone model, the degree of damage decreases from Region 1 to Region 2 to Region 3. The extent of damage (i.e., the size distribution of insulation fragments) is based on experimental observations of target material impacted by stationary jets at varying distances from the break plane. For example, the experimental observations summarized in Section 3.2 clearly indicate that the fraction of insulation reduced to small fragments is much less for steel-jacketed fibrous pillows than for unjacketed fiber blankets. In the NRC's evaluation of BWR suppression-pool strainers,³⁻² such differences were handled through the use of "destruction factors." For example, destruction factors of 0.75, 0.60, and 0.40 were used to represent the fraction of steel-jacketed Nukon® reduced to a sufficiently small size to be transported by blowdown forces from the drywell

to the wetwell of a BWR Mark I containment. Different values were used for other types of insulation.

3.3.2.2 Equivalent-Volume Sphere Model

An alternative approach to distorting the conical ZOI sphere is the so-called "equivalent-volume" sphere model. This model couples the ideas (from Section 3.3.1.1) of a conical isobar within which pressures exceed a particular damage pressure with a spherical shape to capture the major effects of break-plane movement and jet reflection. A version of this model initially was proposed by the BWROG as one of three possible methods for estimating quantities of debris generation.³⁻³ The basic approach has five essential steps.

1. Determine the damage or destruction pressure (P_{dest}) for an insulating construction of interest.
2. Determine the total volume of space swept out by the conical isobar defined by the damage pressure (i.e., $P_x = P_{dest}$ in Section 3.3.1.1).
3. Convert the total volume within the isobar to a sphere of radius R .
4. Place the origin of the sphere at a specific, postulated break location and determine the total quantity of insulation of the selected type that is within the sphere.
5. Move the origin of the sphere to all other candidate break locations and repeat the exercise.¹⁹

The radius of the equivalent sphere is a function of the damage pressure (unique to each type of insulating construction), the diameter of the pipe where the break is assumed to occur, and the fluid medium within the pipe (i.e., steam vs water).

In the BWROG method, multipliers or correction factors were applied to this basic method to account for destruction factors less than 1.0. The NRC's evaluation of this method determined the general approach to be acceptable for insulating construction with low characteristic damage pressure (Ref. 3-4, Appendices B, C, D, F, G, and K). However, for insulations with high damage pressure, the staff recommended that licensees develop the equivalent sphere on the basis of target-area-average pressures instead of the jet centerline pressures.

¹⁹ Computer programs have been developed to calculate the volume of insulation inside the ZOI for all potential break locations within a containment systematically. For example, the volunteer plant assessments performed as part of the NRC's parametric evaluation of recirculation sump performance used the CASINOVA program to perform these computations.³⁻¹¹ This program has the ability to vary the ZOI for each type of material near a particular weld (i.e., the ZOI associated with the damage pressure for a particular material) and to evaluate all high-energy welds systematically. The systematic analysis provides a spectrum of potential insulation debris volumes by insulation type that can be used to determine the size a screen capable of handling the potential debris load to the recirculation sump screens.

3.3.3 Debris-Size Distribution as a Function of Local Jet Pressure

All insulation located within the ZOI generally is assumed to be damaged to some extent. The extent of damage could range from the total destruction of a blanket (or RMI cassette) with all of its insulation turned into debris of very small dimensions to the blanket/cassette being only slightly damaged and even remaining attached to its piping. Available debris-generation tests clearly indicate that the extent of damage (i.e., the size distribution of resulting debris fragments) depends strongly on the magnitude of the jet forces in the immediate proximity to individual insulation components. Qualitatively, increasing the local jet forces (i.e., increasing local stagnation pressures) tends to produce higher fractions of small debris fragments.

The size distribution of debris formed from insulation targets located within the ZOI can be determined only by combining measurements of debris-size distribution with measurements (or analytical estimates) of local stagnation pressure. Unfortunately, the quantitative relationship between the distribution of debris fragment size and local jet pressure has not been investigated thoroughly. Most reports of experimental work on debris generation document the size distribution of resultant debris fragments along with the initial location of the insulation target but do not measure, or estimate, the local jet stagnation pressure. This extension of test data is left to others to develop by applying one of the models described in Section 3.3.1 or 3.3.2. This gap in the published knowledge base on debris generation is being addressed in an ongoing NRC study of PWR recirculation sump performance for a "volunteer plant." The results of this work are anticipated in early 2003. The general method being used to correlate debris size(s) to local jet pressure in the volunteer plant analysis is summarized below.

Using the spherical ZOI damage model, the fraction of insulation of type- i that is reduced to debris within a particular size bin is given by the following integration:

$$F_i = \frac{3}{r_{ZOI}^3} \int_0^{r_{ZOI}} g_i(r) r^2 dr$$

where

- F_i = the fraction of debris of type-i within a particular size bin,
- $g_i(r)$ = the damage distribution for debris type-i,
- r = the radius from the break in the spherical ZOI model, and
- r_{ZOI} = the outer radius of the ZOI.

The volume associated with a particular level of damage is determined by estimating the volume within a particular isobar within the jet (i.e., any insulation located within this isobar would be damaged to the extent, or greater, associated with that pressure). As described in Section 3.3.2.2, the equivalent-volume sphere model can be used to convert this volume to an equivalent spherical volume with an origin at the break plane. Hence, the debris-size distribution can be associated with a particular spherical radius [i.e., $g_i(r)$]. The distribution would be specific to a particular kind of insulation, jacketing, jacketing seam orientation, and banding.

The difficulty associated with this evaluation is the limited database for insulation debris generation. Examples of debris generation data that include debris-size information that can be correlated to local jet pressure include the BWROG AJIT tests (Section 3.2.1.2) and the OPG steam/water debris generation tests (Section 3.2.2.5). However, when these data are subjected to the above integration, sufficient data points are not available to fully characterize the damage distribution function [$g_i(r)$]. For example, the BWROG data for DPSC Mirror® stainless-steel RMI, which was found to be damaged at jet pressures as low as 4 psi, indicates the size distribution shown in Figure 3-19 when the insulation is installed with standard bands.²⁰

Although these data may be suitable for describing the extent of cassette damage in the outer reaches of the ZOI, they do not describe debris generated at locations closer to the break, where the cassette would be subject to substantially higher local stagnation pressures. Information at very high local pressures can be gleaned from limited data collected in the Siemens-Karlstein tests (Section 3.2.2.4).

These tests included measurements of RMI destruction when a cassette was mounted directly in front of the break plane. Under such conditions, the cassette was reduced to small shreds, with a majority of the pieces characterized as smaller than 2-in. (see Figure 3-7.) Unfortunately, no data are available for the damage of this type of insulation at local pressures between 120 psi and approximately 1000 psi. Given the combined body of data, the ZOI integration for small (< 2-in.) debris fragments of stainless-steel RMI can be made by conservatively assuming that insulation of this type subjected to jet pressures greater than 120 psi becomes debris smaller than 2 in.

Similar exercises can be performed for other types of insulation. However, there are gaps in quantitative measurements of debris size with variable local pressure (i.e., position relative to the break plane) for all types of debris. Consequently, conservative assumptions regarding debris size often are used to characterize quantities of transportable debris.

3.4 References

- 3-1. Wysocki, J., and R., Kolbe, "Methodology for Evaluation of Insulation Debris Effects," NUREG/CR-2791, SAND82-7067, Burns and Roe, Inc. and Sandia National Laboratories, September 1982.
- 3-2. Zigler, G., J. Brideau, D. V. Rao, C. Shaffer, F. Souto, and W. Thomas, "Parametric Study of the Potential for BWR ECCS Strainer Blockage Due to LOCA Generated Debris," NUREG/CR-6224, SEA 93-554-06-A:1, Science and Engineering Associates, Inc., October 1995.
- 3-3. BWR Owners' Group, "Technical Support Documentation: Utility Resolution Guidance (URG) for ECCS Suction Strainer Blockage, 4 Vols., Doc. Control 96-266, November 1996.
- 3-4. "Safety Evaluation by the Office of Nuclear Reactor Regulation Related to NRC Bulletin 96-03 Boiling Water Reactor Owners Group Topical Report NEDO-32686, 'Utility Resolution Guidance for ECCS Suction Strainer Blockage,'" Docket No. PROJ0691, August 20, 1998.

²⁰Distributions developed using most conservative applicable data points.

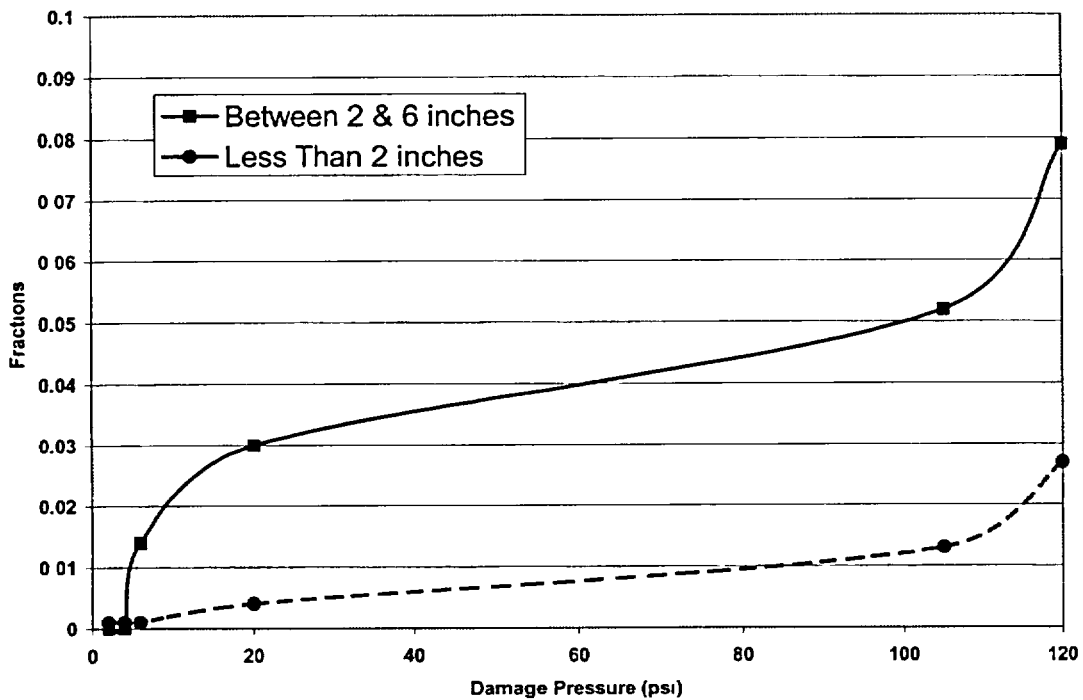


Figure 3-19 Debris Size as a Function of Local Jet Pressure
 (Applicable Only to DPSC SS Mirror® Insulation Based on Available Data)

- 3-5. U.S. Nuclear Regulatory Commission, "Containment Emergency Sump Performance," NUREG-0897, Rev. 1, Nuclear Regulatory Commission, October 1985.
- 3-6. Nuclear Energy Institute (NEI), "Results of Industry Survey on PWR Sump Design and Operations," June 7, 1999
- 3-7. U.S. Nuclear Regulatory Commission, "Assurance of Sufficient Net Positive Suction Head for Emergency Core Cooling and Containment Heat Removal Pumps," Generic Letter 97-04, October 1997.
- 3-8. Moody, F. J., "Prediction of Blowdown Thrust and Jet Forces," Paper 69-HT-31, American Society of Mechanical Engineers, 1969,
- 3-9. Weigand, G., et al., "Two Phase Jet Loads," NUREG/CR-2913 Rev. 4, Sandia National Laboratories, January 1983.
- 3-10. Rao, D. V., B. C. Letellier, K. W. Ross, L. S. Bartlein, and M. T. Leonard, "GSI-191 Technical Assessment: Summary and Analysis of U.S. Pressurized Water Reactor Industry Survey Responses to GL 97-04," NUREG/CR-6762, Volume 2, LA-UR-01-1800, August 2002.
- 3-11. Rao, D. V., C. J. Shaffer, and S. G. Ashbaugh, "GSI-191 Technical Assessment: Development of Debris-Generation Quantities in Support of the Parametric Evaluation," NUREG/CR-6762, Vol. 3, LA-UR-01-6640, Los Alamos National Laboratory, November 2001.
- 3-12. Rao, D. V., C. Shaffer, and E. Haskin, "Drywell Debris Transport Study," NUREG/CR-6369, SEA 97-3105-A:14, 3 Vols., Science and Engineering Associated, Inc., September 1999.
- 3-13. Studsvik Energiteknik, "Component Tests: Paint and Heat Insulation," MXA-4-206, Marviken Power Station, Sweden, September 1997.
- 3-14. Studsvik Material AB, "Steam Jet Dislodgement Tests of Thermal Insulating Material of Type Newtherm 1000 and Caposil HT1," M-93/41, April 1993.

- 3-15. Studsvik Material AB, "Steam Jet Dislodgement Tests of Two Thermal Insulating Materials," M-93-60, May 1993.
- 3-16. Blomqvist, M. and M Delby, ABB-Atom, "Report from Tests Concerning the Effect of Steam Jet on Caposil Insulation at Karlshamn, Carried Out on April 22-23, 1993, and May 6, 1993," SDC 93-1174, June 1993.
- 3-17. Vattenfall Energiesystem, "Metallic Insulation Jet Impact Tests (MIJIT)," GEK 77/95, June 1995.
- 3-18. Zigler, G., et al., "Experimental Investigation of Head Loss and Sedimentation Characteristics of Reflective Metallic Insulation Debris," SEA-95-970-01-A:2 (1996), and NT34/95/e32, "RMI Debris Generation Testing: Pilot Steam Test with a Target Bobbin of Diamond Power Panels."
- 3-19. Ontario Power Generation, "Jet Impact Tests—Preliminary Results and Their Applications," N-REP-34320-10000-R00, April 2001.
- 3-20. Wenzel, H. H., et al., "Blow-down Investigations on the Performance of Insulating Systems—Taking into Account the Regulatory Guide 1.82," B.I.G. V-32.608, Battelle Ingenieurtechnik GmbH, Germany, August 1995.
- 3-21. Regulatory Guide 1.82, Revision 1, "Water Sources for Long-Term Recirculation Cooling Following a Loss-of-Coolant Accident," U.S. Nuclear Regulatory Commission, Revision 1, November 1985, and Revision 2, May 1996.
- 3-22. Studsvik Energiteknik, "The Marviken Full Scale Jet Impingement Tests—Summary Report," MXD-301, September 1982.
- 3-23. American Nuclear Society, "Design Basis for Protection of Light Water Nuclear Power Plants Against the Effects of Postulated Pipe Rupture," ANSI/ANS-58.2-1988, October 1988.
- 3-24. Rao, D. V., B. C. Letellier, C. Shaffer, S. Ashbaugh, and L. S. Bartlein, "GSI-191 Technical Assessment: Parametric Evaluations for Pressurized Water Reactor Recirculation Sump Performance," NUREG/CR-6762, Vol. 1, LA-UR-01-4083, Los Alamos National Laboratory, August 2002.

4.0 AIRBORNE/WASHDOWN DEBRIS TRANSPORT IN CONTAINMENT

Section 4 summarizes the available knowledge regarding transport of insulation debris within the containment from its location of origin to the containment sump pool. The transport of insulation debris would be caused first by the effluences from a high-energy pipe break that would not only destroy insulation near the break, but also would transport that debris throughout the containment, i.e., airborne debris transport. If the break effluences were to pressurize the containment sufficiently to activate¹ the containment spray system to suppress pressurization, the transport of insulation debris would also be driven by the drainage of spray water from the spray heads to the recirculation sump, i.e., washdown debris transport. The knowledge base associated with insulation debris transport is organized in the following subsections.

- Section 4.1 presents an overview of the mechanics associated with airborne/washdown debris transport, including the characteristics of an accident relevant to debris transport, the relevant plant features, the physical processes and phenomena, and the debris characteristics affecting transport.
- Section 4.2 describes the testing relevant to airborne/washdown debris transport that has been performed.
- Section 4.3 describes the analyses relevant to airborne/washdown debris transport that have been performed.
- Section 4.4 summarizes the analytical approaches developed to predict the transport of insulation debris.
- Section 4.5 discusses the basic "rules of thumb" observed during testing and analytical studies.

The phenomena associated with airborne and washdown debris transport is also discussed. These phenomena include the following:

- How substantial quantities of airborne debris in motion would come into contact with

¹The spray system would activate if the containment pressure exceeded the system-activation setpoint. The pressurization of the containment is plant- and accident-scenario-dependent (e.g., the size of the break)

containment structures and equipment and be deposited onto these surfaces.

- How debris would settle gravitationally onto equipment and floors as depressurization flows slow down.
- How airborne debris (usually very fine) would be washed out of the air by the spray droplets except in areas not covered by the sprays.
- How the impact of these sprays onto surfaces and the subsequent drainage of the accumulated water would wash deposited debris down toward the sump pool.
- How containment sprays may degrade insulation debris further through the process of erosion, thereby creating even more of the very fine and most transportable debris.
- How the analysis of debris transport in the containment depends on the type and characteristics of the debris generated by the break (discussed in Section 3).

The containment transport analyses (above the sump pool) provide a description of the debris entering the sump pool in terms of the type of debris, where the debris enters the pool, and when the debris enters the pool. Section 5 discusses the transport of debris within the sump pool. A majority of the testing and analysis relevant to airborne/washdown insulation debris transport was performed to support the suction-strainer-clogging issue for BWRs; however, most of this research is also directly applicable to PWRs. The applicability of BWR research to PWRs is discussed as appropriate.

It also should be noted that debris-transport research has tended to focus on the transport characteristics of fibrous insulation debris. Research has also considered other types of insulation debris, notably experimental RMI debris research, but the potential for fibrous insulation debris to clog a strainer generally has been found to be substantially greater for fibrous debris than for RMI debris. Further research has tended to focus on LDFG over the other types, e.g., HDFG or mineral wool fibrous debris. Therefore, there are gaps in the completeness of debris-transport research.

4.1 Overview of Mechanics

The transport of debris within a PWR would be influenced by both the spectrum of physical processes and phenomena and the features of a particular containment design. Because of the violent nature of flows following a LOCA, insulation destruction and subsequent debris transport are chaotic processes. For example, a piece of debris could be deposited near the sump screen directly or it could take a much more tortuous path—first going to the dome and then being washed by the sprays back down to the sump. A piece of debris could also be trapped in any number of locations. Debris-transport analysis includes the characterization of the accident, the design and configuration of the plant, the generation of debris by the break flows, and both airborne and waterborne debris-transport dynamics.

The NRC convened a panel of recognized experts with broad-based knowledge and experience to apply the Phenomena Identification and Ranking Table (PIRT) process to the transport through a PWR containment of debris generated by a high-energy pipe break.⁴⁻¹ The PIRT process was designed to identify processes and phenomena that would dominate debris-transport behavior. Further, these processes and phenomena were prioritized with respect to their contributions to the reactor phenomenological response to the accident scenario. The NRC also convened a PIRT panel to rank transport processes relative to debris transport within a BWR drywell.⁴⁻²

This section specifically discusses:

- the characteristics of postulated accident scenarios relevant to the transport of insulation debris (Section 4.1.1),
- the plant features that would affect transport of insulation debris (Section 4.1.2),
- the physical processes and phenomena that affect transport of insulation debris (Section 4.1.3), and
- the characteristics of insulation debris that affect its transport (Section 4.1.4).

4.1.1 Accident Characterization Relevant to Debris Transport

Long-term recirculation cooling must operate following the range of possible LOCA accident

scenarios and non-LOCA accident scenarios (e.g., a main steam line break). A comprehensive debris-transport study should consider an appropriate selection of these scenarios. The maximum debris transport to the screen likely will be determined by a small subset of accident scenarios, but this scenario subset should be determined systematically. Many important debris-transport parameters will depend on the accident scenarios.

Perhaps the most important aspect of the accident scenario in regard to debris transport in the containment is the size of the break, which is usually specified as a small, medium, or large LOCA. The break size influences the debris transport in a number of ways:

- The size of the break largely determines the dynamics within the containment of the resultant primary system depressurization. The primary system depressurization period usually is referred to as the blowdown phase. Blowdown dynamics determine transport velocities and flow qualities within the containment, which in turn affect the mechanisms for debris deposition onto structures.
- The size of the break also affects the timing of the accident sequence, i.e., the completion of the blowdown phase, the ECCS injection phase, and the time when the recirculation pumps start to pump water from the sump (recirculation phase). The injection phase corresponds to ECCS injection into the primary system that subsequently establishes the sump pool. The recirculation phase refers to long-term ECCS recirculation.
- The size of the break can also determine whether the containment sprays activate. For large breaks, the sprays likely would activate almost immediately, whereas with a smaller break, the containment pressure rise may not be sufficient to initiate the sprays.
- The size of the break would determine the pumping flow rate from the sump in that the pump flow rate would be limited by the rate of flow from the break after the vessel inventory was replaced.

Debris transport would be affected by the location and size of the break. The location of the break, along with the general design of the containment, determines the patterns of flow throughout the containment. It affects flow

dynamics, how and where debris impacts structures, whether debris would be transported away from the sump or toward the sump, etc. The location of the break relative to the piping insulation would affect the type of debris being transported (refer to Section 3). The location of the break would also affect the sump-pool flow dynamics near the recirculation sump (refer to Section 5).

4.1.2 Plant Features Affecting Debris Transport

A number of features in nuclear power plant containments would significantly affect the transport of insulation debris. These features include the containment's engineered safety features and associated plant operating procedures. Perhaps the most significant containment feature is the containment pressure-suppression system. In a BWR plant, the primary pressure suppression system is its suppression pool and the containment sprays. In a PWR plant, the relatively large free volume functions to keep pressure from becoming excessive, thus, the large free volume is essentially a pressure-suppression system. The containment sprays also help keep pressure from becoming excessive. The containment size was reduced in ice-condenser plants because of their banks of ice, which would condense steam effectively, and in sub-atmospheric plants, where the operating pressure inside the containment is below atmospheric pressure. The most significant difference between PWR and BWR containments with respect to debris transport is the pressure-suppression system, other than the sprays, and its location relative to the postulated break. In BWR containments, the break effluences would flow down toward the suppression pool via downcomer vents, i.e., toward the ECCS suction strainers. In PWR containments, the break effluences would tend to flow generally up toward the large free volume of the containment dome, i.e., away from the ECCS sump screens. For example, in ice-condenser containments, the containment was designed to direct the break flows through the ice banks, which exit into the dome. These flows also would carry the insulation into these regions. This means that for PWR plants, substantial quantities of debris would be propelled away from the lower regions of the

containment and toward the higher regions² of the containment. If it were not for the containment sprays washing the debris down toward the recirculation sump, the debris carried aloft likely would remain in the higher reaches of the containment.

The flow propelling debris upward in the containment could be channeled through relatively narrow passageways in some containment designs, such as an ice condenser bank, where substantial portions of the debris entrained within the flow likely would be deposited inertially within the channel. Such an effect could provide a means for analytically determining a quantity of debris that would not likely subsequently transport downward to the sump. Other structural features would capture debris as it was propelled past the structure. These structures include gratings, piping, and beams.

After the airborne debris is dispersed throughout the containment, the washdown of that debris to the recirculation sump would be determined primarily by the design of the containment spray system, including the drainage of the sprayed water. First, the spray droplets would tend to sweep any remaining airborne debris out of the containment atmosphere, and then the falling droplets would wash debris off surfaces (structures, equipment, walls, floors, etc.). As the drainage water worked its way downward, entrained debris would move along with the flow. However, not all debris would be washed off surfaces and entrained, and the containment sprays may not cover substantial areas within the containment.

Containments are designed, in general, to readily drain the spray water to the sump to minimize water holdup and maximize sump water levels. However, the refueling pools could hold up substantial quantities of water if the pool drains are not open or are blocked by debris. Thus, the design of the refueling pools, including the pool drainage system, can be an important containment feature in regard to debris transport.

The locations where spray drainage enters the sump pool relative to the location of the

²This effect would be lessened somewhat when the pipe break was located higher up in the containment, such as in a main steam line.

recirculation sump are also important. Debris deposited into the pool well away from the recirculation sump would be less likely to transport to the sump screen than debris that was deposited near the sump. Debris transport within the sump pool depends on a number of plant features, including the lower compartment geometry that defines the shape and depth of the sump pool, such as the open floor area, ledges, structures, and obstacles within the pool. In addition, the relative locations of the sump, the LOCA break, and the drainage paths from the upper reaches of the compartment to the sump pool are important to determining pool turbulence, which, in turn, determines whether debris can settle in the pool.

4.1.3 Physical Processes and Phenomena Affecting Debris Transport

Of the full spectrum of physical processes and phenomena that would affect the transport of debris from its source to the sump pool, a subset has been identified that should be considered the most important in debris-transport analysis. These include thermal-hydraulic processes that contribute to the transport and/or deposition of the debris and the debris deposition

mechanisms. Further, these processes and phenomena can be grouped according to transport phase, i.e., the airborne dispersion by the depressurization flows and the subsequent washdown of dispersed debris by the containment sprays. These processes and phenomena are listed in Table 4-1 and described in Tables 4-2 through 4-5.

The complete range of thermal-hydraulic processes affect the transport of insulation debris. Furthermore, the containment thermal-hydraulic response to a LOCA includes most forms of thermal-hydraulic processes. Debris transport is affected by a full spectrum of physical processes, including particle deposition and resuspension for airborne transport and both settling and resuspension within calm and turbulent water pools for both buoyant and nonbuoyant debris. The dominant debris-capture mechanism in a rapidly moving flow likely would be inertial capture, but in slower flows, the dominant process likely would be gravitational settling. Much of the debris deposited onto structures likely would be washed off the structures by containment sprays or possibly even by condensate drainage. Other debris on structures could be subject to erosion.

Category	Airborne Debris Transport	Washdown Debris Transport
Thermal-Hydraulic Processes and Phenomena Affecting Debris Transport	Pressure-Driven Flows Localized Flow Fields Turbulence Liquid Flashing Entrained Liquid Liquid Impaction on Surfaces Surface Condensation Condensation on Debris Sheeting Flow Dynamics	Containment Spray Droplet Fallout Spray Droplet Accumulation Floor Drainage of Accumulated Spray Pool Formation (Other than Sump) Spray Drainage Runoff Break Deluge Ice Melting in Ice Condenser Plant
Debris-Transport Mechanisms	Debris Advection Disintegration Debris Entrapment (Deposition) Gravitational Settling Inertial Impaction Turbulent Impaction Diffusiophoresis Adhesion Resuspension	Spray Droplet Sweepout of Debris Surface Reentrainment of Debris Deluge Transport Accumulation of Entrained Debris Drain Blockage by Debris Pool Entrapment of Debris Debris Erosion (Disintegration)

Table 4-2 Thermal-Hydraulic Airborne Processes and Phenomena	
Processes and/or Phenomena	Description
Pressure-Driven Flows	The bulk flows, i.e., the net or macroscopic flow characteristics of the containment atmosphere. These flows would be the carriers of the debris. System-level thermal-hydraulic codes can predict these bulk flows reasonably well.
Localized Flow Fields	Flow directions and/or velocities that differ from the bulk atmosphere flow characteristics because of localized geometries. Localized flow fields would be most pronounced in the region near the break, where the depressurization jet is expanding and being redirected by structures, equipment, and walls. The flows can be extremely dynamic in this region. Predictions of these localized flow fields likely would require sophisticated CFD code analyses.
Turbulence	Local fluid vortices or flow eddies created by flow around obstacles. These vortices and flow eddies provide locations where debris potentially could settle even though bulk conditions would not predict settling. However, the locations could be transient such that settled debris could be reentrained.
Liquid Flashing	Liquid-to-vapor phase transformation caused by expansion across a choked break plane.
Entrained Liquid	Flow of break fluid that does not flash but continues as a liquid stream that would wet walls impacted by the stream and form pools as the water accumulates on the floor.
Liquid Impaction on Surfaces	Liquid impacting a surface (either entrained liquid or falling water droplets) that would wet that surface, thereby forming a liquid film on the surface. The liquid film would subsequently enhance debris capture by that surface. Debris-transport testing has shown surface wetting to greatly enhance debris deposition.
Surface Condensation	Formation of a liquid film on structure surfaces as a result of condensation of steam from the atmosphere would also wet surfaces. The rate of condensation depends on the rate of heat transfer into a structure, as well as on the moisture content of the atmosphere.
Condensation on Debris	Steam condensation onto debris in general would increase the weight of the debris, thereby enhancing the gravitational settling of that debris.
Sheeting Flow Dynamics	A dynamic sheet of water could be driven across a surface of any orientation by impaction of a liquid stream. This stream could entrain and transport debris already deposited onto that surface. Sheeting would most likely occur because of flows from the break. Before forming a sump pool, the initial break flows to the sump floor would transport debris already deposited on the sump floor (See Section 5).

Table 4-3 Airborne Debris-Transport Mechanisms	
Processes and/or Phenomena	Description
Debris Advection	Transport of airborne debris within the carrier-gas medium by flows at the spectrum of scales from bulk to turbulent eddies.
Disintegration	<p>Further destruction of debris as a result of debris impacting a structure, debris impacting debris, or liquid impacting debris. The most significant aspect of this secondary destruction is the generation of finer debris, such as individual fibers from fibrous insulation, because fine debris was found to readily transport from both the upper reaches of the containment by the containment sprays and within the sump pool. Further, this fine debris forms a thin uniform layer across the entire sump screen, threatening blockage through what has been called a "thin bed effect." Thus, a relatively small amount of disintegration could have a significant effect on screen blockage. Erosion of fibrous debris by falling water and within a turbulent pool has been seen experimentally.</p> <p>The opposite of disintegration, i.e., agglomeration, where debris pieces combine into larger pieces, was not observed during airborne debris-transport testing.</p>
Debris Entrapment (Deposition)	One mechanism or another would eventually trap debris undergoing airborne advection. Debris could be removed directly from the flow stream or through simple fallout of the atmosphere after depressurization completed. These mechanisms are listed next in this table.
Gravitational Settling	Downward relocation (sedimentation) of debris in the containment atmosphere onto structure surfaces under the force of gravity. Gravitational settling becomes an effective deposition mechanism after the bulk flow slows sufficiently so that gravity causes debris to fall faster than flow turbulence can keep the debris in suspension. Thus, gravitational settling would occur in regions well away from the break, where the break flow has dispersed, and after the depressurization completes (post-blowdown).
Inertial Impaction	Capture of debris particles on structure surfaces because of inertially driven impaction. Airborne-debris transport testing has demonstrated that inertial impaction is an effective form of deposition whenever flows are rapid and surfaces are wetted. Substantial debris was found to be deposited onto a grating whenever test flows passed through wetted grating onto miscellaneous structures such as I-beams and pipes, and onto flat surfaces when the flow was forced through a sharp bend. This type of debris deposition would be most effective in the region of the break or along the flow pathway from the break to the larger upper dome.
Turbulent Impaction	Capture of debris on structural surfaces caused by turbulent eddies. Although this form of debris deposition would occur, its importance is much less than deposition by inertial impaction and by gravitational settling. Also, turbulent impaction would be more effective on very fine debris than on larger debris.
Diffusiophoresis	Transport of debris particles toward deposition surfaces because of the concentration gradients of the atmosphere contents. Following a LOCA, the gradient is dominated by steam concentration gradients created by condensation on containment structures. This form of deposition is also secondary to deposition by inertial impaction and gravitational settling.
Adhesion	Permanent retention of debris particles on a structure surface as a result of mechanical interactions with a rough surface or other forces. The flow velocities would be insufficient to remove the debris from the surface again.
Resuspension	Reentrainment of debris previously deposited on structure surfaces into the atmosphere flow stream because of local fluid/structure shear forces.

Processes and/or Phenomena	Description
Containment Spray Droplet Fallout	Falling containment sprays condense steam and cool the containment atmosphere. The interaction of spray droplets with the atmosphere can induce local fluid vortices, eddies, or fields.
Spray Droplet Accumulation	Spray water would accumulate and run off of surfaces, providing another mechanism for debris transport.
Floor Drainage of Accumulated Spray	Spray water accumulating on a floor, other than the sump floor, would drain from that floor by pathways such as floor drains or an overflow onto a lower level.
Pool Formation (Other than Sump)	In some circumstances, spray water can pool at locations other than the sump. Water could pool in a refueling pool if the pool drains were not open or if the drains were blocked by debris.
Spray Drainage Runoff	The drainage of accumulated spray water from surfaces.
Break Deluge	Large flow rate of liquid effluent from a break in the reactor coolant system onto containment structures.
Ice Melt in Ice Condenser Plant	The water from melting ice would drain from the ice banks and thereby transport debris with the ice melt.

Processes and/or Phenomena	Description
Spray Droplet Sweepout of Debris	Transport of airborne debris from the containment atmosphere by containment spray droplets.
Surface Reentrainment of Debris	Reentrainment of debris previously deposited on structure surfaces by containment spray runoff.
Deluge Transport	Relocation of debris from containment structures due to interactions with the deluge of liquid from the ECCS and/or spray system.
Accumulation of Entrained Debris	Debris being transported by containment spray runoff can accumulate together at such locations as floor drains.
Drain Blockage by Debris	Accumulated debris could potentially form a flow blockage at drains, such as floor drains or the refueling pool drains.
Pool Entrapment of Debris	At any location where water could pool, debris could settle to the floor of that pool and remain there.
Debris Erosion (Disintegration)	Further destruction of debris as a result of spray drainage or deluge water impacting the debris. Under these conditions, disintegration is in the form of erosion, where finer debris, such as individual fibers from fibrous insulation, is removed from larger debris. This fine debris tends to transport readily from both the upper reaches of the containment by the containment sprays and within the sump pool. Further, this fine debris forms a thin uniform layer across the entire sump screen, threatening blockage. Thus, a relatively small amount of disintegration could have a significant effect on screen blockage. Erosion of fibrous debris by falling water and within a turbulent pool has been seen experimentally.

4.1.4 Debris Characteristics Affecting Transport

Transport of debris is strongly dependent on the characteristics of the debris formed, including the types of debris (insulation type, coatings, dust, etc.) and the size distribution and form of the debris. Each type of debris has its own set of physical properties, such as density; specific surface area; buoyancy when dry, partially wet, or fully saturated; and settling velocity in water. Several distinct types of insulation are used in PWR plants. The size and form of the debris depend on the method of debris formation, e.g., jet impingement, erosion, aging, operational, etc. The size and form of the debris affect whether it passes through grating or a screen, as well as affecting its transport to the grating or screen. For example, fibrous debris may consist of individual fibers or large sections of an insulation blanket and all sizes between these two extremes.

4.2 Airborne/Washdown Debris-Transport Testing

The NRC, U.S. industry, and international organizations conducted tests to examine different aspects of airborne and washdown debris transport within a nuclear power plant containment experimentally. The results of these tests provided qualitative insights into which physical processes and phenomena were most important and also provided quantitative test data regarding debris characteristics, deposition, and transport. Much of this information was obtained specifically to support the resolution of the BWR strainer-blockage issue; however, the information is also directly applicable to the PWR sump-screen blockage issue, for the most part.

The testing pertinent to airborne/washdown debris transport is listed in Table 4-6. The first four test series pertained to airborne debris transport, but not to washdown debris transport. Conversely, the last two test series in the table pertain to washdown but not airborne debris transport. The single test series sponsored by the BWROG had elements of both airborne and washdown debris transport within the series.

The NRC sponsored three series of small-scale tests designed to examine the transport and capture characteristics of debris within a BWR

drywell caused by steam and water depressurization flows and to examine the transport and erosion characteristics of debris within a drywell by water washdown flows.⁴⁻³

Two test series were designed to study airborne transport of fibrous debris: the separate-effects and the integrated-effects debris-transport tests. In the separate-effects tests, transport characteristics were determined for fibrous debris capture on structures where the test configuration was set up for one type of structure and orientation at a time, e.g., debris transport through a grating. In the integrated-effects testing, a combination of different types of structures was implemented into the test chamber at the same time. A third test series examined the transport and erosion characteristics of debris by water washdown flows within a drywell that impacted fibrous debris with water to determine the extent of transport from a structure and the degree of erosion to the debris that remained on the structure.

To date, only one series of small-scale tests has been performed by U.S. industry that relates to airborne/washdown debris transport. These tests were conducted to provide guidance to utilities for resolution of the BWR strainer-blockage issue, but are qualitatively applicable to the PWR issue as well.

Experiments have been conducted outside the U.S., and the NRC has reviewed data applicable to the resolution of the BWR strainer and PWR sump-screen clogging issues in the U.S. Three of these experiments obtained data that pertain to airborne and/or washdown debris transport. The primary source for this information is a knowledge base report prepared by the NRC for the Organization for Economic Cooperation and Development (OECD).⁴⁻⁴

These tests are summarized in the order listed in Table 4-6.

4.2.1 Airborne Phase Debris-Transport Testing

4.2.1.1 Separate-Effects Debris-Transport Tests

In 1996–1997, the Alden Research Laboratory (ARL) conducted tests for the NRC that were designed to provide a basic understanding of

Table 4-6 Airborne/Washdown Debris-Transport Testing

Test Description	Sponsor, Laboratory, and Date	Debris Source	Transport Medium	Objectives	Significant Limitations	Reference
Airborne-Phase Debris Transport						
Separate-Effects Debris-Transport Tests	NRC ARL 1997	Injection of Prepared LDFG Debris	Fan-Driven Air	Obtain basic data related to inertial capture of small insulation debris generated by a postulated MSLB. Possible degradation and erosion mechanisms by airflow were a secondary objective.	Limited debris sizes and loadings. One-dimensional flow fields. Non-prototypical congestion of structures. Use of airflow rather than steam flow. Only one type of insulation debris tested (LDFG).	NUREG/CR-6369 (Volume 2)
Integrated-Effects Debris-Transport Tests	NRC CEESI 1997	Air-Blasted LDFG Debris	Blowdown Air Jet	Obtain debris-transport data under integrated conditions prototypical of a BWR drywell following a postulated LOCA.	Use of airflow rather than steam flow. Surface wetness applied by spray mist rather than steam condensation. Only one type of insulation debris tested (LDFG).	NUREG/CR-6369 (Volume 2)
HDR Facility Blowdown Experiments (Full-Scale)	Owens-Corning HDR 1985	Steam-Blasted LDFG	Blowdown Steam Jet	Obtain containment thermal-hydraulic blowdown data. Two tests conducted to determine capability of LDFG insulation to withstand impact of high-pressure steam-water blast and to determine debris size distribution.	Limited debris-transport testing and data collection (for most of the test, debris-transport data were a by-product).	NEA/CSNI/R (95) 11 and NUREG-0897, Rev. 1
Karlshamn Steam Blast Tests	ABB-Atom Karlshamn 1992	Steam-Blasted Aged Mineral Wool	Blowdown Steam Jet	Investigate the dislodgment of insulation and subsequent transport in the containment following a LOCA.	Test scaling was too small to realistically simulate thermal-hydraulic conditions in a BWR drywell. Transport velocities were not typical of conditions expected in a nuclear power plant, i.e., the flows were too slow.	NEA/CSNI/R (95).11

Table 4-6 Airborne/Washdown Debris-Transport Testing

Test Description	Sponsor, Laboratory, and Date	Debris Source	Transport Medium	Objectives	Significant Limitations	Reference
Airborne/Washdown Combined-Phase Debris Transport						
BWROG Debris-Transport Tests	BWROG CD 1996	Injection of Prepared LDFG and RMI Insulation and Paint Chips	Steam/ Water Jet	Obtain insulation debris-transport data applicable to transport of debris from a BWR drywell to the wetwell through the downcomers and main vents. Specifically, obtain conservative estimates of the transport fractions for both the blowdown and washdown phases.	Test scaling was too small to realistically simulate thermal-hydraulic conditions within a BWR drywell.	NEDO-32686
Washdown-Phase Debris Transport						
Separate-Effects Insulation Debris Washdown Tests	NRC/SEA 1997	Air-Blasted and Prepared LDFG Debris	Sprayed Water	Obtain water-driven debris erosion data for debris captured by floor gratings.	Testing was small-scale. Only one type of insulation debris tested (LDFG)	NUREG/CR-6369 (Volume 2)
Oskarshamn NPP Containment Washdown Tests (Full-Scale)	ABB-Atom Oskarshamn NPP 1994	Old and New Insulation Material (Unknown Type)	Sprayed Water	Investigate the transport of insulation material by the containment spray system in a full-scale plant.	Most test conditions including type of insulation were not reported. Debris preparation and initial distribution may not have been typical of a postulated LOCA	NEA/CSNI/R (95) 11

LOCA-generated fibrous insulation debris capture on typical BWR containment structures as a result of an inertial capture process. Because these data were obtained for basic structural components that are common to both PWR and BWR containments, the results of these tests are generally applicable to all BWR and PWR containment designs. A complete description of the tests, including apparatus descriptions, procedures, and data, is documented in Volume 2 of Ref. 4-3.

The structural congestion (pipes, gratings, I-beams, and vents) within containments would affect the transport of fibrous debris, and substantial quantities of impacted debris likely would remain stuck (captured) on these structures. The tests were designed to examine the following.

1. The role of debris inertia on the capture during airborne transport of fibrous debris on typical BWR drywell structures (similar structures exist in PWRs). A number of different structures were tested to examine the effects of shape and orientation relative to the direction of flow.
2. The effect of surface wetness on retention of fibrous debris by surfaces impacted by debris. It was suspected that surface wetting resulting from steam condensation would significantly enhance the efficiency of capture.
3. Possible degradation and erosion mechanisms for captured large pieces (e.g., trapped against a grating) during blowdown. Such fibrous debris would be subjected to high-velocity steam flow intermixed with water droplets, thereby potentially further degrading the debris pieces.

A once-through flow tunnel was constructed of plywood panels with a blower at the upstream end of the test section and an air-filtering plenum downstream of the test section. The primary test section had a cross section with inner dimensions of 4 ft by 4 ft and a length of 8 ft. Because airflow velocities within this test section were limited to about 50 ft/s, a smaller 2-ft by 2-ft test section was inserted within the larger test section in selected tests to achieve velocities of up to 150 ft/s. The smaller test section was 5 ft long. The test apparatus is shown in Figure 4-1.

Perforated plates and a honeycomb structure were used to achieve a uniform velocity distribution. In addition, the head loss across this flow-conditioning device was calibrated with respect to tunnel velocities and later used to establish specified test section velocities.

Test obstructions consisted of individual components and combinations of individual components, with the individual components including I-beams, gratings, pipes, and a vent cover. Single-component tests involved mounting one or two objects side by side within the test tunnel with the objects being the same type, having identical cross sections, and being aligned similarly to the flow. In combined-component tests, combinations of components (one or more shapes) were mounted with different orientations, i.e., different alignments to the flow, and sometimes positioned so that front-mounted components partially shielded rear-mounted components. Thus, the effects of component proximity wake effects and shielding were evaluated.

Obstruction surfaces were wetted in most tests by spray injection nozzles located upstream of the test section. The duration of the spray controlled the extent of surface wetness (either 10 s or 30 s). Most tests were conducted with a 10-s prewet time.

The fibrous insulation debris was injected into the tunnel through a rupture disk capping one end of each of two pressurized 4-in. polyvinyl chloride (PVC) pipes. The pipes' sections were suspended from the tunnel ceiling downstream of the flow-conditioning structure and filled with preshredded insulation. Air was pumped into the pipe until the rupture disk failed, so that the jet of escaping air dispersed the insulation debris. The fibrous insulation debris was generated from heat-treated LDFG blankets.

Forty-eight tests were conducted to examine a variety of test conditions. The test parameters included

- the flow velocity (24–150 ft/s),
- the wetness of structure surfaces (dry to draining water film conditions),
- the type of structure (I-beams, piping, gratings, and Mark II vents),
- the approximate debris size, and
- the debris loading (6.3–12.5 g/ft²).

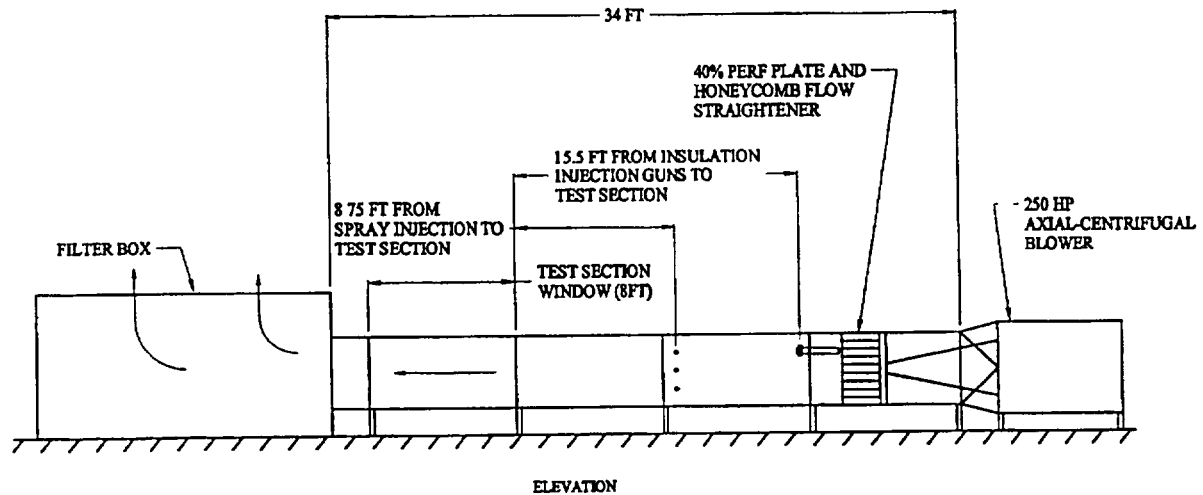


Figure 4-1 Separate-Effects Insulation Debris-Transport/Capture Test Apparatus

Within the ranges of tested parameters, the test data exhibited the following trends.

- Gratings captured more fibrous insulation debris than did other types of structures. For example, in combination-component tests in which the grating was placed downstream of other structures (pipes and I-beams), the grating captured substantially more debris than all other upstream structures combined.
- Surface wetness clearly influenced the extent of debris capture on structures, especially for pipes and I-beams. When pipes and I-beams were dry, these surfaces essentially did not capture debris. Capture on floor gratings was affected by wetness but was less sensitive to the degree of wetness than were other structure types. Typical debris capture by a wetted pipe is shown in Figure 4-2.
- Tests with dual gratings in series showed substantially more debris capture on the upstream grating (averaging about 25%) than on the downstream grating (about 12%), most likely because the largest debris was removed from the flow stream by the upstream grating. Note that the capture percentages reflect the fraction of the mass of debris approaching a particular structure that subsequently was captured by that structure.
- Mark II vents with wetted surfaces captured about 12% of small debris on the cover plate and the simulated drywell floor.
- Break-up or disintegration of fibrous debris captured on a grating was negligible when 6-in. by 6-in. thin pieces (1/8 to 1/2-in. thick) of insulation were subjected to gas velocities approaching 140 ft/s.
- Gravitational settling (i.e., debris settling to the tunnel floor) was negligible for all tests except the Mark II vent geometry (settling was not included in the vent-capture percentage).

These separate-effects tests had the notable limitations of

1. relatively light debris loadings on the structures compared with expected BWR conditions,
2. a modest assortment of debris sizes,
3. nonprototypical congestion of structures, and
4. overly simplified flow fields approaching the structures.

The debris loading approaching a structure refers to the density of debris pieces per unit of cross-sectional flow area. The principal concern was that debris captured on a structure could be knocked free (reentrained) by the impact of additional debris under conditions of heavy debris loading, thereby effectively reducing the capture efficiency for that structure. To ensure conservative estimates for debris capture, additional data were needed for heavier, more prototypical debris loadings. Therefore, additional experiments of a more representative

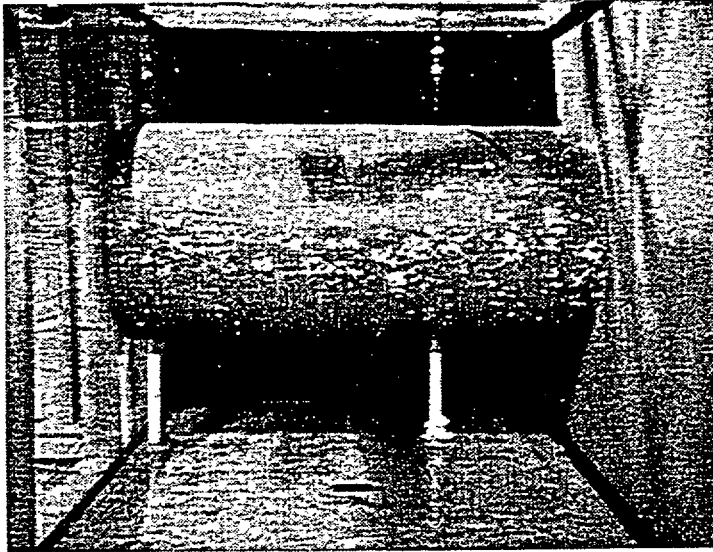


Figure 4-2 Typical Fibrous Debris Capture by a Wetted Pipe

and integrated nature were performed to further understand the role of fibrous insulation debris inertial capture.

4.2.1.2 Integrated-Effects Debris-Transport Tests

Although the separate-effects tests described in Section 4.2.1.1 provided valuable data, those tests still had the notable limitations listed above. The integrated debris-capture tests were designed to minimize the limitations noted for the separate-effects tests. The primary objective of these tests was to provide integrated fibrous-debris-capture data to benchmark analytical models and methods used to predict debris transport within a BWR drywell. The integrated-effects tests also combined debris generation with debris transport. The integrated debris-transport tests were conducted at the CEESI air-blast facility in 1997. A complete description of the tests, including apparatus descriptions, procedures, and data, is documented in Volume 2 of Ref. 3. Because these data were obtained for basic structural components that are common to both PWR and BWR containments, the results of these tests are generally applicable to all BWR and PWR containment designs.

The CEESI facility was capable of storing as much as 11,000 ft³ of air at 2,500 psia. In these tests, a dispersing 1,100-psi air jet was used to destroy insulation blankets and then transport

the debris through test chambers that contained obstructions. The insulation blankets were mounted and restrained in a manner designed to maximize their destruction and therefore maximize the amount of debris impacting the structures. Debris sizes ranged from individual fibers to partially intact blankets. The structures for debris capture were more complex and more prototypical than those used in the separate-effects testing. The flow patterns in the integrated testing were also more complex, (more three-dimensional) than those for the separate-effects testing. The data from these integrated tests were compared with the data from the separate-effects tests for insights into the effects of complex structural arrangements and fluid flows on debris capture.

The main test chamber, which is shown in Figure 4-3, consisted of a large horizontal cylinder with an inner diameter of 9.4 ft and a length of 93 ft. In addition, a 32-ft auxiliary chamber of the same diameter was attached with a flanged collar at the exit end of the main chamber in a horizontal "L" configuration. The upstream end of the main chamber, behind the air-jet nozzle, was blocked almost completely so that only a small portion of the air could exit the chamber in the reverse direction. The purpose of the auxiliary chamber was to investigate fibrous debris capture associated with flows undergoing a change in direction; in this case, a 90° bend.

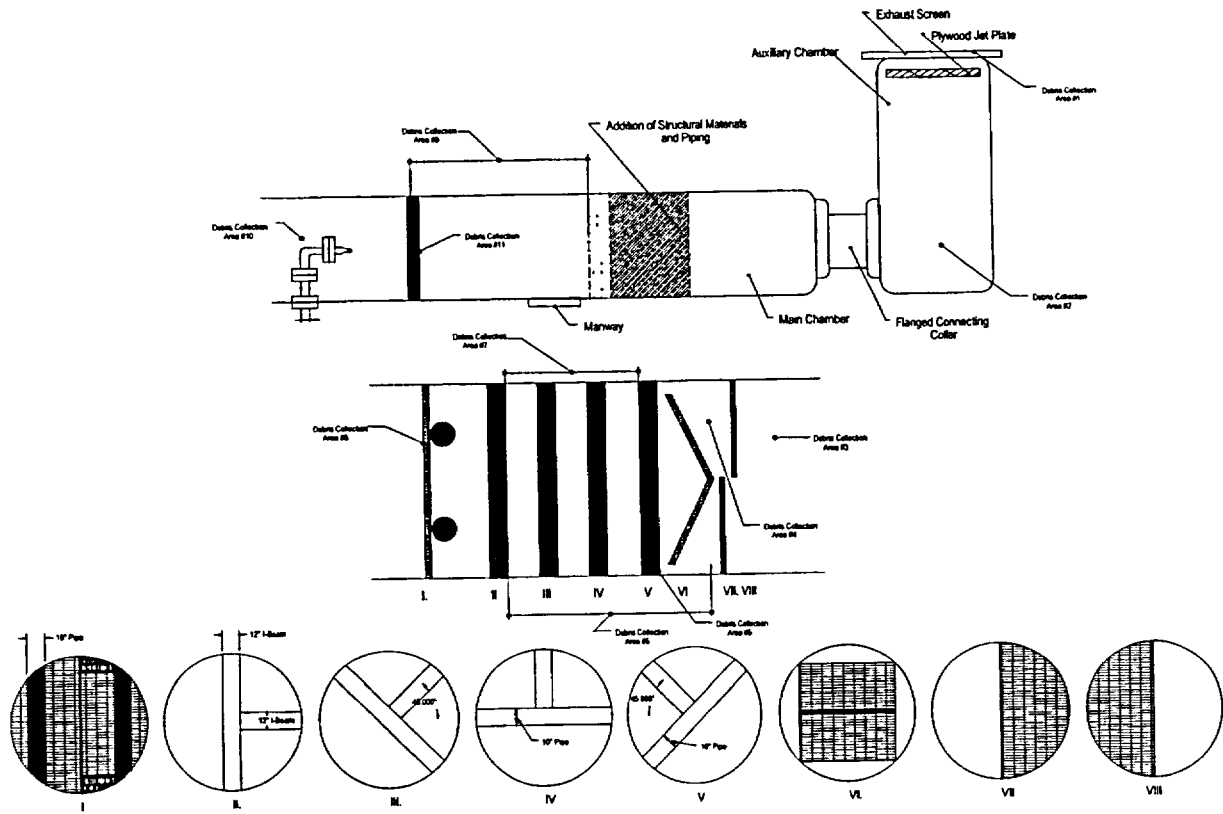


Figure 4-3 CEESI Air-Jet Test Facility

Target insulation blankets were mounted a few feet downstream of the air-jet nozzle. The blankets were mounted on a 12.75-in. outer diameter pipe that extended across the main test chamber at mid-height and positioned directly in front of the air jet nozzle. The target pipe mount was secured to rails so that the target could be positioned any distance from the jet out to 30 ft from the nozzle. The targets consisted of canvas-covered LDFG insulation blankets that were usually 3 ft long with either two or three stainless-steel bands placed around them to hold the blanket in place. Metal jackets were not used to encapsulate the blankets. A 1.5-ft-long blanket was used in one test.

The structural test section contained an assemblage of structural components (gratings, pipes, and I-beams) designed to simulate a prototypical section of a BWR drywell. The design focused on maintaining the same surface-to-volume ratios as found in BWR containments, and, to the extent practical, the structures were oriented in a manner analogous to the orientations found in actual plant

conditions. These structural components are also shown schematically in Figure 4-3.

All I-beams were 12 in. from upper to lower flange, and all pipes were 10 in. in diameter. I-beams were oriented with their web into the direction of airflow. Starting from the front (the flow entrance) of the structural test section, the test section contained the following structural subassemblies.

- A continuous grating with two vertically oriented pipes directly behind it
- I-beams with a full-length beam oriented vertically and a half-beam oriented horizontally
- I-beams with a full-length beam oriented 45° from vertical
- Horizontally oriented pipe with a half I-beam oriented vertically
- A pipe oriented 45° from vertical
- A V-shaped grating (approximately 56°) that obstructed about 57% of the total test-chamber flow area.

- Two half-section gratings separated axially by 22 in., referred as the split grating.

In the separate-effects tests, surface wetness was shown to affect the capture efficiency of structures profoundly. Therefore, surface wetness was a primary concern in the integrated tests. In the CEESI tests, structures were prewet with misters positioned throughout the test section. The mister system, which was constructed from PVC pipe, sprayed warm water as fine droplets from a high-pressure (150-psig) source. The misting system was operated long enough (approximately 10 min) to form a draining water layer.

The size of the jet nozzle was designed to minimize air usage while still allowing the jet to continue long enough for the debris-generation and debris-transport processes to complete (i.e., all debris was either deposited onto a surface or passed through the test chamber). The nozzle discharge was monitored and recorded. Developmental tests determined that at least 10 s were required for a 4-in. diameter nozzle and 12 s were required for a 3-in. diameter nozzle. Facility operators were able to approximate the jet-duration time specified for a particular test. Air-jet discharge was initiated using a rupture disk.

The developmental tests were instrumented with Pitot tubes to monitor and map the flow distributions before the flow entered the congested test section. The airflow velocities entering the area containing the congestion of structural components generally ranged from 25 to 50 ft/s. These velocities were in good agreement with velocities predicted for the tests using a commercially available CFD code. These velocities were also comparable to CFD-predicted velocities for a typical BWR drywell. After the flows dissipate into pressure-driven flows, BWR steam-flow velocities were predicted to generally range from about 30 to 50 ft/s. Therefore, the airflow velocities in the CEESI tests were considered prototypical of steam-flow velocities that would exist in a BWR drywell following a postulated LOCA.

Ten production tests that examined a variety of test conditions regarding debris transport were conducted. In addition, four of the developmental tests also provided useful debris-transport data. The test parameters included:

- the nominal nozzle diameter, either 3 or 4 in.,
- the duration of the air-jet flow (5 to 24 s),
- the surface wetness, and
- the distance between the nozzle and the target.

Most of the tests were conducted using a nominal 4-in. diameter nozzle, a flow duration of 12 to 17 s, and wet surfaces. One of the fibrous-debris transport tests (Test H7) was conducted with all surfaces deliberately maintained dry to illustrate the effect of surface wetness on debris capture. In addition, the mister system partially malfunctioned in two tests, resulting in incomplete surface wetness and a subsequent reduction in debris capture.

The distance between the nozzle and the target was initially adjusted until the optimum distance for maximum target destruction was found; a distance of ~120 in. (L/D of 30) appeared to maximize destruction. Insulation debris consisted of pieces of bare fiberglass insulation of various sizes, pieces of shredded canvas, agglomerated pieces containing both insulation and canvas, and large sections of the canvas cover that remained relatively intact and sometimes contained substantial quantities of insulation. The bare insulation was divided into three general size groups—large, medium, and small. Samples of debris pieces are shown in Figure 4-4.

The tests demonstrated the ability of structural components to capture debris. The average overall transport fraction for small debris in the CEESI was 33% of the total debris generated, i.e. ~2/3 of the generated debris was captured, primarily by inertial impaction, within the test facility.

Once again, gratings were found to be the most effective at catching fibrous debris. The debris captured by the split grating in Test H2 is shown in Figure 4-5. Note that the upstream gratings had captured the large debris already. The capture efficiencies for the split grating and for each test are plotted in Figure 4-6 as a function of debris loading. The corresponding separate-effects data also are shown. This figure clearly shows the effect of surface wetness and debris loading and the general agreement between the separate and integrated effects tests.

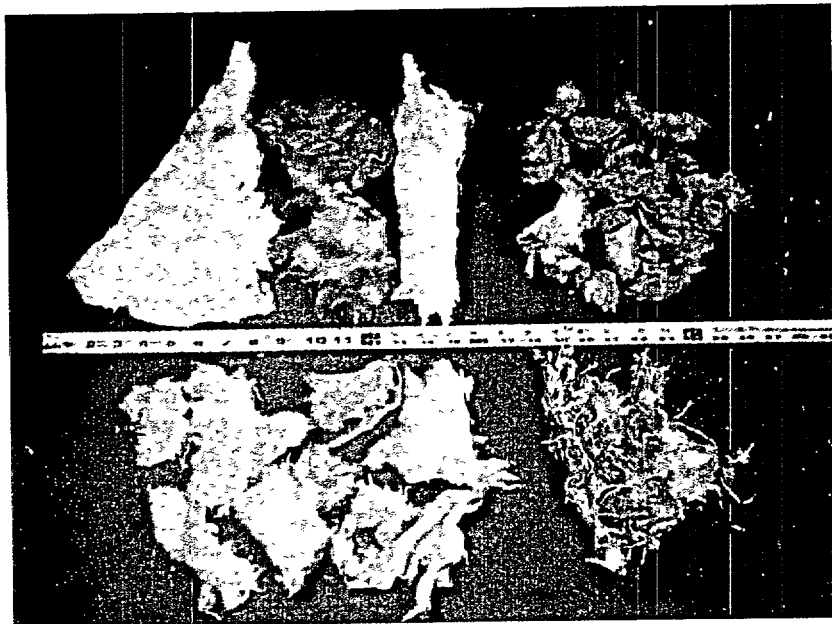


Figure 4-4 Samples of Debris Generated in the CEESI Tests



Figure 4-5 Typical Debris Deposition on a Grating in CEESI Tests

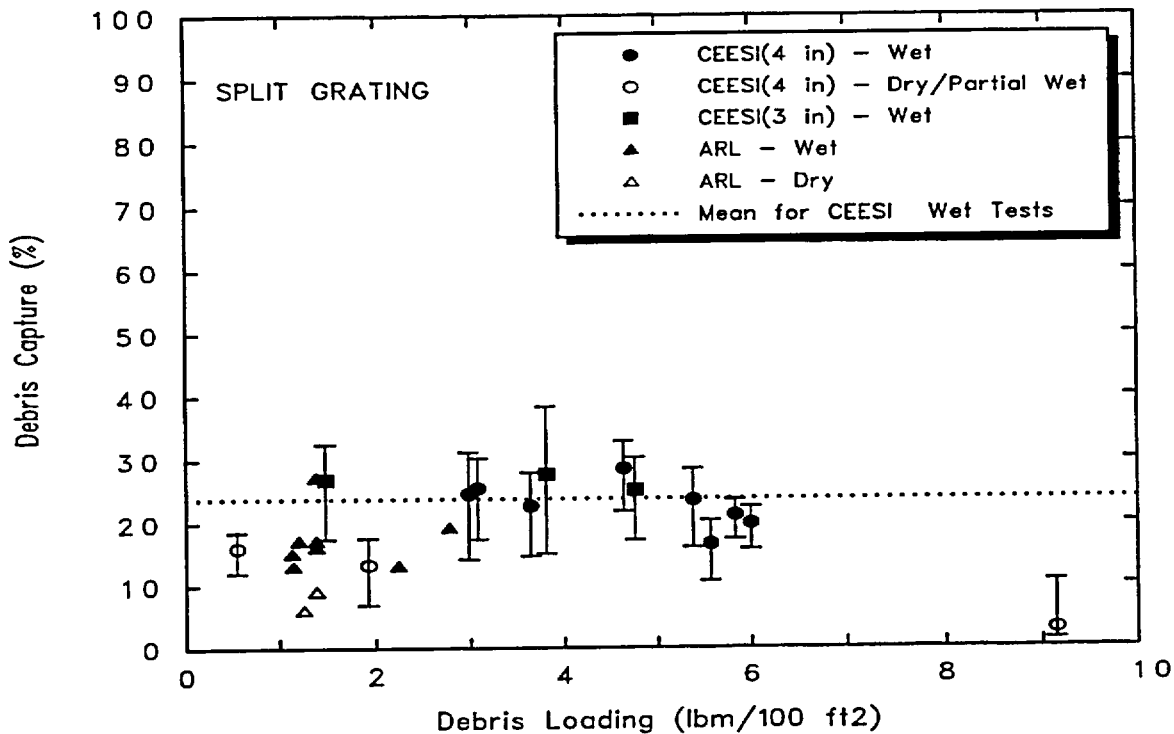


Figure 4-6 Capture of Small Debris by Grating

The average fractions of small debris captured by each test structure component are shown in Table 4-7. Note that the first continuous grating stopped almost all of the larger debris and that the capture fraction for the continuous grating was not obtained. This was because of the failure of the mister system to wet the continuous grating adequately (i.e., this grating illustrated dry behavior).

The 90° bend between the two chambers caused debris to be captured at the bend, which was maintained wet by a mister in the auxiliary chamber. Seventeen percent of the debris entering the auxiliary chamber was trapped on the chamber wall as a direct result of the bend. The I-beams and pipes captured a lesser but still substantial amount.

The capture fractions were found to be relatively independent of the debris mass loading (i.e., lbm/ft²) impacting the structures. The integrated-effects tests' capture data were consistent with the separate-effects tests data, indicating that the finer aspects of the local flow fields (e.g., eddies and wakes) do not influence debris capture significantly. The separate-

effects and integrated-effects tests clearly established that a fraction of the small and large debris would be deposited as the debris transported through the drywell following a blowdown. The most likely locations for the deposition in a BWR are the floor gratings located at different elevations. These captured pieces would potentially be subjected to subsequent washdown water flows.

4.2.1.3 Blowdown Experiments at Heissdampfreaktor (HDR) Facility

A decommissioned 100-MW_{th} superheated steam reactor, HDR, was refitted as a testing facility for LWR safety research.⁴⁴ The reactor vessel, without its internals, was decontaminated and modified for blowdown testing. For a blowdown test, the vessel was typically charged initially to 11 MPa and 310°C. Note that U.S. PWRs typically operate at a pressure of about 15 MPa.

About 40 blowdown tests were performed during the late 1970s and the 1980s. In general, the aim of these experiments was the qualification of equipment under accident conditions. Some of

Structure Type	Debris Capture
I-Beams and Pipes (Prototypical Assembly)	9%
Gratings	
V Shaped Grating	28%
Split Grating	24%
90° Bend in Flow	17%

the tests lasted for less than a second; during others, the content of the pressure vessel was allowed to expand until the vessel pressure dropped to containment pressure. The diameter of the nozzle was 0.45 m, and the break was initiated using a rupture disk. A deflector plate was installed in front of the nozzle to break up the jet. The tests were reviewed in regard to their applicability to debris generation; this review is discussed in Ref. 4-5.

The transport behavior of the insulation debris was not an objective of the experiments; it was only a by-product. Insulation material that was present for operational purposes was damaged badly in the first experiments and replaced by other insulation types in an effort to limit the damage. Different insulation types were used, including jacketed mineral wool (fibrous), foam glass, encapsulated fiberglass, covered glass wool, and RMI.

The HDR containment measures about 20 m (66 ft) in diameter and 60 m (200 ft) high and is subdivided into a number of compartments. The break compartment is situated about 25 m (82 ft) above the sump. The water from the break had to pass down through four floors to reach the sump.

Although debris transport was not an objective of the experiments, three observations were made regarding the transport of insulation debris within the HDR.

- Debris was found in rooms adjacent to the break compartment, as well as in the break compartment, for each type of insulation except RMI, indicating more limited transport for RMI than for other types of debris. However, only one RMI test specimen was used, so this test result may not be representative of the behavior of large amounts of RMI debris.

- The mineral wool insulation originally installed before the first blowdown experiment was torn from the piping during blowdown. This debris was caught in large flocks at railings and at other obstacles, as well as in stagnation areas. This observation provided initial indications of how fibrous debris would be captured.
- Almost no insulation debris was found in the sump, which was four floors beneath the break compartment. However, the post-test investigation did not examine the distribution of individual fibers. The predominant pathway for the blowdown flows would have been toward the larger compartments, i.e., the upper dome. Also note that these tests did not consider washdown debris transport from the operation of containment sprays, which certainly would have washed debris to the sump.

The results from these tests in regard to debris transport were only qualitative; even the distribution of insulation debris collected within the break and adjacent compartments was not quantified. However, insights were gained that supported later debris-transport testing.

4.2.1.4 Karlshamn Steam Blast Tests

Experiments were conducted by ABB-Atom at the Karlshamn fossil-fueled power plant to determine the relative distribution of insulation debris in the containment.⁴⁻⁴ These experiments were conducted in a small-scale test assembly that was subdivided into a few inner volumes. The outer dimensions of the assembly were 3.33 m by 2.56 m, and the assembly was 4.25 m high. The assembly was divided into four levels, as shown in Figure 4-7. Floor gratings connected the upper three levels. The lowest level simulated a wetwell, and the connection between the lowest level and the level above simulated a vent downcomer. The only water

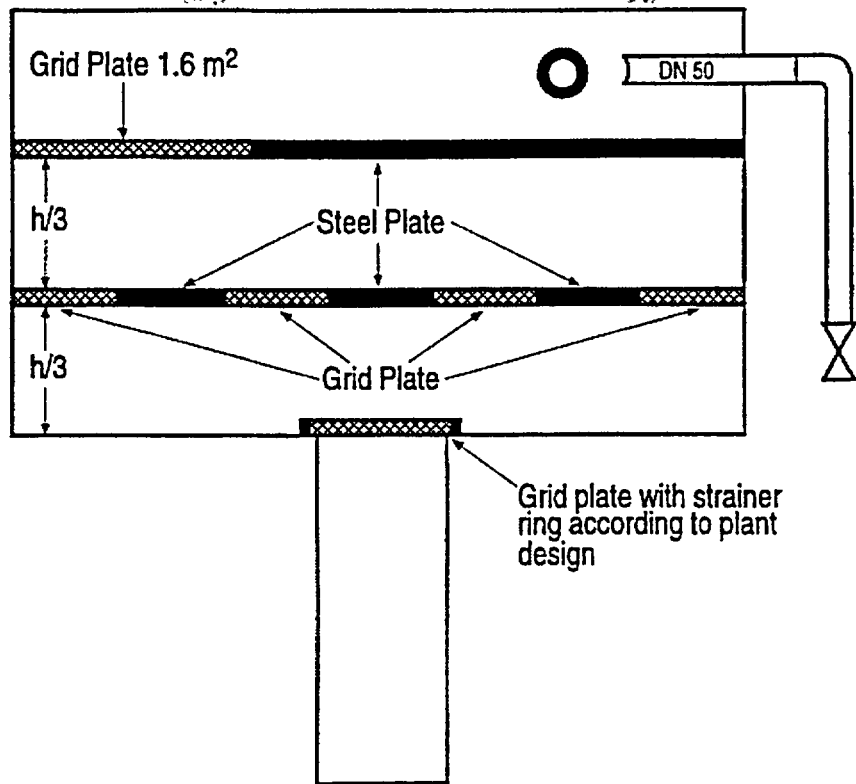


Figure 4-7 ABB-Atom Containment Experimental Arrangement

involved in these tests was condensed steam. Fibrous insulation was attached to a pipe in the upper level of the test apparatus, where it was exposed to a steam jet driven by an 8-MPa steam source.³ The jet fragmented the insulation, and the insulation debris was dispersed within the test apparatus by the steam flow and displaced air.

Most of the fibrous insulation debris was distributed in the upper parts of the test apparatus. The gratings held debris back, debris adhered to walls where steam condensed, and debris accumulated in areas of low flow velocity. Only minor quantities of the debris reached the wetwell level through the downcomer vent. In fact, the quantities reaching the wetwell were about 3% or less of the total quantity of dislodged insulation. As expected, the quantities of debris transported to the wetwell were found to be dependent on the transport velocities.

³An unknown amount of pressure was lost as the steam flowed through 75 m of pipeline from the source to the jet.

These findings are consistent with debris-transport test results from later, more sophisticated testing, even though the later testing showed much more debris transported to the wetwell. The peak bulk flow velocities in the Karlshamn tests were about 1 m/s, whereas the transport velocities were much faster following a postulated LOCA in an actual plant (and in the later, more typical tests conducted by the NRC). In the Karlshamn tests, debris was able to settle gravitationally at all levels, whereas at typical transport velocities, the flow turbulence would generally be much too high to allow settling anywhere near the break. After break flows disperse sufficiently into compartments well away from the break, flow velocities and turbulence can be expected to slow sufficiently to allow gravitational settling, as was seen in the Karlshamn tests. Thus, the Karlshamn tests might be considered representative of debris transport in some areas of PWR containments but not in the region of the break. The Karlshamn results might also be representative of debris transport following very small LOCAs. In general, the Karlshamn tests results have

limited applicability to the U.S. PWR sump-screen-blockage issue because the test scaling was not representative of U.S. containments and the debris transport velocities were not typical of expected velocities.

4.2.2 Airborne/Washdown Combined Phase Debris-Transport Testing

4.2.2.1 BWROG Testing of Debris Transport Through Downcomers/Vents

The NRC issued NRC Bulletin 96-03, "Potential Plugging of Emergency Core Cooling Suction Strainers by Debris in Boiling-Water Reactors," on May 6, 1996. All BWR licensees were requested to implement appropriate measures to ensure the capability of the ECCS to perform its safety function following a LOCA. The bulletin noted that plant-specific analyses to resolve this issue are difficult to perform because a substantial number of uncertainties are involved. These uncertainties included the amount of debris that would be transported to the suppression pool. The BWROG then developed the URG⁴⁻⁶ to provide utilities with:

- guidance on the evaluation of the ECCS potential strainer clogging issue for their plants,
- a standard industry approach to resolution of the issue that is technically sound, and
- guidance consistent with the requested actions in the bulletin for demonstrating compliance with 10 CFR 50.46.

The URG includes guidance on a calculational methodology for performing plant-specific evaluations. The NRC reviewed the BWROG URG document and issued the staff's SER on August 20, 1998.⁴⁻⁷

The BWROG sponsored tests designed to gather data on the transport of insulation debris from a BWR drywell to the wetwell through downcomers and main vents. The overall objective of this test program was to determine conservative estimates for the blowdown and washdown-transport fractions. As described in Ref. 4-6, transport fractions were measured through a 1/8-scale Mark I main vent and a Mark II downcomer for saturated steam, saturated water jets, and coolant water flows. Thus, the dynamics of debris transport were simulated in subscale containment configurations and scaled blowdown rates. A total of 33 tests was

conducted with fibrous insulation, RMI insulation, and paint chips. The tests investigated the effects of

- simulated debris preparation,
- full-scale prototypical gratings,
- blowdown jet orientation and duration,
- duration of debris washdown process,
- flow rate and pipe orientation, and
- debris introduction location.

Drums were used to construct containment vessels configured for the Mark I and Mark II vent designs, as shown schematically in Figures 4-8 and 4-9. The apparatus was simplified in that it did not contain any of the structural congestion typical of reactor containments, e.g., piping, wire trays, etc. A catch basket was attached to the end of the vent to trap the exiting debris. The drums were approximately 30 in. in diameter and 41 in. high (~125 gal.). For the Mark I configuration, prototypically-sized grating was placed at one level to estimate the effect of gratings on transport. Gratings were placed at two levels in the Mark II configuration. The system pressure, washdown flow rates, and debris quantities were measured in the tests.

For fibrous debris transport, it was concluded that

- the transport of all fibrous debris from the lower drywell volume is not a certainty;
- only the finest fiber debris fragments in Mark I containments may be carried from the lower drywell down the main vents;
- for the Mark II configuration, the average transport of fine fibers never exceeded 56%;
- for fiber debris larger than the distance between the bars of a typical grating, the transport fraction from the Mark I lower containment was 33%; and
- debris hang-up on the grating was dependent on grating location relative to the pipe-break location.

For RMI debris transport, it was concluded that

- nearly all of the small stainless-steel RMI foils transport from the lower Mark I containment volumes and
- an average of 10% of the small stainless-steel RMI foils transport from the lower Mark II containment volumes.

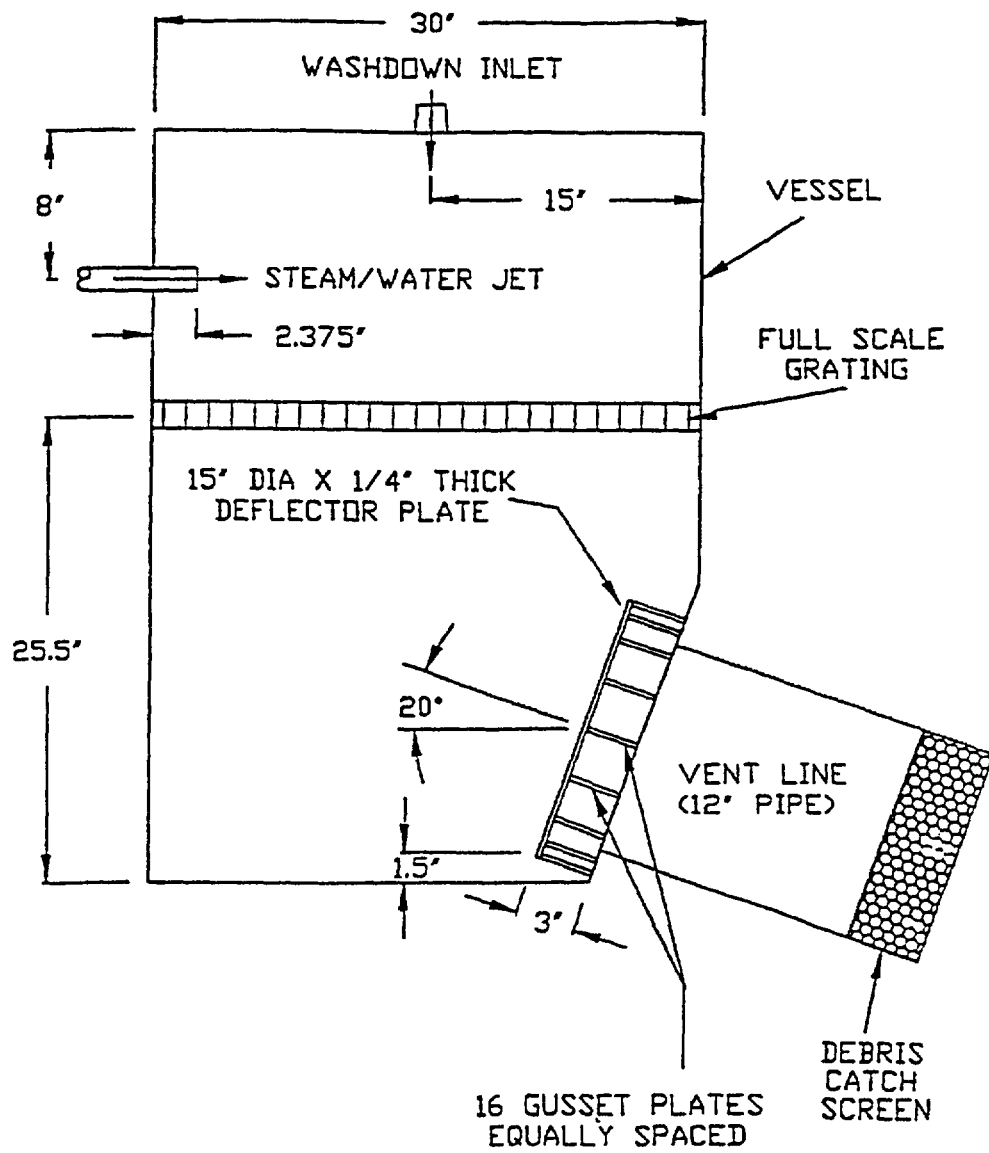


Figure 4-8 Schematic of 1/8-Scale Mark I Configuration Test Apparatus

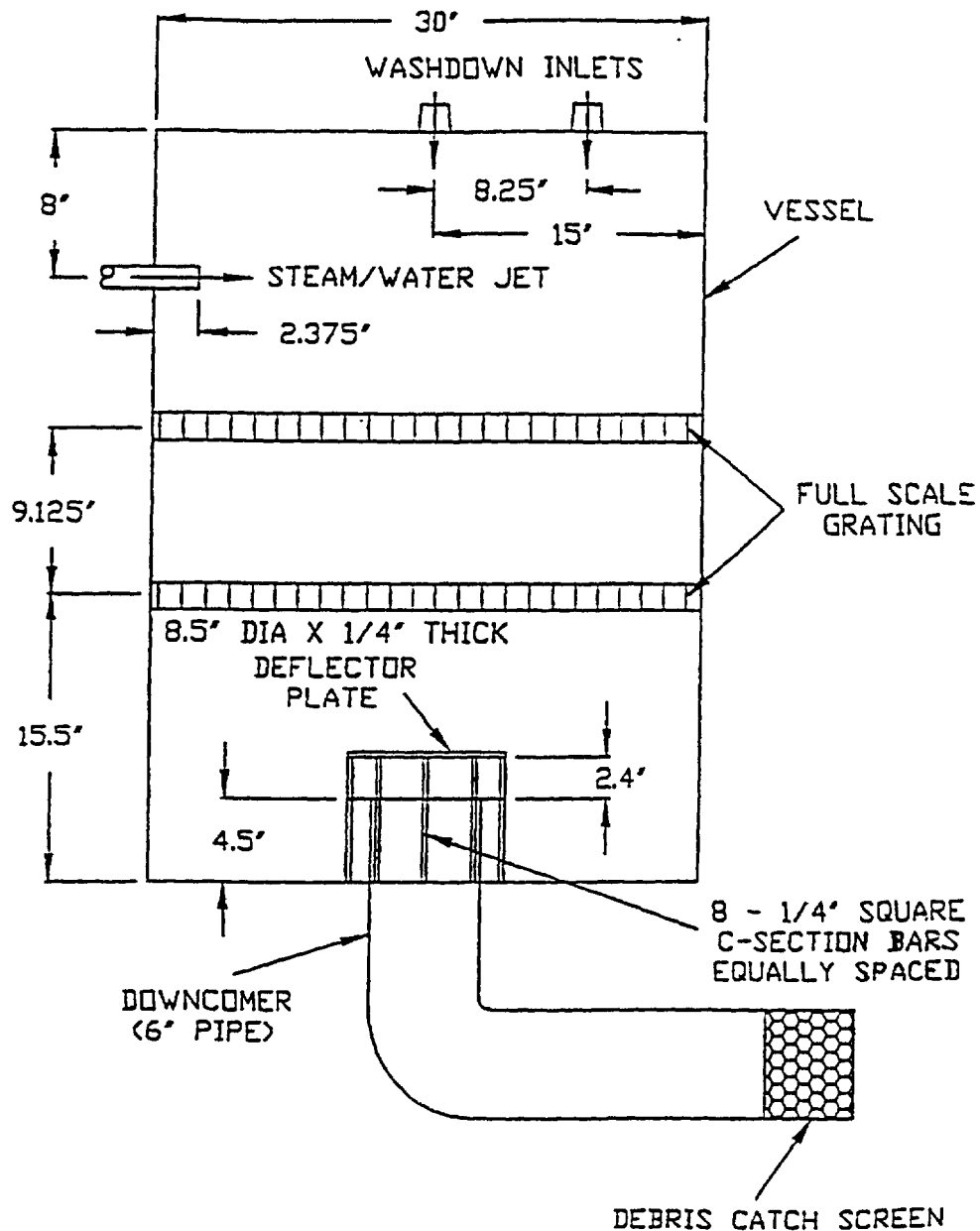


Figure 4-9 Schematic of 1/8-Scale Mark II Configuration Test Apparatus

The BWROG recommended 100% fine-fibrous debris transport through the drywell to the vent downcomers for the Mark I and III containment designs and 56% for the Mark II design. The transport of the large fibrous debris depended on the location of the debris relative to the gratings. For RMI debris, the BWROG again recommended 100% for the Mark I and III designs, but only 10% for the Mark II design. These numbers were for airborne and washdown debris transport combined.

The NRC review of the BWROG URG document^{4,7} with regard to the drywell debris transport determined that the guidance in the URG was nonconservative for Mark II containments. The NRC staff concluded that the same transport fractions used for the containments of Mark I and Mark III designs should also be used for the Mark II containments, i.e., 100% transport.

The primary criticism of the BWROG drywell debris-transport tests was of the scaling of the tests in that the drums were simply too small to simulate realistically the thermal-hydraulic conditions within a BWR drywell following a postulated LOCA. The test conditions, such as blowdown flow rates through the drum, may not have been prototypical. The BWROG did not perform any separate-effects testing to support the test results, which were for testing where all the effects were integrated. Much of the BWROG's claim of conservative results was based on exclusion of structures (piping, cable trays, etc.), which were not present in the experiments; however, the NRC-sponsored testing determined that the debris deposition on these structures was secondary in importance to the grating that was present in the test.

4.2.3 Washdown-Phase Debris-Transport Testing

4.2.3.1 Separate-Effects Insulation Debris Washdown Tests

Debris captured on structures during the blowdown phase following a LOCA would subsequently be subjected to transport and/or erosion by water flows from long-term recirculation cooling and containment sprays (washdown phase). For a BWR plant, the primary concern is the erosion and waterborne transport of debris captured on a floor grating directly below the broken pipe. In this situation, the debris would be pummeled by recirculation water flow that would cascade from the break to the drywell floor. Pieces of debris continually impacted by falling water could erode, allowing debris to pass through the grating and continue traveling toward the strainers. A series of tests was conducted in 1997 at a facility operated by SEA to examine the potential effect of washdown erosion. A complete description of the tests, including apparatus descriptions, procedures, and data, is documented in Volume 2 of Ref. 4-3.

The primary objective was to obtain experimental data that could be used to estimate the extent and timing of erosion during the washdown phase that would occur to insulation captured by floor gratings. The tests were to study the erosion of fibrous debris of different sizes at a variety of flow rates with the objective of answering two questions.

- What fraction of a piece of debris would erode and subsequently be transported to the drywell floor?
- Does the rate of erosion decrease with time, potentially reaching an asymptotic behavior?

These tests were conducted within a 5-ft-long, 2-ft by 2-ft vertical test chamber constructed of 0.5-in. clear polycarbonate to allow complete visualization of the tests. Figure 4-10 is a schematic of the test apparatus. An aluminum grating with 1-in. by 4-in. cells, which is characteristic of gratings used in BWR drywells, was placed at the bottom of this test chamber to hold the pieces of debris. Water was pumped into the top of the test chamber. Three simulated pipes were positioned to break up the structure of the injected flow before the water reached the debris. The simulated pipes were constructed of Plexiglas and were 2 in. in diameter.

A 400-gal. tank was used as a water reservoir for recirculation purposes. A 250-gpm centrifugal pump pumped water from this tank to the top of the test chamber through a 4-in. diameter PVC pipe. A debris catcher of fine-mesh wire screen was installed below the test chamber to catch insulation debris and erosion products, thereby preventing their recirculation back into the test chamber. A second filter was fitted to the pump suction to guarantee complete filtration of the debris from the pump inlet flow. A valve in the PCV pipe controlled the flow; the flow rate was monitored by a calibrated flow meter.

The simulated pipes conditioned the flow entering at the top of the test chamber; i.e., the bulk flow was broken up in a prototypical fashion. In this manner, water impacting the debris was spread relatively uniformly across the test chamber. In tests simulating spray-induced washdown, a removable spray head was attached to the PVC outlet.

Debris of various sizes was placed on the gratings and pipes and subjected to water flow typical of containment spray nozzles and break flow. Tests were conducted with room-temperature water using pieces of insulation generated by an air-jet impingement.

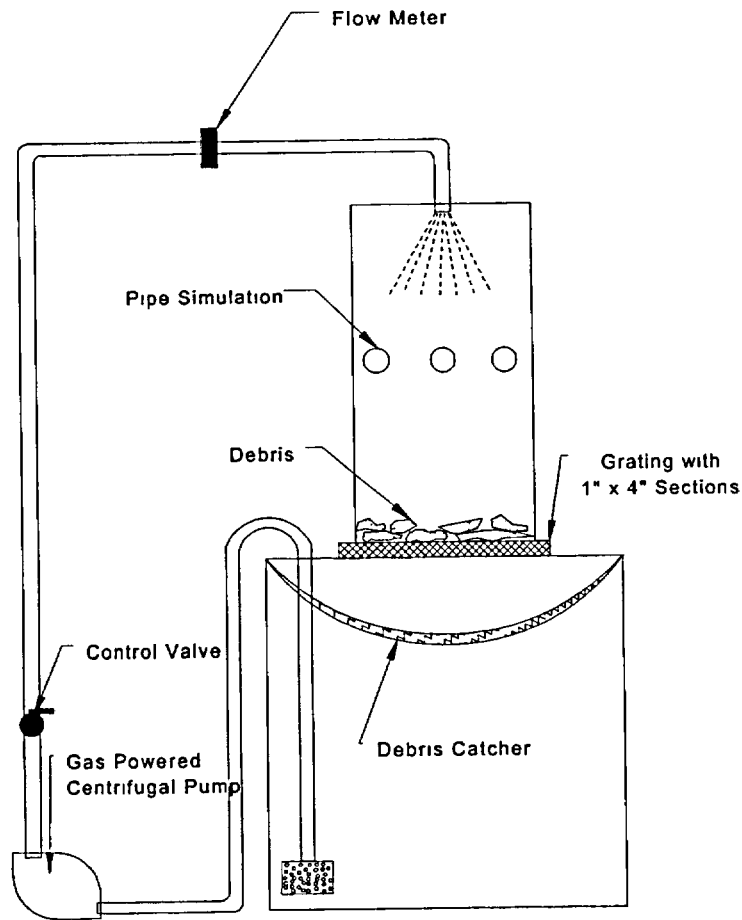


Figure 4-10 Schematic of Washdown Test Apparatus

Both the debris size and the water flow rate were varied to simulate washdown of small debris by containment sprays, as well as erosion and transport of large debris by break flows. Twenty-six parametric tests were conducted that examined a variety of test conditions. The test parameters included

- the water flow rate;
 - the type of flow conditioning, i.e., with or without the removable spray head;
 - the duration of the flow;
 - the size and condition of the debris;
 - the mass of the debris; and
 - the thickness of the debris bed.
- LDFG was tested, and four sizes of debris were tested to represent the range of debris expected following a LOCA:
- Fine Debris. This debris consisted of insulation pieces of loosely attached individual fibers less than an inch long. This debris was obtained directly from the CEESI air-jet transport tests. Such fine debris was typically found attached to wet surfaces such as pipes and gratings.
 - Small Debris. This debris was characterized having a light, loose, and well-aerated texture with an average density lower than 0.25 lbm/ft^3 . The pieces were typically about 1.5 in. in size and possessed little of the insulation's original structure. This debris also was obtained from the CEESI air-jet transport tests and was used primarily in the spray tests.
 - Medium Debris. This debris consisted of pieces of insulation typically about 4 in. by 6 in. in size. This debris was formed by one of two methods.

- Generated in the CEESI air jet tests where, although torn, the pieces kept some of the original structure of the insulation
- Intact insulation cut with scissors into medium-sized pieces
- **Large Debris.** This debris consisted of relatively large pieces of insulation ranging in size from 10 in. by 10 in. to 18 in. by 18 in. This debris was cut into predetermined sizes manually. Note that the air-jet tests clearly demonstrated that large pieces of debris produced by jet impingement tended to retain most of the original insulation structure.

Within the ranges of tested parameters, the data exhibited the following trends.

- Little or no erosion is possible for insulation pieces covered in canvas when they are subjected to washdown flow resulting from either the break overflow or containment spray.
- Most of the small pieces of debris resting on the grating bars will be washed down by water within approximately 15 min, after which the washdown reaches an asymptote.
- A significant fraction of the medium pieces would be eroded and transported.
- Large pieces will not be forced through the grating even at high flows. The pieces will remain on the grating and may erode with time. Erosion also exhibits a relatively constant rate behavior, as shown in Figure 4-11. The typical condition of debris after exposure to water is shown in Figure 4-12.
- The product of the erosion of large debris is fine debris, i.e., individual fibers and small clumps of fibers, that is likely to remain suspended in a pool of water with minimal turbulence.

Test Conclusions

- All finer debris (smaller than the grating cells) captured on the grating as a result of inertial capture would most likely be washed down when it is subjected to break and/or containment spray flows.
- A significant fraction of the medium pieces would be transported. For break overflows, most of the medium pieces likely would

transport. For containment spray flows, perhaps 50% would transport.

- Erosion of large debris is dependent on both time and flow rate. At low flow rates typical of containment sprays, the erosion of large pieces is negligible, especially considering that containment sprays are operated only intermittently. At water flow rates typical of break flow, the rate of erosion is substantial (as high as 25% for a 3-h duration). For such conditions, an erosion rate of 3 lbm/100-ft²/h is recommended.

4.2.3.2 Oskarshamn Nuclear Power Plant Containment Washdown Tests

ABB-Atom conducted experiments at the Oskarshamn BWR nuclear power plant to investigate the transport of insulation material by the containment spray system.⁴⁻⁴ After old and new insulation material was spread out on the diaphragm floor between the drywell and the wetwell, the containment spray system was activated. The distribution of the insulation material was determined after the experiments. In these experiments, a maximum of 5% of the material was transported into the wetwell.

The results of these tests have little value, primarily because the type and condition of the debris were not mentioned in the published report. Debris washdown is highly dependent on the type of insulation, the size of the debris, and the placement of the debris relative to the sprays and the vent downcomers. Based on U.S. NRC-sponsored testing, larger pieces of RMI debris placed well away from the inlet to the downcomer likely would have a very low transport fraction; conversely, fine fibrous debris likely would have a much higher transport fraction. These tests are mentioned here for completeness, but more information is needed for these tests to be useful.

4.3 Airborne/Washdown Debris-Transport Analyses

The NRC, U.S. industry, and international organizations have developed methodologies and performed analyses to estimate the airborne and washdown transport of debris within U.S. nuclear power plant containments. The results of these analyses provided qualitative and quantitative insights into the physical processes

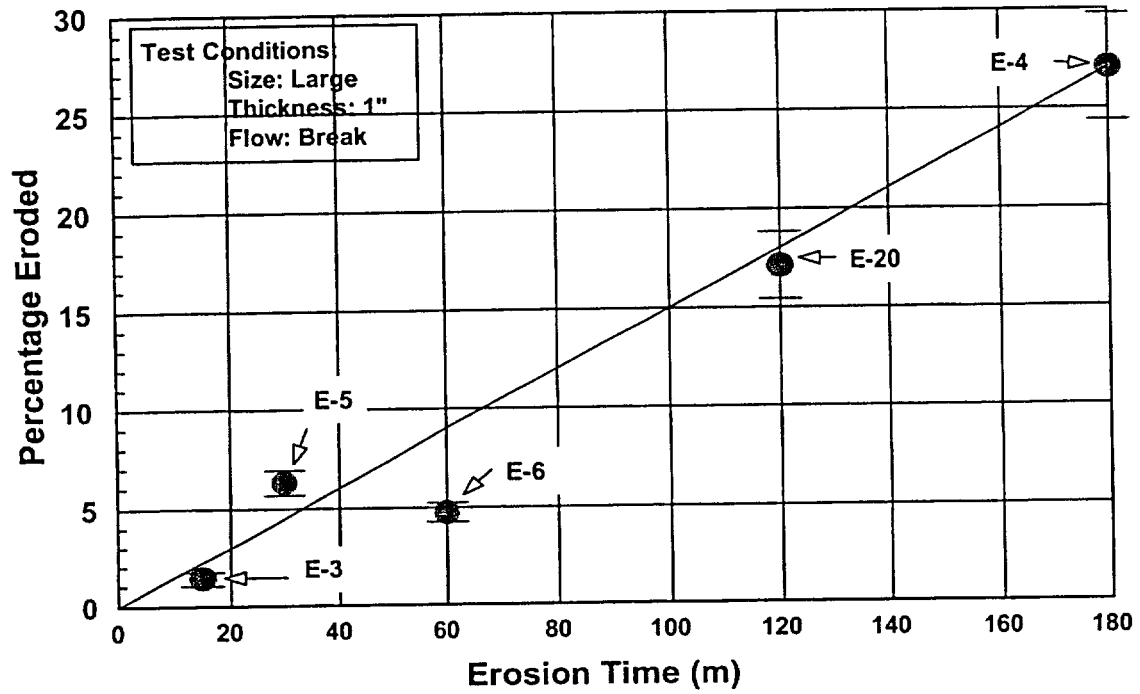


Figure 4-11 Time-Dependency of 1-in. Insulation Blanket Material Under Break-Flow Conditions

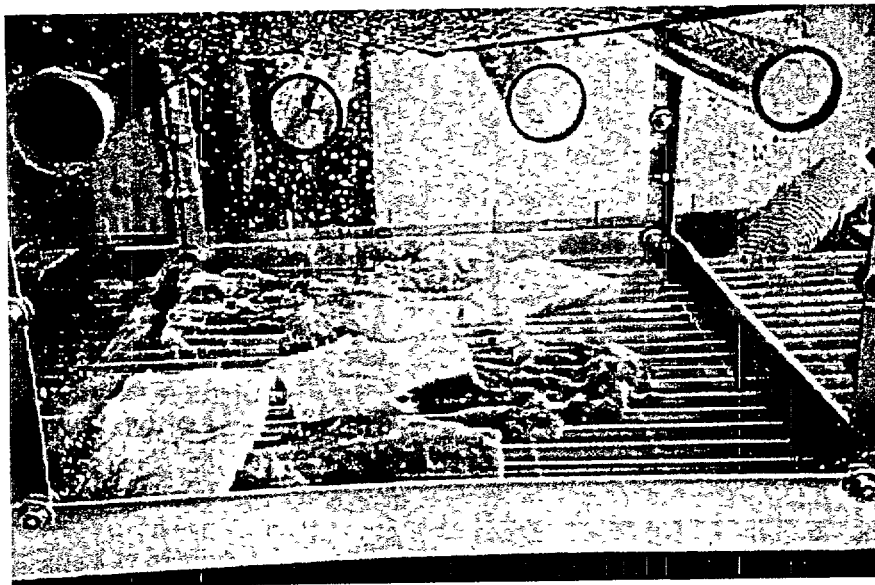


Figure 4-12 Typical Condition of Debris After Exposure to Water

and phenomena that govern debris transport. As mentioned earlier, much of this information was obtained specifically to support the resolution of the BWR strainer blockage issue; however, that information also is directly applicable to the PWR sump-screen blockage issue for the most part.

The analyses pertinent to airborne/washdown debris transport are listed in Table 4-8. These analyses include the following.

- Brief evaluations of operational incidents that occurred at the Gundremmingen-1 nuclear power plant (1977) in Germany and at the Barsebäck-2 nuclear power plant (1992) in Sweden in which insulation debris was generated and transported. These incidences both occurred at plants that had similarities to U.S. BWR plants (Section 4.3.1).
- The NRC sponsored the development of debris-transport PIRTs for both BWR and PWR nuclear power plants in the U.S. (Section 4.3.2).
- The Karlshamn debris-transport tests were simulated with the MELCOR code to test the ability of the code to predict the transport of insulation debris (Section 4.3.3.1).
- The NRC sponsored the DDTS to estimate BWR drywell debris-transport fractions using a bounding analysis approach (Section 4.3.3.2).
- The NRC sponsored a detailed analysis of debris generation and transport within a volunteer U.S. PWR nuclear power plant (Section 4.3.3.3).
- The BWROG developed their URG to support utility plant-specific analyses (Section 4.3.4.1).
- The NRC sponsored a parametric evaluation of the potential for sump-screen blockage within operating U.S. PWR plants. The evaluation included a generic estimate of the containment debris-transport fractions (Section 4.3.4.2).

4.3.1 Evaluations of Operational Incidents

4.3.1.1 Evaluation of Incident at Gundremmingen-1

An event occurred at the German BWR reactor Gundremmingen-1 (KRB-1) in 1977 in which the 14 SRVs of the primary circuit opened during a transient.^{4,4} The SRVs were located inside the

containment at a pipe attached to the main steam line between the reactor pressure vessel and the high-pressure turbine. The valves blew directly into the surrounding containment where the pipes had been insulated with fiberglass insulation reinforced with wire mesh and jacketed with sheet zinc. The piping insulation was extensively damaged.

After the incident, approximately 450 m³ (16,000 ft³) of water was found in the sump; about 240 m³ (8500 ft³) of the water originated in the coolant circuit; the rest was delivered by the CSS. This water transported a substantial quantity of insulation debris into the control drive mechanism compartment directly below the SRVs. The floor was covered with flocks of insulation material, but no larger parts of the insulation, such as sheet metals or textiles, were transported there. A thick layer of fiberglass insulation was found at the strainers installed in front of ducts leading from this compartment into the sump. Because recirculation from the sump was not required, the layer of insulation debris on the strainers had no further consequences. Therefore, it is not known whether recirculation from the sump was possible. No details regarding the quantities of debris generated and transported were made available for further analysis. Nevertheless, the potential for clogging recirculation strainers with insulation debris generated by an operational incident was clearly demonstrated.

4.3.1.2 Evaluation of Incident at Barsebäck-2

An event occurred at the Barsebäck-2 BWR nuclear power plant on July 28, 1992, during a reactor restart procedure after the annual refueling outage.^{4,4} The reactor power was below 2% of nominal when an SRV opened inadvertently because of a leaking pilot valve. The main valve opened when the reactor pressure had reached 3.0 MPa (435 psig). The steam was released as a jet directly into the containment. The containment is basically an upright cylinder with the drywell in the upper part and the wetwell directly beneath. Vertical pressure-relief pipes connect the drywell and the wetwell, and their openings are flush (covered by gratings) with the drywell floor. The containment was isolated when the drywell pressurized, so the blowdown pipes into the wetwell cleared. The containment vessel spraying system and the ECCS were started automatically.

Table 4-8 Airborne/Washdown Debris-Transport Analyses

Test Description	Sponsor, Analyst, and Date	Debris Source	Transport Medium	Objectives	Evaluation Products	Reference
Evaluation of Operational Incidences						
1977 Incident at Gundremmingen-1	OECD --- 1996	Damage to Operational Fiberglass Insulation	Inadvertent Opening of 14 SRVs and Containment Sprays	Understand debris transport that occurred during an operational incident at a nuclear power plant.	Qualitative information only. No details regarding quantities of debris generated and transported were made available for analysis. However, the potential for clogging recirculation strainers with insulation debris generated by an operational incident was clearly demonstrated.	NEA/CSNI/R (95) 11
1992 Incident at Barseback-2	OECD --- 1996	Damage to Operational Fiberglass Insulation	Inadvertent Opening of SRV and Containment Sprays	Understand debris transport that occurred during an operational incident at a nuclear power plant.	The quantities of debris generated and the dispersion of that debris were estimated. However, the relative quantities transported by airborne dispersion vs debris washdown could not be determined.	NEA/CSNI/R (95) 11
Phenomena Identification and Ranking Tables (PIRTs)						
BWR PIRT	NRC PIRT Panel 1997	Postulated LOCA-Generated Insulation Debris	BWR LOCAs	Use PIRT process to identify phenomena and to rank their importance as related to transport of LOCA-generated debris within U.S. BWR drywells and advise the NRC staff regarding debris-transport analyses and experimentation.	PIRT tables identified phenomena that could potentially influence debris transport within BWR drywells and ranked them according to their perceived importance with the highest-ranked phenomena clearly flagged.	INEEL/EXT-97-00894
PWR PIRT	NRC PIRT Panel 1999	Postulated LOCA-Generated Insulation Debris	PWR LOCAs	Use PIRT process to identify phenomena and to rank their importance as related to transport of LOCA-generated debris within U.S. PWR containments and advise the NRC staff regarding debris-transport analyses and experimentation.	PIRT tables identified phenomena that could potentially influence debris transport within PWR containments and ranked them according to their perceived importance with the highest-ranked phenomena clearly flagged.	LA-UR-99-3371, Rev. 2

Table 4-8 Airborne/Washdown Debris-Transport Analyses

Test Description	Sponsor, Analyst, and Date	Debris Source	Transport Medium	Objectives	Evaluation Products	Reference
Airborne/Washdown Debris-Transport Evaluations						
MELCOR Simulation of 1992 ABB-Atom Karlshamn Tests	SEA SEA 1995	Steam-Blasted Fibrous Debris	Blowdown Steam Jet	Test the ability of the MELCOR code to simulate insulation-debris transport.	The MELCOR code predicted results that compared well with the experimental debris-transport results. However, it was determined that the Karlshamn flow velocities were atypically too slow and that the MELCOR code would not likely perform well at typical flow velocities where inertial impaction would be a primary deposition mechanism because MELCOR does not model inertial impaction.	SEA-95-970-01-A:5
Drywell Debris Transport Study (DDTS)	NRC SEA 1997	BWR LOCA-Generated Debris	LOCA Steam-Water and Containment Sprays	Using a bounding analysis approach, the fractions of postulated LOCA-generated debris that subsequently would be transported to the wetwell were estimated. The analysis considered both the blowdown and the washdown phases.	Transport fractions for fibrous insulation debris were estimated using assumptions appropriate for an upper-bound estimate and a less conservative central estimate. In addition, the study provided engineering insights into debris transport processes that were useful when judging appropriateness of utility-generated debris-transport fractions.	NUREG/CR-6369
PWR Volunteer Plant Analysis	NRC LANL 2002	PWR LOCA-Generated Debris	PWR LOCAs	Develop and demonstrate a methodology for estimating the debris-transport fractions within PWR containments.	Generalized methodology was developed and demonstrated by estimating the transport fractions for a specific LOCA in the volunteer plant.	TBD

Table 4-8 Airborne/Washdown Debris-Transport Analyses

Test Description	Sponsor, Analyst, and Date	Debris Source	Transport Medium	Objectives	Evaluation Products	Reference
Generalized Debris-Transport Guidance						
BWROG URG	BWROG BWROG 1996	BWR LOCA- Generated Debris	BWR LOCAs	Provide guidance to the operators of U.S. BWR nuclear power plants regarding the resolution of the BWR strainer blockage issue. This guidance included methodology for estimating the drywell debris transport fractions.	The URG for ECCS Suction Strainer Blockage was developed. (The NRC staff subsequently reviewed the URG; their review comments noted where they agreed or did not agree with the URG.)	NEDO-32686
Transport Fractions for Parametric Evaluation	NRC LANL 2002	PWR LOCA- Generated Debris	PWR LOCAs	Generic composite debris-transport fractions were estimated to support the parametric evaluation of the potential for sump-screen blockage in U.S. PWR plants.	A set of transport fractions was estimated based on both documented research and on-going research that could be applied in a generic fashion to all U.S. PWR plants for the specific purposes of the parametric evaluation and therefore are not generally applicable to plant-specific analyses. These transport fractions, defined as the fraction of the ZOI insulation subsequently transported to the sump screen, tended to favor the plant situation and thus should not be treated as conservative.	NUREG/CR-6762

About 200 kg (440 lb) of fibrous insulation debris was generated and about 50% of this debris subsequently reached the wetwell, resulting in a large pressure loss at the strainers about 70 min after the beginning of the event. Gratings in the drywell did not hold back the insulation material effectively. The approximate distribution of insulation debris within the drywell following the event was

- 50% on the beamwork, mainly concentrated in three areas: inside the drywell "gutter," near the outer containment wall, and on or near the grid plates over the blowdown pipes;
- 20% on the wall next to the affected pipe, from which most of the insulation originated, and on the components around the safety valve;
- 10% on the wall opposite the affected pipe;
- 12% on the walls above the grating lying above the safety valve; and
- 8% on the grating above the safety valve.

The debris was transported by steam and airflow generated by the blowdown and by water from the CSS. It could not be determined how the transport developed with respect to time and whether the blowdown or washdown processes transported the major part of the debris found in the wetwell.

The generation and transport of large amounts of fibrous debris by the simple erroneous opening of a safety valve were observed. The transport included the short-term transport resulting from the steam and air blast and the longer-term washdown transport associated with operation of the containment spray system. The extent of damage and of transport appeared to be remarkably large given the small leak size and low reactor pressure. The locations of debris on such surfaces as the walls suggest the significance of inertial impaction as a deposition mechanism near the location of the break.

4.3.2 Phenomena Identification and Ranking Tables

4.3.2.1 BWR PIRT

The NRC sponsored the formation of a PIRT panel of recognized experts with broad-based knowledge and experience to identify and rank the phenomena and processes associated with the transport of break-generated debris through a BWR containment drywell following the

initiation of one or more accident sequences.⁴⁻² The primary objective of the BWR PIRT was to support the DDTs, which is discussed in Section 4.3.3.2. The PIRT process was designed to enhance the DDTs analysis by identifying processes and phenomena that would dominate debris-transport behavior. Further, these processes and phenomena were prioritized with respect to their contributions to the reactor phenomenological response to the accident scenario. The PIRT panel also evaluated the plans for experimental research, the experimental results, and the analytical results. Their final report was updated to reflect the final results of the DDTs. The phenomena ranked as having the highest importance with respect to debris transport within a BWR drywell are listed in Table 4-9.

4.3.2.2 PWR PIRT

Like the BWR PIRTs discussed in Section 4.3.2.1, the NRC sponsored the formation of a PIRT panel of recognized experts with broad-based knowledge and experience to identify and rank the phenomena and processes associated with the transport of debris in PWR containments following the initiation of one or more accident sequences.⁴⁻¹ The PWR PIRT has been used to support decision-making regarding analytical, experimental, and modeling efforts related to debris transport within PWR containments.

A modest database of experimental and technical results existed to support this PIRT effort. The PIRT panel initially focused on a Westinghouse four-loop PWR with a large dry ambient containment as the base configuration and a double-ended, cold-leg, large-break LOCA for the baseline scenario. Following the initial effort, the PWR PIRT considered the other two existing U.S. PWR containment designs, i.e., the sub-atmospheric and ice condenser containments. The event scenario was divided into three time phases: blowdown between event initiation and 40 s, post-blowdown between 40 s and 30 min, and sump operation between 30 min and 2 days. Each phase was characterized with respect to physical conditions, key phenomena and processes, and equipment operation. The containment was partitioned into three components:

- the containment open areas, excluding the potential pool in the bottom of the

Processes and/or Phenomena	Description
Pressure-Driven Flows	These flows represent the bulk flows, i.e., the net or macroscopic flow characteristics of the containment atmosphere.
Localized Flow Fields	Flow direction and/or velocities that differ from the bulk atmosphere flow characteristics because of localized geometries.
Liquid Flashing	Liquid to vapor phase transformation because of expansion across choked break plane.
Recirculation Deluge (Steaming)	Large flow rate of liquid effluent from a low-elevation break in the reactor coolant system (e.g., recirculation line) onto drywell structures or from sprays when activated.
ECCS Deluge	Large flow rate of liquid effluent from ECCS onto drywell structures.
Drywell Floor Pool Formation, Overflow, and Flow Dynamics Following Recirculation Line Break	Creation of a water pool on the drywell floor sufficiently deep to allow overflow into wetwell transfer piping. Flow dynamics include multi-dimensional flow patterns and velocities, free-surface behavior, and turbulent mixing.
Surface Wetting	Formation of a liquid film on structure surfaces due to condensation of steam from the atmosphere or impaction of water droplets onto structure surfaces.
Structural Congestion (Porosity)	Variations in fluid flow area and flow as related to the density of the structures in the drywell, and due to the tortuousness of the flow paths around these structures.
Debris Advection/Slip	Transport of airborne debris within the carrier gas medium.
Inertial Impaction	Capture of debris on structure surfaces due to inertial impaction.
Adhesion	Permanent retention of debris particles on a structure surface due to mechanical interactions with a rough surface or other forces.
Recirculation Deluge (Steaming) Related Transport	Relocation of debris from drywell structures due to interactions with the deluge of liquid from recirculation pipe breaks, or sprays.
Debris Transport and Deposition within Pool	Relocation of debris in the drywell floor pool towards the wetwell vent pipe entrances.

- containment and the debris-generating ZOI in the vicinity of the break;
- the containment structures; and
- the containment floor upon which a liquid pool forms in the lower containment elevations.

The panel identified a primary evaluation criterion for judging the relative importance of the phenomena and processes important to PWR-containment debris transport. The criterion was the fraction of debris mass generated by the LOCA that is transported to the sump entrance. Each phenomenon or process identified by the panel was ranked relative to its importance with respect to the transportation of debris to the sump entrance. Highly-ranked phenomena and processes were judged to have a dominant effect with respect to the primary evaluation

criterion. Medium-ranked phenomena and processes were judged to have a moderate effect with respect to the primary evaluation criterion. Low-ranked phenomena and processes were judged to have a small effect with respect to the primary evaluation criterion.

The results of the panel's identification and ranking efforts were tabulated, and all processes and phenomena were ranked according to perceived relative level of importance, i.e., high, medium, or low. (See the PWR-PIRT final report for complete tabulation). The processes ranked as high are shown in Table 4-10. In the table, the processes and phenomena are grouped by accident phase and containment location. Most of the high-importance processes dealt with debris transport on the containment floor, where the sump pool was either forming or

Transport Phase	Containment Component		
	Open Areas	Structures	Floor
Blowdown (0–40 s)	Gravitational settling	None	None
Post-Blowdown (40 s–30 min)	Droplet motions Debris sweepout	Surface draining Deluge transport Disintegration Entrapment	<u>Pool Behavior</u> Formation Agitation Flow dynamics Film entry transport Liquid entry transport Disintegration Settling Transport
Sump Operation	None	None	<u>Pool Behavior</u> Agitation Flow dynamics Sump-induced flow Reentrainment Transport Sump-induced overflow

had already formed. (These processes and phenomena are the subject of Section 5.) Only seven processes were listed with high importance for the containment above the sump pool, which is the subject of this section. Definitions of these seven processes are provided in Table 4-11.

During blowdown, gravitational settling of large pieces of debris generated by the break-jet flow was ranked as high. During post-blowdown, the four processes associated with the containment above the sump pool deal with debris washdown by the containment sprays. During the sump-operation phase, no processes were ranked as high except those dealing with sump-floor debris transport.

4.3.3 Airborne/Washdown Debris-Transport Evaluations

4.3.3.1 MELCOR Simulation of Karlshamn Tests

Using the MELCOR code, SEA simulated one of the Karlshamn tests to demonstrate the ability of the code to simulate insulation debris transport.⁴⁻⁸ As discussed in Section 4.2.1.4, these tests were conducted in a small-scale test

assembly, shown schematically in Figure 4-7, that was subdivided into a few inner volumes. A steam jet was used to fragment insulation and disperse its debris within the test apparatus. Most of the fibrous insulation debris was distributed in the upper parts of the test apparatus. The gratings held debris back, debris adhered to walls where steam condensed, and debris accumulated in areas of low flow velocity.

The MELCOR code, which was developed at Sandia National Laboratories for the NRC, is a fully integrated computer code that models the progression of severe accidents in LWR nuclear power plants.⁴⁻⁹ Thermal-hydraulic behavior is modeled with a lumped-parameter approach using control volumes connected by flow paths. Each volume is defined spatially by its volume vs altitude; may contain a gravitationally separated pool of single- or two-phase water; and can have an atmosphere consisting of any combination of water vapor, suspended water droplets, or noncondensable gases. Noncondensable gases are modeled as ideal gases with temperature-dependent specific heat capacities. The flow paths connect volumes and define paths for moving hydrodynamic materials.

Processes and/or Phenomena	Description
Gravitational Settling	Downward relocation (sedimentation) of debris in the containment atmosphere onto structure surfaces under the force of gravity.
Droplet Motions	Movement of droplets introduced into containment by the spray system.
Debris Sweepout	Transport of debris through the containment by liquid droplets from the containment spray system.
Surface Draining	Movement of liquid streams from higher elevations to lower elevations.
Deluge Transport	Relocation of debris from containment structures as a result of interactions with the deluge of liquid from the ECCS and spray system.
Disintegration	Breakup of relatively large pieces of debris into smaller particles that can be reentrained into the flow stream caused by the impact of falling liquid streams from the break, fan coolers, and liquid draining off surfaces.
Entrapment	Capture of debris in local structural "pooling points," i.e., locations that allow the accumulation and storage of draining condensate and associated transported debris.

The governing thermal-hydraulic equations conserve mass, momentum, and energy. The MELCOR code contains models to predict the transport and behavior of aerosols that directly couple to the thermal-hydraulic models. The aerosol deposition processes modeled include gravity, diffusion, thermophoresis, and diffusiophoresis.

The MELCOR code results compared well with the experimental results; however, this high degree of comparability does not extend to the conditions typical of postulated LOCAs. The peak bulk flow velocities in the Karlshamn tests were about 1 m/s, whereas the transport velocities were much faster following a postulated LOCA in an actual plant. The atypically slow flow velocities in the Karlshamn tests allowed the debris to settle gravitationally at all levels, whereas at typical transport velocities, the flow turbulence generally would be much too high to allow settling anywhere near the break. After break flows disperse sufficiently into compartments well away from the break, flow velocities and turbulence can be expected to slow sufficiently to allow gravitational settling as was seen in the Karlshamn tests. Thus, the Karlshamn tests might be considered representative of debris transport in some areas of PWR containments, but not in the region of the break. Alternatively, the Karlshamn results might be representative of debris transport following very small LOCAs.

After a complete review of the Karlshamn simulation, it was concluded that although the MELCOR code did a good job of predicting debris transport within the Karlshamn tests apparatus, the code could not reliably be used to predict debris transport within a containment where the flow velocities and flow turbulence would be too high to allow significant debris settling. Also, it should be noted that the MELCOR code does not model inertial impaction of an aerosol, which would be substantial near the break region of the containment. Therefore, system-level codes such as MELCOR were used to estimate thermal-hydraulic conditions within a containment following a LOCA, but not to predict debris transport.

4.3.3.2 BWR Drywell Debris Transport Study (DDTS)

In September 1996, the NRC initiated a study, referred to as the DDTS, to investigate the transport and capture characteristics of debris in BWR drywells using a bounding analysis approach. Understanding the relatively complex drywell debris-transport processes was an essential aspect of predicting the potential for strainer clogging in the estimation of debris transport in the drywell. These processes involve the transport of debris during both the reactor blowdown phase through entrainment in steam/gas flows and the post-blowdown phase

by water flowing out of the break and/or containment sprays. The erosion characteristics of debris caused by air and water flows must also be considered. The focus of the DDTs was to provide a description of the important phenomena and plant features that control or dominate debris transport and the relative importance of each phenomenon as a function of the debris size. Further, these analyses were to demonstrate calculational methodologies that can be applied to plant-specific debris-transport estimates. It also should be noted that the DDTs focused almost entirely on the transport of LDFG insulation debris.

Because of its complexity, the problem was broken into several individual steps. Each step was studied either experimentally or analytically, and engineering judgment was applied where applicable data were not available. The results of the individual steps were quantified using a logic-chart approach to determine transport fractions for (1) each debris size classification, (2) each BWR containment design, (3) both upper bound and central estimates, and (4) each accident scenario studied. The complexity is illustrated in Figure 4-13 for both the blowdown and washdown phases.

Upper bound estimates provide transport fractions that are extremely unlikely to be exceeded. Because each upper bound estimate represents the compounding of upper bound estimates for each individual step, the overall upper bound transport fractions are highly conservative. The central estimates were developed using a more realistic, yet conservative, representation of each individual step. Although the central-estimate transport fractions were deemed closer to reality, the estimates lacked the assurance of not being exceeded under any accident condition.

Early in the study the thermal and hydraulic conditions that would govern debris transport were analytically assessed by performing end-to-end scoping calculations that encompassed the possible debris-transport and capture processes. These calculations included both a series of hand computations and system-level computer code calculations (i.e., MELCOR, RELAP, and CFD). All calculations were designed to examine selected specific aspects of the overall problem. The calculation results were used to subdivide the problem into several components that could be solved individually

through the separate-effects experiments, analytical modeling, and engineering calculations. The calculations also identified vital database elements necessary to quantify transport.

Experiments and further analytical studies were undertaken to provide a basis for quantifying debris transport during blowdown, washdown of debris by ECCS water flow, and debris sedimentation on the drywell floor. In particular, three sets of experiments, which are discussed in Section 4.2, were designed and conducted as part of this study. Detailed CFD simulations were used to determine likely flow patterns that would exist on the drywell floor during ECCS recirculation and the likelihood of debris sedimentation under these conditions.

Transport fractions were estimated for each of the BWR containment designs (i.e., Mark I, Mark II, and Mark III) for a spectrum of postulated accident scenarios. Two major types of piping breaks were studied: main steam line (MSL) breaks and recirculation line (RL) breaks. Both throttled and unthrottled ECCS break overflow was considered. Containment sprays were considered to operate intermittently or not at all.

A simplified logic-chart method was chosen to integrate the problem subcomponents into a comprehensive study. An example logic chart is shown in Figure 4-14. A separate logic chart was generated for each scenario and each containment design. Individual steps in the logic charts were solved using available knowledge tempered by conservative engineering judgment. Finally, the logic charts were quantified and the results were tabulated.

The logic chart subdivides the problem into five independent steps: (1) LOCA type, (2) debris classification, (3) debris distribution after blowdown, (4) erosion and washdown, and (5) sedimentation in the drywell floor pool. Because the debris size distribution was not within the scope of this study, a size distribution from a BWROG study⁴⁻⁶ was used in the DDTs to illustrate the computation of overall debris-transport fractions. Four size classifications are shown in the chart: small, large-above, large-below, and canvassed. Because large debris does not pass through floor grating, the large debris classification was subdivided into debris formed above any grating and debris formed below all gratings. Overall transport fractions were applied to all insulation within the ZOI.

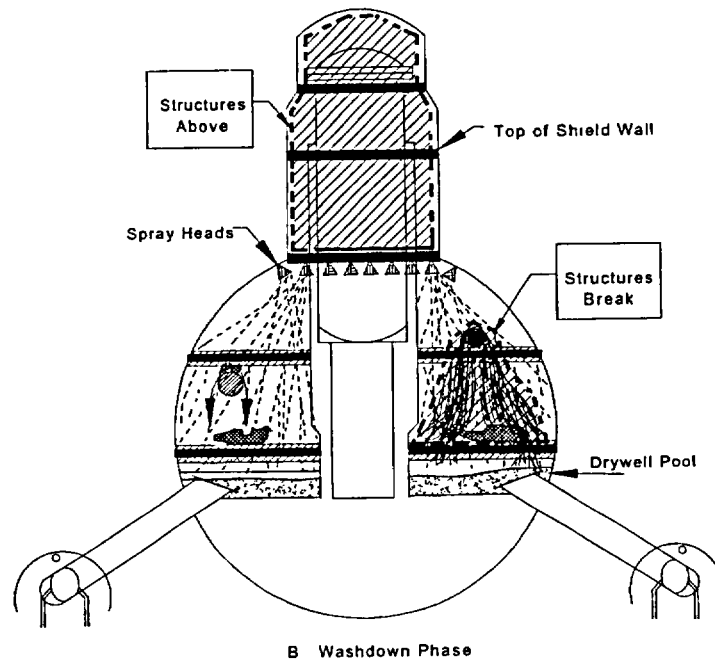
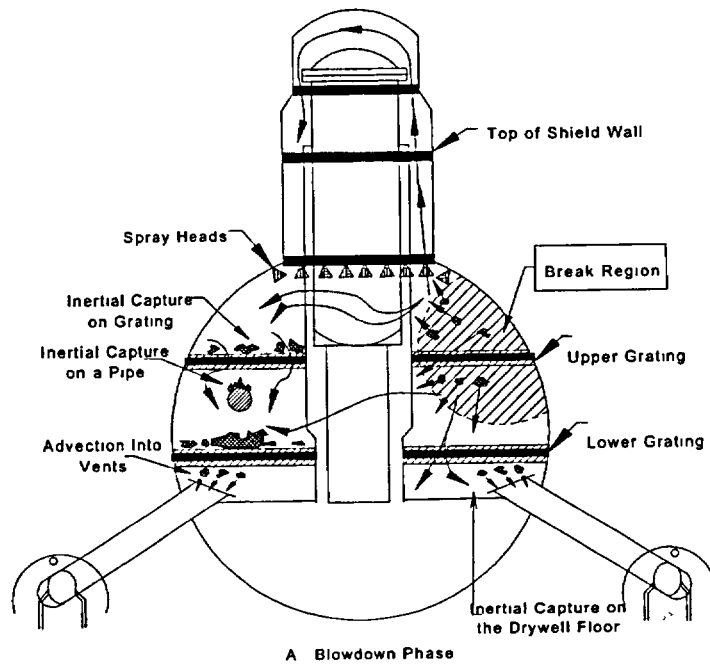


Figure 4-13 Schematic Illustrating the Complexity of Drywell Debris Transport

LOCA Type	Debris Classification	Distribution After Blowdown	Erosion and Washdown	Drywell Floor Pool	Path No.	Fraction	Final Location		
MARK I CENTRAL ESTIMATE MSL BREAK ECCS THROTTLED SPRAYS OPERATED FIBROUS INSULATION	Small Pieces 0 22	Adverted to Vents			1	1.144E-01	Vents		
		0 52 Enclosures			2	2.200E-03	Enclosures		
		0 01			Waterborne	3	0.000E+00	Vents	
		Drywell Floor			0 00				
		0 01			Sediment	4	2.200E-03	Floor	
					1 00				
					Waterborne	5	8.800E-07	Vents	
					0 01				
		Condensate Drainage			Sediment	6	8.712E-05	Floor	
		Structures-Above			0 99				
		0 04			Adheres	7	8.712E-03	Structures-Above	
					0 99				
					Waterborne	8	1.100E-04	Vents	
					0 01				
		Sprays/Condensate			Sediment	9	1.089E-02	Floor	
		Structures-Break			0 99				
		0 10			Adheres	10	1.100E-02	Structures-Break	
					0 50				
					Waterborne	11	3.520E-04	Vents	
					0 01				
		Sprays/Condensate			Sediment	12	3.485E-02	Floor	
		Structures-Other			0 99				
		0 32			Adheres	13	3.520E-02	Structures-Other	
					0 50				
					Waterborne	14	5.100E-04	Vents	
					1 00				
					Sprays/Condensate	Sediment	15	0.000E+00	Floor
		Structures-Break			0 01				
					0 00				
		0 15			Adheres	16	5.049E-02	Structures-Break	
			0 99						
			Waterborne	17	2.890E-03	Vents			
			1 00						
Large-Above			Sprays/Condensate	Sediment	18	0.000E+00	Floor		
0 34			Structures-Other	0 00					
			0 01						
			Adheres	19	2.861E-01	Structures-Other			
			0 99						
MSL Break			Adverted to Vent	20	3.600E-02	Vents			
1 00			0 90 Enclosures	21	4.000E-04	Enclosures			
Large-Below			0 01						
0 04			Waterborne	22	0.000E+00	Vents			
			0 00						
Drywell Floor			Sediment	23	1.600E-03	Floor			
			1 00						
			Waterborne	24	0.000E+00	Vents			
			0 00						
			Sprays/Condensate	Sediment	25	4.000E-06	Floor		
Structures-Break			1 00						
0 01			Adheres	26	3.960E-04	Structures-Break			
			0 99						
			Waterborne	27	0.000E+00	Vents			
			0 00						
			Sprays/Condensate	Sediment	28	1.600E-05	Floor		
Structures-Other			1 00						
0 04			Adheres	29	1.584E-03	Structures-Other			
			0 99						
Canvassed				30	4.000E-01	Structures/Floor			
0 40				Total	1.000E+00				

Figure 4-14 Sample Drywell Debris Transport Logic Chart

Accordingly, the canvassed classification included intact blankets located within the ZOI. The third column shows where the debris is expected to reside following the end of blowdown. Drywell structures were divided according to location in the drywell:

- structures located above the containment spray heads (which are not subject to spray flows),
- structures located directly below the break (which can be subjected to recirculation break flows), and
- all other structures subjected to sprays but not to break flows.

Additionally, small debris can be deposited directly onto the floor by mechanisms such as vent capture or entrapment within an enclosure such as the reactor cavity. Large debris generated above any grating was assumed to reside on a grating either below the break or not below the break. Large debris deposited above the spray heads or in enclosures was not considered credible. Each branch in the erosion and washdown column simply calculated the amounts of captured debris that remained on the structures after being subjected to the appropriate washdown flows (i.e., recirculation break flow, containment spray flow, and condensate drainage). Similarly, each branch in the drywell floor pool column asks how much of the debris settles to the floor and remains there.

Analyses supporting the DDTs included a variety of calculations designed to examine selected specific aspects of the overall problem. These included hand calculations, system-level code calculations, and CFD calculations. The computer code calculations that were performed in support of the DDTs are described in the following paragraphs.

MELCOR Code Calculations

The MELCOR computer code was used to examine the thermal-hydraulic conditions within the drywell following a postulated LOCA. The simulations were based on the BWR Mark I reference plant analyzed during the NUREG/CR-6224 strainer-blockage study.⁴⁻¹⁰ Insights were obtained regarding containment pressures and temperatures, bulk flow velocities, the time required to clear the vent downcomer of water, rate of steam condensation on drywell structures and

subsequent thickness of films, rate of accumulation of water on the drywell floor, and transport of noncondensable gases to the wetwell. Several key observations were made of these MELCOR calculations, including those in the following list.

- The drywell pressure increased rapidly to about 3 atm (44 psia) in about 1 s, corresponding to the clearing of the downcomer vents. Further pressurization was prevented by the pressure-suppression system. After a relatively short period of 5 to 10 s, the pressures decreased again.
- The water in the downcomer vent pipes was purged from the pipes in about 1 s.
- Steam immediately condensed upon contact with surface structures until the temperature of the surface equilibrated with the steam environment. For example, the total rate of condensation within the drywell for the high MSL break peaked at 1170 lbm/s at about 2.5 s.
- Water films with a thickness of 200 to 400 μm accumulated on the structures in as little time as 1 s, depending on the location of the surface relative to the pipe break.
- Peak flow velocities as high as 820 ft/s were found near the break, and flow velocities through the vent downcomer pipes exceeded 660 ft/s. Elsewhere in the drywell, the velocities varied considerably from one location to another.
- The majority of the nitrogen gas initially located in the drywell was forced into the wetwell in about 3 s. The residence time for a tracer gas injected into the drywell along with the break source was generally less than 2 s.
- A pool of water accumulated on the drywell floor and in the reactor cavity sumps, as was expected. In the MSL breaks, the pool would not overflow into the downcomer vent pipes because the depth of the water was only about a quarter of the depth required to overflow. In the recirculation line break (RLB), the results were considerably different. The overflow through the downcomer vent began at 5 s for the low RLB. The asymmetrical pressures acting on the drywell floor pool pushed the accumulated water to the backside of the pedestal from the break; after the drywell pressures peaked, the pool became two-phased. The raised water level caused the

water to overflow into the vents at the backside. The drywell pool leveled out again after the primary system was depressurized.

RELAP Code Calculations

Calculations were performed with the RELAP computer code to characterize the break flow, (i.e., rate of flow and thermodynamic state as a function of time). Following a main steam line break (MSLB), essentially dry steam expands into the containment. The steam mass-flow rate falls from an initial value of close to 6000 lbm/s (assuming blowdown from both ends of the broken pipe) to about 1000 lbm/s within a period of 50 s, whereas the steam velocity remains essentially at the sonic velocity of about 700 ft/s. Water enters the drywell in the form of fine droplets (approximately 5 μm) of entrained water, but the water content is not likely to be large enough to completely wet the debris during its generation.

Following an RLB, the initial flow would be mainly water, but after a period of 5 to 10 s, a mixture of water and steam is discharged at high velocities. During this phase, the dynamic pressures far outweigh the corresponding pressures during the initial 5 s after the break. Because the debris generation is proportional to the dynamic pressure, these results suggest that for an RLB, most of the fibrous insulation debris will be produced in the later stages of the accident. The total mass flow rate remains fairly high (approximately 20,000 lbm/s) throughout the blowdown phase of an RLB compared with the flow rate for a similar size MSLB; however, the water content of the exit flow is very large. In these conditions, it is expected that all of the structures located in the path of the jet will be drenched with water, and the insulation materials in the vicinity of the break are likely to be thoroughly wet before the break jet produces significant debris. Additionally, it is likely that the majority of the debris generated will follow the steam component of the break flow rather than the liquid component. The DDTS assumed that 80% of the debris would be transported with the steam and 20% would be transported with the water.

CFD Calculations

Substantial quantities of insulation debris could land on the drywell floor during the primary

system depressurization or be washed down to the drywell floor from drywell structures after being captured during depressurization. From there, the debris could be transported from the floor into the vent downcomers. Therefore, determining the potential for debris to remain captured on the floor was a necessary step in the overall debris-transport study. This determination was made based on simulating the drywell floor pool for a variety of conditions using a commercially available CFD code. The primary objective of this analysis was to evaluate the potential for fibrous debris to settle in drywell pools and to estimate the fractions of the debris that would be transported to the suppression pool. The study considered Mark I, II, and III designs for variations in pool depth and entrance conditions to the pools.

The CFD results needed to be benchmarked to prototypical experimental data to correlate pool turbulence levels with the conditions that allowed debris to settle. This was accomplished by simulating the ARL Pennsylvania Power and Light Company (PP&L) flume tests with the CFD code and then correlating the code-predicted turbulence level for a given test with the PP&L test results that showed whether fibrous debris actually settled in each test. The PP&L flume tests are documented in "Results of Hydraulic Tests on ECCS Strainer Blockage and Material Transport in a BWR Suppression Pool" (1994).⁴⁻¹¹ The maximum levels of turbulence that allowed debris to settle were determined and applied to the drywell floor pool simulation results. Two maximum levels were determined, one for small debris and one for large debris.

The results of each of the drywell floor pool simulations consisted of graphical pictures of pool flow behavior, such as two- and three-dimensional color pictures of flow velocities and flow turbulence in the form of specific kinetic energy. These turbulence levels then were compared with the maximum levels for debris settling determined by the code calibration. If pool turbulence were higher than the levels found to keep debris in suspension, then debris would not likely settle. On the basis of this graphical data, engineering judgment was used to determine the likelihood for debris settling for each pool configuration. With noted design-specific exceptions, drywell floor pools formed by recirculation break flows are considered likely to transport the majority of insulation debris into

the vent downcomers, and pools formed by the containment sprays are likely to retain debris.

Debris Transport Quantification Results

A summary of the upper bound and central estimated transport fractions for a postulated LOCA in the mid-region of the drywell are presented in Tables 4-12 and 4-13 for the MSLBs and the RLBs. As previously noted, the DDTs focused on the transport of LDFG insulation debris. A complete set of results can be found in Ref. 4-3.

The central estimate transport fractions shown in Table 4-12 are the fractions for the MSLB scenarios in which the operators throttle the ECCS back to the steaming mode and the containment sprays are operated intermittently. This scenario was chosen for summary purposes because it is the most likely scenario that operators would follow. Conversely, the upper bound estimate transport fractions in Table 4-12 are the fractions for the MSLB scenarios in which the ECCS is not throttled back to the steaming mode and the sprays are operated. This scenario was chosen for the upper bound estimate because it represents the worst-case scenario in terms of debris transport. Similarly, the transport fractions shown in the Table 4-13 summary for RLB scenarios are those for ECCS throttling and spray operation

for the central estimates and no throttling and spray operation for the upper bound.

Transport fractions corresponding to Tables 4-12 and 4-13 for all of the insulation initially located within the ZOI are provided in Table 4-14. These transport fractions were determined using the BWROG debris-size distribution of 0.22, 0.38, and 0.40 for small, large, and canvassed debris. The large debris was subdivided further into large-above and large-below categories using engineering judgment. These subdivisions were 80% and 90% above the grating for the central and upper bound estimates, respectively.

Several general conclusions can be drawn from these results.

- The total fraction of debris transported depends strongly on the assumed size distribution of the debris and the location of the break.
- Small debris readily transports toward vent entrances with a substantial amount captured, primarily by the gratings.
- A majority of the large debris generated above any grating is not likely to transport to the vents.
- A majority of the large debris generated below all gratings will likely transport into the vents.

Plant Design	Central Estimate			Upper Bound Estimate		
	Small Debris	Large Debris		Small Debris	Large Debris	
		Above Any Grating	Below All Gratings		Above Any Grating	Below All Gratings
Mark I	0.52	0.01	0.90	1.0	0.05	1.0
Mark II	0.74	0.01	0.90	1.0	0.05	1.0
Mark III	0.55	0	0.90	0.93	0.03	1.0

Plant Design	Central Estimate			Upper Bound Estimate		
	Small Debris	Large Debris		Small Debris	Large Debris	
		Above Any Grating	Below All Gratings		Above Any Grating	Below All Gratings
Mark I	0.86	0.02	0.94	1.0	0.30	1.0
Mark II	0.89	0.02	0.95	1.0	0.30	1.0
Mark III	0.72	0.01	0.90	1.0	0.30	1.0

Table 4-14 Study Transport Fractions for All Insulation Located in ZOI

Plant Design	Main-Steam-Line Break		Recirculation-Line Break	
	Central	Upper Bound	Central	Upper Bound
Mark I	0.15	0.31	0.23	0.39
Mark II	0.20	0.31	0.24	0.39
Mark III	0.16	0.29	0.20	0.39

The study concluded that the URG-recommended transport fractions for Mark II containments underestimate debris transport. For Mark I and Mark III drywells, the study concluded that the URG appears to provide reasonable estimates, provided the plant contains a continuous lower grating with no large holes. However, although the RG 1.82, Rev. 2 recommended assumption of 100% transport of transportable debris was found to provide a reasonable upper bound for breaks located below the lowest grating, the recommendation greatly overestimates debris transport for breaks located above the lowest grating. Finally, the study concluded that licensees should pay close attention to plant features that are unique to their plant and how they were modeled in this study. If necessary, the logic charts provided in this study can easily be modified to account for plant-specific features, such as number and arrangement of floor gratings. They also are flexible enough to accommodate new evidence and assumptions related to debris size and distribution.

The DDTS is documented in the three-volume NUREG/CR-6369 report.⁴⁻³ The main volume, Volume 1, summarizes the overall study, in particular, the debris-transport quantification and transport fractions. The experiments conducted to support this study are documented in detail in Volume 2. The analyses conducted to support this study are documented in detail in Volume 3. The DDTS reports provide reasonable engineering insights that can be used to evaluate the adequacy of the debris-transport fractions used in the utility strainer-blockage analyses

4.3.3.3 PWR Volunteer Plant Analysis

The primary objective of this analysis was to develop and demonstrate an effective methodology for estimating containment debris transport that could be used to assess the debris transport within PWR plants. The transport

analysis consisted of airborne debris transport, where the effluences from a high-energy pipe break would destroy insulation near the break and then transport that debris throughout the containment, and washdown debris transport caused by operation of the containment sprays. The airborne/washdown debris-transport analysis provides the source term for the sump-pool debris-transport analysis.

The volunteer plant chosen for detailed analysis has a large, dry cylindrical containment with a hemispherical dome constructed of steel-lined reinforced concrete with a free volume of approximately 3 million cubic feet. The nuclear steam supply system is a Westinghouse reactor with four steam generators. Each of the steam generators is housed in a separate compartment that vents upward into the dome. Approximately 2/3 of the free space within the containment is located in the upper dome region, which is relatively free of equipment. The lower part of the containment is compartmentalized. The internal structures are supported independently so that a circumferential gap exists between the internal structures and the steel containment liner. Numerous pathways, including the circumferential gap, interconnect the lower compartments.

The containment spray system has spray train headers at four different levels, but about 70% of the spray nozzles are located in the upper dome. The compartments in the lower levels are not covered completely by the spray system, including even the compartments containing spray heads. Therefore, significant areas exist where debris washdown by the sprays would not occur. The sprays activate when the containment pressure exceeds 18.2 psig. If the sprays do not activate, debris washdown likely would be minimal.

The insulation composition for the volunteer plant is roughly 13% LDFG, 86% RMI, and 1% Min-K. The volunteer plant analysis focused on

debris transport for LDFG insulation because LDFG insulation debris causes much more head loss on a sump screen than does a comparable amount of RMI insulation debris, and there was relatively little Min-K in the containment. (Although the analysis focused on the transport of LDFG insulation debris, the transport of the RMI and Min-k insulation debris were also estimated.)

The LDFG debris in the volunteer plant analysis was subdivided into four categories; the transport of each category of debris was treated separately. All insulation located within the break-region ZOI is assumed to be damaged to some extent. The damage could range from the total destruction of a blanket, with all of its insulation turned into small or very fine debris, to the blanket being only slightly damaged and even remaining attached to its piping, perhaps with some insulation erosion occurring through a rip in the blanket cover. The four categories and their properties are shown in Table 4-15.

The primary difference between the two smaller categories and the two larger categories was whether the debris was likely to pass through a grating. The fines were then distinguished from the small pieces because the fines would tend to remain in suspension in the sump pool under even relatively quiescent conditions, whereas the small pieces would tend to sink. Further, the fines tend to transport a little more like an aerosol in the containment air/steam flows and are less quick to settle when airflow turbulence drops off than the small pieces. The distinguishing difference between the large and intact debris was whether the blanket covering was still protecting the LDFG insulation. The primary reason for this distinction was whether the containment sprays could erode the insulation material further. Estimates were made for a distribution among the four categories based on available data and previously accepted engineering judgments. (The database for LOCA generated debris size distributions is sparse.)

The debris-transport methodology decomposed the overall transport problem into many smaller problems that were either amenable to solution or could be judged conservatively in a manner similar to that used in the DDTs (see Section 4.3.3.2).⁴⁻³ The volunteer plant PWR debris-transport methodology necessarily differed from the DDTs BWR transport methodology because

of differences in plant designs. Because debris will for the most part travel with the effluences from the break, a majority of the debris not captured in the break region likely would be blown upward into the dome region. Conversely, in the DDTs study, the break effluences flowed predominantly to the suppression pool. Although debris blown into the upper compartment may be washed back down into the lower compartment by the containment sprays, the washdown pathway can be a tortuous one that certainly could result in substantial debris entrapment.

The DDTs methodology of using logic charts to decompose the transport problem in the volunteer plant worked well within the region of the break. However, outside the region of the break, the complexity of the lower region inner compartments made that approach unreasonable. Therefore, in the volunteer plant analysis, debris capture was estimated first in the break region using the logic chart approach, and then a less sophisticated approach was used for the remaining containment.

In the region of the break, the MELCOR code was used to determine the distribution of flows from the region. Based on the reasoning that fine and small debris will disperse relatively uniformly with the flows and, to a lesser extent, the large debris, the MELCOR flow distributions become the dispersion distributions. Debris capture along these flow pathways was estimated using appropriate capture fractions; e.g., the debris capture fractions for debris passing through gratings were measured. (See Sections 4.2.1.1 and 4.2.1.2.) Another example of debris capture that can be readily justified is debris capture at the personnel access doorways between the steam generator compartments and the sump annulus. Here, the flow must make either one or two 90° bends, and it was determined and measured experimentally that debris would be captured onto a wetted surface at a sharp bend in the flow.

Outside the region of the break, the containment free volume was subdivided into a number of regions based on geometry and the locations of the containment sprays. Within each volume region, the surface area was subdivided according to both its orientation and its exposure to wetness. Because debris gravitationally settles onto horizontal surfaces, the floor areas

Table 4-15 Debris Size Categories and Their Capture and Retention Properties

Fraction Variable	Size	Description	Airborne Behavior	Waterborne Behavior	Debris Capture Mechanisms	Requirements for Crediting Retention
D_F	Fines	Individual fibers or small groups of fibers.	Readily moves with airflows and slow to settle out of air even after completion of blowdown.	Easily remains suspended in water, even relatively quiescent water.	Inertial impaction Diffusiophoresis Diffusion Gravitational settling Spray washout	Must be deposited onto surface not subsequently subjected to containment sprays or to spray drainage. Note that natural circulation airflow likely will transport residual airborne debris into a sprayed region. Retention in quiescent pools without significant flow through the pool may be possible.
D_S	Small Pieces	Pieces of debris that easily pass through gratings.	Readily moves with depressurization airflows and tends to settle out when airflows slow.	Readily sinks in hot water, then transports along the floor when flow velocities and pool turbulence are sufficient. Debris subject to subsequent erosion by flow water and turbulent pool agitation.	Inertial impaction Gravitational settling Spray washout	Must be deposited onto surface not subsequently subjected to high rates of containment sprays or to substantial drainage of spray water. Retention in quiescent pools (e.g., reactor cavity). Debris subject to subsequent erosion.
D_L	Large Pieces	Pieces of debris that do not easily pass through gratings.	Transports with dynamic depressurization flows but generally stopped by gratings.	Readily sinks in hot water and can transport along the floor at faster flow velocities. Debris subject to subsequent erosion by flow water and by turbulent pool agitation.	Trapped by structures (e.g., gratings) Gravitational settling	Must be either firmly captured by structure or on a floor where spray drainage and/or pool flow velocities are not sufficient to move the object. Debris subject to subsequent erosion.
D_I	Intact	Damaged but relatively intact pillows.	Transports with dynamic depressurization flows or may remain attached to its piping.	Readily sinks in hot water and can transport along the floor at faster flow velocities. Debris assumed still encased in its cover and thereby not subject to significant subsequent erosion by flow water and turbulent pool agitation.	Trapped by structures (e.g., gratings) Gravitational settling Not detached from piping	Must be firmly captured either by a structure or on a floor where spray drainage and/or pool flow velocities are not sufficient to move the object. Intact debris subsequently would not erode because of its encasement.

were treated separately from the other areas. The exposure to wetness determines the extent of debris washdown; therefore, areas subjected to containment sprays were treated differently than areas simply wetted by steam condensation. As the containment pressurizes following a LOCA, break flows carrying debris would enter all free volumes within the containment. Larger debris would tend to settle out of the break flows as the flow slowed down after leaving the break region. However, the fine and smaller debris more likely would remain entrained so that it would be distributed more uniformly throughout the containment. In the volunteer plant analysis, the fine and small debris was distributed according to free volume. The larger debris was distributed according to where it would fall out of the flow as the flow slowed. After the debris was dispersed to a volume region, it was assumed to have deposited within that region. The surface area distribution fractions were estimated using the areas tempered by engineering judgment.

Debris deposited throughout the containment subsequently would be subject to potential washdown by the containment sprays, the drainage of the spray water to the sump pool, and, to a lesser extent, by the drainage of condensate. Debris on surfaces that is hit directly by containment spray is much more likely to transport with the flow of water than debris on a surface that is merely wetted by condensation. Debris entrained in spray water drainage is less easy to characterize. If the drainage flows are substantial and rapid moving, the debris likely would transport with the water. However, at some locations, the drainage flow could slow and be shallow enough for the debris to remain in place. As drainage water drops from one level to another, as it would through the volunteer plant floor drains, the impact of the water on the next lower level could splatter it sufficiently to transport debris beyond the main flow of the drainage, thereby capturing the debris a second time. In addition, the flow of water could erode the debris further; generating more of the very fine easily transportable debris. The drainage of spray water from the location of the spray heads down to the sump pool was evaluated. This evaluation provided insights for the transport analysis, such as identifying areas not impacted by the containment sprays, the water drainage pathways, likely locations for drainage water to pool, and locations where

drainage water plummets from one level to the next.

The retention of debris during washdown must be estimated for the debris deposited on each surface, i.e., the fraction of debris that remains on each surface. These estimates, which are based on experimental data and engineering judgment, were assigned somewhat generically. For surfaces that would be washed by only condensate drainage, nearly all deposited fine and small debris likely would remain there. For surfaces that were hit directly by sprays, a majority of the fine and small debris likely would transport with the flow. Large and intact debris likely would not be washed down to the sump pool because of the screens or gratings across the floor drains and the size of those drains. For, surfaces that are not sprayed directly but subsequently drain accumulated spray water, such as floors close to spray areas, the retention fractions are much less clear.

4.3.4 Generalized Debris-Transport Guidance

4.3.4.1 BWR URG Guidance for Drywell Debris Transport and the NRC Review

Based on the small-scale testing summarized in Section 4.2.2.1, the BWROG provided guidance regarding options for estimating the fraction of the damaged insulation generated in the drywell that would be transported subsequently to the suppression pool.⁴⁻⁶ It should be noted that the BWROG approach combined debris generation and drywell debris transport into a combined methodology such that the URG recommends fractions of the damaged insulation within the ZOI that should be considered likely to transport to the suppression pool for each type of insulation. The NRC staff reviewed the BWROG guidance to determine its adequacy.⁴⁻⁷

A number of aspects were considered by the BWROG in determining the recommended fractions. First, the debris was categorized into three groups such that the transport of each group could be considered independently of the other groups. Based on the condition of debris recovered in the AJIT tests, the damaged fibrous insulation was categorized as fines, large pieces, and blankets. The damaged RMI debris was categorized as small pieces (<6 in.²), large foils (>6 in.²), and intact assemblies.

The fibrous "fines" and the RMI "small pieces" generally were considered transportable because they would easily pass through a typical grating. A continuous grating would stop virtually all of the other debris categories.

For fibrous debris, the "large pieces" and "blankets" were effectively treated in the BWROG analyses as a combined group referred to as "blanket material." In both cases, a grating effectively stopped them from transporting, and both were subjected to erosion by break overflow. The insulation within the inner 3 L/D was assumed completely destroyed into transportable debris.

The BWROG used AJIT data to derive the relative fractions of the insulation destroyed into one of three size categories. These fractions depended on the type of insulation and, for some insulation types, on whether the insulation originally was located above or below the lowest elevation grating in the drywell. The BWROG calculated these fractions as integral values averaged over the entire ZOI. These URG fractions are listed in Table 4-16. For example, 77% of the damaged NUKON™ within the ZOI was considered "blanket material" and the remaining 23% was "fines."

The BWROG estimated the transport fractions for each debris category for both fibrous and RMI debris. These fractions are listed in Table 4-17. The BWROG recommended that 100% of the fibrous fines and the RMI small pieces be considered as transported to the suppression pool for Mark I and Mark III plants as a combined result of both blowdown and washdown processes and for both MSL and RL breaks. However, for Mark II plants, the

BWROG limited the transport of fibrous fine debris to 50% for MSL breaks and 56% for RL breaks and RMI small debris to 10% for MSL breaks and 5% for RL breaks. These estimates were based on small-scale experimental data and the analysis of the water flow on drywell floors.

For larger debris, either fibrous or RMI, no direct transport to the suppression pool was assumed for debris generated above the lowest grating. For larger pieces of fibrous debris generated below the lowest grating, a fraction of this debris was assumed to transport directly to the suppression pool. For Mark I and Mark III plants, this fraction was estimated at 70%, but for Mark II plants, the estimate was reduced to 30%. Larger pieces of RMI (generated either above or below a grating) were not assumed to transport to the suppression pool. The remaining mode of transport applicable to fibrous debris was erosion by break overflow. Here, an assumed 25% of blanket material remaining in the drywell would be located so that it would be plummeted by the break overflow and 25% of this material would be eroded away and transported to the suppression pool, resulting in 6.25% of blanket-material transporting to the suppression pool. Lacking appropriate data, an erosion fraction of 1.0 was assumed for calcium-silicate, Koolphen-K, and Min-K insulations (nonfibrous). The URG did not address breaks that could result in debris being generated both above and below the lowest grating. Further, the URG did not specifically address offset or split gratings where depressurization flows could partially bypass the gratings.

Table 4-16 Fractions of Blanket Material with Low Transport Efficiency

Insulation Material	Fraction of Blanket Material with Low Transport Efficiency
NUKON™	0.77
Temp Mat™	0.84
K-Wool	0.78
Knauf®	0.70
NUKON™ Jacketed with Sure-Hold Bands	0.85
Calcium-Silicate with Aluminum Jacketing	0
Koolphen-K®	0.74

Table 4-17 URG Drywell Transport Fractions			
Fibrous Insulation Debris		RMI Debris	
Size Category	Transport Fraction	Size Category	Transport Fraction
Fines	1.0 for Mark I and III 0.5 for Mark II MSLB 0.56 for Mark II RLB	Small Pieces	1.0 for Mark I and III 0.1 for Mark II MSLB 0.05 for Mark II RLB
Blanket Material Above Grating	No Direct Transport 25% Erosion of 25% of Pieces = 6.25%	Large Foils Above Grating	No Transport No Erosion
Blanket Material Below Grating	70% Direct + 6.25% Erosion of Remaining 30% for Mark I and III 30% Direct + 6.25% Erosion of Remaining 70% for Mark II	Large Foils Below Grating	No Transport No Erosion

These debris-generation and debris-transport fractions were developed further into combined debris-generation and transport fraction for each type of insulation. Unjacketed NUKON™ debris generated above the lowest grating, for example, 23% of the damaged insulation, was turned into fine debris that subsequently transports directly to the suppression pool. Then, 6.25% of the remaining 77% (blanket material) was eroded away and also transported for a total of 28% of the ZOI insulation transported into the suppression pool (i.e., $0.23 + 0.0625 \times 0.77 = 0.28$). Below the lowest grating, the total debris transported would consist of the 23% fines, 70% of the 77% blanket material, and 6.25% of the nontransport blanket-material that subsequently was eroded (i.e., $0.23 + 0.70 \times 0.77 + 0.0625 \times 0.30 \times 0.77 = 0.78$). Combined debris-generation and transport fractions for the Mark I and Mark III plants are listed in Table 4-18.

The BWROG did not develop transport factors for materials other than insulation materials. Where an approved transport factor is not available, licensees should either assume a factor of 1.0 or perform the testing/analysis necessary to justify another factor.

NRC Evaluation

The URG recommendations were based primarily on data from small-scale debris-generation and transport tests conducted by the BWROG. Because the staff had several concerns related to scaling small-scale transport test data to BWR conditions, the staff conducted

confirmatory research to verify the accuracy of guidance provided by the URG. Specific concerns included whether or not the flow rates and flow durations in the small-scale tests were prototypical of conditions that would exist in BWR drywells following a LOCA. The staff's analysis indicated the BWROG test flow velocities were on the order of 50% of prototypical velocities for a postulated large MSL break. It was not clear to the staff in evaluating the BWROG test program whether the test results were reasonable, conservative, or nonconservative if scaled to a full-sized plant. Therefore, the staff concluded that there is inadequate substantiation for the BWROG claim that the use of these test results would conservatively bound the drywell transport fraction. The NRC-sponsored DDTS (see Section 2.2.3)⁴⁻³ demonstrated that a high percentage of fine debris could transport to the suppression pool and that the transport of the debris is both plant-specific and break-specific.

Estimating the erosion of large fibrous debris depends on estimating the quantity of debris subjected to erosion, the rate of erosion, and the duration of the erosion. The URG estimate of 25% of the debris being subjected to erosion was based on engineering judgment and was considered by the BWROG to be sufficient to ensure a conservative estimate of the mass of eroded debris. The staff evaluation of the URG guidance for assuming erosion of large fibrous debris concluded that the guidance is adequate provided that the unthrottled ECCS flow does not continue for more than 3 h. The staff concluded that licensees should determine an

Material	Above Grating	Below Grating
Darchem DARMET®	0.50	0.50
Transco RMI	0.50	0.50
Jacket NUKON™ with Modified Sure-Hold Bands, Camloc® Strikers, and Latches	0.15	0.15
Diamond Power MIRROR® with Modified Sure-Hold Bands, Camloc® Strikers, and Latches	0.50	0.50
Calcium-Silicate with Aluminum Jacketing	0.10	0.10
K-Wool	0.27	0.78
Temp-Mat™ with Stainless-Steel Wire Retainer	0.21	0.76
Knauf®	0.34	0.80
Jacketed NUKON™ with Standard Bands	0.28	0.78
Unjacketed NUKON™	0.28	0.78
Koolphen-K®	0.45	0.45
Diamond Power MIRROR® with Standard Bands	0.50	0.50
Min-K	1.0	1.0

*Same fractions used for steam and water breaks

appropriate fraction for their analysis if unthrottled flow continues for more than 3 h. Note that NRC-sponsored research demonstrated that erosion of NUKON™ occurs at a linear rate (see Section 2.1.1.5), which facilitates scaling NUKON™ erosion. Based on the overall level of conservatism in the URG guidance, the staff concluded that the URG guidance regarding the prediction of the erosion of large fibrous debris by break overflow was acceptable.

The staff reviewed the URG destruction fractions, i.e., the determination of the fractions of the destroyed insulation that would remain in "blanket material" form with low transport efficiency. On the basis of NRC-sponsored research, the staff noted a number of strengths and conservatisms associated with the URG guidance. The blanket arrangement used in the BWROG tests was conservative, (e.g., the orientation of blanket seams and jacket latches relative to the air-jet nozzle). The BWROG tests oriented seams and latches to maximize blanket destruction. In BWR drywells, insulation blankets could be protected by other structures located in the jet pathway, and this protection was not taken into account in the tests. In the BWROG air-jet tests, the insulation blankets were oriented normal to the air jet to maximize destruction, but in BWR drywells, the majority of the piping (>65%) and therefore the insulation

blankets would be located parallel to the jet flow. Thus, much less of the blanket would be subjected to the full jet flow. The weakness of the BWROG test data was that they were very limited for several types of insulation, specifically Temp-Mat, K-wool, and some of the RMI. However, the staff concluded that the URG methods for determining the ZOI and debris generation are sufficiently conservative to outweigh this weakness.

The primary criticism of the URG drywell debris-transport guidance was the substantially reduced transport fractions applied to the Mark II containments relative to the Mark I and III containments. The NRC-sponsored tests of the Mark II geometry did not identify any basis to conclude that the transport fraction for a Mark II containment would be different from that of a Mark I or a Mark III containment. Given the uncertainty associated with estimating the debris transport fraction, which includes the uncertainty associated with estimating size distribution and quantities of insulation damaged, the staff concluded that the BWROG transport fractions for fibrous debris in Mark II containments are both nonconservative and unacceptable and that Mark II containments should use the same transport fractions as the Mark I and Mark III containments.

4.3.4.2 Transport Fractions for Parametric Evaluation

The NRC sponsored a parametric evaluation to demonstrate whether sump failure is a plausible concern for operating PWR plants in the U.S.^{4-12, Vol 1} The results of the parametric evaluation formed a credible technical basis for decision-making regarding the resolution of the PWR sump-screen issue. Among the limitations of the parametric evaluations was the necessity of assuming and applying generic debris-transport fractions to all PWR plants, knowing that transport fractions are highly plant-specific. The development of these generic transport fractions is discussed in detail in Volume 4 of Ref. 4-12.

A number of simplifying assumptions were necessary to keep the parametric evaluation tractable for each of the 69 operating PWR plants. In addition, the assumptions generally were slanted in favor of sump failure not being a plausible concern. For the purposes of the parametric evaluation, the containment airborne and washdown-transport fractions were combined with the sump-pool transport fraction. That is, the transport fraction used in the parametric evaluation was the fraction of the insulation originally contained within the ZOI that subsequently was transported to the sump screen.

To further simplify the evaluation, one set of transport fractions was applied to all types of insulation debris in the analysis. The insulations types for all the PWRs were categorized for the purposes of this evaluation as either fibrous, reflective metallic, particulate (e.g., calcium-silicate), or foam. The foam insulation was neglected from further analysis on the basis that it would float above the screens and therefore not contribute to head loss.⁴ The generic parametric evaluation transport fractions were used to estimate the transport of fibrous insulation, reflective metallic insulation, and particulate insulation alike.

⁴Note that this assumption was suitable for the purposes of the parametric evaluation but *not* necessarily for plant-specific analyses in that some foam types might not be sufficiently buoyant to float over a sump screen and even buoyant debris would impact, at least to some extent, a sump screen that is not completely submerged.

With respect to sump-screen head loss, the parametric evaluation quickly determined that the head loss associated with fibrous insulation debris would be substantially greater than the head loss associated with the RMI debris. Hence, the study focused on fibrous insulation debris head loss for any plant reporting significant fibrous insulation in the containment. For plants claiming that all or nearly all of their insulation was RMI, the parametric evaluation examined the RMI head loss to determine the likelihood of that plant's sump screen becoming clogged by RMI debris alone.⁵

The head loss associated with calcium-silicate was not evaluated specifically because of the general lack of head loss data for calcium-silicate. The parametric evaluation simply determined the likely quantities of calcium-silicate to transport to the sump screens and added those quantities to the assumed quantity of general particulate transport down from the containment, an approach that definitely is not suitable for plant-specific analyses. Because the presence of calcium-silicate in a fibrous debris bed has been found to substantially enhance the head loss associated with that bed over and above the corresponding head loss without the calcium-silicate present, this approach represents an underestimate (possibly a huge underestimate) of the head loss associated with calcium-silicate. The problems associated with not evaluating the blockage potential associated with calcium-silicate insulation were noted in the evaluation.

It was assumed that 33% of the ZOI insulation was damaged into a form that has been loosely

⁵ It should be noted that in all likelihood no PWR containment would be completely free from fibrous debris. As discussed in Section 2, any containment should be expected to contain a certain amount of miscellaneous dust, which would partially consist of fibers. This type of fibrous debris is referred to as 'latent fibers' and little, if any, data exists at this time to quantify the amount of latent fiber within containment. Latent fibers would be easily washed by the containment sprays to the sump where the fibers would tend to accumulate on the sump screen forming a thin, uniform bed of fibrous debris. In addition, a plant relying primarily on RMI insulation would most likely use other types of insulation in locations where the use of RMI was not practical, and such a plant likely would have other non-insulation materials within the containment that contained fibers, such as fire barrier materials.

referred to as "transportable debris."^{4-12, Vol 3} In other words, 67% of the insulation would not likely transport to the sump because the debris pieces would be larger debris or even partially destroyed insulation blankets still attached to their respective piping. However, erosion of the larger pieces as a result of the impact of water flow is known to happen. Therefore, the 33% was enhanced to 40% to account for erosion.⁶ In this manner, the evaluation could neglect further consideration of the transport of the larger debris.

The transport fractions used in the parametric evaluation were based on ongoing NRC-sponsored research into debris transport, including small-scale testing, and on engineering judgment. The results and conclusions from this research had not been completely formulated at the time of the evaluation. The engineering judgment relied on debris-transport research from the corresponding resolution of the strainer-blockage issue for the BWR plants, as well as the ongoing PWR-related research.

The transport fractions used in the parametric evaluation are shown in Table 4-19. In the parametric evaluation, selected parameters were treated using a range of values that were denoted as favorable and unfavorable with respect to the potential for sump blockage. A favorable position was slanted toward not illustrating a credible concern regarding sump blockage. The favorable/unfavorable difference in the transport fractions was a result of the transport fraction associated with transport within the sump pool.

These transport fractions served their purpose in the parametric evaluation but should not be used in detailed PWR debris-transport analyses in lieu of plant-specific debris-transport fractions. As stated, the purpose of the parametric evaluation was simply to demonstrate a plausible concern using very limited plant-specific information. Thus, plant-specific analyses should use plant-specific data. The plant-specific transport fractions could exceed those of the parametric evaluation.

4.4 Types of Analytical Approaches

Analytical work has clearly demonstrated that system-level codes (for example, the MELCOR

⁶ An assumption that 10% of the large debris was eroded into fines debris ($0.1 \times 0.67 = 0.07$)

code) do not have the capability to realistically simulate debris transport except for limited transport conditions. The same can be said of CFD codes. The aerosol-transport models in these codes do not usually have inertial impaction models. Inertial impaction models exist for specific circumstances, such as at a bend in a pipe, but these models are not generally applicable to the variety of specific flow situations within containments, even if these situations could be modeled thermally-hydraulically. An exception would be the transport of small debris at relatively slow flow velocities, such as the Karlshamn experiments. (See Section 4.3.3.1.) Here the debris deposition was primarily a result of gravitational settling, which was the dominant deposition mechanism in those tests and is modeled in MELCOR. However, these types of codes are very useful for characterizing thermal-hydraulic conditions within the containment. These codes can predict the flow velocities and distributions, rates of condensation, surface film thicknesses, temperatures, pressures, etc., reasonably well.

One method of reducing the debris-transport fractions is to evaluate specific locations where debris is likely to be trapped and not subsequently washed down to the sump pool. For example, debris carried by flow exiting the break region compartment by way of a door that makes one or more 90° bends may likely become trapped where containment sprays would not impact the trapped debris. Debris-transport testing clearly demonstrated inertial debris capture whenever the flow makes a sharp change of direction and the associated surfaces are wetted. Most surfaces within the containment would be wetted quickly by steam condensation. These experimentally justified specific debris-capture locations could conceivably add up to a significant reduction in the debris-transport fraction.

The logic chart approach developed in the DDTs analyses, discussed in Section 4.3.3.2, might be used to decompose the problem, such that individual parts of the overall transport problem can be resolved by adapting experimental data tempered with engineering judgment. This approach works best where there are relatively few flow pathways and substantial inertial capture along those pathways because of sharp bends in the flow or structures such as gratings. For simpler containments, the approach might be applied to the entire

Transport Conditions	Favorable Estimate	Unfavorable Estimate
Small LOCA (SLOCA) with Sprays Inactive	0.05	0.10
SLOCA with Sprays Active	0.10	0.25
All Medium LOCAs (MLOCAs) and Large LOCAs (LLOCAs)	0.10	0.25

containment, but the approach likely would be difficult to apply for more complex flow situations. The approach should usually still be applicable to the region of the break, even if the flows in the overall containment are too complex for a logic-chart type of analysis.

It might be appropriate to assume a relatively uniform dispersion for the fine and small debris outside the break region for some analyses. After the inertially impacted deposition is estimated, the remaining airborne debris is distributed according free volume. Outside of the break region, the depressurization flows should slow dramatically as the flows expand. As the flows expand and slow, inertial impaction deposition would become much less important, and as the flow turbulence subsides, gravitational settling would dominate debris capture. Without inertial impaction, the debris would tend to follow the movement of steam and air until settling becomes effective.

The larger debris cannot be dispersed uniformly. Rather, the larger debris would simply fall out after the transport velocities slowed, such as when the depressurization flows entered the containment dome. Large debris ejected into the containment dome would most likely simply fall to the floor of the uppermost levels.

4.5 Rules of Thumb

It is difficult to formulate general rules of thumb appropriate to airborne and washdown debris transport in a PWR containment. Airborne and washdown debris transport are both plant-specific and accident-specific. However, the following general and somewhat simplistic observations apply to airborne and washdown debris transport.

- Fine and small debris transport more readily than does the larger debris.

- Substantial inertial deposition can be expected in the region of the break.
- Outside the region of the break, gravitational settling would dominate debris deposition after the flow turbulence decreased significantly to allow settling.
- If the containment spray system were activated, then substantial quantities (if not most) of fine and small debris impacted by the sprays likely would be washed down to the sump pool.

4.6 References

- 4-1. B. E. Boyack, T. S. Andreychek, P. Griffith, F. E. Haskin, and J. Tills, "PWR Debris Transport in Dry Ambient Containments – Phenomena Identification and Ranking Tables (PIRTs)," Los Alamos National Laboratory report LA-UR-99-3371, Revision 2, December 14, 1999.
- 4-2. G. Wilson, et al., "BWR Drywell Debris Transport Phenomena Identification and Ranking Tables (PIRTs)," Final Report, Idaho National Engineering Laboratory report INEL/EXT-97-00894, Lockheed Martin Idaho Technologies Co., Idaho Falls, ID, September 1997.
- 4-3. D. V. Rao, C. Shaffer, and E. Haskin, "Drywell Debris Transport Study," U.S. Nuclear Regulatory Commission, NUREG/CR-6369, Volume 1, September 1999.
Volume 2, D. V. Rao, C. Shaffer, B. Carpenter, D. Cremer, J. Brideau, G. Hecker, M. Padmanabhan, and P. Stacey, "Drywell Debris Transport Study: Experimental Work," September 1999.
Volume 3, C. Shaffer, D. V. Rao, and J. Brideau, "Drywell Debris Transport Study: Computational Work," September 1999.

- 4-4. "Knowledge Base for Emergency Core Cooling System Recirculation Reliability," NEA/CSNI/R (95) 11, Prepared by U.S. Nuclear Regulatory Commission for the Principal Working Group 1 (PWG-1), International Task Group, Committee on the Safety of Nuclear Installations, Organization for Economic Cooperation and development (OECD) Nuclear Energy Agency (NEA), February 1996.
- 4-5. A. W. Serkiz, "Containment Emergency Sump Performance," U.S. Nuclear Regulatory Commission, NUREG-0897, Revision 1, October 1985.
- 4-6. "Utility Resolution Guidance for ECCS Suction Strainer Blockage," BWROG, NEDO-32686, Rev. 0, November 1996.
- 4-7. "Safety Evaluation by the Office of Nuclear Reactor Regulation Related to NRC Bulletin 96-03 Boiling Water Reactor Owners Group Topical Report NEDO-32686, 'Utility Resolution Guidance for ECCS Suction Strainer Blockage,'" Docket No. PROJ0691, NRC-SER-URG, August 20, 1998.
- 4-8. C. J. Shaffer, "Demonstration of MELCOR Code Capability to Simulate Insulation Debris Transport Within a BWR Drywell," Computational Analysis Report, SEA-95-970-01-A:5, October 23, 1995.
- 4-9. R. O. Gauntt, et al., "MELCOR Computer Code Manuals," Volumes 1 and 2, Revision 2, NUREG/CR-6119, SAND2000-2417, Sandia National Laboratories, October 2000.
- 4-10. G. Zigler, J. Bridaeu, D. V. Rao, C. Shaffer, F. Souto, W. Thomas, "Parametric Study of the Potential for BWR ECCS Strainer Blockage Due to LOCA Generated Debris," Final Report, U.S. Nuclear Regulatory Commission, NUREG/CR-6224, October 1995.
- 4-11. K. W. Brinckman, "Results of Hydraulic Tests on ECCS Strainer Blockage and Material Transport in a BWR Suppression Pool," EC-059-1006, Revision 0, May 1994.
- 4-12. D. V. Rao et al., "GSI-191: Parametric Evaluations for Pressurized Water Reactor Recirculation Sump Performance," NUREG/CR-6762, Volume 1, 2002.
- Volume 2, D. V. Rao, B. C. Letellier, K. W. Ross, L. S. Bartlein, and M. T. Leonard, "Technical Assessment: Summary and Analysis of U.S. Pressurized Water Reactor Industry Survey Responses and Responses to GL 97-04," 2002.
- Volume 3, C. J. Shaffer, D. V. Rao, and S. G. Ashbaugh, "Technical Assessment: Development of Debris-Generation Quantities in Support of the Parametric Evaluation," NUREG/CR-6762, 2002.
- Volume 4, S. G. Ashbaugh and D. V. Rao, "Technical Assessment: Development of Debris Transport Fractions in Support of the Parametric Evaluation," 2002.